Boosting the innate immune response to enhance antibiotic efficacy: Mechanistic and quantitative insights by amalgamating *in vitro*, *in vivo* and *in silico*

Inaugural-Dissertation

to obtain the academic degree

Doctor rerum naturalium (Dr. rer. nat.)

submitted to the Department of Biology, Chemistry, Pharmacy

of Freie Universität Berlin

by

Sebastian Niklas Franck

Berlin, 2020

Declaration of Authorship

I hereby confirm that I have authored the submitted dissertation independently and without the use of sources and aids other than those indicated. No other person's work has been used without due acknowledgment in the main text of the thesis. This dissertation has not been submitted in the same or similar form in any previous doctoral procedure.

Sebastian Niklas Franck

Die vorliegende Dissertation wurde von 2016 bis 2020 unter der Leitung von Prof. Dr. Charlotte Kloft am Institut für Pharmazie der Freien Universität Berlin angefertigt.

1. Gutachter:	Prof. Dr. Charlotte Kloft
2. Gutachter:	Dr. Jean-Claude Sirard
Disputation am:	08.07.2021

Abstract

Therapy of bacterial infectious diseases is an increasingly challenging task due to the emergence of resistance, which has become a major threat for global healthcare in the last years. In particular, lower respiratory tract infections are contributing extensively as the leading infectious cause of death in the world. The dynamics in the development of new bacterial resistance mechanisms highlight this alarming trend. Currently, combining at least two antibiotics is the most important and ultimo-ratio strategy to overcome an infection in patients being severely infected with highly resistant bacterial strains. However, the emergence of bacterial resistance is already restricting current approaches and illustrates the high priority of novel advanced strategies.

Hence, the pursuit of innovative treatment regimens is urgently required to address this challenge. One strategy is the use of immunostimulatory drugs in combination with antibiotics to contribute minimising both, the emergence of antibiotic resistance in pathogens and treatment failure. Targeting the innate immune response has the advantage of interacting with the host rather than the pathogen and, accordingly, being able to delay bacterial resistance development. In combination with currently available antibiotic drugs, the novel approach is rapidly accessible to support anti-infective therapy and sustain effectiveness of antibiotic drugs.

The present thesis aims to develop non-conventional combination regimens of antibiotic and immunostimulatory drugs to treat clinically most relevant bacterial species in terms of lower respiratory tract infections. The main objectives were to initially select potential drug combination partners *in vitro*, evaluate their preclinical exposure-response relationship *in vivo*, and define the efficacy of this combination regimen by applying pharmacometric approaches *in silico*. By amalgamating these methods, mechanistic and quantitative insights and an enhanced understanding of the applied combination were intended to ultimately allow a translation into a clinical setting.

The *in vitro* investigations characterised the bacterial strains *Klebsiella pneumoniae*, *Pseudomonas aeruginosa*, *Staphylococcus aureus* and *Streptococcus pneumoniae* and assessed the single and combined effects of the utilised antibiotic and immunostimulatory drugs by conducting conventional susceptibility and checkerboard studies. Antibacterial effects of immunostimulatory drugs could be exerted by direct, i.e. drug-mediated, or indirect, i.e. modulator-mediated, effects. For that purpose, modulator-mediated effects were assessed in a newly developed time-kill curve assay allowing growth in cell-pretreated medium. Here, drug-mediated effects were excluded, no distinct modulator-mediated effects were determined and no potential interactions in combination with antibiotics were shown.

Based on the conducted *in vitro* studies and state-of-the-art knowledge, the combination of the antibiotic amoxicillin and the immunostimulatory drug monophosphoryl lipid A (MPLA) was selected aiming to characterise the dynamic interplay of the drugs, the pathogen and the host *in vivo* in a murine pneumonia model in collaboration with project partners at the Institut Pasteur de Lille. Both drugs were investigated

after administration to mice 12 h after infection with *Streptococcus pneumoniae* in monotherapy or a combined treatment regimen. Exploiting pharmacokinetic and pharmacodynamic data from the mouse infection model, the preclinical exposure-response relationship of this combination was characterised in an overarching pharmacometric analysis:

Quantification of orally administered amoxicillin in mouse serum was enabled by the successful development, validation and application of a rapid, simple and highly sensitive liquid chromatography tandem mass spectrometry assay leading to fully described concentration-time profile of amoxicillin. The pharmacodynamic effects of amoxicillin and MPLA were comprehensively characterised *in vivo* by assessing the bacterial burden at the infection site lung and the spleen as surrogate of sepsis, by survival and by different markers representing the physical condition and the immune response of the animal. In combination, the bacterial burden was substantially reduced, and survival was improved. The innate immune response was simultaneously affected by the bacterial strain as well as the immunostimulatory drug.

The developed semi-mechanistic pharmacokinetic/pharmacodynamic model provided quantitative insights on basis of the generated *in vivo* data. MPLA coadministration reduced the amoxicillin clearance at maximum by 40.9% for a dose of 1.2 mg/kg amoxicillin. On top of this pharmacokinetic interaction, a pharmacodynamic interaction was determined: The combined treatment was superior to both monotherapies with MPLA enhancing the efficacy of amoxicillin after 48 h by more than 50% compared to amoxicillin alone after 48 h. MPLA was able to boost the innate immune response by 1.40-fold. This effect was rather delayed and benefitted of the contrarily immediate response of amoxicillin. Combining MPLA cotreatment with amoxicillin concentrations above the minimal inhibitory concentration for ≥3.23 h, a survival rate of ≥95% was achieved with MPLA reducing the required time of amoxicillin concentrations above the minimal inhibitory concentration by 1.23 h compared to monotherapy. Additionally, survival of mice in the combined treatment approach at highest amoxicillin dose (1.2 mg/kg) was increased 1.35-fold to 90.3% after 14 d compared to monotherapy. To investigate the potential benefits of this therapeutic approach in a clinical setting, important steps towards a translation to humans were performed. Whereas adequate and plausible translation of the pharmacokinetics of amoxicillin was possible, the innate immune response was not completely characterised and, accordingly, not translatable. Still, valuable insights into interactions of bacteria, the drugs and the host were established and critical aspects hampering a translation were identified.

To conclude, applying pharmacometric approaches increased the understanding of the pathophysiology of the infection and allowed a link between pharmacokinetics and pharmacodynamics. The characterised boost of the immune system and the enhanced antibacterial efficacy clearly indicated the potential of immunostimulatory drugs to function as combination partner of antibiotic drugs to treat bacterial infections in humans in future.

Zusammenfassung

Die Therapie von bakteriellen Infektionskrankheiten ist eine immer schwieriger werdende Herausforderung, da sich der deutliche Anstieg in der Entstehung von bakteriellen Resistenzen in den letzten Jahren zu einer großen Bedrohung für die globale Gesundheitsversorgung entwickelt hat. Insbesondere Infektionen der unteren Atemwege verursachen in Relation zu anderen Infektionskrankheiten den weltweit größten Anteil an Todesfällen. Die Dynamik in der Entwicklung neuer bakterieller Resistenzmechanismen verdeutlicht diesen alarmierenden Trend. Gegenwärtig ist die Kombination von mindestens zwei Antibiotika die wichtigste Strategie zur Behandlung einer Infektion bei Patienten, die mit hochresistenten Bakterien infiziert sind. Das Auftreten bakterieller Resistenzen schränkt jedoch bereits jetzt die derzeitigen Behandlungsansätze ein und verdeutlicht die hohe Priorität neuartiger fortgeschrittener Strategien.

Um dieser Herausforderung zu begegnen, ist die Verfolgung innovativer Behandlungsansätze dringend erforderlich. Eine Strategie ist der Einsatz von immunstimulierenden Arzneistoffen in Kombination mit Antibiotika, die dazu beitragen sollen, sowohl die Entstehung von Antibiotikaresistenzen als auch das Versagen der Behandlung zu minimieren. Die Stimulation der angeborenen Immunantwort hat den Vorteil, dass direkt mit dem Wirt statt vor allem mit dem Erreger interagiert wird. Dementsprechend kann die bakterielle Resistenzentwicklung verzögert werden. In Kombination mit derzeit verfügbaren Antibiotika ist dieser neuartige Ansatz vergleichsweise schnell umzusetzen, um die Therapie von Infektionskrankheiten zu unterstützen und die Wirksamkeit der antibakteriellen Arzneistoffe aufrechtzuerhalten.

Die vorliegende Arbeit zielt darauf ab, nichtkonventionelle Kombinationstherapien von antibiotischen und immunstimulierenden Arzneistoffen zu entwickeln, um die klinisch relevantesten Bakterien als Auslöser von Atemwegsinfektionen zu behandeln. Die Hauptziele waren zunächst die Auswahl potenzieller Arzneistoffkandidaten *in vitro*, die Bewertung ihrer präklinischen Expositions-Wirkungsbeziehung *in vivo* und die Definition der Wirksamkeit dieses Kombinationsschemas durch Anwendung pharmakometrischer Modelle *in silico*. Durch das Vereinigen dieser Methoden sollten mechanistische und quantitative Erkenntnisse sowie ein verbessertes Verständnis der angewandten Kombination letztendlich eine Übertragung in die klinische Praxis ermöglichen.

In den *In-vitro*-Untersuchungen wurden die Bakterienstämme *Klebsiella pneumoniae*, *Pseudomonas aeruginosa*, *Staphylococcus aureus* und *Streptococcus pneumoniae* charakterisiert und die Einzel- und Kombinationswirkungen der eingesetzten antibiotischen und immunstimulierenden Arzneistoffe durch konventionelle Empfindlichkeits- und Interaktionsstudien bewertet. Die Wirkung von immunstimulierenden Arzneistoffen kann durch direkte, d.h. arzneistoffvermittelte, oder indirekte, d.h. modulatorvermittelte Effekte ausgeübt werden. Zu diesem Zweck wurden die modulatorvermittelten Wirkungen in einem neu entwickelten Assay bewertet, der das zeitabhängige Wachstums- bzw.

Absterbeverhalten der Bakterien in einem modulatorenthaltendem Medium ermöglicht. Dabei wurden arzneistoffvermittelte Effekte ausgeschlossen, keine eindeutigen modulatorvermittelten Effekte festgestellt und keine potenziellen Wechselwirkungen in Kombination mit Antibiotika gezeigt.

Auf der Grundlage der durchgeführten *In-vitro*-Studien und den neusten Erkenntnissen aus der aktuellen Literatur wurde die Kombination des Antibiotikums Amoxicillin mit dem immunstimulierenden Arzneistoff Monophosphoryl Lipid A (MPLA) ausgewählt, um das dynamische Zusammenspiel der Arzneistoffe, des Erregers und des Wirts Maus in einem Pneumonie-Modell in Zusammenarbeit mit Partners des Institut Pasteur de Lille zu charakterisieren. Beide Arzneistoffe wurden den Mäusen einmalig 12 h nach einer Infektion mit *Streptococcus pneumoniae* als Monotherapie oder in einem kombinierten Therapieansatz verabreicht.

Unter Nutzung pharmakokinetischer und pharmakodynamischer Kenntnisse wurde die präklinische Expositions-Wirkungs-Beziehung dieser Kombination in einer übergreifenden pharmakometrischen Analyse charakterisiert:

Die Quantifizierung von oral verabreichtem Amoxicillin in Mäuseserum wurde durch die erfolgreiche Entwicklung, Validierung und Anwendung eines schnellen, einfachen und hochempfindlichen Flüssigkeitschromatographie-Tandem-Massenspektrometrie-Assays ermöglicht, der die Erfassung eines vollständig beschriebenen Konzentrations-Zeit-Profils von Amoxicillin ermöglichte. Die pharmakodynamischen Effekte von Amoxicillin und MPLA wurden *in vivo* umfassend charakterisiert, indem die bakteriellen Konzentrationen an dem Ort der Infektion, der Lunge, und der Milz als Surrogat für Sepsis, das Überleben und verschiedene Marker, die die Gesundheit und die Immunantwort der Mäuse repräsentieren, bestimmt wurden. In Kombination beider Arzneistoffe wurde die bakterielle Konzentration erheblich reduziert und die Überlebensrate deutlich gesteigert. Die angeborene Immunantwort wurde gleichzeitig sowohl durch die Pathogene als auch durch den immunstimulierenden Arzneistoff beeinflusst.

Das entwickelte semi-mechanistische pharmakokinetische/pharmakodynamische Modell lieferte quantitative Erkenntnisse auf der Grundlage der generierten *In-vivo*-Daten. Die gleichzeitige MPLA-Gabe verringerte die Amoxicillin-Clearance in Abhängigkeit von der Amoxicillin-Dosis linear um maximal 40.9%. Zusätzlich zu dieser pharmakokinetischen Interaktion wurde eine pharmakodynamische Interaktion bestimmt: Die Kombinationstherapie war den jeweiligen beiden Monotherapien überlegen, da MPLA die Wirksamkeit von Amoxicillin nach 48 h um mehr als 50% gegenüber der alleinigen Amoxicillingabe steigerte. MPLA konnte die angeborene Immunantwort um das 1.40-Fache verstärken. Dieser Effekt trat verzögert auf und profitierte von dem im Gegensatz dazu sofortigen Effekt von Amoxicillin. Die Kombination der MPLA-Behandlung mit Amoxicillin-konzentrationen oberhalb der minimalen Hemmkonzentration für mindestens 3.23 h erreichte eine Überlebensrate von 95%. So reduzierte MPLA die benötigte Zeit von Amoxicillinkonzentration

oberhalb der minimalen Hemmkonzentration um 1.23 h. Zudem konnte in der Kombinationstherapie bei einer Amoxicillindosis von 1.2 mg/kg das Überleben nach 14 Tagen im Vergleich zur Monotherapie um das 1.35-fache auf 90.3% gesteigert werden. Um den potenziellen Nutzen dieses therapeutischen Ansatzes in einem klinischen Umfeld zu untersuchen, wurden wichtige Schritte in Richtung einer Übertragung auf den Menschen unternommen. Während eine adäquate und plausible Übertragung der Pharmakokinetik von Amoxicillin möglich war, konnte die angeborene Immunantwort nicht vollständig charakterisiert werden und war dementsprechend nicht übertragbar. Dennoch konnten wertvolle Erkenntnisse über die Wechselwirkungen zwischen Bakterien, den Arzneistoffen und dem Wirt gewonnen und kritische Aspekte, die eine Übertragung behindern, identifiziert werden.

Zusammenfassend lässt sich festhalten, dass die Anwendung pharmakometrischer Ansätze das Verständnis der Pathophysiologie der Infektion verbesserte und eine Verbindung zwischen Pharmakokinetik und Pharmakodynamik ermöglichte. Die charakterisierte Stärkung des Immunsystems und die verbesserte antibakterielle Wirksamkeit zeigten deutlich das Potenzial immunstimulierender Arzneistoffe, in Zukunft als Kombinationspartner von Antibiotika zur Behandlung bakterieller Infektionen beim Menschen zu fungieren.

Acknowledgements

I would like to use the opportunity to express my gratitude to all of my companions, who have supported me scientifically, morally and financially over the last 3.5 years as doctoral student at the Department of Clinical Pharmacy and Biochemistry at the Institute of Pharmacy of the Freie Universitaet Berlin:

In particular, I would like to sincerely thank my supervisor *Professor Charlotte Kloft* to provide an opportunity to perform my doctoral research in such a fabulous environment. Thank you for the multiple inspiring discussions, your enthusiasm, your ideas and our common process of learning about the characteristic features of mice. I always appreciated your valuable feedback and advice, and the possibility to fully evolve within the project.

Professor Sebastian Wicha, I would also like to express my sincere gratitude to you. Thank you for offering a second working environment to me in Hamburg and having answers to my questions, your encouragement and constant interest, your excellent input and our regular and vivid discussions about how to further improve the work.

My gratitude to the *Joint Programming Initiative of Antimicrobial Resistance* for creating the ABIMMUNE project, addressing the relevance of the present topic and allowing me to work in an international collaboration financed by the *Bundesministerium für Bildung und Forschung*.

Within this consortium, I would like to particularly thank "*Team Lille*", namely *Jean-Claude Sirard* and *Fiordiligie Casilag*, for an excellent collaboration and for providing an amazing preclinical database. Thank you for giving us insights into your preclinical experiments, for your enthusiasm in discussing the recent findings and for your patience and willingness to help in answering our multiple questions about the specifications of your experiments.

Thanks to the Graduate Research Training Programme *PharMetrX*, namely Prof. Charlotte Kloft and Prof. Wilhelm Huisinga, for giving me, as Training+ student, the opportunity to be part of the module curriculum and regular meetings. The scientific insights provided an environment facilitating me the first steps into the field of pharmacometrics and the friendly and familiar atmosphere supported the interdisciplinary exchange.

Thank you*, Dr. Robin Michelet*, for your interest in the project, our fruitful discussions and your support in finalising the work. I appreciated your extensive knowledge and ideas promoting the progress of the project.

Thank you, *Tania Fuhrmann-Selter*, for your valuable daily support – not only by preparing the practical biochemistry courses but also in the lab. Your impressive ability to give a hand in preparing samples or performing microbiological experiments and our common discussions about the multiple bioanalytical challenges simplified daily work and were a great pleasure.

Thank you, *Dr. Jan Joseph* and PharmaMS, for your valuable helping hands in setting up the instruments and your support in the development of the bioanalytical method.

Thank you, *Dr. Ingo Siebenbrodt*, for the smooth organisation of any teaching-related activities in the practical courses and seminars.

Thanks to all present and former colleagues and friends in the working groups in Berlin and Hamburg who accompanied me on the way: Lunchbreaks, Lidl or canteen walks, conferences, evening activities, fun, laughs, creative atmosphere, scientific exchange, mutual support, dinners, drinks – a great time, socially and scientifically!

Thank you, *Johanna S.*, for our several discussions and the great ideas that evolved and being there any time by just opening the door next to me. Your enthusiasm for teaching and research motivated and inspired me.

Thank you, *Astrid*, for your endless support in developing the *in silico* models. As partners in thesis writing, our mutual support motivated me in finalising the thesis.

Thank you, *in vitro* team: *Eva* for introducing me into the AK as my mentor and the *in vitro* infection environment; *Josi* for our joint discussions about the MS and *Luis*, *Lisa A.* and *Christine* for all the fun we shared! And thank you, *in silico* experts *Franzi*, *Khalid*, *Ana-Marija*, *David B.*, *David U., Ferdi*, *Francis*, *Iris*, *Lisa E.*, *Anna*, *Andrea*, *Johanna M.* and *Viki* for all your input and reviewing activities in any *in silico*-related questions.

For reviewing parts of the present thesis, a big applause for: *Astrid* and *Johanna*, *Luis*, *Josi*, *Ferdi*, *David B.*, *Francis*, *Alix* and *Anneke*! Thank you all for your valuable input.

To my *family* for their endless support and being there for me: Thank you all for making this possible. To my "non-scientific" *friends*, thank you, for the distraction from the scientific work. And finally, thank you, *Janina*, for your patience, support and understanding and recalling parts of life being more important than work.

Table of contents

Abbreviations

ACN	Acetonitrile
AIC	Akaike information criterion
AMPK	Adenosine monophosphate-activated protein kinase
AMX	Amoxicillin
ANOVA	Analysis of variance
Ara4N	4-amino-4-deoxy-L-arabinose
ATCC	American Type Culture Collection
ATP	Adenosine triphosphate
AUC	Area under the concentration-time curve
AUC_{AMX}	AUC of orally-administered AMX
AUC/MIC	AUC divided by MIC
BAL	Bronchoalveolar lavage
Balb/cJ	Inbred Balb/cJRj mouse strain
BLQ	Below the LLOQ
BSV	Between-subject variability
BW	Body weight
CAL	Calibrator
CAMHB	Cation-adjusted Mueller-Hinton broth
cAMP	Cyclic adenosine monophosphate
CCL2	C-C chemokine ligand 2
CCL20	C-C chemokine ligand 20
CD8	Cluster of differentiation 8
C_e	Apparent drug concentration in effect compartment
$C_{e,\ lung}$	AMX concentration in the lung effect compartment
$C_{e,\ spleen}$	AMX concentration in the spleen effect compartment
CFU	Colony forming unit(s)
CI	Confidence interval
CL	Clearance
CL_{AMX}	Clearance of AMX monotherapy without monophosphoryl lipid A interaction
CLSI	Clinical and Laboratory Standards Institute
$C_{lung,\ time}$	Bacterial number in the lung at a certain time point
C_{max}	Maximal concentration in serum

$C_{max, lung}$	Maximal concentration in lung
C_{max}/MIC	C_{max} divided by MIC
$C_{max, spleen}$	Maximal concentration in spleen
C_p	Drug concentration in serum
$C_{spleen, time}$	Bacterial number in the spleen at a certain time point
cumhaz	Cumulative hazard
CV	Coefficient of variation
CXCL2	C-X-C chemokine ligand 2
df	Degree of freedom
DMSO	Dimethylsulfoxide
EC_{50}	Drug concentration to achieve half of the maximum killing effect
EGA	Exploratory graphical analysis
ELISA	Enzyme-linked immunosorbent assay
EMA	European Medicines Agency
E_{max}	Maximum killing effect
ESA	Exploratory statistical analysis
ESI	Electrospray ionisation
EtOH	Ethanol
EUCAST	European Committee on Antimicrobial Susceptibility Testing
f	Free, unbound
FBS	Foetal bovine serum
FC	Code of experiment performed by Fiordiligie Casilag
$FC_{AMX+MPLA}$	Fractional change of CL_{AMX} in presence of MPLA depending on the AMX dose
FKBP5	FK506 binding protein 5
FO	First-order estimation
FOCE	First-order conditional estimation
FOCE+I	First-order conditional estimation with interaction
G6P	Glucose-6-phosphate
Gal	D-galactose
GalNAc	N-acetyl-D-galactosamine
GC	Growth control
Glc	D-glucose
GlcNAc	N-acetyl-D-glucosamine

GM-CSF	Granulocyte macrophage colony-stimulating factor
GOF	Goodness-of-fit
H	Hill factor
Hep	L-glycero-D-manno-heptose
H_{lung}	Hill factor of AMX in lung
HPLC	High performance liquid chromatography
H_{spleen}	Hill factor of AMX in spleen
h(t)	Hazard distribution function
I	Susceptible at increased exposure
ICH	International Conference for Harmonisation
IIV	Interindividual variability
IL-X	Interleukin-X (e.g. IL-6: Interleukin-6)
IOV	Interoccasion variability
IQR	Interquartile range
ITGB2L	Integrin beta chain-2
JPIAMR	Joint Programming Initiative on Antimicrobial Resistance
k_a	First-order absorption rate constant
k_{AMX}	First-order killing rate constant of AMX in spleen
Kdo	3-deoxy-D-manno-oct-2-ulosonic acid
k_{e0}	First-order rate constant for drug transfer to effect compartment
$k_{e0,\ lung}$	First-order killing rate constant for effect delay in lung
$k_{e0,\ spleen}$	First-order killing rate constant for effect delay in spleen
k_g	First-order growth rate constant in lung
$k_{kill,\ lung}$	First-order killing rate constant for treatment-unrelated killing in lung
$k_{kill,\ spleen}$	First-order killing rate constant for treatment-unrelated killing in spleen
k_{lag}	First-order rate constant for delay in onset of bacterial growth in lung
$k_{MPLA,\ spleen}$	First-order rate constant for killing effect of MPLA in spleen
k_{net}	First-order rate constant for net bacterial growth
k_{tr}	First-order transit rate constant
LC-MS/MS	Liquid chromatography-tandem mass spectrometry
LHB	Lysed horse blood
LLOQ	Lower limit of quantification
LLP	Log-likelihood profiling

LOD	Limit of detection
log	Natural logarithm
log10	Decadic logarithm
LPS	Lipopolysaccharides
LRT	Likelihood-ratio test
LTRI	Lower respiratory tract infection(s)
McF	McFarland turbidity standard
MDR	Multi-drug resistance
MeOH	Methanol
MGT	Mean generation time
MHB	Mueller-Hinton broth
MIC	Minimal inhibitory concentration
MMP8	Matrix metalloproteinase-8
MPI	Max Planck Institute
MPLA	Monophosphoryl lipid A
mRNA	Messenger ribonucleic acid
MRSA	Methicillin-resistant *Staphylococcus aureus*
MS	Mass spectrometry
MTT	Mean transition time
MyD88	Myeloid differentiation factor 88
m/z	Mass-to-charge ratio
n	Number
NaCl	Sodium chloride
$N_{bacteria,\ lung}$	Number of bacteria in lung
$N_{bacteria,\ spleen}$	Number of bacteria in spleen
$N_{bacteria,\ t=0}$	Initial number of bacteria in spleen
NC3Rs	National Centre for the Replacement, Refinement and Reduction of Animal Research
NEG-	Negative control of not-stimulated supernatant
NEG+	Negative control of not-stimulated supernatant with addition of MPLA
NF-κB	Nuclear factor κ of activated B-cells
NGP	Neuronal guidance protein
NMLE	Nonlinear mixed-effects
OAT	Organic anion transporters

ODE	Ordinary differential equation
OFV	Objective function value
PAO1	*Pseudomonas aeruginosa* ATCC 15692
PBS	Phosphate buffered saline
pcVPC	Prediction-corrected VPC
PD	Pharmacodynamic(s)
$PD_{CFU/lung}$	PD in terms of number of bacteria of SP1 in lung
$PD_{CFU/spleen}$	PD in terms of number of bacteria of SP1 in spleen
$PD_{survival}$	PD in terms of survival
pdf(t)	Probability density function
PK	Pharmacokinetic(s)
PK_{AMX}	PK in terms of AMX concentrations
PPARγ	Peroxisome proliferator-activated receptor γ
PPB	Plasma protein binding
$PRED_{bin}$	Population prediction of a bin
$PRED_{ij}$	Population prediction of the i^{th} individual at the j^{th} observation
PROK2	Prokineticin 2
Pr(t)	Probability function
PT	Peak time
Q	Intercompartmental clearance between central and peripheral compartment
QC	Quality control
qXXh	Drug administration every XX hours (e.g. q12h: every 12 h)
R	Resistant
R^2	Coefficient of determination
RPMI1640	Roswell Park Memorial Institute 1640
RSE	Relative standard error
RSS	Residual sum of squares
RT-PCR	Reverse transcriptase polymerase chain reaction
RUV	Residual unexplained variability
S	Susceptible at standard dosing regimen
S100A9	S100 calcium-binding protein A9
SA	Surge amplitude
SC	Sterility control

SE	Standard error
SP1	*Streptococcus pneumoniae* serotype 1
S(t)	Survival function
STIM	MPLA-stimulated supernatant
SW	Surge width at half maximum intensity
Swiss	Outbred RjOrl:Swiss (CD-1) mouse strain
$T_{>EC50}$	Time period of total drug concentrations exceeding the EC_{50}
t_{lag}	Lag time
TLR4	Toll-like receptor 4
t_{max}	Time of C_{max}
$T_{>MIC}$	Time period of total antibiotic concentrations exceeding the MIC
TNFα	Tumour necrosis factor α
TRIF	Toll-interleukin-1 receptor-domain-containing adapter-inducing interferon-β
TTE	Time-to-event
ULOQ	Upper limit of quantification
UP	Ultra-pure
V	Volume of distribution
V_c	Volume of distribution of central compartment
V_p	Volume of distribution of peripheral compartment
VPC	Visual predictive check
WHO	World Health Organization
x_{ij}	Independent variable of the i^{th} individual at the j^{th} observation
Y_{ij}	Vector of the dependent variable for the i^{th} individual at the j^{th} observation
ZTBT16	Zinc finger and BTB region containing-16

Symbols

α	Significance level
β	Exponential rate constant of the Gompertz distribution function
β_i	Extent of covariate effect of a covariate i
γ	Shape parameter
Δ	Difference
$\varepsilon_{add,\,ij}$	Additive ε_{ij}
$\varepsilon_{exp,\,ij}$	Exponential ε_{ij}
ε_{ij}	RUV parameter value for the i^{th} individual at the j^{th} observation
$\varepsilon_{prop,\,ij}$	Proportional ε_{ij}
η_{ik}	IIV for the i^{th} individual at the k^{th} parameter
Θ	Vector of fixed-effects parameters
θ_{ik}	Typical value of the k^{th} parameter and the i^{th} individual
θ_k	Typical value of the k^{th} parameter
λ_0	Baseline hazard
L_i	Likelihood of the i^{th} individual of a certain observation
LL	Twice the negative natural logarithm of the likelihood function
ρ	Correlation coefficient
σ^2	Variance
χ_2	Chi-squared distribution
Ω	Omega matrix, variance-covariance matrix
$\omega^2_{1,1}$	Diagonal element of the first element of the omega matrix
$\omega_{1,2}$	Off-diagonal element of the first and second element of the omega matrix
ω^2_k	Variance of the typical value of the k^{th} parameter

1 Introduction

1.1 Current challenges of anti-infective therapy

The rational use of our armoury of anti-infective drugs provides the basis for a successful treatment of bacterial infections. Unfortunately, the emergence of bacterial resistance challenges this common understanding. Hence, rapid solutions to tackle resistant bacteria are vital.

Almost no effective therapeutic options were present in case of bacterial infections, until antibacterial agents were introduced in the early 1930s starting with the accidental discovery of penicillin by Alexander Fleming in 1928. The beginning of a successful treatment of such infections was enabled and revolutionised society and economy. Subsequently, antibiotic therapy was optimised with development of new antibiotic classes and by targeting specific pathogens, and consequently applied throughout the world with highest efficacy. Until today, the use of antibiotics is still well appreciated to overcome a bacterial infection. Nevertheless, major challenges go along with the use of antibiotics. Nowadays, treatment is often associated with low effectiveness or failure due to resistant bacterial strains. Several reasons for the emergence of bacterial resistance are discussed: Excessive and inappropriate usage of antibiotics in humans [1], spread of resistant bacteria in a global environment, unconsidered veterinary use [2] or insufficient awareness of this challenge [3]. For this purpose, an appropriate dosing of an appropriate antibiotic drug at the right time with accompanying adherence is essential aiming at the right exposure at target site for a known pathogen [4].

Still, the increasing pace in emergence of infections with resistant bacteria threatens human health and leads to pathogens that are even resistant to more than one antibiotic class [5]. In addition, almost no newly developed antibiotics are entering the market [6]. Among other reasons, high costs with limited profit margins in combination with a high effort to establish and a long time period to launch a new drug not only cause the lack of new antibiotics, but also lead to the shutdown of several industrial research units. Hence, a shift to usage of ultimo-ratio antibiotics is recognisable and, ultimately, may lead to a return to a pre-antibiotic era in case that the increasingly challenging task is not tackled [7].

In this context, lower respiratory tract infections (LRTI), defined as infections affecting trachea, bronchial tubes and alveoli of the lung, are currently the leading infectious cause of death in the world with 2.38 millions of death in 2016 [8]. Pneumonia as one possible form of LRTI is most often reported. In general, LRTI caused 4.40% of all death and was listed in the top 10 of global causes of mortality in 2016. In particular, children below the age of 5 years were mostly affected by those infections. In addition, approximately 336 million people were infected with a bacterial strain causing LRTI. Hence, LRTI are mainly addressed by the alarming trend in emergence of bacterial resistance and treatment failure, and it is urgently required to reveal alternative treatment options.

1.2 Key pathogens of pneumonia

As introduced, LRTI have a key role in the area of infectious diseases. These infections are caused by multiple pathogenic bacteria over a broad spectrum. Clinically most relevant bacterial species causing LTRI are *Klebsiella pneumoniae*, *Pseudomonas aeruginosa*, *Staphylococcus aureus* and *Streptococcus pneumoniae*. All of those potentially display the emergence of different resistance mechanisms against various antibiotic drugs and point at the need to develop treatment options that can be implemented fast into a clinical setting compared to development of completely novel drugs.

S. pneumoniae is a Gram-positive bacterial species contributing more to bacterial pneumonia than all other aetiologies together with increasing resistance rates [8]. The species is classified into 90 serotypes depending on the immunochemistry of their capsular polysaccharides. Here, *S. pneumoniae* serotype 1 is one of the most prevalent serotypes associated with complicated pneumonia [9]. Most bacterial strains of *S. pneumoniae* are susceptible to beta-lactamase-labile beta-lactams as amoxicillin (AMX). However, the bacterial resistance of *S. pneumoniae* to beta-lactams has emerged rapidly over the last years [10,11]. *S. pneumoniae* is characterised as an extremely fastidious organism being alpha-haemolytic, building diplococci and producing hydrogen peroxide contributing to virulence and affecting other microorganisms [12]. Another Gram-positive microorganism being able to cause LRTI and occurring as cocci is *S. aureus*. Due to expression of beta-lactamases, most bacterial strains of *S. aureus* are resistant against beta-lactamase labile drugs [13]. A difficult to treat strain of the species *S. aureus* is the methicillin-resistant *S. aureus* (MRSA) that is resistant to most antibiotics.

Two Gram-negative bacteria being a potential cause of LRTI are *K. pneumoniae* and *P. aeruginosa*. *K. pneumoniae* is a rod-shaped microorganism of the group of *Enterobacteriaceae* and among LRTI and other infections especially responsible for urinary tract infections. The strain is characterised by growing fast and rampant on agar plates occurring as mucous structures due to a strong expressed capsule [14]. Here, the emergence of multi-drug resistance (MDR) by e.g. producing carbapenemases is an enormous challenge [15]. *P. aeruginosa* is a non-fastidious, rod-shaped microorganism producing a characteristic blue-green pigment and being capable of forming biofilms. Similar to *K. pneumoniae*, emergence of MDR is a common challenge in treating such infections [16].

All of these bacterial species with their concomitant reported resistance mechanisms are reported as priority pathogens in the global priority list by the World Health Organization (WHO, [17]) with increased scientific, political and public awareness.

1.3 Novel treatment options to tackle the emergence of resistance

To fight the emergence of bacterial resistance, the beforehand mentioned challenges have to be tackled and research has to be prioritised on potential solution pathways. Hence, it is urgently required to investigate novel treatment options that are accessible rapidly to support anti-infective therapy.

Here, several approaches are discussed: At the moment, last resort antibiotics or combinations of several antibiotics are used in case of severe infections to overcome the challenge of resistance. Recent research activities have focussed on identifying antibiotics exerting synergistic effects. A combination of two or more already licensed drugs is a cost- and time-efficient solution. Next to combining antibiotics, a combination of an antibiotic drug with non-bacterial targeted drugs, showing adjuvant effects with antibiotics, is a potential option [18]. These antibiotics can either be well-established drugs, or, alternatively, neglected and disused antibiotics. The latter mentioned strategy aims to repurpose those antibiotics that had not been used for several years. Here, it is hypothesised that resistance mechanisms are less widespread in contrast to commonly used drugs and activity against MDR bacteria is still given [19]. Potential combination partners of such antibiotics are e.g. antibodies, probiotics, bacteriophages or antimicrobial peptides [18]. Other possible combination partners in this therapeutic concept are immunostimulatory drugs. Stimulating the innate immune response is hypothesised to support the antibiotic drug effect and ultimately physiological reaction to overcome an infection [20].

The non-conventional combination regimen of antibiotic drugs and a simultaneous stimulation of the innate immune response may contribute to develop non-traditional approaches for treatment of LRTI and to address the urgency of the current situation. The rationale of such combinations aims at saving the effectiveness of the antibiotics, reducing the emergence of resistance, avoiding the use of last-resort antibiotics and, ultimately, preventing the return to a pre-antibiotic era.

1.3.1 Key antibiotics

Key antibiotics can either be newly developed, well-established or neglected and disused. The lack of new entities entering the market limits the usage of newly-developed drugs. Furthermore, an immediate broad usage of newly-developed antibiotics provokes the development of new resistance mechanisms and could restrain the sustainability of these drugs. In case of well-established drugs, emergence of resistance is increasing. Hence, sustaining the drug's effectiveness is crucial. Certain disused and neglected antibiotics still represent important weapons to fight bacteria due to low resistance rates. Still, there are several reasons for their neglected usage for each of the drugs over the last decades, such as more efficient drugs, substantial adverse events or improved formulations of other drugs increasing the adherence of the patient [21]. In addition, only limited knowledge about certain drug characteristics is available from time decades ago necessitating an entire characterisation of physicochemical and pharmacokinetic (PK) properties allowing to reduce the dose accompanied by reduced toxicity. For that purpose, it is important to ensure that their re-use is carried out rationally and efficacy and safety are proven.

The antibiotic drugs colistin, fosfomycin and streptomycin are representative agents of disused and neglected antibiotics and will briefly be introduced in context of this thesis regarding their activity spectrum, mechanism of action, special characteristics and specific requirements of *in vitro*

investigations. In addition, the antibiotic AMX will be outlined. Despite not belonging to the disused and neglected antibiotics, AMX was included as standard of care for LRTI. Being classified as essential medicine by the WHO [22], its effectiveness must be sustained and the emergence and spread of bacterial resistance must be avoided.

Amoxicillin. AMX is a well-established and characterised beta-lactam antibiotic being discovered 1972 and showing a favourable safety profile with negligible reported adverse reactions, such as allergic reactions or candidiasis [23]. It is a semi-synthetic compound with relatively polar and hydrophilic characteristics (Figure 1.1) leading to poor, but still sufficient solubility in water [24] with high reported permeability indicating belonging to class I of the biopharmaceutics classification system for low AMX doses [25].

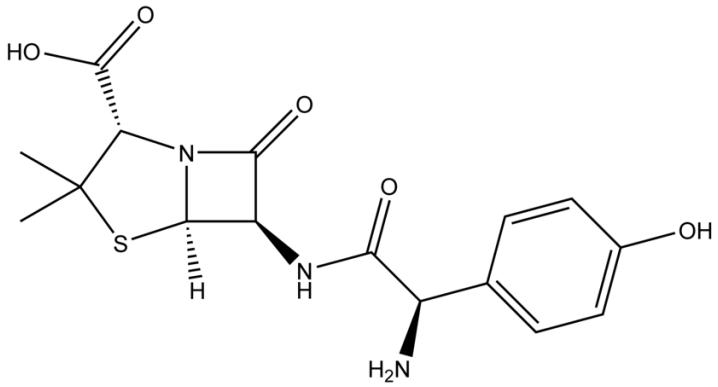

Figure 1.1: Chemical structure of amoxicillin.

Next to several other bacterial infections, AMX has been widely used in the clinics for respiratory tract infections mainly caused by *S. pneumoniae* in the last decades due to its high effectiveness. As beta-lactam antibiotic, AMX interacts with the cell-wall synthesis of a broad spectrum of Gram-negative and -positive bacteria by inhibiting the cross-linkage between peptidoglycan polymer chains [26]. The broad clinical usage of AMX already led to the emergence of resistance against several bacterial species of the genus Klebsiella and Pseudomonas. Even Staphylococci and Streptococci have shown increasing resistance rates [27]. Possible resistance mechanisms include a reduced affinity to penicillin-binding proteins, a reduced penetration into bacteria or efflux pumps [23,28]. To overcome the most reported resistance mechanism of inactivation of AMX via beta-lactamases, the drug is often combined with the beta-lactamase inhibitor clavulanic acid to prevent this degradation. Due to its mechanism of action, AMX is typically classified as an antibiotic with time-dependent effects, i.e. the effect is best described by the percentage of time within a dosing interval, in which drug concentrations exceed the minimal inhibitory concentration (MIC), typically assessed in serum [29]. With maximum total daily doses of 3 g, AMX is commonly administered orally or intravenously maximum six times daily depending on the kind and site of the infection, as well as patient characteristics, such as age, body weight and renal function.

The drug exhibits low plasma protein binding (PPB) with 17% and is preferentially eliminated unmetabolised by renal excretion with 60% and 75% of an orally or intravenously administered dose, respectively [26]. Another elimination pathway is a possible metabolic conversion leading to two major metabolites without any antibacterial activity [30]. Maximum serum concentrations (C_{max}) range from 2.72 to 14.0 mg/L with C_{max} occurring between 0.9 and 1.2 h after oral administration of a single 500 mg dose [23,28,31-34].

Colistin. Colistin, also termed polymyxin E, is a polymyxin antibiotic and was discovered in the late forties of the last century. Because of its reported nephrotoxicity and neurotoxicity leading to a narrow therapeutic window, colistin has been used very sparsely for the last decades [35]. However, recent studies report colistin to be less toxic as expected, highly effective and few bacterial strains expressing colistin resistance, which may allow usage for treatment of pneumonia [36]. Colistin is a mixture of different cyclic polypeptides, mainly colistin A and B, that exist as sulphate salts used orally to treat gastrointestinal infections or as methanesulphonate salts being activated *in vivo* by hydrolysation and used parenterally [37]. After reaching C_{max} with concentrations between 3.60 and 13.2 mg/L at an intravenous infusion of 160 mg colistin methanesulphonate over 15-60 min, parenterally administered colistin is eliminated renally by tubular secretion [38,39]. After association with the bacterial membrane of Gram-negative bacteria by binding to anionic lipopolysaccharides (LPS) and electrostatic interaction, a rearrangement of the cell membrane occurs: Magnesium and calcium are displaced and membrane permeability is increased [36,40]. Colistin is highly active against selected Gram-negative bacteria including *K. pneumoniae* and *P. aeruginosa* and used as last-resort antibiotic for MDR bacteria [40]. Resistance can occur due to various mutations and phenotypical adaptation processes, including downregulation of LPS production and expression of degrading enzymes or efflux transporters [36]. Still, due to its neglected use in the last decades, only a few organisms are resistant against colistin [41].

Fosfomycin. Discovered in 1969 and produced by Streptomyces species, fosfomycin is generally well-tolerated and active against a wide range of bacterial strains including various MDR bacteria. Whereas orally administered fosfomycin is globally utilised for the treatment of urinary tract infections, an intravenous formulation is only licensed in Europe [42]. Due to reluctant global use of fosfomycin, emergence of resistance has been restrained [43]. Nevertheless, a high percentage of resistant strains of *K. pneumoniae* and *P. aeruginosa* has been reported [44,45]. Fosfomycin interacts with the formation of bacterial peptidoglycan structures and, hence, inhibits biosynthesis of bacterial cell wall components resulting in cell lysis and bacterial death [46]. For fosfomycin uptake into the bacterial cell, transport mechanisms, mainly glycerol-3-phosphate and the hexose phosphate transporters, are involved, whose expression is increased by glucose-6-phosphate (G6P). Additionally, immunostimulatory effects, such as suppression of interleukin-2 (IL-2) production or modulation of cytokine production, have been reported [44]. Both, time-dependent [44] and concentration-dependent [47] effects have been described mainly depending on the targeted microorganism [48]. To obtain sufficient plasma concentrations,

intravenous dosing regimens propose administration of 3 to 4 g fosfomycin three times daily as short-term infusion up to maximum daily doses of 20 g for life threatening infections [44,49,50]. Fosfomycin is excreted unchanged by glomerular filtration without being metabolised [36] after reaching C_{max} values in plasma after intravenous administration of 3 g with concentrations ranging between 22.0 and 23.0 mg/L [51].

Streptomycin. Streptomycin is an aminoglycoside antibiotic derived from different Streptomyces species. First isolated in 1943, streptomycin was widely used after its discovery. Due to a high rate of reported resistances and dose-limiting adverse drug effects, such as ototoxicity and nephrotoxicity, streptomycin is used sparsely today. Optimised instead of standard dosing regimens propose reduced toxicity and enable a repurposed use of streptomycin [52]. Streptomycin is only administered parenterally with a C_{max} value of approximately 43.6 mg/L at a dose of 800 mg and eliminated by glomerular filtration without being metabolised hepatically [53]. After binding the 30S subunit of bacterial ribosomal structures, streptomycin interferes with protein synthesis of bacteria by inhibiting formation of an initiation complex during translation. Streptomycin is concentration-dependent active against Gram-negative and -positive bacteria. However, bacterial resistance exists, and streptomycin is only used in combination as last resort antibiotic [54].

1.3.2 Key immunostimulatory drugs

A physiological immune response is a prerequisite for successful antibiotic therapy. Here, the human immune system acts as a powerful and extraordinary helpful instrument to overcome infections. Usually, a contact with potentially harmful microorganisms is not realised by a human, as long as the immune system is fully functional. Even if replicating bacteria are leading to an infection by the microorganism, the immune system can typically handle these infections. Nevertheless, in cases of immuno-compromised or -deficient or critically-ill patients due to concomitant diseases, the immune system may not be able to tackle the infection alone and administration of an antibiotic may be necessary. Here, a host-directed stimulation of the immune system might be appropriate to enhance the therapeutic benefit. In case of administering immunostimulatory drugs, it is essential to reflect on risk factors of stimulating the immune system in case of an infection and consider, whether it might rather help or harm the individual in the specific situation.

By supporting the immune system in manifold processes involved, the antimicrobial effect against the microorganism is increased and the body is assisted to deal with the infection. This antibacterial effect of immunostimulatory drugs can be caused directly, i.e. by drug-mediated effects, or indirectly, i.e. by modulator-mediated effects from stimulated immune cells. Another benefit is that the host rather than the microorganism is targeted by the drugs and, hence, the pressure of antimicrobial resistance is avoided [55]. However, it is essential that an activation of the immune system always leads to an appropriate inflammation at the site of infection. A marked inflammation may involve tissue damage, weaken

especially critical-ill patients and limit the therapeutic benefit. Even an endotoxic shock is a possible reaction of the human body [55]. For this purpose, an important aim of an immune stimulation is to avoid a hyperactivation of the immune system.

Overall, the best option to support antimicrobial therapies in patients is a controlled stimulation of the immune system to enhance the antimicrobial activity and prevent inflammation [55]. In context of this thesis, metformin, monophosphoryl lipid A (MPLA) and pioglitazone have been investigated as potential candidates for combination with antibiotics due to their immunostimulatory activities.

Metformin. Metformin, a typically well-tolerated antidiabetic drug of the class of biguanides, currently is standard treatment of type 2 diabetes. The exact mechanism of metformin's pleiotropic actions is still not completely understood. Generally, the antidiabetic effect is caused by decreasing intestinal glucose absorption and hepatic gluconeogenesis, and by improving insulin sensitivity. One reported mechanism of action includes the inhibition of the mitochondrial complex I, causing a decline in adenosine triphosphate (ATP) production. Thus, the adenosine monophosphate-activated protein kinase (AMPK) is activated to initiate production of ATP leading to an increased uptake and usage of glucose and reduced gluconeogenesis [56]. In addition, metformin shows anti-inflammatory, immunostimulatory and antimicrobial effects. Various studies have reported a higher risk for respiratory tract infections in case of increased glucose concentrations in the airway surface liquid [57,58], that can be reduced by metformin. Furthermore, AMPK activation in cancer cells has been reported to lead to immunostimulatory effects by interacting with regulation of cluster of differentiation (CD) 8 T-cells [59,60]. The recommended oral dosing regimen of metformin is 500 to 1000 mg twice up to three times daily with a maximum of 3 g per day leading to C_{max} values ranging from 1.60 to maximum 5.00 mg/L [61-63]. Metformin is excreted unchanged and renally by glomerular filtration and tubular secretion.

Monophosphoryl lipid A. MPLA, a toll-like receptor 4 (TLR4) agonist with a favourable safety profile [64] and a LPS derivative, is licensed as adjuvant component with immunostimulatory properties for vaccines including Fendrix® (hepatitis B, [65]) or Cervarix® (human papilloma virus, [66]) and is produced by *Salmonella minnesota* R595. LPS as parent components and typically located in the cell membrane of Gram-negative bacteria are structured in three different parts (Figure 1.2). A core oligosaccharide is linking the glycolipid anchor lipid A, that has a heterogenic composition and differs in degree or type of fatty acids [67], and an O-specific polysaccharide [68].

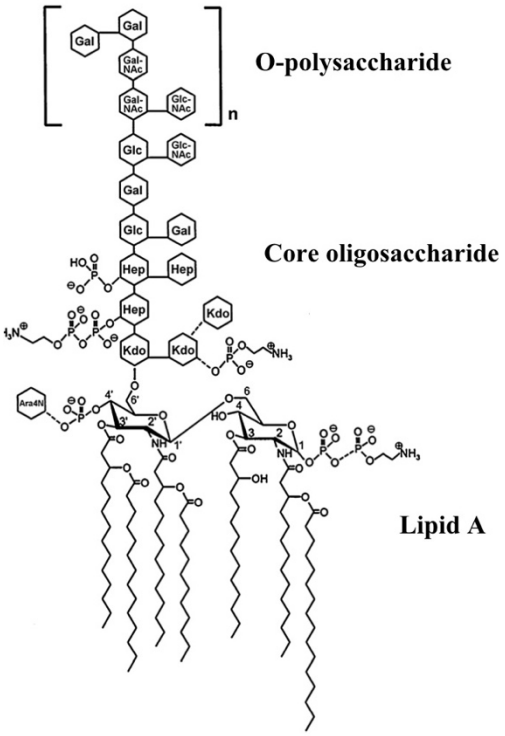

Figure 1.2: General structure of a lipopolysaccharide molecule from *Salmonella minnesota* (modified from Kilar et al. [68]). Abbreviations: Gal: D-galactose; GalNAc: N-acetyl-D-galactosamine; Glc: D-glucose; GlcNAc: N-acetyl-D-glucosamine; Hep: L-glycero-D-manno-heptose; Kdo: 3-deoxy-D-manno-oct-2-ulosonic acid; Ara4N: 4-amino-4-deoxy-L-arabinose. The fatty acids of bacterial lipid A may vary in number or composition in terms of length, saturation and hydroxylation.

LPS affect the human immune system by interacting using their lipid anchor lipid A with the TLR4 and myeloid differentiation protein 2 complex leading to TLR4 dimerisation and activation of downstream cascades. These are either depending on the adaptor protein myeloid differentiation factor 88 (MyD88) or toll-interleukin-1 receptor-domain-containing adapter-inducing interferon-β (TRIF, [69]). MyD88 activation induces the innate immune system to activate cytokine producing cells to generate proinflammatory cytokines, such as interleukin-6 (IL-6), tumour necrosis factor α (TNFα) or interleukin-8 (IL-8), via the nuclear factor κ of activated B-cells (NF-κB) pathways [70]. Via TRIF, a rather delayed production of type I interferons is initiated leading to effective host response [69]. An overstimulation of the immune system with the lipid A structure can cause inflammation, shock symptoms and its associated consequences [71,72]. MPLA is the monophosphorylated and water-soluble form of the lipid A structure of LPS. It is biased to activation of TRIF signalling being equipotent to LPS and only inducing MyD88 pathways to a lesser extent compared to LPS [73]. Thereby, production of proinflammatory cytokines is actively suppressed [74] leading to a substantially decreased toxicity being 100-10000-fold smaller [75]. Hence, MPLA displays less inflammatory activity with still immunostimulatory characteristics [72]. For that reason, MPLA is ideal for use as adjuvant in vaccines and can also serve as potential candidate for immunostimulatory therapy.

Pioglitazone. Pioglitazone is an oral antidiabetic drug of the class of thiazolidinediones being commonly used for treatment of type 2 diabetes. By stimulating the nuclear peroxisome proliferator-activated receptor γ (PPARγ), transcription of specific genes controlling glucose uptake is increased activating glucose uptake into a cell. Besides its antidiabetic effects, also immunostimulatory and anti-inflammatory effects are present. Numerous studies report PPARγ agonists to inhibit the release of inflammatory mediators in immune cells [76-79]. Furthermore, mitochondrial reactive oxygen species are produced enhancing the immune defence [80]. However, exact mechanisms are still unknown and it has to be considered that pioglitazone can also cause lung injuries and possibly worsen LRTI [81]. After absorption, pioglitazone is metabolised into various pharmacologically active metabolites by cytochrome P450 enzymes [82]. Pioglitazone is extensively bound to plasma proteins with a PPB of 99% and achieves C_{max} values of 1.33 to 1.37 mg/L at a time t_{max} of 2 to 4 h after oral administration of a single dose of 45 mg [83,84].

1.4 Pharmacokinetic/pharmacodynamic approaches in anti-infective therapy

To gain quantitative insights into potential new combination regimens and evaluate their effectiveness, it is mandatory to analyse PK and pharmacodynamic (PD) characteristics extensively aiming at elucidation of exposure-response relationships in a combined PK/PD analysis [85]. These characteristics can be initially studied *in vitro* or *in vivo* and, subsequently, further analysed *in silico*.

In vitro approaches are suitable screening methodologies mainly applied to assess the relationship between a drug and a microorganism at standardised conditions and being useful for designing subsequent *in vivo* investigations. These preclinical studies are usually performed in animals and commonly succeeded by clinical studies in humans. Considering infectious diseases and antibacterial drugs in particular, preclinical studies play a critical role in evaluation of these relationships [5]. Compared to *in vitro* investigations, animal models consider effects of the immune system, that are challenging to reproduce *in vitro*. Most widely, mice are used to investigate antibacterial PK/PD relationships and induce an infection, such as pneumonia [86]. Here, inbred and outbred mice can be differentiated. Whereas the latter ones are characterised by genetic heterogenicity with a competent immune system, inbred mice are genetically homologous and rather have constraints in their immune system [87]. Sampling techniques include among others retroorbital bleeding or less invasive sampling from the tail vein. Drug administration is either performed orally, intravenously or intraperitoneally.

By applying *in silico* approaches, *in vitro* and *in vivo* generated data can be analysed comprehensively. An efficient use of the data is enabled by employing mathematical models that are able to describe underlying processes using a small number of mathematical equations [88]. Existing data is descriptively characterised and, subsequently, enables model-based simulations for extrapolation into a predictive setting. Hence, a continuous and simultaneous evaluation of PK and PD is enabled and even a translation into a clinical setting is possible. Using these pharmacometric approaches, manifold

processes and modifications can be captured and interactions between host, drug and the microorganism can be described, quantified, explained and even used for prediction. Several approaches are available to assess PK and PD *in vitro*, *in vivo* and *in silico*, and will further be introduced.

1.4.1 Quantitative assessment of antibiotic pharmacokinetics

PK comprise studying concentrations of a drug and its metabolites over time in a quantitative manner by considering absorption, distribution, metabolism and elimination of a drug and, thereby, represent exposure. The PK characteristics depend on drug- and species-specific factors, including physicochemical properties, PPB or the administered dose and the health condition, body weight, sex or comparable patient characteristics, respectively. To adequately investigate PK, appropriate bioanalytical quantification methods in biological matrices are required.

Diverse techniques have been developed to determine drug concentrations in context of PK. Here, generating high quality PK data, e.g. accurate, precise and reproducible concentration measurements, is crucial for a reliable PK analysis. Basic information about certain PK characteristics, such as physicochemical properties, are evolved *in vitro* at standardised conditions. To assess a species-specific concentration-time profile of a drug, *in vivo* studies are performed. A certain matrix of a species of interest is sampled and processed appropriately. Commonly, serum is the matrix of choice. Nevertheless, an adequate antibiotic exposure at the site of the infection is a prerequisite for efficient antimicrobial treatment and drug concentrations may be influenced in case of high PPB of the drug.

A highly sensitive and specific method for quantification of drug concentrations is the combination of chromatography and mass spectrometry, particularly in terms of liquid chromatography-tandem mass spectrometry (LC-MS/MS [89]). Initially, the drug of interest is separated from matrix constituents chromatographically with suitable retention times depending among others on the utilised column, an appropriate eluent, pressure and temperature. Subsequently, quantification is accomplished by directing the separated drug to an ion source of a triple quadrupole mass detector measuring the mass-to-charge ratio (m/z) of charged particles. Nowadays, LC-MS/MS assays are preferred as bioanalytical methods compared to other techniques such as bioassays, fluorometric assays or the linkage of chromatographic and other spectrometric approaches due to higher sensitivity, specificity and precision [5].

Subsequently, concentration-time profiles are further analysed and accordingly evaluated by *in silico* approaches. Here, sources of variability between different individuals, within one individual or by the applied assay, trends within the study population and the influence of potential covariates can be assessed.

1.4.2 Determination of pharmacodynamic effects of antibiotics

PD comprise analysis of certain effects of a drug, preferentially representing the response. These drug effects can be expressed in multiple surrogate parameters, such as a reduction of blood pressure or pain,

depending on the affinity of a compound to its target, as well as patient-specific factors, such as genetic factors and several others. In case of bacterial infections, the PD effect can be expressed as the MIC, bacterial burden or survival.

In vitro studies mainly aim at assessing antimicrobial susceptibility often in terms of the MIC and categorise the antibiotic-pathogen relationship in a turbidity-based assay with visual evaluation at a single point in time. In clinics, susceptibility testing is commonly used for prediction of a therapeutic outcome [90]. The most appropriate and basic approach to determine the MIC value is the broth dilution method in a globally standardised and easily conductible procedure [91,92]. Growth of bacteria in a liquid growth medium with static antibiotic concentrations in twofold dilutions is assessed and the MIC is defined as the lowest drug concentration of an antimicrobial agent that inhibits visible growth of the microorganism [90]. The interplay of bacteria and antibiotics is implemented into a specific classification system, which is based on an *in vitro* response of a certain bacterial species to a drug at specific concentrations corresponding to plasma concentrations [91]. According to the European Committee on Antimicrobial Susceptibility Testing (EUCAST) and their reported breakpoint values, a bacterial strain is classified as (i) susceptible at standard dosing regimen with a high likelihood of therapeutic success (S), (ii) susceptible at increased exposure with a high likelihood of therapeutic success due to the increased exposure (I), and (iii) resistant with a high likelihood of therapeutic failure (R, [92]). Extending this approach from one to two simultaneously studied drugs allows to assess possible interactions of two drugs in static checkerboard investigations that could potentially be synergistic, antagonistic or additive [93]. Additional quantification of bacteria at the study endpoint enables gaining additional information in dynamic checkerboard studies. Continuously monitoring the time course of antibacterial effects of one or even more drugs in combination is studied in static time-kill curve experiments with constant drug concentrations over time. However, static conditions do not reflect the dynamic situation of changing drug concentrations over time in a target organ under *in vivo* conditions [94]. By mimicking an *in vivo* concentration-time profile in a dynamic time-kill curve setting, the PD effect of the mimicked PK profile on bacterial growth can be determined. Still, dynamic effects of the immune system are typically not considered in *in vitro* studies and limit the direct translation into a patient setting.

This limitation is considered by performing *in vivo* studies in animal models. Several additional PD parameters can be studied compared to an *in vitro* setting by incorporating the immune system: Evaluation of the bacterial burden at target-site, survival of infected mice or the extent of the stimulation of the immune system by determining e.g. cytokine concentrations is possible. In case of pneumonia, not only bacterial burden in lung, but also in spleen as surrogate for sepsis can be assessed.

Comparable to the evaluation of PK data, detailed information about *in vitro* and *in vivo* PD characteristics can be assessed in subsequent *in silico* analyses.

1.4.3 Exposure-response relationship of antibiotics

To describe the exposure-response relationship comprehensively in a PK/PD analysis and adequately define exposure and response, a relation between PK measures and PD measures is established [95]. Here, it is recommended to use the same *in vitro* and *in vivo* models for generation of PK and PD data favouring the simultaneous investigation of PK and PD [5]. In context of infectious diseases, the exposure-response relationship is determined by the interplay of the drug, the host and the microorganism. Here, the anti-infective drug is directly interacting with the microorganism. The host mainly affects the PK of the drug, while the PD is rather affected by the host's immune response to the infection [5]. However, evidence is given that already nonclinical infection models can predict difficult to assess PD related clinical outcomes without considering the targeted host in a first place [5]. Accounting easily accessible PK information in patients, the PK/PD relationship can be characterised.

Standardised PK/PD indices [96] allow to classify antibiotic drugs and are easily accessible based on PK measurements. PK measures include the area under the concentration-time curve (AUC), the C_{max} value of an dosing interval or the time period of total antibiotic concentrations exceeding the MIC ($T_{>MIC}$), all typically related to a PD measure of bacterial susceptibility in terms of the MIC [95]. In this context, it has to be considered that only the fraction of the drug not bound to plasma proteins is microbiologically active and, hence, the PK/PD indices are typically based on free concentrations indicated by the letter *f* (*f*$T_{>MIC}$, *f* C_{max}/MIC, *f*AUC/MIC [95]). In case of negligible PPB, a simplification to the indices $T_{>MIC}$, C_{max}/MIC, AUC/MIC is possible not considering the unbound fraction. Accordingly, an appropriate PK/PD index is determined in PK/PD studies for a certain drug. Commonly, these indices comprise a classification into so-called time- or concentration-dependent antibiotics. Here, the effects of time-dependent drugs, such as beta-lactams, is best described by $T_{>MIC}$, whereas the effect of concentration-dependent drugs, such as aminoglycosides, is described by the AUC/MIC or C_{max}/MIC ratio [95]. Reaching a certain PK/PD target, e.g. a minimum $T_{>MIC}$, highly increases the probability of a successful treatment. Yet, only the potency of the drug expressed as MIC is related to exposure without considering any additional information about the dynamics of an infection [97]. To accomplish this, a pharmacometric analysis studies the experimentally obtained results beyond a common descriptive analysis, allows to amalgamate information on PK and PD levels, to integrate multiple study data and to translate these results into a clinical setting. Several examples in a preclinical or clinical setting have shown the already mentioned advantages of this approach [5,97-105].

1.5 Objectives

The emergence of bacterial resistance and the resulting loss in effectiveness of antimicrobial drugs limit our treatment options for infectious diseases, such as pneumonia. This major threat requires the pursuit of novel strategies, one of which is combining antibiotics and immunostimulatory drugs. Here, mechanistic and quantitative insights of this innovative treatment option are lacking. Hence, within these

new therapeutic options, as key characteristics the PK and PD behaviour of established drugs needs to be studied systematically. For that purpose, the ABIMMUNE consortium was initiated in context of the Joint Programming Initiative on Antimicrobial Resistance (JPIAMR) to provide a platform, in which bacterial resistance is tackled jointly, and problem-solving approaches are addressed in a global research collaboration.

The objective of this thesis was to initially select potential combination partners *in vitro*, evaluate their PK/PD relationship preclinically, and define the efficacy of this combination regimen by applying pharmacometric approaches *in silico*. Amalgamating these *in vitro*, *in vivo* and *in silico* approaches should enhance the understanding of a potential interaction and motivate a translation into a clinical setting.

In the framework of the *in vitro* investigations, an appropriate choice of the antibiotic and immunostimulatory drugs and bacterial species was addressed as basis for subsequent *in vivo* investigations. Here, the characterisation of the bacterial strains in relation to the respective drugs and the differentiation of drug-mediated and modulator-mediated antibacterial effects of immunostimulatory drugs was mandatory in combination with current state-of-the-art knowledge.

Concretely, the following objectives were addressed consecutively within part I, the *in vitro* screening, to ultimately select an appropriate bacterial strain and an appropriate combination of antibiotic and immunostimulatory drugs. Here, basic research questions were addressed by using common microbiological methods. Based on first results, novel assays were to be developed and refined to assess modulator-mediated effects of the immune system *in vitro*.

- Characterisation of bacterial strains at standard conditions with respect to their specific growth and appropriate handling *in vitro* to generate optimal conditions for evaluation of drug-mediated effects.
- Characterisation of bacterial strains and antibiotic drugs in terms of MIC investigations to ensure investigation of susceptible bacterial strains.
- Determination of any drug-mediated effects of the immunostimulatory drugs in MIC investigations or in combination with antibiotics in static and dynamic checkerboard investigations to allow a subsequent differentiation from modulator-mediated effects.
- Characterisation of bacterial strains at modified growth conditions with respect to their specific growth over time to ensure appropriate growth and comparability to standard growth conditions.
- Determination of the bacterial susceptibility in terms of the MIC against antibiotic drugs in modified growth media to ensure a comparability of antibacterial effects.
- Assessment of drug-mediated and modulator-mediated effects alone as well as in combination with the antibiotic drugs in terms of static and dynamic checkerboards and time-kill curve analysis.

In part II, the *in vivo* analysis, the selected combination regimen shall systematically be investigated in a murine pneumonia model to allow assessment of the preclinical exposure-response relationship based on determined PK and PD parameters. Here, the results of part I as well as bioanalytical research questions were applied to comprehensively evaluate the selected combination.

- Development, validation and application of rapid and highly sensitive bioanalytical quantification methods to allow characterisation of the PK of the selected antibiotic and immunostimulatory drugs and allow evaluation of the exposure-response instead of the dose-response relationship.
- Comprehensive determination of the PD effects of the selected regimen over time in terms of bacterial burden at the site of infection and survival to fully characterise the disease progression in mice with characterisation of pneumonia and sepsis.
- Characterisation of the immune response of the murine innate immune system after infection and stimulation with the selected immunostimulatory drug to assess detailed information about the progression of the immune response.

In part III, the *in silico* analysis, the selected combination should be exploited and characterised with the use of PK/PD knowledge in an overarching pharmacometric analysis to ultimately allow a translation into a clinical setting. Based on part II, the pharmacometric analysis aimed to sequentially consider PK and PD in terms of bacterial burden and survival and to finally apply these results in a translational framework.

- Enabling a pharmacometric analysis of the generated PK data of the selected combination regimen to get quantitative insights into the PK characteristics and potential PK interactions.
- Extension of the PK submodel to a semi-mechanistic PK/PD model considering the bacterial burden in terms of pneumonia and sepsis to ensure a comprehensive characterisation of the exposure-response relationship.
- Establishing an additional link to generated survival data to predict survival based on easily accessible markers.
- Evaluating the interaction between the immune response and the antibiotic effect mechanistically to provide quantitative insights into the combination.
- Performance of translational PK/PD modelling to extrapolate results of the selected combination regimen into a clinical setting.

2 Materials and methods

2.1 Materials

2.1.1 Chemicals and drugs

Acetonitrile, HPLC-MS grade, various LOTs	Fisher Chemical, Thermo Fisher Scientific Inc., Schwerte, Germany
Amoxicillin trihydrate, LOT: LRAA8983	Carl Roth GmbH, Karlsruhe, Germany
Bacillol®-AF, various LOTs	Bode Chemie GmbH, Hamburg, Germany
Calcium chloride dihydrate, LOT: 233199810	Carl Roth GmbH, Karlsruhe, Germany
Colistin sulphate, LOT: LRAA4721	Carl Roth GmbH, Karlsruhe, Germany
Columbia agar (base), various LOTs	Carl Roth GmbH, Karlsruhe, Germany
DensiCheck™ calibration standard, LOT: 837532901	BioMérieux® Inc., Nuertingen, Germany
D-Glucose 6-phosphate sodium, LOT: SLBP5158V	Sigma Aldrich Chemie GmbH, München, Germany
Dimethylsulfoxide, LOT: 1210059-01	Euro OTC Pharma GmbH, Bönen, Germany
Foetal bovine serum, qualified, Brazil, LOT: 42G1360K	Gibco, Thermo Fisher Scientific Inc., Schwerte, Germany
Formic acid, LOT: J653454	VWR International, Darmstadt, Germany
Fosfomycin disodium salt, LOT: 125M4168V	Carl Roth GmbH, Karlsruhe, Germany
Lysed horse blood, LOT: 33449700	Oxoid Ltd., Thermo Fisher Scientific Inc., Basingstoke, United Kingdom
Magnesium chloride hexahydrate, LOT: 293198927	Carl Roth GmbH, Karlsruhe, Germany
Meliseptol®, various LOTs	B. Braun, Melsungen, Germany
Metformin hydrochloride, LOT: LRAA8975	Carl Roth GmbH, Karlsruhe, Germany

Methanol, LC-MS grade, LOT: 16Z0946	VWR International, Darmstadt, Germany
Milli-Q® water, purified by Milli-Q® Reference A+	Merck Millipore, Darmstadt, Germany
MPLA from S. minnesota R595 (Re) TLRpure™, sterile solution, LOT: A100613-100002	Innaxon, Tewkesbury, United Kingdom, provided by Institut Pasteur de Lille, Lille, France
Mueller Hinton broth, unadjusted cation content, various LOTs	Oxoid Deutschland GmbH, Thermo Fisher Scientific Inc., Wesel, Germany
Pioglitazone hydrochloride, LOT: LRAA5299	Carl Roth GmbH, Karlsruhe, Germany
Polysorbate 80, LOT: 12315303	Caesar & Loretz GmbH, Hilden, Germany
Pseudomonas agar (base), LOT: 1942333	Oxoid Deutschland GmbH, Thermo Fisher Scientific Inc., Wesel, Germany
RPMI1640 with GlutaMAX™, LOT: 1880320	Gibco, Thermo Fisher Scientific Inc., Schwerte, Germany
Sheep blood, various LOTs	Oxoid Ltd., Thermo Fisher Scientific Inc., Basingstoke, United Kingdom
Sodium chloride BioXtra, LOT: SLBQ5226V	Sigma Aldrich Chemie GmbH, München, Germany
Streptomycin sulphate, LOT: SLBQ3439V	Carl Roth GmbH, Karlsruhe, Germany
Ultra-pure water, purified by SG LaboStar™ 2-DI/UV	Evoqua Water Technologies, Eschborn, Germany

2.1.2 Bacterial strains

Klebsiella pneumoniae ATCC 43816	LGC Standards GmbH, Wesel, Germany
Pseudomonas aeruginosa ATCC 15691 (PAO1)	Centre d'Etude des Pathologies Respiratoires, Tours, France
Staphylococcus aureus ATCC 29213	Institute for Microbiology and Hygiene, Charité University Hospital Berlin, Germany
Staphylococcus aureus subspecies aureus strain Newman	Institut Pasteur de Lille, Lille, France
Streptococcus pneumoniae serotype 1 (clinical isolate E1586, SP1)	National Reference Laboratory, Ministry of Health, Uruguay

2.1.3 Consumables

BD Falcon™ round-bottom tube, (5 mL, polystyrene, sterile), various LOTs	VWR International, Darmstadt, Germany
Cannulas (various sizes), various LOTs	B. Braun, Melsungen, Germany
CellStar® tubes (50 mL, polypropylene, sterile), various LOTs	Greiner Bio-One GmbH, Frickenhausen, Germany
Centrifuge tubes (15 mL, polypropylene, sterile), various LOTs	ISOLAB Laborgeräte GmbH, Wertheim, Germany
InfinityLab Poroshell 120 Phenyl Hexyl column (RP, 2.1 × 100 mm, 2.7 µm), LOT: B15164	Agilent Technologies, Waldbronn, Germany
Mouse serum, LOT: BS15175.5	Bio&SELL GmbH, Feucht, Germany
Nunc 96-well plates (polypropylene, conical bottom)	Nunc, Thermo Fisher Scientific Inc., Roskilde, Denmark
Nunc 96-well plate cap mats, various LOTs	Thermo Fisher Scientific Inc., Roskilde, Denmark
Petri dishes (polystyrene, ∅ 90 mm, h 14.2 mm, Sterile, without vents), various LOTs	VWR International, Darmstadt, Germany
Pipette tips, various LOTs epT.I.P.S.® Standard (various sizes) Combitips advanced® 10 mL	Eppendorf AG, Hamburg, Germany
Roti®-Store cryo vials, LOT: 185228984	Carl Roth GmbH, Karlsruhe, Germany
Safe lock vials (0.5 mL, 1.5 mL), various LOTs	Eppendorf AG, Hamburg Germany
Syringe filter, Puradisc FP 30/0.2 CA-S (0.2 µm, sterile), various LOTs	GE Healthcare GmbH, Solingen, Germany
Syringe Injekt® Solo (various volumes, sterile), various LOTs	B. Braun, Melsungen, Germany
Tissue culture flasks 25 cm^2 (vented caps, sterile), various LOTs	TPP Techno Plastic Products AG, Trasadingen, Switzerland
Tissue culture plates (48 well, sterile), various LOTs	VWR International, Darmstadt, Germany

2.1.4 Laboratory devices and equipment

Agilent LC-MS/MS system 1290 Infinity II LC system Autosampler G7167B High speed pump G7120A Multicolumn thermostat G7116B Triple quadrupole system G6495A	Agilent Technologies, Waldbronn, Germany
Analytical balance, BP221S	Sartorius AG, Göttingen, Germany
Autoclave, Kronos B23	Newmed, Quattro Castella, Italy
Autoclave, Tuttnauer 2540EL	Tuttnauer, Jerusalem, Israel
Balance, Sartorius MC1 - Laboratory LC 2200P	Sartorius AG, Göttingen, Germany
Centrifuge, Eppendorf 5430R	Eppendorf AG, Hamburg, Germany
Centrifuge, Eppendorf 5417R	Eppendorf AG, Hamburg, Germany
Colony Counter, Handy type	N. Usui & CO. Ltd., Kobe, Japan
Colony Counter, ColonyQuant®	Schuett Biotec GmbH, Göttingen, Germany
Duran® glass bottles (Various sizes)	Schott AG, Mainz, Germany
Glass equipment (Measuring cylinders, funnels, beakers)	VWR International, Darmstadt, Germany
Incubator, GFL 3032	Gesellschaft für Labortechnik mbH, Burgwedel, Germany
Infrared loop steriliser, SteriMax®	WLD-TEC GmbH, Arenshausen, Germany
Inoculation loops	Carl Roth GmbH, Karlsruhe, Germany
Laminar air flow work bench, LaminAir® LB-48-C	Heraeus, Hanau, Germany
Magnetic stirrer with heating, RCT basic	IKA®-Werke GmbH, Staufen, Germany
Microplate shaker, PMS-1000i	Grant Instruments Ltd., Shepreth, United Kingdom
Pipettes, Eppendorf Research (0.01 to 5 mL), Eppendorf Multipette® M4	Eppendorf AG, Hamburg, Germany
Turbidity meter, DensiCheck®	BioMérieux, Nuertingen, Germany
Vortexer, REAX2000	Heidolph Instruments GmbH & CO. KG, Schwabach, Germany

2.1.5 Solutions and media

In general, it was aimed for standardised condition within and between different experiments. For this purpose, prepared solutions were handled in the same way throughout the whole thesis. To also ensure reproducibility between experiments that were performed within the ABIMMUNE collaboration (Chapters 2.2, 2.3 and 2.4), it was paid attention to use same products and batches. That was particularly important for the used batch of foetal bovine serum (FBS) that tends to differ between batches leading to critically different characteristics.

Drug stock solutions. Stock solutions of antibiotic and immunostimulatory drugs were prepared according to the Clinical and Laboratory Standards Institute (CLSI, [91]). To establish a standard procedure for preparation of stock solutions of different drugs or even different lots of the same drug considering the following aspects was mandatory: To target a specific drug concentration, a potency was calculated considering e.g. purity, salt fraction or water content given by the respective manufacturer. The potency was calculated as depicted in Equation 2.1.

$$Potency = assay\ purity \cdot active\ fraction \cdot (1 - water\ content) \quad (2.1)$$

An approximate amount of the drug powder was weighed using a calibrated analytical balance to obtain at least a volume of 10 mL of the aimed concentration of 1 mg/mL of the stock solution. Based on the potency of the drug and the exact weighed amount, the specific volume of the respective diluent needed for the final solution was calculated (Equation 2.2).

$$Volume\ (mL) = \frac{weight\ (mg) \cdot potency\ (\mu g/mg)}{concentration\ (\mu g/mL)} \quad (2.2)$$

Volumes of 1 mL were dispensed into safe lock vials, stored at -80 °C and thawed as needed for preparation of secondary stock solutions or working solutions. Before being used for antimicrobial experiments (Chapter 2.2), thawed and mixed aqueous stock solutions were sterilised by membrane filtration with a cellulose acetate syringe filter with a pore size of 0.2 µm. Stock solutions with organic solvents (Chapter 2.2.2.1), such as dimethylsulfoxide (DMSO), were considered to be self-sterilising [106].

Cation-adjusted Mueller-Hinton broth. Mueller-Hinton broth (MHB) was routinely used as culture medium of choice for susceptibility testing of common bacteria (Chapter 2.2.2, [91]). For preparation of cation-adjusted MHB (CAMHB), 2.1 g of MHB with unadjusted cation content were weighed into a 100 mL glass bottle and suspended in 100 mL Milli-Q® water. The cation content of magnesium and calcium was adjusted to 12.5 mg/L and 25 mg/L, respectively, to standardise conditions. To allow for complete dissolution of MHB, it was heated and stirred for at least 60 min before being autoclaved for 15 min at 121 °C and 2 bar. For fastidious bacterial organisms (Chapter 2.2.1.4), lysed horse blood (LHB) was added after the broth medium cooled down to ≤50 °C under sterile conditions to achieve a final concentration of 5% (v/v). Freshly prepared CAMHB was stored at 4 °C for maximum 7 days.

Sodium chloride solution (0.9%). For antimicrobial experiments (Chapter 2.2), a sodium chloride (NaCl) solution containing 0.9 g NaCl in 100 mL Milli-Q® water was prepared in a 100 mL glass bottle and autoclaved for 15 min at 121 °C and 2 bar. Prepared NaCl solution was stored at 4 °C for maximum 1 month.

Agar plates. Depending on the bacterial strain, a specific amount of the respective agar medium was weighed according to the instructions of the manufacturer and suspended in 1000 mL of MilliQ® water in a 1 L Duran® glass bottle. After heating and simultaneous stirring until clarity of the medium for at least 2 h, it was autoclaved for 15 min at 121 °C and 2 bar. In case of fastidious organisms, 50 mL of sheep blood were added aseptically to 950 mL of the medium after autoclaving at a temperature ≤50 °C (Chapter 2.2.1.4, [91,107]). Ultimately, the medium was evenly poured into petri dishes as a thin layer and was allowed to solidify under sterile conditions. To ensure sterility, two of 30 prepared agar plates were incubated over night as quality controls and checked for growth of any microorganisms. Prepared agar plates were stored for maximum 30 days at 4 °C.

Roswell Park Memorial Institute 1640 medium with 10% foetal bovine serum. To prepare Roswell Park Memorial Institute 1640 (RPMI1640) medium with 10% FBS, 1 mL of heat inactivated FBS was added to 9 mL RPMI1640 in centrifuge tubes under sterile conditions. Solutions were stored at -80 °C and thawed as needed (Chapters 2.2.1.4 and 2.2.4).

2.1.6 Software

Here mentioned software tools with accompanying packages and functionalities were used during the projects at different stages to either perform various investigations or analyse and evaluate generated results. The high-performance computing cluster "Wichlin" at the University of Hamburg, Germany, was used to carry out some higher computationally demanding modelling tasks.

Agilent MassHunter B.08.00	Agilent Technologies, Waldbronn, Germany
ChemDraw® 18.1	PerkinElmer, Waltham, MA, USA
ColonyQuant® 3.2	Schuett Biotec GmbH, Göttingen, Germany
GFortran, GNU Compiler Collection	GNU Project
Microsoft® Office Excel® 16.30	Microsoft Corporation, Redmond, WA, USA
NONMEM® 7.4.1	ICON Clinical Research LLC, Gaithersburg, MD, USA
Pirana® 2.9.7	Certara Inc., Princeton, NJ, USA [108]
PsN 4.7.0	Uppsala University, Uppsala, Sweden [109]
R® 3.6.0	R Foundation, Vienna, Austria
RStudio® 1.2.1335	RStudio Inc., Boston, MA, USA
XQuartz 2.7.11	XQuartz Project, Apple Inc., Cupertino, CA, USA

2.2 Microbiological *in vitro* investigations

This chapter summarises various experimental approaches to assess microbiological characteristics of different antibacterial and immunostimulatory drugs and bacterial strains in *in vitro* experiments. In a first step, the fundamentals of microbiological studies are introduced to in detail describe proper handling of bacteria in *in vitro* studies, e.g. their storage, cultivation, growth conditions or quantification (Chapter 2.2.1). These approaches serve as a basis for subsequently performed investigations of different studies combining drug and bacteria (Chapters 2.2.2-2.2.4).

2.2.1 Predefined principles of microbiological experiments

2.2.1.1 Storage of bacteria

Freezing stocks of bacteria were stored in sterile Roti®-Store cryo vials, which contained glass pellets and a specific medium protecting bacteria from damage during freezing. By preparing a suspension with a turbidity of 2 McF of the respective bacteria from a fresh overnight culture, 0.5 mL of this suspension were added to cryo vials. These vials enabled long-term storage of bacteria at -80 °C.

2.2.1.2 Preparation of subcultures

Temporary short-term removal of bacteria stored in cryo vials from the freezer enabled the preparation of a bacterial subculture. For recultivation, the cryo vial was opened aseptically, a glass pellet was selected using autoclaved tweezers and distributed on an appropriate agar plate. Subsequently, the inoculated agar plate, termed as primary subculture, was incubated over night at 37 °C and kept at 4 °C for short-term storage for maximum 4 weeks afterwards depending on the bacterial strain [91].

The day before a microbiological experiment, a secondary subculture was needed, freshly prepared according to CLSI guidelines [91]. For that purpose, bacterial colonies were picked using sterilised inoculation loops and distributed on an appropriate agar by streaking [107]. This secondary subculture was incubated over night at 37 °C.

2.2.1.3 Bacterial stock suspensions

To prepare bacterial stock suspensions from a secondary subculture (Chapter 2.2.1.2), a specific number of colonies depending on the bacterial strain was picked with a sterile inoculation loop and suspended in 3 mL sterile 0.9% NaCl solution in a round-bottom tube. Turbidity was adjusted to 0.5 McF yielding bacterial stock suspensions with a concentration of approximately $1 \cdot 10^8$ CFU/mL. For standardisation, bacterial suspensions were vortexed before measuring turbidity by using a DensiCheck® densitometer. Commonly, this stock of lag-phase bacteria was used for experiments without any preincubation that would have been needed to have log-phase bacteria.

To confirm the intended bacterial concentrations, bacterial stock suspensions were prepared for each strain and plated on an appropriate agar to quantify bacterial concentrations at the start of each microbiological experiment (Chapter 3.1.1.1).

2.2.1.4 Bacterial specific growth conditions

Depending on the bacterial strain, specific requirements for bacterial growth conditions were present. To account for these various characteristics, specific agars were used. It was aimed to ensure reproducible and isolated shapes of bacterial colonies to allow unrestricted growth and to simplify their counting. Columbia agar without or with 5% (v/v) sheep blood were the agar of choice for *S. aureus* [110] and *S. pneumoniae* [13], respectively (Figure 7.1). For *K. pneumoniae* as well as *P. aeruginosa*, specific Pseudomonas agar, a modification of King's Agar [111], was used.

To assess direct antimicrobial effects, liquid media used were mainly predefined by authorities [13,112]. In contrast to nonfastidious organisms, such as *K. pneumoniae*, *P. aeruginosa* or *S. aureus*, the fastidious *S. pneumoniae* required the addition of 5% (v/v) LHB to CAMHB.

To also assess indirect effects of immunostimulatory drugs (Chapter 2.2.4), additional liquid media were studied. For that purpose, a specific medium was produced by the group of Jean Claude Sirard at the Institute Pasteur de Lille, France, based on an assay developed by Martin Rumbo at the Universidad Nacional de La Plata, Argentina. Briefly, Max Planck Institute (MPI) cells reflecting innate immune responses of alveolar macrophages and being sensitive to bacterial LPS [113] were kept in RPMI1640 with glutaMAX^{TM} and 10% (v/v) heat inactivated FBS and in presence of 30 ng/mL murine granulocyte macrophage colony-stimulating factor (GM-CSF). After preparation of a subculture and subsequent incubation overnight, 5 mL of the cell suspension containing 10^6 cells/mL were stimulated with MPLA at a final concentration of 1 µg/mL. Flasks were incubated for 24 h at 37 °C in 5% CO_2. The resulting supernatant was harvested, centrifuged at 1500 rpm for 5 min in Lille, France, and subsequently sent on dry ice in centrifuge tubes for usage in various experiments at the Freie Universität Berlin, Germany, where it was stored at -80 °C. Next to this supernatant of MPI cells stimulated with MPLA ("STIM"), negative controls consisting of not-stimulated supernatant ("NEG–") or negative controls of direct effects of not-stimulated supernatant with subsequent addition of MPLA ("NEG+") were investigated (Figure 2.1).

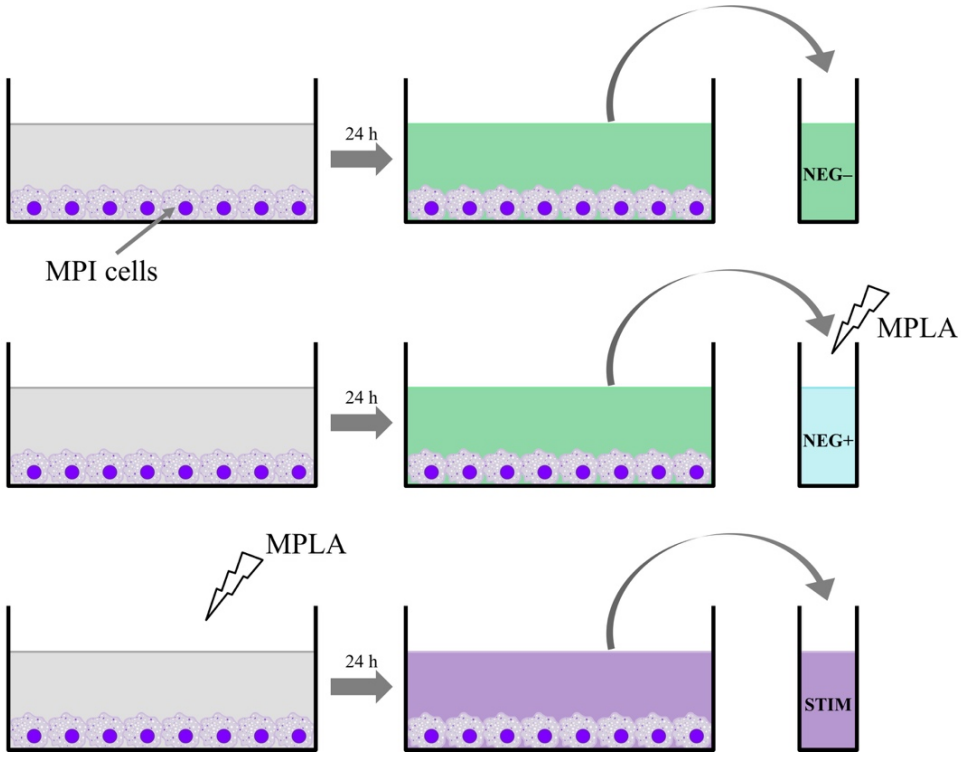

Figure 2.1: Generation of pretreated medium for *in vitro* experiments of direct and indirect effects of monophosphoryl lipid A (MPLA). Max Planck Institute (MPI) cells were either stimulated with MPLA for 24 h ("STIM", bottom row) or not stimulated without ("NEG–", top row) or with ("NEG+", middle row) subsequent addition of MPLA. The supernatant was harvested and stored at -80 °C.

2.2.1.5 Bacterial quantification

Cell counting of incubated bacteria is commonly performed by determining colony forming units (CFU) as surrogate for the actual bacterial concentration. In this thesis, quantification of viable bacteria in a liquid sample of a known volume was performed by a viable plate count method, termed droplet plate assay [110,114], in terms of CFU. Advantages of this method are e.g. less use of material, media and incubator space, less effort and a faster handling, compared to common plate counting methods spreading the sample on the agar plate [114,115].

For the droplet plate assay, a 100 µL aliquot of the bacterial sample was added to 900 µL of sterile 0.9% NaCl solution in round-bottom tubes and subsequently serially diluted tenfold. Bacteria were assumed to be stable in 0.9% NaCl solution for 30 min, since stability was proven for the bacterial strains [110]. Depending on the expected bacterial concentration, preparation of up to the 8^{th} dilution was necessary to allow counting of single and distinct colonies, prevent overlapping of colonies and avoid exceeding the upper limit of quantification (ULOQ) of 500 CFU/100 µL. In a next step, ten drops of a volume of 10 µL were plated on a quarter of an appropriate agar plate for each relevant dilution. After all quarters were filled and NaCl solution vaporised, the agar plate was incubated at 37 °C for 18-24 h. Colonies were counted manually using a colony counter device and each agar plate was photographically

documented using ColonyQuant®. Based on the actual counts, the bacterial concentration expressed as CFU/mL was calculated. In case multiple dilutions of one well showed countable bacterial colonies between 10 and 200 CFU, depending on the bacterial strain, the median was calculated. This approach resulted in a lower limit of quantification (LLOQ) of $1 \cdot 10^2$ CFU/mL. If extremely low bacterial concentrations $<1 \cdot 10^2$ CFU/mL were expected, sampling directly from the well onto the agar plate was justified leading to a LLOQ of $1 \cdot 10^1$ CFU/mL (Chapter 2.2.3). Due to a limitation in the used medium, several time-kill curves studies were performed with a maximum volume of only 1 mL allowing to only take 10 µL from a liquid sample and dilute it in 990 µL NaCl solution (Chapter 2.2.4). Hence, a LLOQ of $1 \cdot 10^3$ CFU/mL resulted, when the first dilution was plated.

2.2.2 Characterisation of the susceptibility of the bacterial strains

2.2.2.1 Investigation of drug-specific requirements

For optimal and reliable susceptibility testing, drug-specific requirements have to be considered and evaluated in terms of fosfomycin, pioglitazone and colistin.

Fosfomycin. Using the antibiotic drug fosfomycin requires the addition of 25 mg/L G6P [13,92,116]. Furthermore, only agar dilution is approved for susceptibility testing with fosfomycin due to inconsistent results for broth dilution methods [13,43]. Nevertheless, the broth dilution method has already been used in literature [47] and will also be applied in these exploratory investigations (Chapter 2.2.2), although performance of the broth dilution method with fosfomycin was not supported by CLSI guidelines [91].

Pioglitazone. Pioglitazone is poorly water-soluble, but highly soluble in methanol (MeOH), ethanol (EtOH) or DMSO [117]. To exclude any substantial killing effect of DMSO, which was used to dissolve pioglitazone, the influence of DMSO, on bacterial growth of *S. aureus* American Type Culture Collection (ATCC) 29213 was investigated against a growth control. 8.9 mL CAMHB were used in appropriate cell culture flasks to which respective solutions of DMSO and CAMHB with a volume of 1 mL were added to obtain final DMSO concentrations of 0%, 1%, 3%, 5% and 10% (v/v). After inoculation with 0.1 mL of a bacterial stock suspension of lag-phase bacteria aiming at a final bacterial concentration of $1 \cdot 10^6$ CFU/mL, the flasks were incubated at 37 °C. Bacterial concentrations were determined over time at 0, 4, 8 and 24 h by using the droplet plate assay (Chapter 2.2.1.5). The influence of pioglitazone itself on bacterial growth was not investigated in this experimental setting.

Colistin. For *in vitro* investigations, the specific physicochemical properties of colistin have to be considered. Hence, adjusting the cation content of calcium and magnesium in CAMHB (Chapter 2.1.5) was crucial to guarantee reproducible results, since these cations may interfere with the interaction of colistin and LPS (Chapter 1.3.1). For determination of the MIC, the sulphate salt is commonly used. Due to reported adhesion of colistin to plastics and a loss of colistin up to 100% depending on the applied concentrations, addition of polysorbate 80 has to be considered [118,119]. To investigate the influence

of polysorbate 80 on the antibiotic effect of colistin, the MIC of colistin and *P. aeruginosa* PAO1 was determined in presence or absence of polysorbate 80, respectively. For that purpose, polysorbate 80 in a concentration of 0.002% (v/v) was added to CAMHB and antimicrobial susceptibility testing was performed as described in Chapter 2.2.2.2.

2.2.2.2 Minimal inhibitory concentration

According to the CLSI guideline M07-A9 [91], a broth dilution procedure was performed to determine the MIC of a specific combination of one drug and a bacterial strain. In 48-well plates with each well being able to take a volume of 1 mL, the experiments were performed (Figure 2.2).

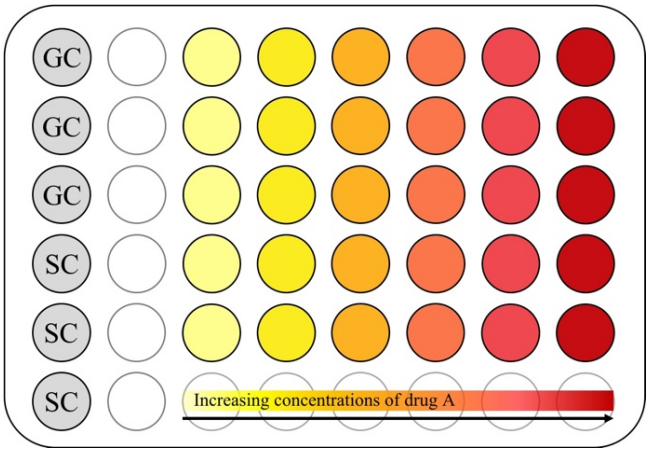

Figure 2.2: Schematic illustration of the determination of a minimal inhibitory concentration with growth control samples (GC, 3 replicates), sterility control samples (SC, 3 replicates) and samples exposed to different concentrations of drug A (5 replicates per concentration level).

As recommended, 890 µL of the bacteria-specific medium were used (Chapter 2.2.1.4). A sterile primary stock solution (Chapter 2.1.5) of the studied drug was diluted to secondary stock solutions in CAMHB: Based on reported breakpoints, drug concentrations were chosen as multiples or fractions of 1.0 mg/L mostly in twofold dilution steps. 100 µL of the secondary stock solution were added to the bacteria-specific media. In most cases, a primary bacterial stock suspension of lag-phase bacteria (Chapter 2.2.1.3) was diluted 1:2 with sterile 0.9% (v/v) NaCl solution to a secondary stock suspension with a bacterial concentration of $5 \cdot 10^7$ CFU/mL in round-bottom tubes. 10 µL secondary bacterial stock suspension were added to each well to achieve a final bacterial concentration of $5 \cdot 10^5$ CFU/mL, that was characteristic and only used for MIC investigations. In case of *S. pneumoniae*, 40 µL of the primary bacterial stock suspension without the 1:2 dilution step were used to consider deviating bacterial concentrations of the stock at 0.5 McF (Chapter 2.2.1.3). The respective volume of the specific medium was adjusted accordingly. In addition, sterility control samples (SC, $n_{replicate}=3$) and growth control samples (GC, $n_{replicate}=3$) were investigated replacing drug and bacteria or solely drug with CAMHB, respectively. The well plate was incubated at 37 °C for 18-20 h and the MIC was determined as the lowest concentration of the drug allowing no visible bacterial growth.

The MIC was determined for multiple combinations of antibiotic or immunostimulatory drugs and bacterial strains at different concentrations (Table 2.1) and classified according to reported breakpoint values by EUCAST [92]. The MIC values of *S. aureus* were determined with strain Newman except of cases, when strain ATCC 29213, also a drug-susceptible strain, was used.

Table 2.1: Investigated concentration ranges (mg/L) of multiple combinations of various antibiotic or immunostimulatory drugs and bacterial strains to determine the minimal inhibitory concentration.

	K. pneumoniae ATCC 43816	*P. aeruginosa* ATCC 15691	*S. aureus* Newman	*S. pneumoniae* serotype 1
Antibiotic drugs				
Amoxicillin	-	-	0.0625-64	0.002-1
Colistin	0.25-16	0.25-16	-	-
Fosfomycin	1-264	0.5-64	0.25-16	-
Streptomycin	0.25-64	2-128	1-64	-
Immunostimulatory drugs				
Metformin	-	-	100-1000*	-
MPLA	-	-	0.0625-1	-
Pioglitazone	-	-	7.5-480*	-

Abbreviations: ATCC: American Type Culture Collection; *K. pneumoniae*: *Klebsiella pneumoniae*; MPLA: Monophosphoryl lipid A; *P. aeruginosa*: *Pseudomonas aeruginosa*; *S. aureus*: *Staphylococcus aureus*; *S. pneumoniae*: *Streptococcus pneumoniae*. * Minimal inhibitory concentration determined with *S. aureus* ATCC 29213.

2.2.3 Drug-drug interaction investigation *in vitro*

With several combinations of antibiotics, immunostimulatory drugs and bacteria, conventional and dynamic checkerboard experiments were performed. The experimental setting was comparable to antimicrobial susceptibility investigations as described in Chapter 2.2.2.2: In addition to sterility and growth control samples and single drug effects, combined drug effects were investigated in this experiments (Figure 2.3). Deviating from the typical MIC setup, 100 µL drug solution of the antibiotic and the immunostimulatory drug, respectively, were added to 790 µL CAMHB for combinations in 48-well plates and samples were initially inoculated with 10 µL of a bacterial suspension with a concentration of $1 \cdot 10^6$ CFU/mL. In addition, single drug effects were investigated with addition of 100 µL drug solution to 890 µL CAMHB as comparison. Drug concentrations were selected based on determined MIC values and reported clinical plasma concentrations (Chapter 1.3). After incubation at 37 °C for 20 h, the checkerboard was evaluated conventionally by turbidity and dynamically by quantifying bacteria using a droplet plate assay (Chapter 2.2.1.5, [120]).

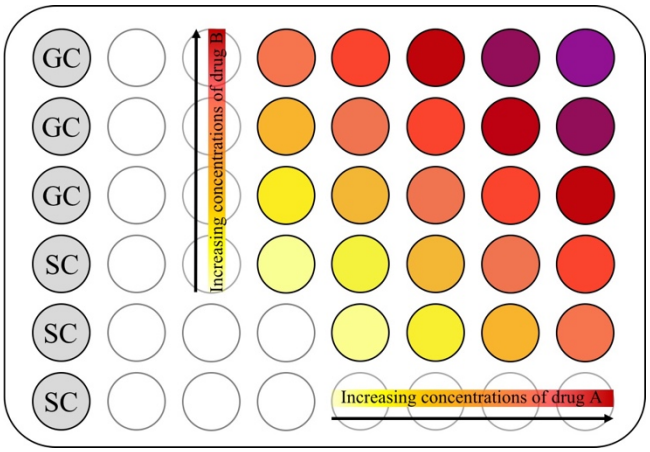

Figure 2.3: Schematic illustration of the experimental setup of a dynamic checkerboard investigation with growth control samples (GC, 3 replicates), sterility control samples (SC, 3 replicates) and samples exposed to different concentrations of drug A and drug B or the combination of both drugs (1 replicate each per concentration level of drug A and drug B).

A variety of specific combinations of bacterial strains and drugs was investigated in this experimental setting (Table 2.2).

Table 2.2: Concentration ranges and tested bacterial strains (*K. pneumoniae* ATCC 43816, *P. aeruginosa* ATCC 15691, *S. aureus* Newman) of multiple combinations of various antibiotic and immunostimulatory drugs studied in a dynamic checkerboard.

		Antibiotic drug		
		Colistin 0.25-2 mg/L	Fosfomycin 1-8 mg/L	Streptomycin 2-32 mg/L
Immuno-stimulatory drug	Metformin 0.625-2.5 mg/L	*K. pneumoniae* *P. aeruginosa*	*K. pneumoniae* *P. aeruginosa* *S. aureus*	*K. pneumoniae* *P. aeruginosa* *S. aureus**
	Pioglitazone 0.375-1.5 mg/L	*K. pneumoniae* *P. aeruginosa*	*K. pneumoniae* *P. aeruginosa* *S. aureus*	*K. pneumoniae* *P. aeruginosa* *S. aureus**

Abbreviations: ATCC: American Type Culture Collection; *K. pneumoniae*: *Klebsiella pneumoniae*; *P. aeruginosa*: *Pseudomonas aeruginosa*; *S. aureus*: *Staphylococcus aureus*; *S. pneumoniae*: *Streptococcus pneumoniae*. * Checkerboard performed with *S. aureus* ATCC 29213.

2.2.4 Immunostimulatory effects in an *in vitro* infection model

This chapter focusses on determining modulator-mediated effects of immunostimulatory drugs on bacteria. For that purpose, the antibacterial and immunostimulatory effects were studied in liquid media provided by the group of Jean Claude Sirard at the Institute Pasteur de Lille (Chapter 2.2.1.4) and compared to commonly used CAMHB. For these investigations, different types of the provided media

were studied. Next to conventional RPMI1640 medium with or without 10% (v/v) heat inactivated FBS, three variations of the MPI cell-pretreated medium were used, introduced as NEG–, NEG+ and STIM in Chapter 2.2.1.4.

2.2.4.1 Bacterial growth in cell growth medium

As basis for investigation of indirect effects, growth of *S. aureus* Newman and *S. pneumoniae* serotype 1 was studied without drug exposure in common bacterial growth media (Chapter 2.2.1.4), RPMI1640 and RPMI1640 with 10% (v/v) FBS. The impact of different concentrations of FBS on bacterial growth was analysed with *S. pneumoniae* serotype 1 by studying 2.5% and 5% in addition. In a 48-well plate, 10 µL or 80 µL of a bacterial stock suspension (Chapter 2.2.1.3) were added to 970 µL or 900 µL medium for *S. aureus* Newman or *S. pneumoniae* serotype 1, respectively, yielding an initial inoculum of $1 \cdot 10^6$ CFU/mL and a total volume of 1 mL. 20 µL of MilliQ® water were added as drug surrogate. Samples were incubated with agitation at 37 °C and bacterial concentrations were determined over time for up to 24 h (0, 1, 2, 4, 8 and 24 h) with a droplet plate assay (Chapter 2.2.1.5).

2.2.4.2 Minimal inhibitory concentration in cell growth and cell-pretreated medium

To evaluate the impact of the cell growth medium on the susceptibility of bacterial strains, the MIC of AMX and MPLA was investigated for direct effects in RPMI1640 with 10% (v/v) FBS as described in Chapter 2.2.2.2 and compared to the MIC determined in common CAMHB. The combinations of AMX (concentration range of 0.0313-0.25 mg/L) or MPLA (concentration range of 0.125-1 mg/L) and *S. aureus* Newman were used as case example.

For indirect effects of MPLA, susceptibility of bacteria in different ratios of STIM and RPMI1640 with 10% (v/v) FBS (22.3%, 45% and 89% (v/v) STIM) was studied.

2.2.4.3 Time-kill curve studies in cell-pretreated medium

In a miniaturised time-kill curve setting, (inhibition of) bacterial growth was monitored over maximum 10 h with quantification of bacteria using the droplet plate method at specific time points (Chapter 2.2.1.5). Here, direct and indirect effects of MPLA were assessed for *S. aureus* Newman and *S. pneumoniae* serotype 1. In addition, both effects of MPLA were studied in combination with AMX for *S. pneumoniae*.

A total volume of 1 mL instead of 10 mL, that are commonly used in standard time-kill curve studies, of NEG+, NEG- or STIM (Chapter 2.2.1.4) were used. In general, the time-kill curve studies were performed as outlined in 2.2.4.1 except for the used media. For the investigated strains *S. aureus* Newman and *S. pneumoniae* serotype 1, an initial inoculum of $1 \cdot 10^6$ CFU/mL was targeted. In this case, 10 µL or 80 µL of a bacterial stock suspension (Chapter 2.2.1.3) were added to 890 µL or 900 µL medium for *S. aureus* Newman or *S. pneumoniae* serotype 1, respectively, yielding a maximum

concentration of STIM of 90% (v/v). To assess direct and indirect effects of MPLA, 100 µL or 20 µL of MilliQ® water were added as drug surrogate for *S. aureus* Newman and *S. pneumoniae* serotype 1, respectively. Differences between study groups were assessed by performing an unpaired, two sample t-test or an analysis of variance (ANOVA, Chapter 2.6.2) for bacterial concentrations at 8 h.

The effect of AMX was investigated in a concentration range of 0.004 to 0.032 mg/L by adding 20 µL of secondary stock solutions (Chapter 2.1.5) instead of MilliQ® water. In addition, the impact of two different batches of NEG-, NEG+ and STIM was investigated with *S. pneumoniae*.

2.3 Bioanalytical assay for quantification of amoxicillin in mouse serum

This chapter describes the development, validation and application of the bioanalytical method to quantify AMX in mouse serum. For this purpose, an LC-MS/MS assay was developed based on an appropriate pretreatment of study samples. To apply the method to analysis of mouse study samples, the method also had to be validated according to current European guidelines [121].

2.3.1 Development of bioanalytical LC-MS/MS assay

2.3.1.1 Preparation of calibrator and quality control samples

Based on two individually prepared antibiotic stock solutions of AMX in MilliQ® water (Chapter 2.1.5), working solutions (1, 10, 100 µg/mL) were subsequently prepared in MilliQ® water in safe lock vials. Aiming at a final concentration range of 0.01-10 µg/mL and 0.01-5 µg/mL for calibrator (CAL) and quality control (QC) samples, respectively, CAL and QC samples were prepared by adding 5 µL of an aqueous working solution of AMX to 45 µL of pooled serum of Swiss mice.

2.3.1.2 Sample pretreatment

For the sample preparation and associated protein precipitation before injection into the LC-MS/MS system, CAL and QC samples were handled in the following way: Different suitable protein precipitation methods were investigated to achieve highest recovery of AMX and determined total AMX concentrations in the samples. To 10 µL of a serum sample, 40 µL of several organic precipitation media, i.e. acetone, acetonitrile (ACN), EtOH or chilled MeOH, which was stored at -20 °C, were added. To ensure sufficient mixture of the samples, each sample was vortexed for 20 s and allowed to rest for 10 min. After centrifugation of samples at 5000 *g* at 20 °C for 10 min, 10 µL of the supernatant were transferred into a 0.5 mL vial. Then, the supernatant was either (i) directly used for injection, (ii) diluted 1:10 (v/v) with 90 µL MilliQ® water or (iii) evaporated and dissolved in MilliQ® water. Processed samples were stored at -80 °C until analysis. Study samples were treated with the finally selected pretreatment method. For injection into the LC-MS/MS system, samples were thawed, vortexed and a volume of 30 µL was transferred onto a 96-well plate. Finally, the well plate was covered and placed in the autosampler for injection.

2.3.1.3 Instrumentation and LC-MS/MS instrument setup

The LC-MS/MS system consisted of an Agilent 1290 Infinity II LC system in combination with a autosampler (G7167B), a high-speed pump (G7120A) and a multicolumn thermostat (G7116B) being connected to a triple quadrupole MS/MS system (G6495A). Necessary instrument settings were configured as well as data acquisition and processing were performed by using the Agilent MassHunter B.08.00 software.

To standardise the temperature and minimise degradation of samples in the autosampler, the autosampler module was set to a constant temperature of 4 °C. 5 µL of a respective sample were transferred into the system with a sampling speed of 200 µL/min. Subsequently, the needle was washed for 20 s using 1:2 (v/v) MeOH and ultra-pure (UP) water to prevent carry-over effects. The sample was injected onto an InfinityLab Poroshell 120 Phenyl Hexyl column (Reversed-phase column, 2.1 × 100 mm, 2.7 µm) and the temperature was maintained at 30 °C in the column compartment. To sufficiently separate AMX from the matrix constituents, a gradient method was chosen. At a flow rate of 0.3 mL/min, different gradient profiles with increasing organic solvent over time were studied using UP water (mobile phase A) and ACN (mobile phase B) both supplemented with 0.1% (v/v) formic acid as eluents.

The triple quadrupole mass spectrometry (MS) system used an electrospray ionisation (ESI) source and was operated in positive ion mode. To monitor the three different transitions of AMX from the precursor ion (*m/z* 366.11) to product ions *m/z* 349, 208 and 114, ion acquisition was operated in a dynamic multiple reaction-monitoring mode. Final parameters and transitions were investigated by direct injection and source parameters were optimised both assisted by Agilent Optimizer Software. The LC-MS/MS used nitrogen as drying, sheath and collision gas.

2.3.2 Validation of bioanalytical LC-MS/MS assay

The developed LC-MS/MS method to quantify AMX in mouse serum was fully validated in line with the European Medicines Agency (EMA) guideline on bioanalytical method validation [121]. The following characteristic criteria of the EMA guideline were evaluated: Selectivity, carry-over, LLOQ, calibration range, accuracy, precision, matrix effect and stability.

Selectivity. To assess selectivity and differentiate between matrix constituents and AMX, at least 6 individual sources of appropriate blank matrix should be considered according to the guideline. In this setting, study samples of untreated mice (Chapter 2.4.1) were evaluated against LLOQ samples of the same run. Since volume of blood in mouse is limited to 50 mL/kg [122] corresponding to approximately 1.25 mL blood per mouse, additional sources of serum, such as pooled serum of study mice or commercial mouse serum, were considered for selectivity investigations as it is also specified as acceptable in the guideline in case of rare matrix. After comparison of detector responses, absence of

interference was accepted as long as the detector response of a matrix sample was less than 20% of the response at LLOQ of a sample with AMX added.

Carry-over. Carry-over was considered to be negligible, if the individual detector response of a blank sample of MeOH injected directly after a high concentration sample of AMX (≥5 µg/mL) was negligible compared to a LLOQ sample with <20% in detector response.

Lower limit of quantification. LLOQ samples had to be determined with sufficient accuracy and precision (see below) and show a ≥5 times higher detector response than a blank sample. To determine the LLOQ, replicates of 0.025, 0.01 and 0.025 µg/mL of AMX spiked samples were investigated. Moreover, the lower limit of detection (LOD) was determined based on calculations according to international guidelines [123] as well as the LLOQ was calculated as comparison in that way.

Calibration range. CAL samples were prepared as described elsewhere (Chapter 2.3.1.1) and handled exactly as study samples including the sample preparation (Chapter 2.3.1.2). On three consecutive days, a blank matrix sample and 7 tiers of CALs were prepared in triplicate and analysed with the developed LC-MS/MS assay. The concentration range from 0.01 to 10 µg/mL was covered. A linear regression of detector response vs. nominal concentration was performed to determine the regression function by which AMX concentrations are calculated. To improve accuracy for lower concentrations of the calibration range, a weighing function of $w=1/(concentration^2)$ was applied in a linear regression analysis. To accept a calibration function, back calculated concentrations were required to be within 85%-115% or 80%-120% at the LLOQ of the respective nominal concentrations. These requirements had to be compliant for ≥75% of all CAL samples.

Accuracy and precision. Within-run and between-run accuracy were assessed by evaluating the deviation of mean determined to nominal concentrations of AMX. Within-run and between-run precision were determined by evaluating the distribution of repeated individual measurements. For accuracy and precision, 4 QC tiers (Chapter 2.3.1.1) with 5 replicates per tier were prepared. Concentrations ranging from the LLOQ to the ULOQ, representing the calibration range, were investigated and analysed on three consecutive days. The guideline requires mean concentrations and the coefficient of variation (CV) of QC samples to be within 85%-115% or 80%-120% at the LLOQ of the nominal concentrations.

Matrix effects. Matrix effects should be investigated to detect significant deviations between various individual matrix samples. For that purpose, respective CAL and QC samples in pooled mouse serum were used and compared to aqueous samples at a low (0.025 µg/mL) and a high concentration (1 µg/mL). To evaluate matrix effects, a matrix factor was calculated as ratio of the peak area in presence of matrix to the peak area in absence of matrix. The CV of the matrix factor of at least 6 lots was required to be ≤15%.

Stability. Stability of AMX was investigated under conditions relevant for application of the developed LC-MS/MS assay to study samples. For that purpose, different criteria were assessed. For autosampler stability, stability of processed samples over 20 h at 4 °C in the autosampler was studied. Long-term stability of serum samples over 6 months was evaluated under storage conditions of -80 °C. For these investigations, up to three replicates of CAL or QC samples at AMX concentrations of 0.01, 0.1, 1 and 5 µg/mL were used. Freeze-thaw stability was determined by exposing the samples to three cycles in a low concentration range from 0.01 to 0.1 µg/mL in triplicate. In addition, short-term stability was evaluated at room temperature for 20 h: Unprocessed serum samples as well as processed samples were studied at multiple concentrations of 0.025, 0.1, 0.5, 1, 2.5 µg/mL and more extensively investigated as demanded. A freshly prepared calibration function was used to determine respective AMX concentrations. Except for autosampler stability, which was evaluated in comparison to sample concentrations at t=0 h, obtained results were compared to nominal concentrations. In general, the mean concentrations at each level were required to be within 85%-115% of the nominal concentrations.

2.3.3 Application of the bioanalytical LC-MS/MS assay

The bioanalytical method was applied to quantify concentrations of AMX in study samples of an *in vivo* performed PK study in mice (Chapter 2.4.1). For analysis of study samples, an in-study validation has to be performed according to the respective EMA guideline [121] to verify the performance of the applied assay. The analytical run was required to consist of blank samples, ≥6 CAL samples and ≥3 QC samples (low, medium, high level) at least in duplicate. As demanded, CAL and QC samples were spiked independently from each other with two separately prepared stock solutions of AMX. CAL, QC and study samples were processed, stored at -80 °C and analysed as one single batch.

The analytical run was accepted, if back calculated concentrations of CAL samples were within 85%-115% or 80%-120% at the LLOQ of nominal concentrations. These criteria had to be fulfilled by ≥75% of all CAL samples. In addition, accuracy of QC samples was required to be within ±15% of nominal values, which had to be the case for ≥67% of all QC samples and ≥50% at each concentration level. Finally, overall mean accuracy and precision of QC samples should not exceed 15%.

2.4 Animal infection model

To assess the PK and PD and the influence of stimulation of the immune system on an infection, several aspects were investigated in an animal infection model in different studies. These pooled *in vivo* studies were performed at and results were provided by the Institut Pasteur de Lille, France, by the group of Jean-Claude Sirard and are described in detail elsewhere [124]. In general, the pooled studies aimed to assess four main study groups (no treatment, solo-agent treatment of either AMX or MPLA, dual-agent treatment of AMX and MPLA). The basics that these animal experiments have in common will be introduced in the next part, before methods of respective individual studies will briefly be explained.

Female outbred RjOrl:Swiss (CD-1) mice as well as inbred Balb/cJRj mice (6-8 weeks old; body weight of ~25 g; Janvier Laboratories, Saint Berthevin, France) were used both depending on the investigated parameter. The experiments were in line with institutional regulations and ethical guidelines (Animal facility agreement C59-350009, Institut Pasteur de Lille, APAFIS#5164, protocol 2015121722429127_v4). Briefly, mice were handled in vertical laminar airflow cabinets and were maintained in individually ventilated cages. *S. pneumoniae* serotype 1 (MIC=0.016 µg/mL) was used as bacterial reference organism to induce pneumonia. For that purpose, mice were anaesthetised intraperitoneally with 1.25 mg ketamine and 0.25 mg xylazine in phosphate buffered saline (PBS) and subsequently infected intranasally with a bacterial suspension of 30 µL with a specified bacterial number of ≈1-4·10^6 CFU/mouse. To investigate the antibacterial effects of AMX and MPLA, treatment was induced 12 h after infection. AMX was administered intragastrically by oral gavage as aqueous solution of AMX powder in 200 µL MilliQ® water. For MPLA, 200 µL of a PBS solution of MPLA were administered intraperitoneally without anaesthesia. A standard single dose of 2.00 mg/kg (50 µg/mouse) was used for MPLA. Contrarily, five different single doses were investigated for AMX (0.20-14.0 mg/kg) in total. To study the combined treatment with AMX and MPLA of an individual mouse, drug administration was performed sequentially with MPLA being administered first. In cases of monotherapy, a dummy drug substituting the specific other drug of the combination consisting of either MilliQ® water or PBS instead of AMX or MPLA, respectively, was commonly not used. If applicable, respective exceptions will be indicated.

In general, following aspects of PK and PD were investigated over time in separately performed studies and for a specific type of mouse and will be introduced in detail hereafter: PK of AMX, bacterial growth kinetics in lung and spleen, survival, body weight profile, gene expression of markers of the immune system, cytokine kinetics in serum, tissue morphology in lung of markers of the immune system and recruitment of immune system-related cells (Table 2.3). All steps of the exploratory graphical analysis (EGA) of the generated *in vivo* data were performed in the software R® (version 3.6.0) with accompanying packages “ggplot2” (version 3.2.1) “survival” (version 2.44-1-1) and “survminer” (version 0.4.6).

Table 2.3: Investigated aspects of pharmacokinetics and pharmacodynamics incl. their respective study code, experimental readout and the used mouse strain of a PK/PD study to assess the antibacterial effects of amoxicillin and monophosphoryl lipid A.

Study	Investigated aspect	Experimental readout	Mouse strain
PK1	PK of AMX	AMX serum concentration (µg/mL)	Swiss
PD1	Bacterial growth kinetics in lung and spleen	Bacterial number (CFU/organ)	Swiss, Balb/cJ
PD2	Survival	Survival per day, %	Swiss
PD3	Change in body weight	% of starting body weight	Swiss
PD4	Gene expression	mRNA expression of markers of the immune system	Balb/cJ
PD5	Cytokine kinetics	Cytokine serum concentration (pg/mL)	Swiss, Balb/cJ
PD6	Tissue morphology	Histological score of markers of the immune system	Swiss
PD7	Cell recruitment	% of total immune system-related cells	Balb/cJ

Abbreviations: AMX: Amoxicillin; Balb/cJ: Inbred Balb/cJRj mouse strain; CFU: Colony forming units; mRNA: Messenger ribonucleic acid; PD: Pharmacodynamic (study); PK: Pharmacokinetic (study); Swiss: Outbred RjOrl:Swiss (CD-1) mouse strain.

2.4.1 Pharmacokinetics of amoxicillin *in vivo*

To determine the PK of AMX in mice, a PK study was designed in collaboration with the Institut Pasteur de Lille. Based on literature, planning of the PK study focused on determination of appropriate sampling time points to reduce the number of studies itself and the number of mice that have to be investigated. Three different PK studies (PK1.1, PK1.2, PK1.3) were performed to assess the PK of AMX in Swiss mice mainly differentiating in the administered dose of AMX and the murine infection status (Figure 2.4). To in the first two studies ensure quantification of AMX with concentrations above the LLOQ, the dose (14.0 mg/kg) was relatively high compared to doses administered in PD experiments and the dose that was determined for the third PK study (0.40 mg/kg). In addition, a dummy dose was administered for MPLA in study PK1.1. Serum samples of treated mice beginning with 12.167 h up to 24 h after infection were collected throughout the study with up to 7 sampling time points in total. Per time point, 3-4 serum samples were obtained from 3-4 individual mice, i.e. one sample per individual mouse. For PK study PK1.1 and PK1.3, only one sample was taken per individual mouse over the entire study time in a destructive study design. Such a terminal sample allowed to sample >100 µL of serum per individual mouse. In case of PK1.2, two samples were obtained from one individual mouse at 12.167 and 14 h, at 12.5 and 15 h or at 13 and 18 h after infection, respectively, allowing to sample an additional

intermediate sample of ≈50 µL. Subsequently, serum samples were processed as follows: After sampling by using retroorbital bleeding without anaesthesia, samples were stored in Microtube Z-Gel collection tubes. To obtain serum, the collected samples were processed subsequently by centrifugation at 10000 *g* for 5 min. Samples were stored at -80 °C. For quantification, samples were applied to the developed and validated LC-MS/MS assay at Freie Universitaet Berlin (Chapter 3.2) in two different analyses (PK1.1 and PK1.2 in part 1, PK1.3 in part 2 of the application of the assay), both including an in-study validation as described in detail elsewhere (Chapter 2.3.3), and total AMX concentrations were determined neglecting the minor PPB of 17% of AMX (Chapter 1.3.1).

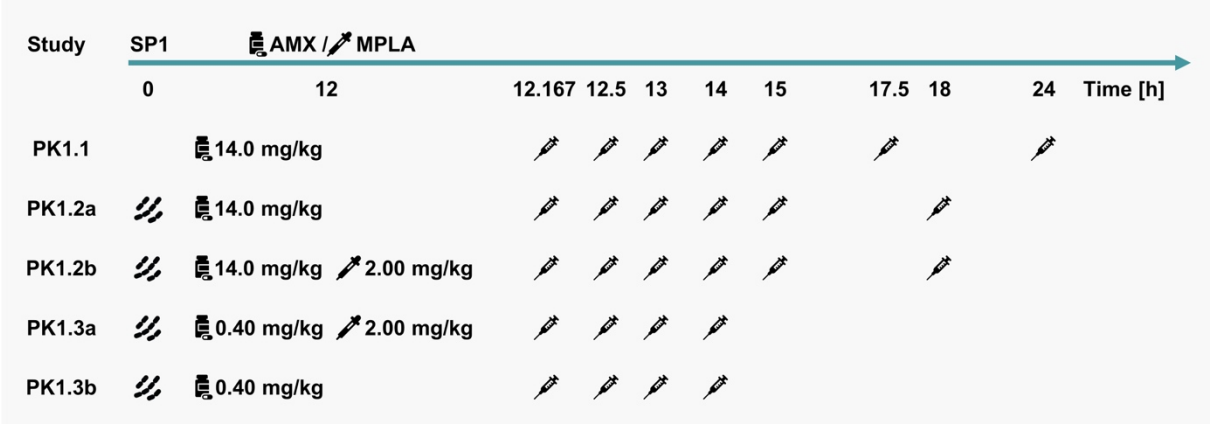

Figure 2.4: Infection, dosing and sampling schedule of three performed pharmacokinetic studies (PK1.1-PK1.3) in non-infected and infected outbred RjOrl:Swiss (CD-1) mice infected with SP1 and treated with AMX or the combination of AMX and MPLA. Abbreviations: AMX: Amoxicillin; MPLA: Monophosphoryl lipid A; SP1: *Streptococcus pneumoniae* serotype 1. Symbols: Bacteria: Infection status of mice with bacteria indicating infected animals; Pillbox: Administered dose of AMX; Pipette: Administered dose of MPLA; Syringe: Sampling of serum.

2.4.2 Bacterial growth kinetics

Several experiments were performed to determine bacterial numbers of *S. pneumoniae* serotype 1 in lung and spleen of Swiss and Balb/cJ mice over time (Figure 2.5). Infection of mice and administration of the investigated drugs were performed as described elsewhere in detail (beginning of Chapter 2.4). A standard dose of 2.00 mg/kg MPLA and three doses of AMX (0.2, 0.4 and 1.2 mg/kg) were studied leading to in total eight study groups being untreated or receiving monotherapy or a combined treatment approach. In case of monotherapy, a dummy dose of the respective other drug was only administered for two out of 11 experiments. After infection with *S. pneumoniae* serotype 1, in total ≤10 different time points between 0 and 48 h after infection were studied. Bacterial numbers were determined in lung and spleen by a destructive sampling method with one sample of lung and spleen per individual using standard droplet plate assays (Chapter 2.2.1.5). Briefly, an individual mouse was sacrificed at a specific time point and the respective entire organs were harvested. Subsequently, the entire organs were added to 1 mL of PBS and homogenised immediately. The organ homogenate was diluted appropriately and

plated on bacteria-specific agar plates. Due to this preparation method, different LLOQ values were possible depending on the dilution that was finally plated. If bacterial numbers of a sample were below the LLOQ, the bacterial number was set to the LLOQ. Bacterial numbers were reported as CFU/organ. For comparison of different study groups, the geometric mean of bacterial numbers per mouse at each time point was calculated per study group.

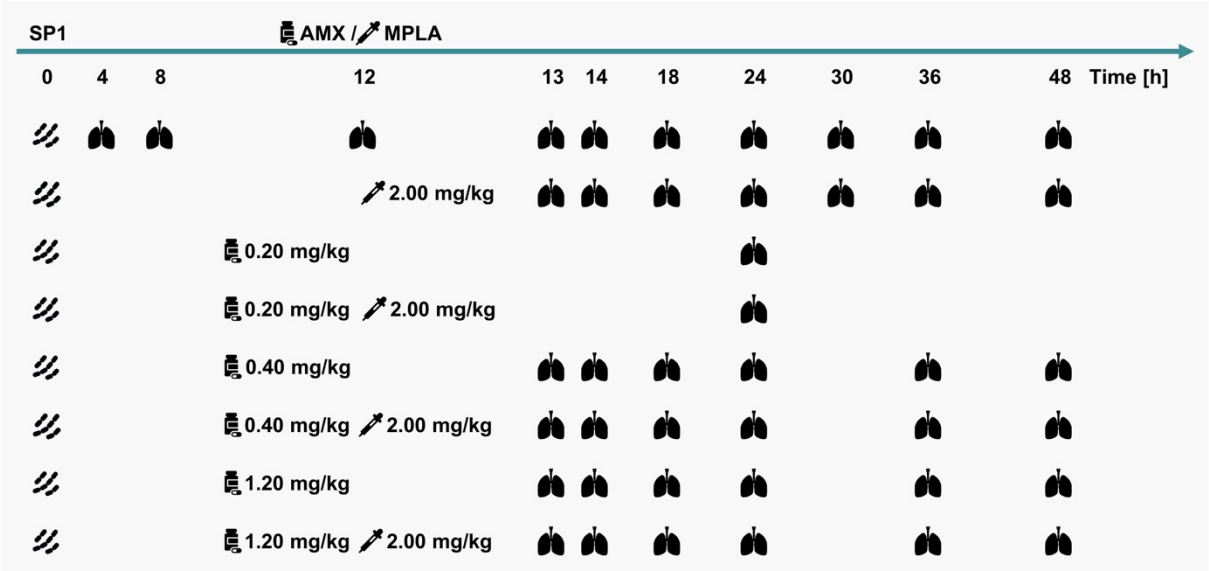

Figure 2.5: Infection, dosing and sampling schedule of several performed pharmacodynamic studies in outbred RjOrl:Swiss (CD-1) or inbred Balb/cJRj mice infected with SP1 and being either untreated or treated with AMX, MPLA or the combination of both drugs. Abbreviations: AMX: Amoxicillin; MPLA: Monophosphoryl lipid A; SP1: *Streptococcus pneumoniae* serotype 1. Symbols: Bacteria: Infection status of mice with bacteria indicating infected animals; Pillbox: Administered dose of AMX; Pipette: Administered dose of MPLA; Lung: Time point of quantification of bacteria in lung.

2.4.3 Survival study

To further evaluate the efficacy of the investigated mono- and combination treatments, the survival status (dead or alive) of infected Swiss mice was monitored over time from the start of infection. After infection with *S. pneumoniae* serotype 1at 0 h, drugs were administered at 12 h. A standard dose of 2.00 mg/kg MPLA and three single doses of AMX (0.4, 0.8 and 1.2 mg/kg) in single or combined treatment as well as untreated mice were studied in eight study groups. Survival was assessed every 24 h after infection over ≤14 d (Figure 2.6) and reported as percent survival compared to the number of mice being investigated per study group.

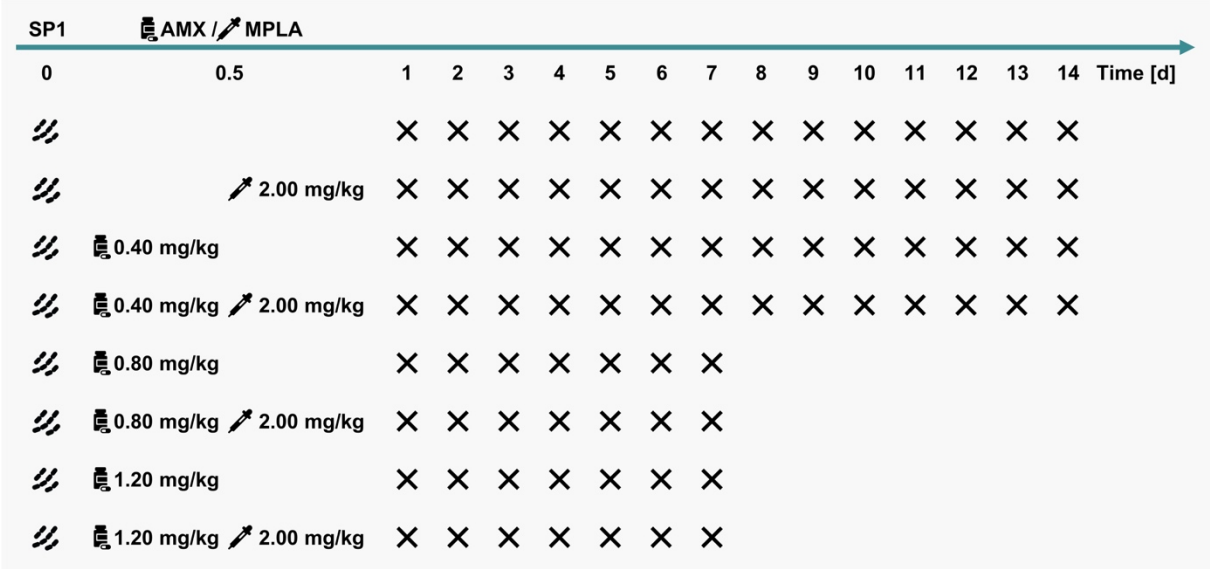

Figure 2.6: Infection, dosing and assessment of survival status or body weight for outbred RjOrl:Swiss (CD-1) mice infected with SP1 and being either untreated or treated with AMX, MPLA or the combination of both drugs. Abbreviations: AMX: Amoxicillin; MPLA: Monophosphoryl lipid A; SP1: *Streptococcus pneumoniae* serotype 1. Symbols: Bacteria: Infection status of mice with bacteria indicating infected animals; Pillbox: Administered dose of AMX; Pipette: Administered dose of MPLA; Cross: Assessment of survival or body weight.

2.4.4 Parameters related to the physical condition and immune system of the animal

In addition to PK of AMX (Chapter 2.4.1), bacterial growth kinetics (Chapter 2.4.2) and survival (Chapter 2.4.3), several other already mentioned parameters were studied and will be reported in this chapter. Here, a brief overview of the studies will be presented, which were in detail performed and analysed by the group of Jean-Claude Sirard at the Institut Pasteur de Lille, France, and scope of their work [124].

2.4.4.1 Body weight profile

Associated with the survival study (Chapter 2.4.3), body weight was assessed simultaneously. For that purpose, mice were weighed at specific time points every 24 h (Figure 2.6). The percentage of the starting body weight of each individual mouse before infection was reported.

2.4.4.2 Gene expression of markers of the immune system

Gene expression of different markers of the immune system was studied in six different study groups in lung (Table 2.4). Balb/cJ mice were either non-infected or infected with *S. pneumoniae* serotype 1. Gene expression of following six study groups was determined: (a) Non-infected mice being untreated (PD4.1) or treated with a standard dose of MPLA (2.0 mg/kg, PD4.2), (b) infected mice being untreated (PD4.3) or treated solely with AMX (0.4 mg/kg, PD4.4), or (c) infected mice being treated with MPLA (2.0 mg/kg, PD4.5) or the combination of MPLA and AMX (0.4 mg/kg, PD4.6).

Table 2.4: Study groups stratified by the infection status of mice being non-infected or infected with *Streptococcus pneumoniae* serotype 1 and corresponding treatment of a PD study aiming to assess relative gene expression of several gene markers of the immune system.

Study group	Infection	Treatment		Mouse strain
		AMX	MPLA	
PD4.1	–	–	–	Balb/cJ
PD4.2	–	–	+	Balb/cJ
PD4.3	+	–	–	Balb/cJ
PD4.4	+	+	–	Balb/cJ
PD4.5	+	–	+	Balb/cJ
PD4.6	+	+	+	Balb/cJ

Abbreviations: AMX: Amoxicillin treatment with a single dose of 0.4 mg/kg; Balb/cJ: Inbred Balb/cJRj mouse strain; MPLA: Monophosphoryl lipid A treatment with a single dose of 2.0 mg/kg; PD: Pharmacodynamic (study).

At different time points (14, 16, 20, 48 h after infection), messenger ribonucleic acid (mRNA) expression of several genes was determined by quantitative real-time polymerase chain reaction (RT-PCR) at the Institut Pasteur de Lille, France [124], and calculated by being normalised to an internal control, in this case the unregulated housekeeping gene β-actin, and gene expression of non-infected and untreated animals. The relative gene expression of the following 15 markers was evaluated from each individual mouse: Cyclic adenosine monophosphate (cAMP), C-C chemokine ligand 2 (CCL2), C-C chemokine ligand 20 (CCL20), C-X-C chemokine ligand 2 (CXCL2), FK506 binding protein 5 (FKBP5), interleukin-12 subunit p40 (IL-12 p40), interleukin-1β (IL-1β), interleukin-4 induced 1 (IL-4i1), IL-6, integrin beta chain 2 (ITGB2L), matrix metalloproteinase 8 (MMP8), neuronal guidance protein (NGP), prokineticin 2 (PROK2), S100 calcium-binding protein A9 (S100A9) and zinc finger and BTB region containing-16 (ZTBT16).

2.4.4.3 Cytokine kinetics in serum

Cytokine kinetics were studied in Swiss and Balb/cJ mice by quantifying pro-inflammatory cytokines in circulating serum over time. Different study groups of non-infected (PD5.3) or infected mice treated with AMX (0.40 mg/kg, PD5.2), MPLA (2.0 mg/kg, PD5.4), a combination of both (PD5.5) or no treatment at all (PD5.1) were investigated (Table 2.5).

Table 2.5: Study groups of a PD study stratified by infection status of mice being non-infected or infected with *Streptococcus pneumoniae* serotype 1 and treatment aiming to assess serum kinetics of five different cytokines.

Study group	Infection	Treatment		Mouse strain
		AMX	MPLA	
PD5.1	+	–	–	Swiss, Balb/cJ
PD5.2	+	+	–	Swiss, Balb/cJ
PD5.3	–	–	+	Swiss, Balb/cJ
PD5.4	+	–	+	Swiss, Balb/cJ
PD5.5	+	+	+	Swiss, Balb/cJ

Abbreviations: AMX: Amoxicillin (0.4 mg/kg); Balb/cJ: Inbred Balb/cJRj mouse strain; MPLA: Monophosphoryl lipid A (2.0 mg/kg); PD: Pharmacodynamic(s); Swiss: Outbred RjOrl:Swiss (CD-1) mouse strain.

Serum was collected and processed as described elsewhere (Chapter 2.4.1). Cytokine concentrations of CCL2, IL-12 p40, IL-6 and TNFα were quantified at different time points (12, 12.167, 12.5, 13, 14, 16, 17, 18, 20, 21, 24, 36 and 48 h after infection) in serum using an enzyme-linked immunosorbent assay (ELISA) at the Institut Pasteur de Lille, France [124].

2.4.4.4 Histopathology in lung of markers of the immune system

Different study groups of non-infected (PD6.1) or infected mice treated with AMX (0.40 mg/kg, PD6.5, or 14.0 mg/kg, PD6.6), MPLA (2.0 mg/kg, PD6.3), a combination of both (PD6.4) or no treatment at all (PD6.2) were investigated to assess the histopathology in lung of mice (Table 2.6).

Table 2.6: Study groups of a PD study stratified by infection of mice being non-infected or infected with *Streptococcus pneumoniae* serotype 1 aiming to assess the histopathology of different immune markers.

Study group	Infection	Treatment		Mouse strain
		AMX	MPLA	
PD6.1	–	–	–	Swiss
PD6.2	+	–	–	Swiss
PD6.3	+	–	+	Swiss
PD6.4	+	+	+	Swiss
PD6.5	+	+	–	Swiss
PD6.6	+	++	–	Swiss

Abbreviations: AMX: Amoxicillin (0.4 mg/kg (+) or 14 mg/kg (++)); MPLA: Monophosphoryl lipid A (2.0 mg/kg); PD: Pharmacodynamic (study); Swiss: Outbred RjOrl:Swiss (CD-1) mouse strain.

Here, Swiss mice were studied, and histopathology was assessed by staining tissue section with haematoxylin and eosin 48 h after infection. A blinded evaluation of the histopathology of the lung samples was performed at the Institut Pasteur de Lille, France [124], and a histological score was calculated for 11 individual markers: (a) Alveolar macrophages, (b) alveolar neutrophilic infiltration, (c) foreign body-related inflammation, (d) intraluminal neutrophils, (e) perivascular mixed inflammatory cells, (f) alveolar haemorrhage, (g) intravascular fibrinous thrombi, (h) microvascular/venular hyperaemia, (i) perivenous/periarterial oedema, (j) fibrin-leukocytic/suppurative pleuritis and (k) mesothelial pleura thickening. The score ranged from 0 (absence of histopathology) to 5 (severe histopathology) being graded in between by 1, 2, 3 and 4 indicating minimal, slight, moderate and marked histopathology, respectively. Each parameter was individually assessed per mouse by specifically trained personal. In addition, a total histological score was calculated to determine overall histopathology by adding up individual scores.

2.4.4.5 Recruitment of immune system-related cells

In Balb/cJ mice, cell recruitment of macrophages, monocytes and neutrophils was investigated directly in lung and by using bronchoalveolar lavage (BAL). Samples of four individual mice were taken 24 h after infection in four different study groups (Table 2.7).

Table 2.7: Study groups stratified the infection status of mice being infected with *Streptococcus pneumoniae* serotype 1 and corresponding treatment of a PD study aiming to assess cell recruitment of macrophages, monocytes and neutrophils in lung.

Study group	Infection	Treatment		Mouse strain
		AMX	MPLA	
PD7.1	+	–	–	Balb/cJ
PD7.2	+	–	+	Balb/cJ
PD7.3	+	+	+	Balb/cJ
PD7.4	+	+	–	Balb/cJ

Abbreviations: AMX: Amoxicillin treatment with a single dose of 0.4 mg/kg; Balb/cJ: Inbred Balb/cJRj mouse strain; MPLA: Monophosphoryl lipid A treatment with a single dose of 2.0 mg/kg; PD: Pharmacodynamic (study).

To evaluate cell recruitment in lung tissue, the number of respective cells was determined by using flow cytometry at the Institut Pasteur de Lille, France [124]. In addition, the number of respective cells was related to the total amount of cells, which was determined as number of all CD45 positive cells representing macrophages, monocytes and neutrophils.

2.5 *In silico* analysis of the combination of amoxicillin and monophosphoryl lipid A

This chapter is mainly dealing with the mathematical background and application of methods that had been employed for a PK/PD analysis of experimental data, that has been generated at the Institut Pasteur de Lille, France. The aim was (i) to define the response of each drug over time in mice, (ii) to identify the interaction of AMX and MPLA in mice and (iii) to establish a basis for subsequent translation into a clinical setting. For this purpose, the used modelling and simulation approaches will be introduced briefly to provide the theoretical understanding of performed analyses. In a next step, the application of these methods will further be elucidated by concretely applying them to the data obtained from the PK/PD studies in mice (Chapter 2.4). Finally, the results of the *in silico* analysis shall be applied to a simulation study exploring the PK/PD model in detail by investigating different dosing regimens and a translation to human.

The modelling itself was performed using the software NONMEM® (version 7.4.1), which was executed by PsN (version 4.7.0). As compiler, GFortran (version 6.3.0) for macOS High Sierra was used. Additional software tools to record, visualise, and evaluate the modelling results were Pirana® (version 2.9.7) including XQuartz (version 2.7.11), RStudio® (version 1.2.1335), and R® (version 3.6.0) with packages “ggplot2” (version 3.2.1), “vpc” (version 1.1.0) and “xpose4” (version 4.6.1).

2.5.1 Mathematical basics of nonlinear mixed-effects modelling

For analysis of experimentally generated results (Chapter 3.3), the approach of nonlinear mixed-effects (NLME) modelling was used and its framework will shortly be introduced. In the area of pharmacometrics, NLME modelling is classified as a top-down approach dealing with empirical to mechanism-motivated models [125-127]. Typically, top-down approaches consist of data generated in (pre-)clinical studies, such as serum concentrations of a certain drug or PD effects over time in a specific patient population. Contrarily to top-down approaches, bottom-up approaches allow a more mechanistic analysis of underlying processes by using detailed physical and physiological information about these processes e.g. on a specific organ level or by using specific drug characteristics [126,128]. Here, physiologically-based PK modelling or systems biology/pharmacology are frequently used approaches. In this context, semi-mechanistic models are a more specific case categorised as compromise of empirical and mechanistic approaches. Here, strongly but appropriately simplified mechanistical models still allow usage of NLME approaches. Compared to empirical models, more physiologically and pharmacologically motivated insights are considered allowing a reliable estimation of parameter estimates to differentiate between drug- and system-specific characteristics.

Based on the respective (pre-)clinical data in top-down approaches, empirical or semi-mechanistic models are developed and PK parameters, such as clearance (CL) or volume of distribution (V), or PD parameters, having e.g. the form of a maximum effect (E_{max}) model, are introduced to describe underlying processes. PK parameters, for instance, are defined in either a compartmental or a

noncompartmental data analysis. While in noncompartmental analysis PK parameters are calculated e.g. by determining the AUC, a compartmental analysis makes use of PK models [128]. Compared to a non-compartmental analysis, the advantage of compartmental models is that they are able to adequately describe the data for only a few data points. By introducing different compartments that are connected by each other, processes are mathematically described as for instance by using a central and peripheral compartment in a two-compartment model that are linked. Various adjustments of these compartments, e.g. varying absorption or elimination kinetics, are possible and were investigated within the process of the model development in this thesis (Chapter 2.5.3.2).

The determination of respective parameters is made either on an individual or a population level [129]. On a population level, characteristics of a certain study population are determined based on individual observations. Here, a typical value of the population with accompanying variabilities and patient-specific covariates are considered. For population analyses, three major approaches were developed: naïve pooling, two-stage approach or NLME modelling [129]. Using naïve pooling, all observations are pooled and considered as derived from one individual. The approach has the advantage that data situations with only one observation per individual are handled, but on the other hand separated assessment of interindividual variability (IIV) and estimates is impossible, and estimates tend to be biased in cases of higher variability [5,128,129]. In a two-stage approach with serial sampling of an individual, individual parameters are derived first, and population parameters are calculated subsequently by descriptive statistics based on the generated data in the first step. Here, IIV might be substantially overestimated, since every individual parameter is already estimated from the original individual data base and potential errors may potentiate [5,130]. Using NLME modelling, all observations are analysed simultaneously with one individual being analysed together with all other individuals [95]. Compared to other compartmental approaches, NLME modelling benefits substantially [129] and is used for datasets displaying large variability, nonlinear PK or several different kinds of PK and/or PD observations [131]. Also, analysis of sparse sampling data is possible [132]. NLME modelling distinguishes fixed-effects and random-effects parameters and, hence, is denoted as mixed-effects modelling. Fixed-effects parameters are mainly characterised by the determined structural population parameters and patient specific covariate parameters that are able to influence the population parameters. Contrarily, random-effects parameters take various levels of variability into account. Mainly, IIV or between-subject variability (BSV), residual unexplained variability (RUV) or intraindividual variability and interoccasion variability (IOV) are employed and will further be introduced partly (Chapter 2.5.1.2). The term “nonlinear” originates from the fact that estimated parameters are related nonlinearly to the dependent variable, e.g. the underlying concentration data [129].

When performing a compartmental analysis by making use of NLME modelling, 3 major steps have to be considered for developing a pharmacometric model: (i) Data management, (ii) development of a

structural model with addition of a statistical and covariate model coming along with usage of an appropriate modeling software with respective estimation methods and (iii) model evaluation [132]. First of all, appropriate data management is mandatory as basis of the whole modelling process. Based on a developed structural model, the generated dataset is analysed and extended by the statistical and the covariate model. By using the software NONMEM® the analysis of the pharmacometric model is performed by specific implemented estimation methods. Subsequently, an evaluation of the developed models is performed to decide for one model revealing the best quality of model parameters and predictive performance for the investigated purpose. Here, various numerical and graphical evaluation techniques are used. The respective parts of a workflow of a NLME modelling study will be outlined briefly in the upcoming parts (Chapters 2.5.1.1-2.5.1.7).

2.5.1.1 Data management

Since the pharmacometric model is only as good as the data base that is used during the analysis, this step often is most critical. For this purpose, the data input has to be as accurate as possible. The underlying data are arranged in one dataset in a specific format that is demanded by the used software NONMEM® (Chapter 2.5.3.1). All information of the performed analysis, such as the determined output at a specific time point, dosing information or individual covariate details, are stored in such a dataset chronologically per individual study subject [88]. In addition, important facts about single measurements are part of the dataset, as for instance the information that a sample has a concentration being below the LLOQ. In a next step, a dataset checkout including comprehensive exploratory statistical analyses (ESA) and EGA has to be performed very precisely to avoid any errors and check for completeness and plausibility. Here, already characteristics of certain distributions of the data or specific influences of certain covariates can be identified and facilitate the modelling process.

2.5.1.2 Pharmacometric model components

A NLME model describes the relation of dependent variables (e.g. concentration of a drug in serum or bacterial numbers in a certain organ) and independent variables (e.g. sampling or dosing time points) by mathematical equations. Based on the selection of an appropriate underlying model and initial parameter estimates, final parameter estimates are calculated that are best able to describe the underlying observations. Here, the model itself can consist of three major parts that will be explained in more detail: (i) the structural, (ii) the statistical and (iii) the covariate model. In the process of developing a pharmacometric model, a structural model with statistical model components is built first before other components, such as variability in a statistical submodel or the covariate effect, are added.

Structural model. Selection of an appropriate structural model is crucial to adequately describe the data as population already without inclusion of any variability. In context of NLME modelling, it is made use of compartments that are considered to structure the model. Compartments represent kinetically

homogeneous parts of the body to which the drug evenly distribute [128]. Due to this compartmental structure, the dependent variable is described simplified by model parameters, e.g. a concentration-time profile by using PK parameters. Compartments can be organised in different constellations with a one- or two-compartment model being the simplest form. Generally, a structural model is expressed as mathematical equation depending on a set of parameters and dependent and independent variables (Equation 2.3).

$$Y_{ij} = f(\Theta, x_{ij}) \tag{2.3}$$

Here, Y is the vector of a dependent variable of interest for all i^{th} individuals of the population at the j^{th} measured time point as a function of independent variables x_{ij} given a vector Θ containing the estimable parameter estimates [126,133]. In a structural model, these mathematical basics are commonly implemented as ordinary differential equations (ODEs).

Statistical model. To explain differences between single measurements, random effects as part of the statistical model are added to a structural model. Describing variability is of high importance to include covariate effects in a next step. Mainly, these random effects are differentiated on two hierarchical levels into IIV and RUV.

Interindividual variability. To assess the extent of variability between different individuals, IIV is introduced as variance of a parameter of the structural model. For instance, the PK parameter *CL* is not expected to be the same among all investigated individuals but will rather differ between them due to e.g. physiological differences. Nevertheless, IIV may not always be estimated reliably for each single parameter of the structural model, e.g. in cases of sparse data. Here, these parameters are treated as fixed parameter estimates without IIV. In general, IIV can be included mathematically in different ways depending on the type of underlying data. Commonly, plausible PK parameters are greater than zero and right-skewed and, hence, log-normally distributed [132]. As a consequence, this exponential relationship is depicted by model parameters θ_{ik} for the i^{th} individual and k^{th} parameter as:

$$\theta_{ik} = \theta_k \cdot e^{\eta_{ik}} \qquad \eta_{ik} \sim \mathcal{N}(0, \omega_k^2) \tag{2.4}$$

Where θ_k is the typical value of the population of a certain parameter k and η_{ik} the deviation from the population value for the i^{th} individual and the k^{th} parameter with a mean of zero and a normal distributed variance ω_k^2. Alternatively, IIV can also be included in an additive way on an arithmetic scale, which is more common for parameters of a PD model [126]. For log-normally distributed data, the variance is typically reported as %CV by converting the variance from the logarithmic to the original dimension. For this easier interpretation, the CV is calculated as depicted in Equation 2.5.

$$CV, \% = \sqrt{e^{\omega_k^2 - 1}} \cdot 100 \tag{2.5}$$

Across a population, correlation between random effects can occur. For this purpose, a covariance term is introduced and represented in an omega matrix Ω. As example, an omega matrix is depicted in Equation 2.6 for two parameters.

$$\Omega = \begin{pmatrix} \omega_{1,1}^2 & \omega_{2,1} \\ \omega_{1,2} & \omega_{2,2}^2 \end{pmatrix} \tag{2.6}$$

Here, the diagonal elements of the matrix are referred as variance terms and the off-diagonal elements as covariance terms of two parameters, here e.g. $\omega_{1,2}$. Unless not explicitly modelled in NONMEM®, covariances are assumed to be zero and parameters to be not correlated [88]. In case of correlation, covariances are typically reported as %correlation coefficient, e.g. $\rho_{1,2}$ (Equation 2.7).

$$\rho_{1,2}, \% = \frac{\omega_{1,2}}{\sqrt{\omega_{1,1}^2 \cdot \omega_{2,2}^2}} \cdot 100 \tag{2.7}$$

Residual unexplained variability. The difference between a single observation of an individual and the model-predicted dependent variable of the respective individual is captured by the RUV including for instance assay variability (e.g. inconsistencies in sample collection, storage, recording of sampling time or imprecision of the bioanalytical method) or model misspecification [132]. Commonly, RUV is mathematically implemented depending on the underlying data in an additive (Equation 2.8), proportional (Equation 2.9), combined (Equation 2.10) or exponential (Equation 2.11) RUV model.

$$Y_{ij} = f(\Theta, x_{ij}) + \varepsilon_{add,ij} \tag{2.8}$$

$$Y_{ij} = f(\Theta, x_{ij}) \cdot (1 + \varepsilon_{prop,ij}) \tag{2.9}$$

$$Y_{ij} = f(\Theta, x_{ij}) \cdot (1 + \varepsilon_{prop,ij}) + \varepsilon_{add,ij} \tag{2.10}$$

$$Y_{ij} = f(\Theta, x_{ij}) \cdot e^{\varepsilon_{exp,ij}} \tag{2.11}$$

In Equations 2.8 to 2.11, ε_{ij} describes the differences between observed measurements and model-predicted dependent variables of the i^{th} individual at the j^{th} observation. It is assumed to be normally distributed and centered around zero as deviations between observation and estimation can occur in two directions, either under- or overprediction of the model. Commonly, RUV is implemented as the determined variance σ^2 of this distribution, often reported as %CV on standard deviation scale. A common strategy for PK data is to start using a combined RUV model that can be simplified subsequently, if one residual variance component is close to zero [126]. PD data, e.g. change to baseline blood pressure, are known to be more variable [134] and for a comparable variance across the range of possible values and, hence, an additive RUV model may be sufficient with the variance being assumed constant over the entire range [132]. Here, RUV is often reported as on a standard deviation scale with the unit of the dependent variable [129]. In a proportional RUV model, the variance is proportional to the magnitude of possible values of the dependent variable.

Interoccasion variability. A possible third level estimating variability between different occasions can also be implemented, when e.g. a drug was administered on two different occasions. This was not part of the present work and, hence, will not be discussed in this framework.

Specific cases affecting the statistical model. Introducing statistical models in the area of NLME modelling also requires mentioning specific factors (e.g. destructive sampling or log-transformed dependent variable) that can occur in data analysis.

In case of destructive sampling with only one sample per individual, it might not be feasible to estimate valid parameter estimates of two hierarchical levels of variability due to the sparseness of the data. Various studies have shown that modelling of destructively assessed PK data are less biased and more accurate by performing NLME modelling instead of naïve pooling or noncompartmental analysis [135,136]. However, with only one sample per individual, the two hierarchical levels of random effects, IIV and RUV, cannot be distinguished [126]. Either RUV can be estimated or RUV can be fixed to a variability of an underlying assay, e.g. the imprecision of a bioanalytical method, and IIV can be estimated instead.

A log-transformation of the underlying dependent variables may be appropriate to better describe the data and facilitate parameter estimation with increased numerical stability in specific cases. Here, an additive RUV model is used corresponding to a proportional RUV model on linear scale.

Covariate model. A covariate is an individual-specific variable that may be able to explain parts of the IIV in the dependent variable and, hence, in the PK and PD of a drug. In consequence of implementing a covariate model, variability of random effects in the statistical model should be reduced. Different covariates can be implemented in various ways. Most important covariates are e.g. body weight or renal function in PK. Commonly, they are classified into continuous (e.g. age, dose, body weight) and categorical (e.g. genotype, race, sex) covariates or intrinsic (e.g. age, height, race) and extrinsic (e.g. dose, smoking status) covariates. A covariate can be associated to different parameters of the structural model in a quantitative relationship [128] and, hence, explain differences in an estimated parameter for several individuals within a population. The way a covariate impacts a parameter of a structural model can be implemented in a linear, exponential or power model next to several other mathematical implementations mostly depending on the data given. Also, several covariates can be combined, if there is a joint effect on a certain parameter. The procedure of selecting the covariates that are best able to explain individual differences includes in a first step the exploration of the underlying data and the covariates comprehensively in an EGA. Subsequently, potential covariates can be selected [132]. Next, the covariate is implemented on specific parameters in an appropriate way. A decision on a covariate is made by e.g. performing a likelihood ratio test (LRT) or making use of graphical analytical tools, such as individual parameter estimates vs. covariates. Foremost, statistically significant covariates are selected that are able to explain variability within a population biologically plausible and with a clinical

relevance. As a consequence of a successful implementation of covariates, differences between individuals can be explained, and dosing may be individualised in a next step by e.g. linking exposure to specific covariates.

2.5.1.3 Parameter estimation

Parameter estimates of a NLME model are identified aiming at the best description of the underlying data on an individual and population level. This estimation of parameters requires advanced numerical analytical tools and is commonly performed by the maximum likelihood estimation approach. Comparable to a linear regression, where the least squares, so the difference between observed and predicted dependent variables, is minimised, a minimisation is performed in the maximum likelihood estimation approach to maximise the likelihood of finding the set of model parameters describing the observed data best. Here, weighing of specific parts of the data is avoided by assuming a normal distribution for the range of possible values of the predicted dependent variable. As likelihood, the difference of the observed from the mean of this distribution is calculated in probability density functions.

$$\mathcal{L}_i(\theta, \omega^2, \sigma^2 | Y_i) = p(Y_i | \theta, \omega^2, \sigma^2) \tag{2.12}$$

In Equation 2.12, L_i is the likelihood of the observations Y for the i^{th} individual given the model parameters θ, ω^2 and σ^2. The corresponding probability density function p aims to determine the set of model parameters θ, ω^2 and σ^2 given the observed data Y for the i^{th} individual that describe the distribution of the observations. For several observations j of i^{th} individuals, the likelihood is the product of the individual likelihoods (Equation 2.13).

$$\mathcal{L}_i(\theta, \omega^2, \sigma^2 | Y_i) = p(Y_i | \theta, \omega^2, \sigma^2) = \prod_{j=1}^{n_i} \mathcal{L}_i\left(\theta, \omega^2, \sigma^2 \middle| Y_{ij}\right) \tag{2.13}$$

To guide the process of model selection, minimising the objective function value (OFV) of the maximum likelihood estimation is aimed for by characterising the fit of the model to the data. The OFV is expressed as minus twice the sum of the natural logarithm of the likelihoods. Accordingly and considering the extent of the statistical model, the OFV is characterised as numerical value indicating how close the predicted data matches the observations. Using that approach, aspects of the statistical model can be estimated simultaneously.

Since analytical solutions for the maximum likelihood estimation were not feasible in context of this thesis given the underlying data base, several approximations can be used as estimation methods to determine parameters of a model that best match the data [137]. Possible estimation methods for NLME models are the first-order estimation (FO) method, the first-order conditional estimation (FOCE) method or the Laplacian method next to several other methods. For the FOCE method, the likelihood is approximated by using a Taylor series expansion [138]. A similar approach considering interaction between IIV and RUV is also available, termed FOCE with interaction (FOCE+I). The FO approach is

a further simplification of the FOCE method. The Laplacian method uses the second derivative instead of only considering the first derivative in the FOCE method, can treat categorical data and is less inaccurate for sparse data [139].

2.5.1.4 Handling data below the lower limit of quantification

To account for dependent variables with concentrations below the LLOQ (BLQ), different methods are proposed to handle these BLQ values [140]. In general, BLQ values should be avoided by e.g. appropriate bioanalytical quantification methods with a broad calibration range or plating of the appropriate dissolution in a droplet plate assay. Nevertheless, BLQ values cannot always be avoided and should be considered for analysis. Discarding these observations in the so-called M1-method may create a bias and lead to concentrations higher as they actually are [140]. Also, setting these observations to 0 or to LLOQ/2 may create a bias, if concentrations are much lower (M5- and M7-method, respectively). For this purpose, the so-called M3-method is of advantage, where the BLQ observations are treated as categorical data and the likelihood that a concentration is below the LLOQ is estimated (Chapter 2.5.3.2, [141]. Since continuous and categorical data are analysed simultaneously, the Laplacian estimation algorithm has to be used.

2.5.1.5 Pharmacokinetic/pharmacodynamic modelling

Present observations on a PK and PD level in the same time period enable to perform integrated PK/PD modelling. PK and PD components are linked by using various approaches, such as direct link or separate e.g. effect compartments [142]. As a consequence, an effect of a certain drug or a specific treatment regimen is evaluated based on PK information in addition to the expected PD effects. PK/PD modelling is performed in a sequential or simultaneous approach [143]. In the letter case, all PK and PD data are analysed simultaneously. Applying a sequential approach, modelling of PK and PD data is performed in two consecutive steps.

2.5.1.6 Time-to-event analysis

Time-to-event (TTE) analysis is a statistical framework frequently employed to analyse survival data and evaluate the influence of relevant PK and PD parameters on survival (Chapter 2.5.3.2). The impact of certain predictors, e.g. different study groups or PK/PD parameters, can be estimated and a link between disease progression and a certain clinical outcome, such as survival status, is possible. Three different approaches exist in context of TTE modelling to describe survival data: a nonparametric, a semi-parametric and a parametric approach [144]. Non-parametric approaches, such as the Kaplan-Meyer method, are only descriptive, i.e. used to calculate the survival probabilities at different time points. No time-varying covariates can be evaluated on survival probability nor are simulations possible. In semiparametric approaches, such as a cox-proportional hazard model, no baseline hazard distribution is assumed and, hence, no simulation studies are possible. The most complex approach is the parametric

approach. This statistical method uses a specific parametric distribution of the outcome events, in this case time of death, and, consequently, hazard and survival are completely parametrically specified. Here, simulating survival is possible from the established parametric distribution of survival times. Due to the mentioned advantages, the latter approach will be introduced in detail in the following part.

In survival analysis, the time from start of the study until occurrence of a response, termed event, is evaluated. Most often, survival studies are performed in context of TTE analysis with a binary outcome of either being alive or dead. Such an event can only occur once per individual. However, it has to be distinguished at what time point an event occurs, especially if the exact time of the event is unknown. For this purpose, the term censoring was introduced [145]. Right-censored events include all individuals that stay alive until the end of a study, whereas left-censored events include individuals that are known to have had an event before start of the study. Interval-censored events are characterised by having the event in between two observation time points. By also including these individuals with a not exact time of the event, a possible bias of the results by neglecting them is avoided [144].

Assuming a parametric distribution that is able to describe the risk of observing an event, in this case death, at a specific time point a hazard function *h(t)* is generated relating individuals being alive to dead individuals [146]. Several existing distributions have been used as hazard functions and will shortly be introduced. The hazard itself is rather a propensity than a probability with the unit 1/time. In TTE analyses, the most suited distribution that is able to describe the underlying hazard is chosen. As distribution several different mathematical implementations are qualified. Most frequently used distributions with regard to survival analysis are the constant hazard distribution [147], Gompertz [147,148] and Weibull hazard distributions [147,149]. The constant hazard distribution describes a first-order dying of an individual with a constant hazard over time, termed baseline hazard λ_0 (Equation 2.14).

$$h(t) = \lambda_0 \tag{2.14}$$

Applying the Gompertz distribution, an decrease or increase in hazard over time is possible. The Gompertz distribution is characterised by a baseline hazard λ_0 and an exponential rate constant β (Equation 2.15).

$$h(t) = \lambda_0 \cdot e^{\beta \cdot t} \tag{2.15}$$

In the Weibull distribution a shape parameter γ and a scale parameter λ are included to describe the hazard (Equation 2.16). Here, the hazard can be constant (γ=0), decreasing (0<γ<1) or increasing (γ>1) over time.

$$h(t) = \lambda \cdot \gamma \cdot (\lambda \cdot t)^{\gamma - 1} \tag{2.16}$$

In addition, several other distributions can be evaluated displaying mainly unimodal distributions. Next to the not more in detail discussed log-logistic function [150], the log-normal distribution [150,151] or

other distribution proposed by Klein et al. and Zufferey et al. [145,152], the surge function [153] can also be applied. The surge function describes a periodic increase and decrease in hazard by including the surge amplitude *SA*, the half of the surge width at half maximum intensity *SW*, the peak time *PT* and a shape parameter γ (Equation 2.17).

$$h(t) = \frac{SA}{\left[\frac{(t-PT)^2}{SW^2}\right]^{\gamma} + 1} \tag{2.17}$$

For a better understanding of the described possible distribution that are able to characterise the hazard in a survival analysis, the hazard functions are visualised schematically in Figure 2.7.

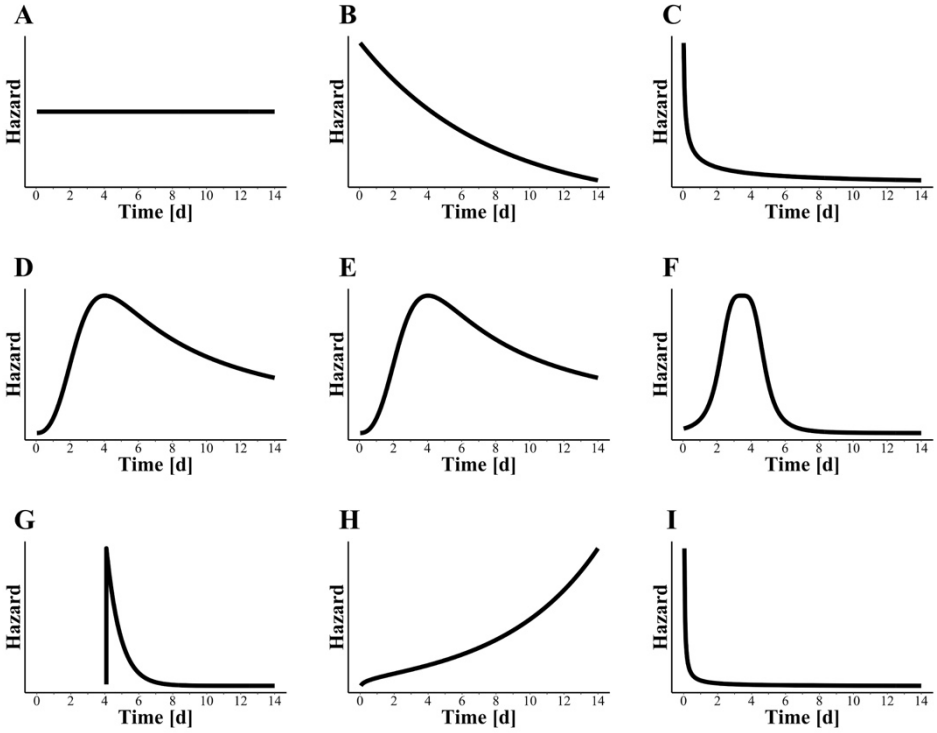

Figure 2.7: Distributions that are able to describe the risk of observing an event in hazard functions: (A) Exponential distribution, (B) Gompertz model with decrease in hazard over time, (C) Weibull distribution with decrease in hazard over time, (D) log-logistic function, (E) log-normal function, (F) surge function [153], (G) hazard function according to Zufferey et al. [152], (H) exponential power function, (I) Pareto function according to Klein et al. [145].

The probability of being alive until a certain study time t is described by the survival function *S(t)* and can be derived from the hazard function *h(t)*:

$$S(t) = e^{-cumhaz} = e^{-\int_0^t h(t)dt} \tag{2.18}$$

Where survival is a function of the cumulative hazard within a specific time interval [154]. The probability density function *pdf(t)* describes the likelihood of observing an event at a specific time. In case of an event at an exact time point, the *pdf(t)* is calculated as outlined in Equation 2.19.

$$pdf(t) = S(t) \cdot h(t) \tag{2.19}$$

In general, the *pdf(t)* obtained as product of hazard and the survival function. However, for calculation of the probability *Pr(t)*, the event censoring approach is relevant. For interval-censored events, the *Pr(t)* is calculated by accounting the survival status between specified time points (Equation 2.20).

$$Pr_{interval-censored}(t) = S\left(t_{start\ of\ interval}\right) - S(t_{end\ of\ interval}) \tag{2.20}$$

For a non-interval censored event, survival can be evaluated at the last observation (right censored events (Equation 2.21)) or the first observation time (left-censored (Equation 2.22)).

$$Pr_{right-censored}(t) = S(t) \tag{2.21}$$

$$Pr_{left-censored}(t) = 1 - S(t) \tag{2.22}$$

Hazard functions can be connected to possible time-varying or constant covariates, certain predicted PK/PD parameters or e.g. the time course of infection that may all be able to explain different survival patterns. Thereby, a link between a PK/PD model to the additional PD marker survival is established. These covariates are also implemented in different ways, mostly included as change in hazard. Potential covariates are commonly encoded exponentially in a hazard model to avoid a negative hazard:

$$h_{cov}(t) = h(t) \cdot e^{\beta_1 x_1 + \beta_2 x_2 + .. + \beta_n x_n} \tag{2.23}$$

Where β_i (i=1, …, n) are coefficients characterising the extent of potential covariate effects of different covariate values x_i (i=1, …, n) [146,152,155]. In addition, the effect of a covariate can be modelled centred to the median value of the covariate [156]. Next to the reported exponential implementation of a covariate effect on the hazard, this effect can also be modelled by an inhibition model [153]. Also, a covariate effect can be added directly to a respective model parameter, e.g. in an additive or exponential parametrisation [156].

In this setting, multiple PK and PD properties are allowed to influence the hazard function and are implemented as covariates including categorical and continuous variables. Model selection criteria were used to select a final covariate model (Chapter 2.5.2).

2.5.1.7 Simulations

Based on a developed PK/PD and TTE model, *in silico* simulations are performed to further investigate the model and assess the outcome of a model in case of a different input to the model [101]. Here, relevant questions can be asked about various aspects of the project, e.g. the influence of different dosing regimens on drug exposure. Optimally, these questions are answered by performing *in silico* simulations based on a predictive model. Using this approach, questions are addressed that otherwise would have required the realisation of additional experiments and, hence, simulations serve to reduce an intensive use of resources and the number of individuals investigated in a study.

Generally, *in silico* simulations are categorised into two types: Deterministic and stochastic simulations [126]. Deterministic simulations are based on fixed-effects parameters and do not allow variability via random effects and, hence, no IIV and RUV are included. Here, a unique output is generated given a constant input. Deterministic simulations are performed to obtain e.g. a PK or PD profile of a typical individual of the population and explore how the system reacts to e.g. changes in the administered dose. Contrarily, stochastic simulations, also termed Monte Carlo simulations, explicitly include random effects.

Possible applications of simulation studies comprise the evaluation of a performed study with respect to altering characteristics of the study. For instance, dose adjustments, a longer observation period or prediction of a specific outcome under certain assumptions can be assessed as well as extreme scenarios can be evaluated (Chapter 2.5.4). Also, simulations are used to evaluate the developed PK/PD and TTE model by simulation-based diagnostics, e.g. visual predictive checks (VPCs, Chapter 2.5.2).

2.5.2 Pharmacometric model evaluation

During the entire development process of a pharmacometric model, a comprehensive model evaluation is essential at each single stage to decide about the predictive performance of the model, next steps and on selecting a proper model. It is mandatory to check if underlying assumptions of the model can be accepted. Here, it is crucial to judge about a model rather as "context-of-use" approach, i.e. research question, instead of classifying into right or wrong [128]. Next to important factors that prove stability, such as a successful convergence of parameter estimation, another major step in model evaluation is the comparison of predicted model parameters to literature for plausibility. Other model evaluation techniques are classified into numerical and graphical evaluation techniques and are explained in more detail. In the early stages of model development, it is advisable to focus on more simple evaluation techniques, such as LRT or goodness-of-fit (GOF) plots. More complex evaluation techniques (e.g. VPC or bootstrap analysis) are typically rather used in a more advanced stage of model development. In general, all model evaluation techniques should be considered collectively, if a decision for one model has to be made.

2.5.2.1 Numerical evaluation techniques

For comparison between nested or non-nested pharmacometric models, the objective function value (OFV) or the Akaike information criterion (AIC), respectively, are used together with parameters of precision.

Objective function value and likelihood ratio test. During all stages of model development, evaluation of models according to their OFV is a key factor (Chapter 3.4.1). As already described in Chapter 2.5.1.3, the OFV is expressed as the minimisation of minus twice the sum of the natural logarithm of the likelihood function (*-2LL*). Generally speaking, this means: The smaller the OFV in

comparison of specific models, the better the fit of the respective model. In comparison of two nested models, a LRT is performed [132]. Here, it is tested for a statistically significant improvement in a "full model" with e.g. a certain parameter being estimated compared to a "reduced model" with e.g. the respective parameter typically fixed to zero. The difference of the *-2LL* of these two nested models is assumed to follow a χ^2 distribution. A decrease of more than 3.84 ($p \leq 0.05$, $\alpha=0.05$, *df*=1) of the OFV is accepted as statistically significant for these nested models differentiating in one parameter. With a different number of parameters *df* or different tested significant levels α, the values of the χ^2 distribution, that determine a statistically significant difference, change accordingly.

Akaike information criterion. The AIC is an extension of the maximum likelihood principle and a useful tool to compare two non-nested models [157].

$$AIC = -2LL + 2p \tag{2.24}$$

In equation 2.24, p is the total number of parameters of the model and *-2LL* refers to the OFV. Here, a higher number of model parameters increases the AIC value and serves as penalising term [132]. The model with the lower AIC value is selected as the superior model.

Precision parameters. During the pharmacometric model development process, it is aimed for high precision of the parameter estimates. Precision of a model is expressed either as relative standard error (RSE) or as accompanying confidence interval (CI). RSE are determined for each estimated parameter of the model. For this purpose, the variance-covariance matrix of fixed-effects or random-effects parameters is used. This is computed in the so-called covariance step as the inverse of the Fisher information matrix. The square-roots of the diagonal elements of the variance-covariance matrix are computed to assess the standard error (SE). The computed SE are expressed as RSE in a next step, depicted in Equation 2.25 for a certain fixed-effects parameter [88]. For random-effects parameters, imprecision is also often expressed on a standard deviation scale rather than on a variance scale illustrated for an IIV parameter in Equation 2.26. Since random effects are typically reported as %CV, this transformation is justified.

$$RSE_{\theta}, \% = \frac{SE_{\theta}}{\theta} \cdot 100 \tag{2.25}$$

$$RSE_{\omega^2}, \% = \frac{SE_{\omega^2}}{2 \cdot \omega^2} \cdot 100 \tag{2.26}$$

Acceptable ranges depend on various aspects, but typically RSE should be <30% for fixed-effects and <50% for random-effects parameters [132]. Based on determined RSE, a CI is derived assuming normal distribution. Typically, the 95% CI is calculated, depicted in Equation 2.27 for a certain fixed-effects parameter estimate.

$$95\%\ CI = \theta \pm 1.96 \cdot SE \tag{2.27}$$

Other more advanced numerical evaluation techniques are also present to determine a CI, such as a bootstrap analysis or the log-likelihood profiling (LLP), and are shortly outlined next.

Bootstrap analysis. Alternatively to already described possibilities of determining parameter imprecision, bootstrapping is another numerical evaluation technique to assess CIs [158]. Compared to a RSE, bootstrapping has the advantage that no specific assumptions of distributions of the parameter are used [126]. By applying a resampling technique, multiple datasets are generated by randomly choosing individuals from the dataset with replacing. Typically, 1000 bootstrap datasets are generated being necessary to determine a 95% CI [132]. Model parameters are estimated for these datasets. To successfully evaluate the generated results, a convergence rate of 90% is aimed for and also proves for robustness of the model. Statistics of successfully converged estimations are calculated and summarised for each parameter of the model. Statistics including the 95% CI and e.g. the median can be compared to the original model estimates and relative deviations can be calculated.

Log-likelihood profiling. Another approach to determine the uncertainty of a model and define parameter precision and identifiability is the LLP. LLP is commonly applied, if RSEs are very high or not obtainable during parameter estimation (Chapter 3.4.1.2). Here, the aim is to investigate the global minimum and the surrounding area of the OFV in detail with the corresponding limits indicating significance. The parameter of interest is fixed to values over a broader range close to the final parameter estimate and other parameters will be estimated [109]. The OFVs are investigated for differences and the minimum should be identified. Results can also be evaluated by plotting the OFVs against the investigated values of the tested parameter estimate, determining the lowest point of the OFV curve and identifying the parameter estimate visually. By applying LLP, the 95% CI is determined by identifying the limits of the parameter value that are within a difference of 3.84 (α=0.05, *df*=1) between the OFV at the minimum and the respective others.

2.5.2.2 Graphical evaluation techniques

In addition to numerical evaluation techniques, graphical evaluation of a developed pharmacometric model is a useful technique to directly visualise the fit of a model and identify model misspecifications. Typically, graphical evaluation techniques comprise GOF plots and VPCs.

Goodness-of-fit plots. GOF plots are classified as a basic prediction-based diagnostic tool being created on an individual or population level. For a better evaluation of a model, the GOF plot can also be stratified, e.g. by different study groups. Several combinations of certain factors are analysed in this setting typically consisting of the observed dependent variable, the predicted dependent variable or the difference of both, termed residuals, and a few will shortly be introduced. A typically investigated basic plot comprises observations versus predictions on individual or population level aiming for being evenly scattered around the line of identity [159]. Obvious trends not matching the line of identity may be strong indicators for a model misspecification. A modification of the model may be appropriate in this

case. Residuals plotted against predictions or time should be centred evenly around zero with most values within ±2 standard deviations of the individual values [132]. A normalisation of the residuals is possible to facilitate interpretation and consider the commonly given magnitude of the data, expressed as weighed residuals or conditional weighed residuals in case FOCE has been used as estimation method. Also, observations and predictions are evaluated over time for an impression of the profile of predicted in comparison to observed data. Here, the individual predictions should match the observations and central or time-dependent tendencies should be identified. In case of covariates implemented in the model, the selection of covariates is supported by exploring the relationship of individual estimates of a certain parameter versus possible values of a covariate [88]. For continuous covariates, a scatter plot is evaluated aiming to detect obvious trends in this relationship. Contrarily, categorical covariates can be evaluated in boxplots.

Visual predictive check. VPCs are classified as a simulation-based graphical evaluation technique. A VPC is the graphical representation of a simulation output that is evaluated together with the original observations commonly against time. Here, the general trend as well as variability of the data is assessed. In a first step, a large number of datasets is simulated given the model to be investigated [88]. Typically, a simulation with 1000 replicates is performed and the distribution of observations and predictions is analysed in a next step. For this purpose, the results of these analyses are represented in a figure containing various factors. The original individual data points are depicted concomitantly with the 2.5^{th}, 50^{th} and 97.5^{th} or 5^{th}, 50^{th} and 95^{th} percentiles of the observations, corresponding to a 95% or 90% prediction interval, respectively [159]. For the simulated data, the 2.5^{th}, 50^{th} and 97.5^{th} or 5^{th}, 50^{th} and 95^{th} respective percentiles are calculated and displayed including the 95% CI around the respective percentiles. Smaller prediction intervals may be appropriate in specific cases, e.g. in a sparse data situation [88]. In case of observations and predictions below the LLOQ and usage of the so-called M3-method, the fraction of samples below the LLOQ is additionally simulated [160]. An important factor when performing a VPC analysis is an appropriate grouping, termed binning, of the data. As one strategy, observed and simulated data should be evenly distributed with an approximate equal number of observations per bin and statistics are calculated for these bins. A bin itself is classified as a small interval of the independent variable, usually time. Due to binning, large differences in the sample size over time leading to an erratic-looking profile can be avoided. Another drawback of common VPCs is that a heterogeneity in the study design, e.g. different doses, may interpretation of a VPC getting challenging. Here, either a stratification into different study groups or extending the VPC principle to prediction-corrected VPCs (pcVPC) may be appropriate. pcVPCs remove the variability coming from different dosing or covariate relationships by normalising the observations or predictions to the typical population prediction of the respective observation or prediction and scaling to the median of the independent variable of a bin [161].

$$pcY_{ij} = \frac{Y_{ij}}{PRED_{ij}} \cdot \widehat{PRED_{bin}} \quad (2.28)$$

In Equation 2.28, the prediction-corrected dependent variable of the i^{th} individual at the j^{th} observation (pcY_{ij}) depends on a certain dependent variable of the i^{th} individual at the j^{th} observation (Y_{ij}), the corresponding population prediction of the i^{th} individual at the j^{th} observation ($PRED_{ij}$) and the median prediction of the bin ($\widehat{PRED_{bin}}$).

2.5.3 Pharmacokinetic/pharmacodynamic analysis of the combination of amoxicillin and monophosphoryl lipid A

The combination of AMX and MPLA was comprehensively investigated *in silico* based on the available diverse and thorough data that was generated in the pooled *in vivo* studies at the Institut Pasteur de Lille, France. The aim of this analysis was (i) to describe and predict the PK and the PD of AMX alone and in combination with MPLA based on AMX concentrations and bacterial numbers and (ii) to define a PK/PD marker to predict probability of survival. Finally, the developed PK/PD and TTE model should enable a translation into a clinical setting.

In a stepwise and consecutive approach, a PK analysis of the *in vivo* study was performed, and the respective PD parts (Chapters 3.3.2-3.3.3) were linked to enable the assessment of the overarching objective of this analysis. Here, three parts of the comprehensive *in vivo* study in mice being infected with *S. pneumoniae* serotype 1 and either untreated as control or treated with AMX and MPLA coadministration were chosen and investigated in detail: PK of AMX, bacterial numbers in lung and spleen, and survival of mice.

For the purpose of an errorless analysis, i.e. by e.g. identifying obvious trends in the data base, comprehensive ESA and EGA of generated data were conducted. It was mandatory to review the generated experimental data extensively for plausibility and completeness. The methods and required information of reported and studied parameters for thorough ESA and EGA were already outlined in respective chapters of the pooled *in vivo* studies (Chapters 2.4.1, 2.4.2 and 2.4.3).

In these chapters, the outline of the semi-mechanistic PK/PD and TTE analysis is described in detail. After introducing specific requirements and giving a short explanation of the underlying datasets (Chapter 2.5.3.1), the model development strategy of the PK/PD model and connected survival analysis is outlined (Chapter 2.5.3.2). Subsequently, basics of a simulation study will be introduced (Chapter 2.5.4) to investigate the feasibility of a translation into a clinical setting (Chapter 2.5.5).

2.5.3.1 Dataset generation

As outlined in Chapter 2.5.1.1, datasets were generated separately for the analysis of PK, PD and survival data in a first step based on the required specific structure for NONMEM®. All dependent variables were investigated against the time after infection with doses of AMX being administered at

12 h. In specific situations, certain datasets were also combined in one dataset to ensure a simultaneous analysis of PK and PD or evaluate the influence of the time course of AMX or bacterial numbers on survival.

In the PK dataset, AMX serum concentrations were specified by the unit µg/mL. All concentrations that had been determined with the developed bioanalytical method were included in the dataset. To consider determined AMX concentrations below the LLOQ, a BLQ column was introduced indicating if a concentration was below (BLQ=1) or above (BLQ=0) the LLOQ. In addition, following potential categorical covariates that may influence the PK of AMX were introduced to the dataset: Infection status of the investigated mice (non-infected, infected) and treatment options (untreated, monotherapy with AMX, monotherapy with MPLA, combination therapy of AMX and MPLA).

Contrarily to the PK, bacterial numbers of the generated PD data were naturally log-transformed [100] and were specified by the unit log CFU/organ. Thereby, parameter estimation was facilitated and bacterial growth, typically being exponentially, was well characterised by the natural logarithm. For graphical visualisation and numerical comparison of the observed and predicted data, bacterial numbers were transformed into log10 CFU/organ after the estimation process. To separate the assessed numbers in lung or spleen, the origin of the samples was specified in a column defining the compartment and an additional column was added to the dataset specifying the origin of the data (lung=3, spleen=4). To consider determined bacterial numbers below the LLOQ, a BLQ column was introduced indicating if a number was below (BLQ=1) or above (BLQ=0) a specific LLOQ that differed between single observations and, hence, was added to the dataset in a LLOQ column. Missing samples (e.g. deceased mice, wrongly handled sample; 4 samples (Chapter 3.3.2)) were excluded from the dataset. Following potential covariates that may influence the bacterial numbers were introduced to the dataset: Administration of a dummy drug substituting either AMX or MPLA (yes, no), dose of AMX (0.4-14 mg/kg), treatment options (untreated, monotherapy with AMX, monotherapy with MPLA, combination therapy of AMX and MPLA), and possible types of mouse (Swiss, Balb/cJ).

To characterise survival, a NONMEM®-compatible dataset common for survival analysis was generated. Here, dependent variable values were included by considering a differentiation between exact events as well as right- and interval-censored events. The following potential covariates were included to investigate a predictive PK/PD marker: The maximum concentration of AMX, the AUC of AMX (AUC_{AMX}), the dose of AMX, bacterial numbers in lung at 24 or 48 h, bacterial numbers in spleen at 24 or 48 h, the AUC of bacterial numbers in lung or spleen, cotreatment with MPLA, and study groups.

2.5.3.2 Pharmacometric model development strategy

The aim of this analysis was to combine PK and PD of the investigated combination of AMX and MPLA in one semi-mechanistic PK/PD model. For this purpose, the PK/PD model was developed stepwise.

First of all, the PK submodel was developed to characterise the PK of AMX based on determined serum concentrations of AMX in mice including absorption of AMX from the gut into the blood after intragastrical administration by oral gavage and subsequent distribution, metabolism and excretion of AMX. To evaluate the antibacterial effect of the investigated combination, bacterial numbers of *S. pneumoniae* serotype 1 in lung and spleen over time were studied in a semi-mechanistic PK/PD analysis that was structured into (i) a bacterial disease submodel development, (ii) an effect compartment submodel development and (iii) the linkage to a disease and treatment submodel. Based on the developed PK/PD model, the evaluation of the additional PD parameter survival was finally assessed by applying survival analysis. The modelling strategy mainly based on mathematical considerations aiming to describe the underlying data. Proceeding from the developed schematic structure (Figure 2.8), the PK/PD model was extended gradually. The detailed model development process will be introduced in the following.

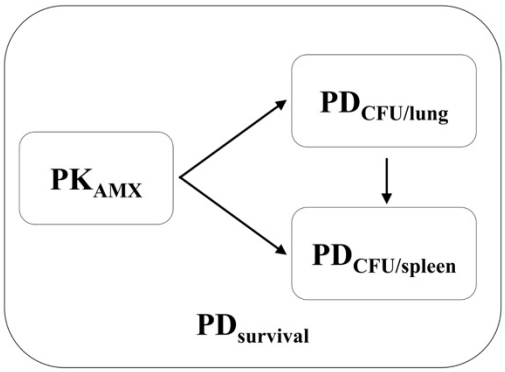

Figure 2.8: Model development process of a semi-mechanistic PK/PD model aiming to describe the PK of AMX (PK_{AMX}), the bacterial number of *Streptococcus pneumoniae* serotype 1 in lung and spleen ($PD_{CFU/lung}$ and $PD_{CFU/spleen}$, respectively) and survival of mice ($PD_{survival}$). Abbreviations: AMX: Amoxicillin; CFU: Colony forming units; PD: Pharmacodynamic(s); PK: Pharmacokinetic(s).

Model evaluation was performed as outlined in Chapter 2.5.2 to evaluate the predictive performance and guide model development. Briefly, various numerical and graphical evaluation techniques were deployed mainly focusing on the OFV, VPC and bootstrap analyses. Evaluation of the OFV aimed at a decrease of more than 3.84 (α=0.05, *df*=1). VPCs were performed with 1000 simulations with RUV or IIV (PK submodel only) and the resulting 90% prediction interval of observed and simulated data was investigated. Among others, parameter precision was assessed by bootstrap analyses with 1000 simulations. For a better understanding of single processes of the entire PK/PD model, specific structural model parts were evaluated and compared between single study groups. Here, the concentration-time profiles of AMX and bacterial numbers in all compartments were further investigated on a PK and PD level. Also, specific single parts of the structural model, such as bacterial growth without any killing or the pure killing effect of AMX without any other additional killing effects, as well as the time-dependent evolvement of single parameter estimates against time or respective concentrations were considered. To

directly assess the efficacy of the investigated combination, reduction in bacterial numbers in the respective study groups compared to bacterial numbers of untreated mice was evaluated.

Pharmacokinetic submodel. For AMX concentrations, typical PK compartment models (one-, two-, three-compartments) with oral administration, linear and nonlinear absorption and elimination processes and with or without a lag time were investigated. To consider several study samples with AMX concentrations below the LLOQ, these observations were treated as categorical data and the likelihood being below the LLOQ was estimated in the so-called M3-method (Chapter 2.5.1.4).

In the setup of the PK study, IIV was investigated, since it was at least partly sampled twice per individual mouse. This source of variability was included for various parameters in an exponential statistical model assuming PK parameters to be log-normally distributed (Equation 2.4). RUV was encoded as RUV model combining an additive and proportional RUV (Equation 2.10) obtaining the estimated RUV on the standard deviation scale and aimed for simplification to a proportional RUV model.

Potential covariates, such as the mouse type (Swiss, Balb/Cj), MPLA coadministration (yes, no) and the dose of AMX (0.4-14 mg/kg), were investigated: Their influence on the model parameters clearance, volume of distribution, intercompartmental clearance or absorption rate constant as categorial (mouse type, MPLA coadministration) or continuous (AMX dose) covariate was evaluated. The influence of MPLA coadministration on certain model parameters was evaluated by allowing MPLA as binary covariate to proportionally with the AMX dose change respective PK submodel parameters.

$$P = \theta_1 + \theta_2 \cdot DOSE \tag{2.29}$$

In Equation 2.29, θ_1 is the typical model-predicted value of a PK parameter P in mice that were not treated with MPLA, and θ_2 is a value for the influence altering θ_1 in case of MPLA coadministration and also depending on the dose of AMX ("DOSE").

Bacterial disease submodel. The bacterial disease submodel was developed to describe the growth of *S. pneumoniae* serotype 1 in lung and spleen of untreated animals. Hence, various options to describe bacterial growth will be introduced. These were investigated to characterise the number of bacteria in lung ($N_{bacteria,\ lung}$, Equation 2.30) and spleen ($N_{bacteria,\ spleen}$) and define important underlying processes in a simple growth model. Based on the visual time course of bacterial numbers in lung of untreated mice, a first-order growth rate constant (k_g) describing the natural growth of the bacterial strain was introduced affected by a delay in onset of growth (first-order rate constant k_{lag}) as an exponential term having less influence on k_g with increase in time [97]. To also capture the observed natural bacterial elimination processes in terms of treatment-unrelated killing and natural death kinetics, an additional first-order rate constant ($k_{kill,\ lung}$) term was introduced [101].

$$\frac{dN_{bacteria,lung}}{dt} = k_g \cdot \left(1 - \left(e^{-k_{lag} \cdot t}\right)\right) \cdot N_{bacteria,lung} - k_{kill,lung} \cdot N_{bacteria,lung} \qquad (2.30)$$

Typically, k_g and $k_{kill,\ lung}$ are represented as a single first-order rate constant k_{net} (k_{net}=k_g-$k_{kill,\ lung}$, [101]), connecting the often interdependent processes of growth and death. Such simplifications and additional parametrisations like limiting bacterial growth to a maximum value [162] or changes of mentioned parameters, e.g. bacterial killing as E_{max} model [97,101] or avoiding the direct estimation of k_{lag} within an exponential term by prebacterial compartments [101] were investigated and evaluated for improvement in OFV and AIC.

To capture the transit process of bacteria from lung to spleen, several approaches published in literature [101,134,163-166] were investigated and will shortly be introduced. Since data showed a delay in occurrence of bacteria in spleen of >12 h, parametrisations being able to include this delay were studied. Typically, these approaches are used to describe e.g. time-dependent signal transduction [165], the process of cell conversion [163,164] or a delay in absorption of a specific drug comparable to a lag time [166]. Furthermore, transit models are able to delay the transition from one to another compartment. Here, a series of differential equations added in a stepwise fashion for a specific number of compartments is placed between two respective compartments of interest. Each step represents a progression of transit to a next stage. These compartments are commonly characterised by not being affected by other parameters than a first-order transit rate constant (k_{tr}). As only one step is rate limiting, only k_{tr} is used instead of different rate constants characterising in- and outflow from a compartment [134]. This constant was computed by dividing the actual number of transit compartments (n), with $n+1$ indicating the number of transitions, by the estimated mean transition time (MTT):

$$k_{tr} = \frac{n+1}{MTT} \qquad (2.31)$$

Here, the greater the number of transit compartments and the smaller k_{tr} are, the greater the delay is. To specifically define the number of transit compartments instead of manually adding them, an advanced approach was utilised as proposed by Savic et al. [166]. Here, the number of compartments is estimated.

$$\frac{dN(n)}{dt} = input \cdot k_{tr} \cdot \frac{(k_{tr} \cdot t)^n \cdot e^{-k_{tr} \cdot t}}{n!} - k \cdot A(n) \qquad (2.32)$$

In Equation 2.32, $dN(n)/dt$ represents the rate of change of a certain number of bacteria in the n^{th} compartment at time t and $N(n)$ the actual number of bacteria in this compartment at time t. The first-order transit rate constant k_{tr} captures the transit from the n^{th-1} to the n^{th} compartment given a certain input, e.g. the dose in case of describing the absorption of a drug. The optimal number of compartments is characterised by n. The transit into the last compartment is described by a first-order disappearance rate constant k. Since data are commonly not informative enough, the constant k can be set to k_{tr} [101]. In a PK model, typically absorption into the central compartment as last step of transition is identified by a first-order absorption rate constant k_a. The factorial function of $n!$ is approximated by using a Stirling approximation (Equation 2.33).

$$n! \approx \sqrt{2\pi} \cdot n^{n+0.5} \cdot e^{-n} \tag{2.33}$$

In case of transferring bacteria from lung to spleen, this approach was adjusted. Here, in- and outflow of bacteria into transit compartments were given by bacterial numbers entering the transit compartments from lung and leaving into spleen, respectively (Equation 2.34).

$$\frac{dN(n)}{dt} = N_{bacteria,lung} \cdot k_{tr} \cdot \frac{(k_{tr} \cdot t)^n \cdot e^{-k_{tr} \cdot t}}{n!} - k_{tr} \cdot N(n) \tag{2.34}$$

The presented approaches to describe the transit of bacteria from lung to spleen were investigated in detail to adequately capture the underlying processes.

In spleen, implementation of an analogous growth submodel as in lung was studied by applying different growth and kill kinetics. Here, either a separate first-order growth rate constant for spleen or a common first-order growth rate constant for lung and spleen were investigated. The same procedure was applied for bacterial elimination kinetics as described for lung.

Effect compartment submodel. To set a basis for a subsequent link of the PK submodel of AMX concentrations in serum and the bacterial disease submodel accounting for distribution to the bacterial target sites lung and spleen, separate effect compartments were investigated [101,134,142]. By allowing the transfer of AMX from serum to lung or spleen compartments, a concentration-dependent time delay was introduced between the respective compartments and different in- and outflow kinetics (first-order, Michaelis Menten) were investigated. Thus, a time delay between administration of AMX and AMX being present in lung and spleen and being able to exert an effect on bacteria was captured. By e.g. using first-order in- and outflow, the concentration of AMX in the effect compartment (C_e) was determined as follows:

$$\frac{dC_e}{dt} = k_{e0} \cdot C_p - k_{e0} \cdot C_e \tag{2.35}$$

With k_{e0} being a first-order rate constant for the antibiotic transit and C_p and C_e being the concentrations of AMX in serum and the certain effect compartment, respectively. The higher k_{e0} was, the more rapidly the effect compartment equilibrated and, hence, more closely followed serum concentrations. In this setting, two independent effect compartments as well as one single effect compartment for lung and spleen were studied.

Disease and treatment submodel. The separately developed PK, bacterial disease and effect compartment submodels were extended to a joint disease and treatment submodel. In a first step, a sequential PK/PD analysis without individual PK data using population parameter estimates of the PK submodel was performed. All population parameter values of the respective PK submodel were fixed to their final estimates. Next, an extension to a simultaneous analysis of individual PK and PD data was studied.

For characterising the effect of AMX on bacteria, different mathematical implementations, such as a simple linear, a power, an ordinary E_{max}, a sigmoidal E_{max} model or a Richards model [167] were applied to the lung and spleen compartment and investigated: In comparison, the sigmoidal E_{max} model (Equation 2.36) served as reference and alternative models were evaluated for worsening in the model performance.

$$E(C_e) = \frac{E_{max} \cdot C_e^H}{EC_{50}^H + C_e^H} \tag{2.36}$$

In Equation 2.36, $E(C_e)$ is the drug effect of a defined antibiotic concentration, E_{max} is the maximum killing effect, EC_{50} is the AMX concentration to achieve the half maximum killing effect, C_e is the apparent AMX concentration in lung or spleen and H is the Hill factor.

Since no PK information for MPLA were collected and only one dose of MPLA was investigated, the influence of MLPA treatment had to be analysed as binary covariate (yes, no) and studied for the ability of MPLA to increase natural bacterial elimination effects characterised by $k_{kill,\ lung}$ or $k_{kill,\ spleen}$. This effect was mathematically implemented as proportionality factor affecting the first-order kill rate constants starting with drug administration at 12 h after infection.

In context of the disease and treatment submodel, possible PD interactions of AMX and MPLA were investigated to detect potential synergistic or antagonistic effects of both drugs in combination. Since MPLA was only studied at a single dose and no MPLA concentrations were determined (Chapter 4.2.1), no comprehensive response surface modelling evaluating Bliss Independence or Loewe Additivity was possible [168]. Nevertheless, to characterise, if MPLA had a significant effect on the efficacy of AMX, the potential of MPLA to modify the effect of AMX was investigated, e.g. by implementing an influence on the maximum killing effect E_{max} or the concentration of AMX needed to achieve half of the maximum effect EC_{50} according to the "General Pharmacodynamic Interaction Model" proposed by Wicha et al. [98]. The effect of MPLA was implemented as fractional change of respective effect parameters. The 95% CI of these estimated change parameter were evaluated, where the inclusion of 1 in the 95% CI indicated no significant change.

For the PD study of bacterial numbers, implementation of IIV was limited due to the fact that only one lung and spleen sample were taken from each individual mouse. As already outlined, this setting did not allow to reliably estimate more than one hierarchical level of variability simultaneously. Hence, only RUV was estimated in a first step and implemented additively on a logarithmic scale. To address this challenge in a next step and still investigate the implementation of IIV, RUV was aimed to be fixed to a characteristic experimental variability to allow estimation of IIV for different parameters of the PD model.

Time-to-event model. In order to investigate survival, a base model was developed for the respective study groups separately in a first step. Subsequently, an overall base survival model was jointly

evaluated for all generated data to characterise the survival in all individuals and quantify the impact of potential covariates. Here, the same baseline hazard was assumed for all individuals, as only one observation per individual mouse existed due to the nature of the study and no random effects could be estimated. Generally, various introduced hazard functions (Chapter 2.5.1.6) were investigated and evaluated to choose the distribution that best described the survival data. In this setting, multiple PK and PD properties were allowed to influence the hazard function and were implemented as covariates including categorial and continuous variables. On a PK level, mono- or combination therapy, the dose of AMX, C_{max} of AMX, AUC_{AMX}, or the actual concentration at a certain time t (C(t)) and respective combinations of single covariates were investigated. PD predictors included bacterial numbers at 24 h or 48 h in lung or spleen ($C_{lung,\ time}$, $C_{spleen,\ time}$), as well as the area under the bacterial number-time curve in lung or spleen ($AUC_{lung,\ time}$, $AUC_{spleen,\ time}$) or the actual bacterial number at time t ($CFU(t)$). In addition, PK/PD parameters, such as $T_{>MIC}$, the time period of AMX concentrations above the EC_{50} ($T_{>EC50}$), AUC/MIC or C_{max}/MIC, were evaluated.

2.5.4 Simulations: Exploration of the pharmacokinetic/pharmacodynamic model

To further explore the developed semi-mechanistic PK/PD model deterministic simulation studies were performed. Here, the general trend of the population and, consequently, the system itself was evaluated instead of results of individual mice with focussing on evaluating results in the lung. The simulation studies with higher numbers of observations over time aimed (i) to investigate longer than actually studied time periods, (ii) multiple dosing regimens in dose fractionation studies, (iii) varying characteristics of the investigated strain in terms of the MIC in susceptibility studies and (iv) prediction of PK/PD indices. On basis of a simulated dataset containing eight individuals, each individual representing one study group with observations every 5 min over a total time period of 48 h, deterministic simulations were performed.

Longer time period. To analyse the prediction of the PK/PD model over a longer time period than 48 h, a dataset of eight individuals, each representing one study group (Chapter 2.4.2), with observations every 30 min over one week was investigated in a simulation study. Bacterial numbers in lung over time were evaluated.

Dose fractionation study. A simulation-based dose fractionation study [169] was performed aiming to evaluate a wide range of total doses in different dosing regimens over a study period of 48 h in lung. For this purpose, total doses being below and above the actually studied doses were investigated. Different fixed total doses (n_{dose}=19) ranging from 0.05 to 30.0 mg/kg were either administered at 12 h after infection as single dose or fractionated into multiple administrations over 36 h after drug administration. In case of multiple doses, AMX was administered twice or in triplicate at 12 h and 36 h (q24h) or at 12 h, 24 h and 36 h (q12h) after infection, respectively. The time course of AMX concentrations in serum and bacterial numbers in lung was simulated. To judge the efficacy of the

therapy and assess detailed information about the significance of the study, the different dosing regimens were compared.

Susceptibility study. In a next step, the dose fractionation study was extended to a susceptibility study investigating altering characteristics of the bacterial strain being responsible for the infection. The experimentally employed bacterial strain of *S. pneumoniae* serotype 1 with a MIC value of 0.016 mg/L was characterised as susceptible. Based on the dataset of the dose fractionation study, MIC values above this MIC value were included to also cover resistant *S. pneumoniae* over the range of 0.016 to 8 mg/L (n_{MIC}=6). To allow a differentiation of the susceptibility of the bacterial strain, the MIC value was mathematically implemented as a factor being able to adjust the originally estimated parameter $EC_{50,base}$ in lung normalised to the MIC of 0.016 mg/L (Equation 2.37 [169]) under the assumption that EC_{50} increases linearly.

$$EC_{50} = \frac{EC_{50,base}}{0.016} \cdot MIC \tag{2.37}$$

Prediction of PK/PD indices. Finally, the generated results of the dose fractionation and susceptibility study were used to identify a PK/PD index being able to describe the relationship between drug exposure and reduction of bacterial numbers best. For this purpose, the behaviour of bacterial numbers in lung in relation to the PK/PD indices $T_{>MIC}$, C_{max}/MIC and AUC/MIC was analysed, and the selected parameter linked to the survival model.

2.5.5 Translational approaches: From mouse to human

Translational approaches were applied to translate the generated semi-mechanistic PK/PD model in mice (Chapter 3.4.1) to humans and allow prediction of a clinical setting. In this chapter, basic translational approaches will shortly be introduced to lay fundamentals of performed investigations.

Allometric scaling. One empirical approach to assess the predictability of a PK/PD model is the allometric scaling approach. Here, model parameters are extrapolated based on certain assumptions from preclinical studies to humans in an interspecies scaling approach. Typically, allometric scaling is employed in drug development, if no comparable parameters are present for humans. As a consequence, scaled parameter estimates are applied in PK/PD studies that want to simulate a clinical setting based on preclinical investigations. In detail, parameters are scaled accounting for species body weight based on similarities in anatomy and physiology. The basic assumption of allometric scaling in this context is that physiological processes are proportional between different species and correlated with body weight [170]. In a best-case scenario, data of more than two animal species [171] are pooled to allow for a reliable translation to human. In general, an extrapolated parameter is calculated in a power function (Equation 2.38, [172]).

$$parameter_{human} = parameter_{animal} \cdot \left(\frac{BW_{human}}{BW_{animal}}\right)^{exponent} \tag{2.38}$$

In Equation 2.38, the human PK parameter ($parameter_{human}$) is calculated based on the determined or estimated parameter in an animal ($parameter_{animal}$), the human and animal body weight (BW_{human} and BW_{animal}, respectively) and an exponent that typically is a multiple of 0.25. A body weight of 70 kg is regularly assumed for BW_{human}.

In a PK analysis, allometric scaling is regularly used to predict the PK parameters *CL*, *V* and, derived from both, the elimination half-life [173]. Depending of the investigated parameter, the beforehand mentioned basic assumption may be adjusted. PK parameters of volume (e.g. volume of a central compartment) are typically directly proportional to body weight leading to an exponent of 1 [170,174]. Extrapolations of the PK parameter *CL* are predictive, if the drug of interest is mainly excreted renally [172]. Here, an exponent of 0.75 has been proposed. In general, extrapolation of the parameter *CL* is challenging due to various simultaneous involved processes, such as passive glomerular filtration, active tubular secretion and active and passive reabsorption processes, that differ between the studied species. For this purpose, an extension of the basic allometric scaling approach is possible for *CL* by accounting for the kidney function in animal and human and calculating a correction factor [175]. The correction factor in this thesis assumed species specific glomerular filtration rates, kidney blood flows, body weights and kidney weights according to Davies et al. [122]. This may especially be appropriate in case of active renal secretion of a drug. Typically, rates, such as the heart rate or PD first-order rate constants, decrease with an increase in body weight, since physiological processes are regularly faster in small animals compared to humans [171,176]. Thus, an exponent of -0.25 is applied to first-order rate constants. The reason for this behaviour is that reported exponents are empirically derived from several studies and experiences. For instance, experimentally derived exponents of 0.8-1.1 are regularly observed for V_c [170] and exponents of 0.35 or 1.39 were observed for *CL* [177].

In this project, allometric scaling was performed to compare the extrapolated parameters to parameters reported in literature to prove comparability between species and plausibility of determined parameter estimates. On the PK level, *CL*, *Q*, V_c and V_p were scaled using the described allometric approach with typical exponents 0.75 for *CL* and *Q* and 1 for volume terms.

Translation into clinical setting. In the next step, the semi-mechanistic PK/PD model describing bacterial numbers in lung was extrapolated from mouse to human to investigate, if a clinical setting can be predicted. Here, a PK submodel describing AMX concentrations in humans was selected from literature in a first step (Chapter 3.4.2) and, subsequently, linked to the developed PD model. Applying the allometric scaling approach, an appropriate adjustment of PD parameters was investigated. In this setting, dose fractionation and susceptibility studies were performed as described beforehand (Chapter 2.5.4) over a study period of 48 h in lung. For this purpose, a simulation dataset was generated with different fixed total doses ranging from 0.1 to 6000 mg (n_{dose}=17) that were either administered at 12 h after infection as single dose (q48h) or fractionated into multiple administrations over 36 h after drug administration. In case of multiple doses, AMX was administered twice, thrice, five- or six-times every

24 h (q24h), 12 h (q12h), 8 h (q08h) or 6 h (q06h), respectively. An extension to a susceptibility study was performed by investigating *S. pneumoniae* with MIC values over the range of 0.016 to 8 mg/L (n_{MIC}=6) as described elsewhere (Chapter 2.5.4). The time course of AMX concentrations in serum and bacterial numbers in lung were simulated and PK/PD indices were evaluated.

2.6 Statistics

For statistical analysis of generated data, various statistical evaluation techniques, next to already introduced model evaluation techniques (Chapter 2.5.2), were used and are described in detail in this chapter.

2.6.1 Descriptive statistics

Measures of central tendency. Various localisation parameters were used to assess measures of central tendency: The median (Equation 2.39) is less prone to outliers and was used for datasets of only a few samples (n≤4) with expected higher dispersion [126].

$$\tilde{x}_{median} = \begin{cases} x_{\frac{n+1}{2}} & for\ uneven\ n \\ \frac{1}{2}\left[x_{\frac{n}{2}} + x_{\left(\frac{n}{2}+1\right)}\right] & for\ even\ n \end{cases} \tag{2.39}$$

The arithmetic mean (Equation 2.40) was used for data that were symmetrically distributed and not skewed [126].

$$\bar{x}_{arithmetic} = \frac{1}{n}\sum_{i=1}^{n} x_i \tag{2.40}$$

Especially for PK data that are commonly skewed in a log-normal distribution, the geometric mean was used (Equation 2.41, [126]).

$$\bar{x}_{geometric} = \sqrt[n]{\prod_{i=1}^{n} x_i} \tag{2.41}$$

Measures of variability. Dispersion parameters, such as the range (Equation 2.42), standard deviation σ (Equation 2.43), variance σ^2 (Equation 2.44), the CV (Equation 2.45) or the 95% CI (Equation 2.27), contain information about distribution of the data and were used to describe the precision of the generated data.

$$Range = x_{maximum} - x_{minimum} \tag{2.42}$$

$$\sigma = \sqrt{\frac{1}{n-1}\sum_{i=1}^{n}(x_i - \bar{x})^2} = \sqrt{\sigma^2} \tag{2.43}$$

$$\sigma^2 = \frac{1}{n-1}\sum_{i=1}^{n}(x_i - \bar{x})^2 \tag{2.44}$$

$$CV, \% = \frac{\sigma}{\bar{x}} \cdot 100 \tag{2.45}$$

2.6.2 Hypothesis testing

For exploratory statistical analysis of experimental data (3143), significant differences between two different study groups were determined for n≥3 experiments. For that purpose, the prerequisites of normal distribution and homogeneity of variance were evaluated by a Shapiro-Wilk test or F-test, respectively [178]. If criteria of normal distribution or homogeneity of variance were met, an unpaired two sample t-test was used. In the opposite case, a Welch t-test was used. The significance level α was set to 0.05 indicating a 5% risk of rejecting the null hypothesis when it was true. For >2 study groups, the Levene test was utilised to test for homogeneity of variance. Depending on whether criteria were met or not met, a one-way ANOVA or a Kruskal-Wallis test were performed, respectively, to compare ≥2 groups. Statistical tests were executed by using the software R with its package "stats" (version 3.6.0) and "car" (version 3.0-5).

For comparison of survival data, a log-rank test was used to evaluate differences between two single study groups with a significance level α of 0.05. This non-parametric test assumes no underlying distributions of the survival data and was calculated with the software R and its package "survminer" (version 0.4.6).

2.6.3 Linear regression analysis

A linear regression analysis was used to characterise the linear statistical relationship between two continuous variables [126]. A dependent variable y_i (e.g. LC-MS/MS detector response) was related to an independent variable x_i (e.g. concentration of CAL samples). Unknown model parameters β_0 (e.g. intercept with y-axis of calibration function) and β_1 (e.g. slope of the calibration function) were estimated based on dependent variables and independent variables given a regression equation containing an error term ε (Equation 2.46).

$$y_i = \beta_0 + \beta_1 x_i + \varepsilon_i \tag{2.46}$$

For that purpose, a minimisation criterion, in this case the residual sum of squares (RSS) of observed and predicted dependent variables, was used aiming to be minimised (Equation 2.47).

$$RSS = \sum_{i=1}^{n} (y_i - (\beta_0 + \beta_1 x_i))^2 \tag{2.47}$$

The coefficient of determination (R^2) was evaluated to decide on the goodness of fit of the regression analysis [126] with 1 being a perfect fit. The R^2 for an analytical assay should be >0.98 [126]. Linear regression analysis was performed in R with its package "stats" (version 3.6.0).

3 Results

3.1 Microbiological *in vitro* investigations

In the present chapter, results of microbiological investigations are summarised. Bacterial strains were classified into susceptible or resistant and several combinations of antibiotics, immunostimulatory drugs and bacterial strains were investigated regarding their direct and indirect effects *in vitro*.

3.1.1 Predefined principles of microbiological experiments

3.1.1.1 Bacterial stock suspension

Bacterial stock suspensions of each strain were adjusted aiming for bacterial concentrations of $1 \cdot 10^8$ CFU/mL (Chapter 2.2.1.3). In general, these concentrations were confirmed for *K. pneumoniae* (median: -6% for $n_{experiment}$=9, with 3-4 replicates each), *P. aeruginosa* (median: +24% for $n_{experiment}$=11, with 2-6 replicates in each) and *S. aureus* (median: ±0% for $n_{experiment}$=21, with 2-4 replicates each, Table 3.1). Minor deviations $\leq \pm 5.80 \cdot 10^7$ CFU/mL from the targeted concentrations were acceptable and mainly occurred due to a not consistent and reproducible surface of used glass vials that was not avoidable by standardising the process. Different from these three strains, *S. pneumoniae* serotype 1 revealed deviating bacterial concentrations. A turbidity of 0.5 McF corresponded to a median bacterial concentration of $1.20 \cdot 10^7$ CFU/mL (median: -88% for $n_{experiment}$=16, with 3-4 replicates each). To consider these results in all conducted experiments, the volume of 10 µL of the bacterial stock suspension that is commonly added to experiments was adjusted for *S. pneumoniae* serotype 1 to e.g. a volume of 80 µL to achieve a bacterial concentration of $1 \cdot 10^6$ CFU/mL in a total volume of 1 mL.

Table 3.1: Median bacterial concentrations and minimum and maximum concentrations indicated as range of a bacterial stock suspension with a turbidity of 0.5 McFarland determined by a McFarland densitometer.

Bacterial strain	Median bacterial concentration [CFU/mL]	Range of bacterial concentrations [CFU/mL]
Klebsiella pneumoniae ATCC 43816	$9.40 \cdot 10^7$	$7.20 \cdot 10^7$ - $1.32 \cdot 10^8$
Pseudomonas aeruginosa ATCC 15691	$1.24 \cdot 10^8$	$9.50 \cdot 10^7$ - $1.58 \cdot 10^8$
Staphylococcus aureus Newman	$1.00 \cdot 10^8$	$4.50 \cdot 10^7$ - $1.30 \cdot 10^8$
Streptococcus pneumoniae serotype 1	$1.20 \cdot 10^7$	$8.00 \cdot 10^6$ - $3.20 \cdot 10^7$

Abbreviations: ATCC: American Type Culture Collection; CFU: Colony forming units.

3.1.2 Characterisation of the susceptibility of the bacterial strains

3.1.2.1 Investigation of drug-specific requirements

Pioglitazone and colistin showed specific characteristics *in vitro* (Chapter 2.2.2.1) that were investigated in exploratory experiments to ensure reliable results.

Pioglitazone. Based on graphical analysis, bacterial growth was comparable for growth control and DMSO concentrations of 1%, 3% and 5% (v/v) over time ($n_{experiment}$=1, Figure 3.1). Highest differences were observed at 4 h in the logarithmic phase of bacterial growth. Nevertheless, addition of 5% DMSO reduced bacterial concentrations only by maximum 0.500 log10 CFU/mL at 4 h and 0.0583 log10 CFU/mL after 24 h. Contrarily, at a DMSO concentration of 10%, a distinct impact on bacterial growth was revealed by decreasing growth by 1.12, 0.656 and 0.429 log10 CFU/mL compared to growth control after 4, 8 or 24 h, respectively.

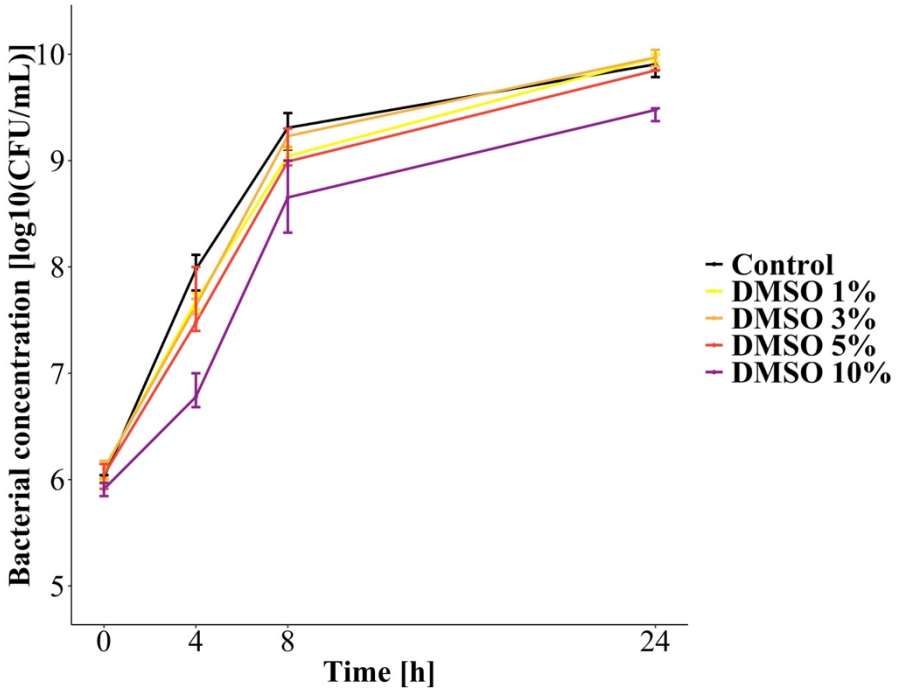

Figure 3.1: Impact of DMSO on bacterial growth of *Staphylococcus aureus* ATCC 29213 ($n_{experiment}$=1). The median of bacterial concentrations of bacteria exposed to 0% (control), 1%, 3%, 5% and 10% (v/v) is depicted as line including the range of minimum and maximum concentrations of up to 3 plated and quantified dilutions of one well. Abbreviations: ATCC: American Type Culture Collection; CFU: Colony forming units; DMSO: Dimethylsulfoxide.

Since DMSO concentrations in planned experiments were not larger than 5%, the use of DMSO as solvent for pioglitazone and additive to microbiological studies was justified. In addition, DMSO was added to growth and sterility control samples in all experiments conducted with pioglitazone (Chapters 2.2.2-2.2.3).

Colistin. With addition of polysorbate 80, the MIC value of colistin against *P. aeruginosa* PAO1 (1 mg/L (Chapter 3.1.2.2)) did not change. Reported significant changes in the MIC value were not confirmed. Hence, microbiological investigations with colistin were performed according to CLSI guidelines [91] without polysorbate 80.

3.1.2.2 Minimal inhibitory concentration

The MIC values were determined as the lowest concentration of a respective drug that prevents visible growth of a bacterial strain by using a broth dilution susceptibility testing as depicted in Figure 3.2 for the MIC determination of streptomycin against *P. aeruginosa* ATCC 15691 with an MIC value of 32 mg/L.

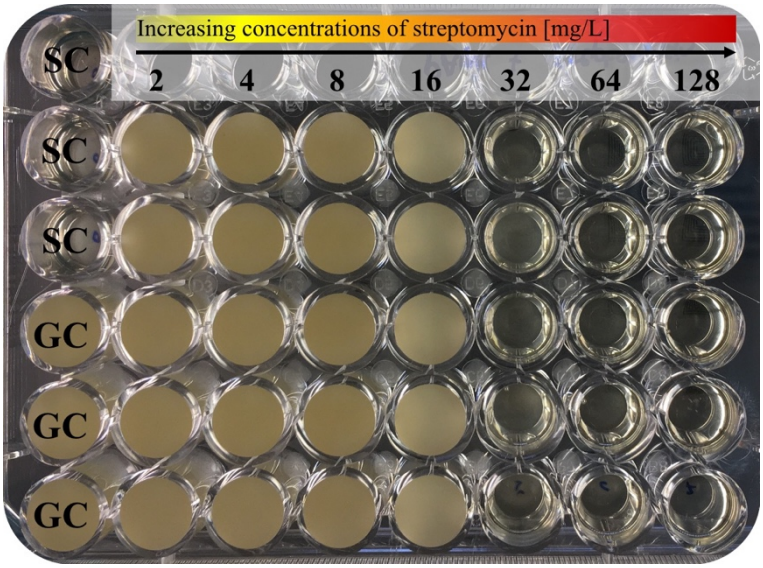

Figure 3.2: Determination of the minimal inhibitory concentration of streptomycin against *Pseudomonas aeruginosa* ATCC 15691 with sterility control samples (SC, 3 replicates), growth control samples (GC, 3 replicates) and samples exposed to different concentrations of streptomycin (2-128 mg/L; 5 replicates per concentration level). The lowest concentration of streptomycin that prevented visible growth was 32 mg/L.

In relation to the bacterial strain, antibiotics were classified according to reported breakpoint values by EUCAST (Table 3.2, [92]).

Table 3.2: Clinical breakpoints (mg/L) of amoxicillin, colistin, fosfomycin and streptomycin against *K. pneumoniae*, *P. aeruginosa*, *S. aureus* and *S. pneumoniae* reported by EUCAST guidelines [92].

Antibiotic drug	*K. pneumoniae*			*P. aeruginosa*			*S. aureus*			*S. pneumoniae*		
	S	I	R	S	I	R	S	I	R	S	I	R
Amoxicillin	≤4	8	≥16	-[1]	-[1]	-[1]	-[1]	-[1]	-[1]	≤0.5	1	≥2
Colistin	≤1	2	≥4	≤1	2	≥4	-[2]	-[2]	-[2]	-[2]	-[2]	-[2]
Fosfomycin	≤16	32	≥64	-[1]	-[1]	-[1]	≤16	32	≥64	-[1]	-[1]	-[1]
Streptomycin	-[1]	-[1]	-[1]	-[1]	-[1]	-[1]	-[1]	-[1]	-[1]	-[1]	-[1]	-[1]

Abbreviations: EUCAST: The European Committee on Antimicrobial susceptibility Testing; *K. pneumoniae*: *Klebsiella pneumoniae*; *P. aeruginosa*: *Pseudomonas aeruginosa*; *S. aureus*: *Staphylococcus aureus*; *S. pneumoniae*: Streptococcus pneumoniae; Susceptibility classification according to EUCAST (I: Susceptible at increased exposure; R: Resistant; S: Susceptible at standard dosing regimen). [1]No breakpoints reported by EUCAST; [2]Colistin not effective against Gram-positive bacteria.

Due to determined MIC values of the investigated antibiotics (Table 3.3), bacterial strains were in general susceptible against these antibiotics according to the mentioned breakpoints. Partly, inconsistent replicates per concentration level for the determination of the MIC of colistin and fosfomycin against *K. pneumoniae* were obtained and led to a classification as resistant in case of fosfomycin: In both cases, multiple single wells did not follow the general trend of the reported MIC values. However, these investigations rather aimed at identifying if bacterial strains were susceptible or resistant and, hence, the MIC value was reported despite the mentioned outliers.

For immunostimulatory drugs, a MIC value was not determinable within the tested concentration ranges and at least higher than the actual investigated concentrations. Hence, tested bacterial strains were assumed to be resistant against investigated immunostimulatory drugs.

Table 3.3: Determined minimal inhibitory concentrations ($n_{experiment}$=1-3 with 5 replicates) of multiple combinations of various antibiotic or immunostimulatory drugs and bacterial strains.

	K. pneumoniae ATCC 43816	*P. aeruginosa* ATCC 15691	*S. aureus* Newman	*S. pneumoniae* serotype 1
Antibiotic drugs				
Amoxicillin	-	-	0.25 mg/L	0.016 mg/L
Colistin	1 mg/L*	1 mg/L	-	-
Fosfomycin	64 mg/L*	32 mg/L	4 mg/L	-
Streptomycin	2 mg/L	32 mg/L	32 mg/L	-
Immunostimulatory drugs				
Metformin	-	-	>1000 mg/L**	-
MPLA	-	-	>1 mg/L	-
Pioglitazone	-	-	>480 mg/L**	-

Abbreviations: ATCC: American Type Culture Collection; *K. pneumoniae*: *Klebsiella pneumoniae*; MPLA: Monophosphoryl lipid A; *P. aeruginosa*: *Pseudomonas aeruginosa*; *S. aureus*: *Staphylococcus aureus*; *S. pneumoniae*: Streptococcus pneumoniae; * Minimal inhibitory concentration determined in 1 of 3 experiments; **Minimal inhibitory concentration determined with *S. aureus* ATCC 29213.

3.1.3 Drug-drug interaction investigation *in vitro*

As representative of the checkerboard investigations, the combination of streptomycin and pioglitazone against *S. aureus* ATCC 29213 will be presented in detail. In a conventional representation, pioglitazone had no antimicrobial effect in the evaluated concentration range indicated by turbid wells (Figure 3.3). Concentrations of streptomycin ≥16 mg/L caused bacterial killing with bacterial concentrations being below the visual detection limit (≈$5 \cdot 10^7$ CFU/mL).

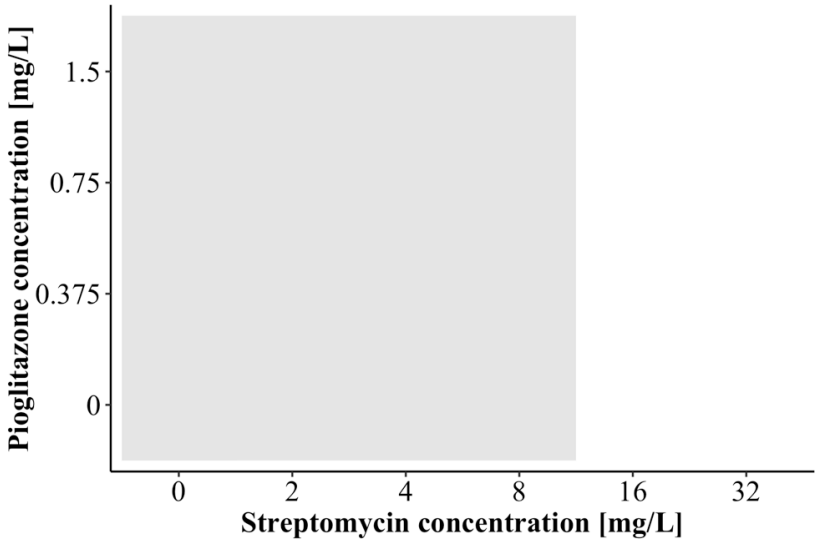

Figure 3.3: Conventional checkerboard of the combination of streptomycin (concentration range of 0-32 mg/L) and pioglitazone (concentration range of 0-1.5 mg/L) against *Staphylococcus aureus* ATCC 29213 ($n_{experiment}$=1) with differentiation between turbid (grey) and clear wells (white). Abbreviations: ATCC: American Type Culture Collection.

Evaluating all checkerboard experiments conventionally by visual assessment of turbidity did not reveal any altered effects by addition of metformin or pioglitazone to one of the studied antibiotics (Figure 3.3**)** compared to the single antibiotic drug effect. Both immunostimulatory drugs did not have an effect by their own in the tested concentration ranges. Hence, no interaction was determined by visual differentiation between turbid and clear wells.

Quantification of bacterial concentrations in each well after 20 h revealed a dynamic checkerboard plot (Figure 3.4). Streptomycin as single drug decreased bacterial concentrations from the starting inoculum of 6 log10 CFU/mL to a concentration below the LLOQ of 2 log10 CFU/mL at the highest drug concentration studied in this setting, compared to a growth control sample characterising maximum growth of 8.42 ±0.47 log10 CFU/mL. At a streptomycin concentration of 16 mg/L, bacterial concentrations were reduced by 1.26 log10 CFU/mL. Comparable to a conventional checkerboard assay that indicated clear wells without visible growth, the dynamic checkerboard showed bacterial growth with concentrations close to the visual detection limit at a streptomycin concentration of 16 mg/L. Addition of pioglitazone did not alter bacterial concentrations alone as well as in combination with streptomycin as depicted in Figure 3.4. Except for the highest concentrations of pioglitazone in combination with 16 mg/L streptomycin, bacterial concentrations were within a range 0.5 log10 CFU/mL per concentration level of streptomycin. Consequently, dynamic evaluation by quantifying bacteria in each single well showed comparable results between monotherapy and the combined treatment approach.

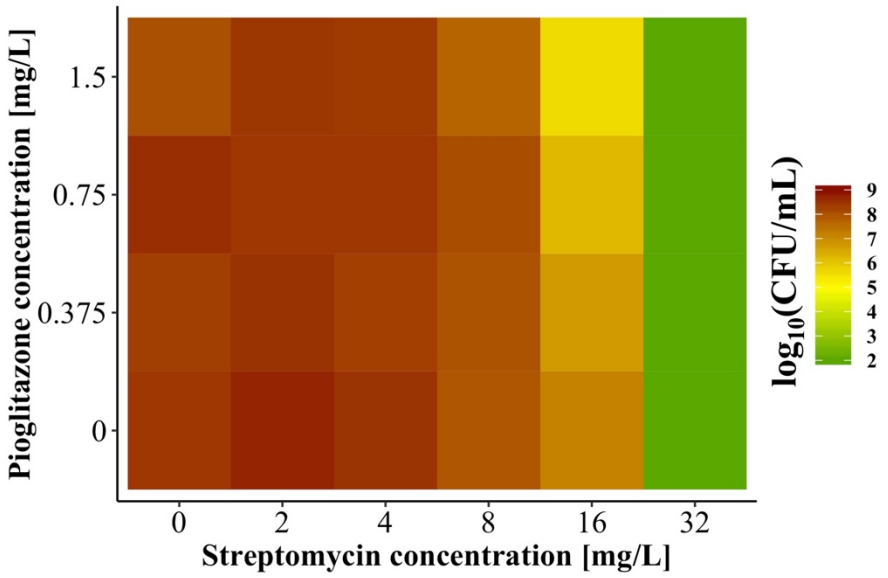

Figure 3.4: Dynamic checkerboard of the combination of streptomycin (concentration range of 0-32 mg/L) and pioglitazone (concentration range of 0-1.5 mg/L) against *Staphylococcus aureus* ATCC 29213 at an initial inoculum concentration of 6 log10 CFU/mL ($n_{experiment}$=1) displaying bacterial concentrations as log10 CFU/mL. Samples with bacterial concentrations below the LLOQ were set to the LLOQ of 2 log10 CFU/mL. Abbreviations: ATCC: American Type Culture Collection; CFU: Colony forming units; LLOQ: Lower limit of quantification.

3.1.4 Immunostimulatory effects in an *in vitro* infection model

After focussing on direct effects of antibiotics and immunostimulatory drugs in the previous chapters, the present chapter will mainly deal with indirect effects of immunostimulatory drugs and the influence of the immune system *in vitro*.

3.1.4.1 Bacterial growth in cell growth medium

Bacterial growth of *S. aureus* Newman and *S. pneumoniae* serotype 1 was visually noticeable in CAMHB and RPMI1640 with or without FBS over time. Bacterial growth in RPMI1640 with FBS led to a shift in the colour of phenol red from a bright pink to a weak yellow indicating a pH shift from a pH value of 8.2 to more acidic conditions below the pH value of 6.6 (Figure 7.2). This pH shift was not present in RPMI1640 without FBS indicating less bacterial growth probably due to missing nutrients in form of FBS.

Comparing bacterial concentrations over time in different media, *S. aureus* Newman revealed typical growth behaviour in CAMHB (Figure 3.5). Subsequent to a lag phase of 2 h, an increase in bacterial concentrations occurred up to a stationary phase at concentrations $>5 \cdot 10^8$ CFU/mL. In contrast, *S. aureus* Newman indicated a delay in transition from lag- into log-phase bacteria in RPMI1640 with FBS and displayed showed growth after approximately 4 h. After 8 h, maximum bacterial growth was achieved at $1 \cdot 10^7$ CFU/mL being reduced by 1.5 log10 CFU/mL compared to CAMHB. RPMI1640

without any supplementation indicated a comparable increase as CAMHB within the first 8 h. However, bacterial concentrations decreased afterwards to approximately $1 \cdot 10^7$ CFU/mL at 24 h.

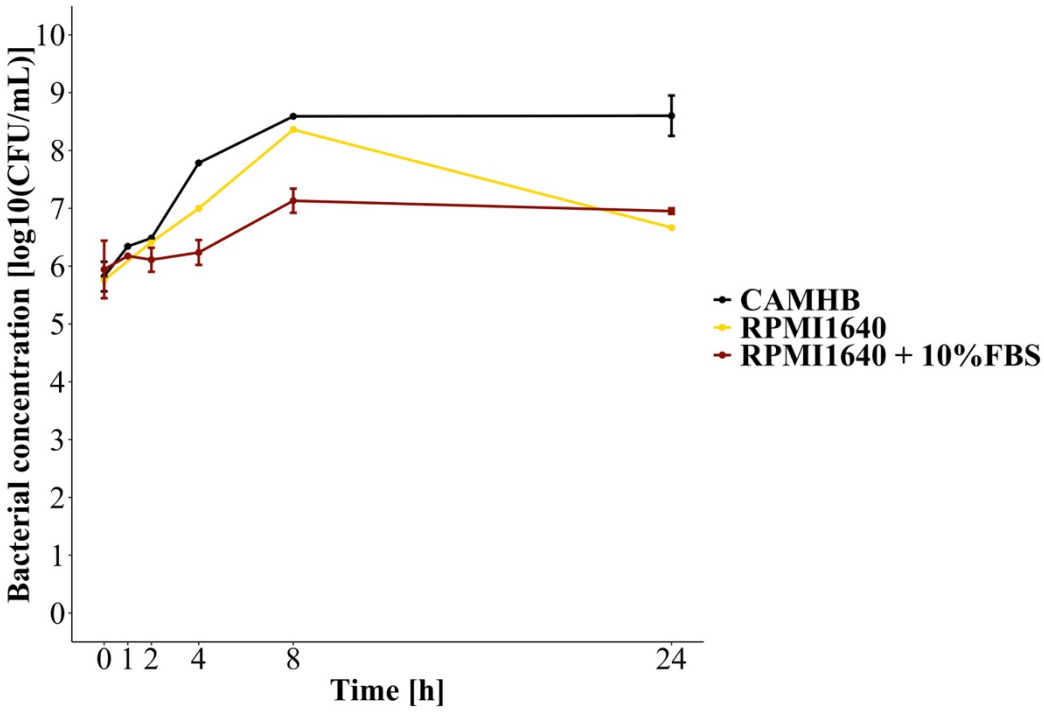

Figure 3.5: Bacterial growth of *Staphylococcus aureus* Newman versus time on a semi-logarithmic scale in (i) CAMHB ($n_{experiment}$=1-2), (ii) RPMI1640 without FBS ($n_{experiment}$=1) and (iii) RPMI1640 with 10% (v/v) FBS ($n_{experiment}$=2). The median (line) with minimum and maximum bacterial concentrations of the median of single experiments as error bar is depicted for each studied case. Abbreviations: CAMHB: Cation-adjusted Mueller-Hinton broth; CFU: Colony forming units; FBS: Foetal bovine serum; RPMI1640: Roswell Park Memorial Institute 1640 medium.

In line with *S. aureus* Newman, *S. pneumoniae* serotype 1 showed typical bacterial growth in the bacteria-specific growth medium achieving maximum concentrations of $1 \cdot 10^9$ CFU/mL at approximately 6 h (Figure 3.6). In RPMI1640 without supplementation, bacterial concentrations were constant within the first 5 h and finally decreased to bacterial concentrations of approximately $1 \cdot 10^4$ CFU/mL. Addition of FBS to RPMI1640 with increasing concentrations promoted growth of *S. pneumoniae* serotype 1 accordingly to $1 \cdot 10^6$ CFU/mL for 10% (v/v) addition of FBS at 8 h. In contrast to *S. aureus* Newman, addition of FBS allowed improved growth behaviour of *S. pneumoniae* serotype 1 compared to RPMI1640 without addition of FBS.

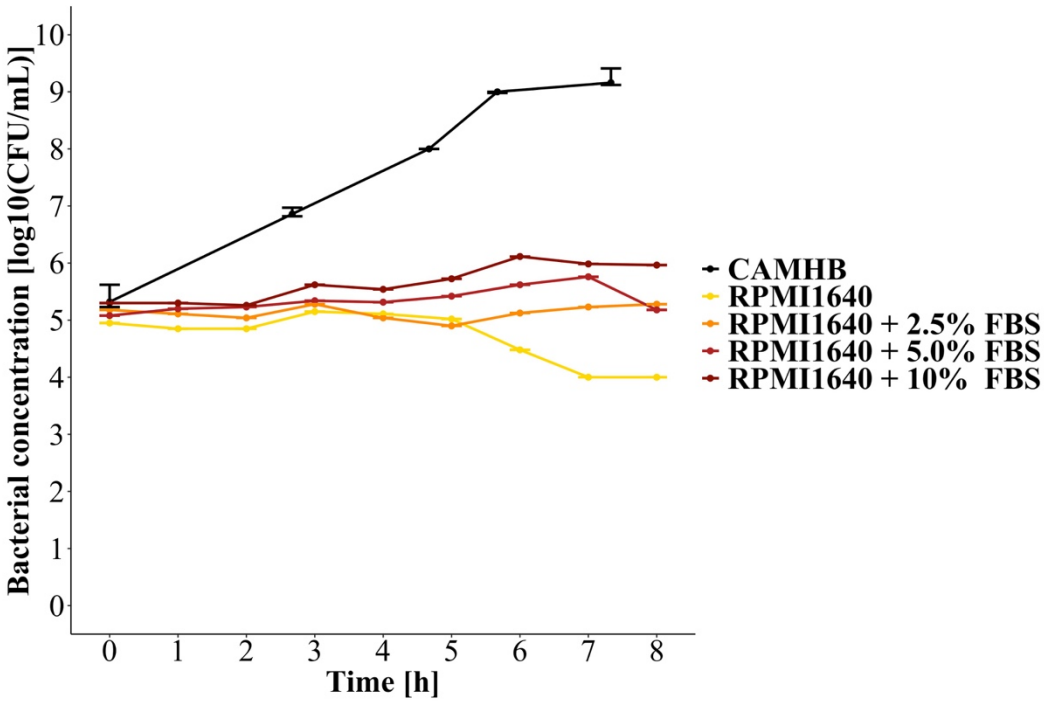

Figure 3.6: Bacterial growth of *Streptococcus pneumoniae* serotype 1 versus time on a semi-logarithmic scale in CAMHB ($n_{experiment}$=1, with 3 replicates) and RPMI1640 with 0%, 2.5%, 5% and 10% (v/v) FBS (each $n_{experiment}$=1 with 1 replicate). The median (line) with minimum and maximum bacterial concentrations of the median of single experiments as error bar is depicted for each studied case. Abbreviations: CAMHB: Cation-adjusted Mueller-Hinton broth; CFU: Colony forming units; FBS: Foetal bovine serum; RPMI1640: Roswell Park Memorial Institute 1640 medium.

3.1.4.2 Minimum inhibitory concentration in cell growth and cell-pretreated medium

The MIC value of AMX against *S. aureus* Newman in RPMI1640 supplemented with 10% FBS was 0.125 mg/L ($n_{experiment}$=3 with 2 replicates each). Compared to the determined MIC value in CAMHB (Chapter 3.1.2.2), the MIC was reduced twofold. In addition to the turbidity of the suspension indicating bacterial growth, a change of the colour of the solution due to presence of the pH indicator phenol red occurred as described in Chapter 3.1.4.1, bacterial growth at AMX concentrations <0.125 mg/L was shown.

To evaluate the impact of the cell growth medium and direct effects of MPLA, the MIC of MPLA against *S. aureus* Newman was determined in RPMI1640 with 10% (v/v) FBS. No antibacterial effect for concentrations <1 mg/L ($n_{experiment}$=1 with 2 replicates) was observed. Furthermore, indirect effects of MPLA were studied in this experimental setting by investigating different ratios of STIM and RPMI1640 with 10% (v/v) FBS. Up to a composition of 89% STIM bacterial growth was observed and, hence, antibacterial effects of the cell-pretreated medium, i.e. indirect effects of MPLA, were excluded in this experimental setting.

3.1.4.3 Time-kill curve studies in cell-pretreated medium

Based on MIC determinations (Chapters 3.1.2 and 3.1.4.2), interaction analysis of the antibiotic and immunostimulatory drugs was not performed using checkerboard assays, since no distinct differences were observed in that setting. As a consequence, miniaturised time-kill curve studies were conducted.

The time-kill curve experiments representing direct and indirect effects of MPLA against *S. aureus* Newman unveiled only minor differences between the study groups (Figure 3.7). The bacterial concentration-time profiles indicated a transition from lag- to log-phase bacteria at approximately 4 h. Maximum bacterial concentrations were reached at 8 h. Compared to growth in CAMHB, a delay of 2 h of the transition occurred as also reported for the cell growth medium RPMI1640 with 10% (v/v) FBS (Figure 3.5). Nevertheless, bacteria cultivated in this cell growth medium reached lower maximum concentrations than NEG- (7.13 log10 CFU/mL (RPMI1640 with 10% (v/v) FBS, Figure 3.5) vs. 8.17 log10 CFU/mL (NEG-)). Considering the relatively large variability in the respective study groups, no distinct differences between NEG- ($n_{experiment}$=3), NEG+ ($n_{experiment}$=3) and STIM ($n_{experiment}$=6) were detected, which were also confirmed as not statistically significant differences by an ANOVA analysis (p=0.0298, α=0.05). Only a minor trend indicating slightly slower growth kinetics for STIM compared to NEG- was recognisable with NEG+ samples showing no clear trend towards one of the other groups.

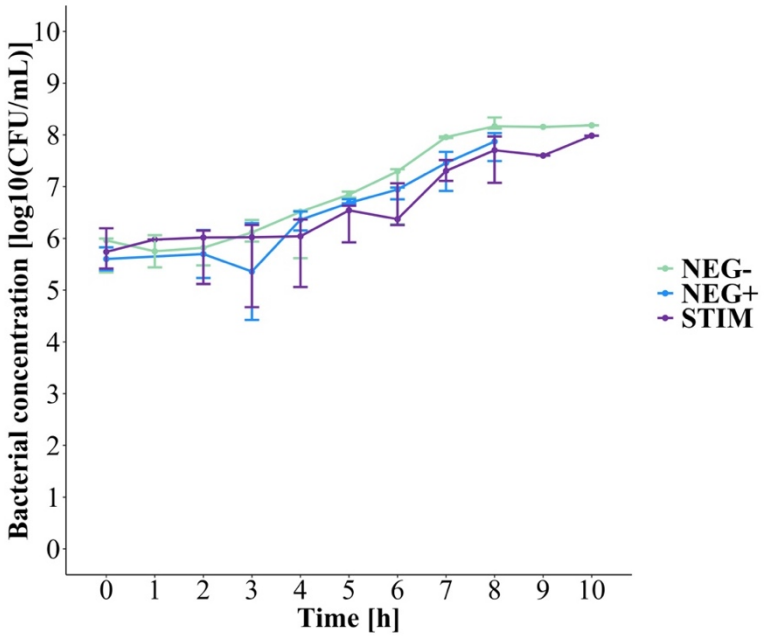

Figure 3.7: Bacterial growth of *Staphylococcus aureus* Newman versus time on a semi-logarithmic scale in NEG- ($n_{experiment}$=3 with 2 replicates each), NEG+ ($n_{experiment}$=3 with 2 replicates each) and STIM ($n_{experiment}$=6 with 2 replicates each). The median (line) with minimum and maximum bacterial concentrations of the median of single experiments as error bar is depicted for each studied case. Abbreviations: CFU: Colony forming units; MPLA: Monophosphoryl lipid A; NEG+: Negative control of not-stimulated supernatant with addition of MPLA; NEG-: Negative control of not-stimulated supernatant; STIM: MPLA-stimulated supernatant.

Evaluating direct and indirect effects of MPLA in *S. pneumoniae* serotype 1 showed that growth of bacteria was enhanced in NEG- compared to RPMI1640 with 10% (v/v) FBS (Figure 3.6). Maximum bacterial concentrations were achieved after 6 to 8 h in standard cell growth medium (Figure 3.6) and delayed and >1.5 log10 CFU/mL higher in NEG- (Figure 3.8). After stimulation of MPI cells with MPLA and investigation of growth over time in resulting STIM, bacterial growth was slightly increased compared to NEG- depending on the used batch. Nevertheless, the difference between NEG- and STIM independent from the used batch was defined as not statistically significant ($p=0.0159$, $\alpha=0.05$). Addition of MPLA to NEG- (termed NEG+) revealed comparable bacterial concentration-time profiles to NEG- and STIM with no statistic differences between all three ($p=0.0161$, $\alpha=0.05$). Bacterial concentrations increased from the starting inoculum of 5.82 log10 CFU to 8.01 log10 CFU after 8 h. Especially at 8 h, higher deviations between the three investigated groups were shown. Nevertheless, also higher variability occurred and made evaluation more challenging. Another fact to consider when evaluating antibacterial effects in cell-pretreated media was the usage of different batches of the medium. As depicted in Figure 3.8, differences of 0.47 log10 CFU in median concentrations for the two different batches of NEG- occurred at 8 h. This trend was less obvious for NEG+ and STIM.

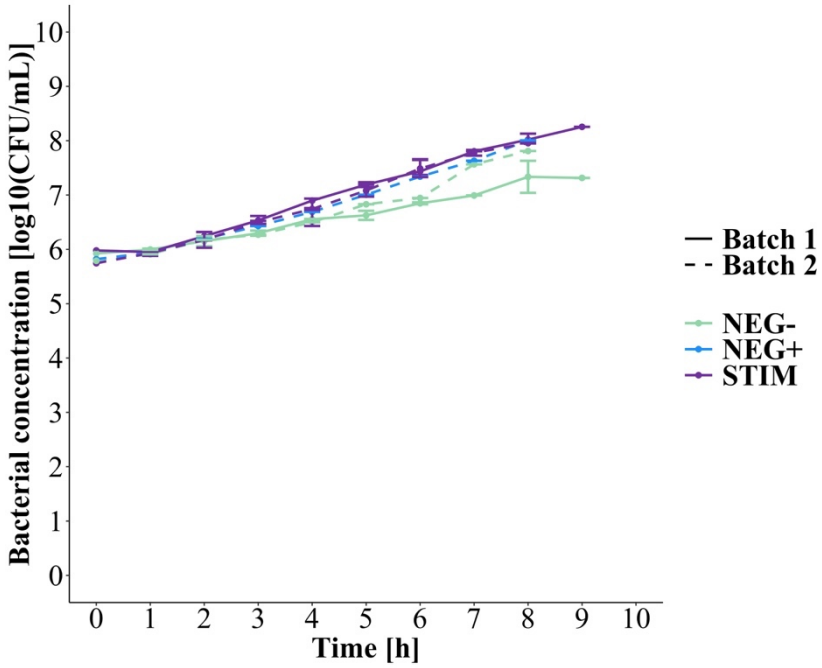

Figure 3.8: Bacterial growth of *Streptococcus pneumoniae* serotype 1 versus time on a semi-logarithmic scale in NEG- ($n_{experiment}=2$ with 2 replicates, each, in batch 1; $n_{experiment}=1$ with 2 replicates, each, in batch 2), NEG+ ($n_{experiment}=1$ with 2 replicates) and STIM ($n_{experiment}=3$ with ≥2 replicates, each, in batch 1; $n_{experiment}=2$ with 2 replicates, each, in batch 2). The median (line) with minimum and maximum bacterial concentrations of the median of single experiments as error bar is depicted for each studied case. Abbreviations: CFU: Colony forming units; MPLA: Monophosphoryl lipid A; NEG+: Negative control of not-stimulated supernatant with addition of MPLA; NEG-: Negative control of not-stimulated supernatant; STIM: MPLA-stimulated supernatant.

In this experimental setting, antibacterial effects were only evaluated over maximum ~10 h in detail, since bacterial concentrations were less informative in a long-term study. A stationary phase was reached after approximately 8 h and bacterial concentrations decreased starting at 16 h, potentially being reduced to bacterial concentrations below the LLOQ at t>24 h. (Figure 7.3).

To further investigate the indirect effects of MPLA in combination with AMX, time-kill curve studies of AMX in NEG- and STIM were performed. As expected, lower bacterial concentrations were observed with increasing concentrations of AMX (Figure 3.9). At subinhibitory concentrations of AMX (<MIC (0.016 mg/L)) in STIM, they were reduced by 0.18 and 0.57 log10 CFU/mL at 5 h at AMX concentrations of 0.004 and 0.008 mg/L, respectively, compared to bacterial growth in STIM without AMX. Reduction of growth in NEG- was comparable. Still, slightly lower bacterial concentrations were observed in NEG- compared to STIM at each AMX concentration level. This trend of increased growth in STIM was inverse for inhibitory concentrations (≥MIC) of AMX. Here, bacterial growth was less affected in NEG- by AMX. At an AMX concentration of 0.016 mg/L in STIM, initial killing to 5.38 log10 CFU/mL at 3 h was observed and followed by regrowth to 5.85 log10 CFU/mL at 5 h. A further increase of AMX concentrations to 0.032 mg/L resulted in bacterial killing without regrowth with a reduction in growth to 2.73 and 3.45 log10 CFU/mL at 8 h in STIM and NEG-, respectively.

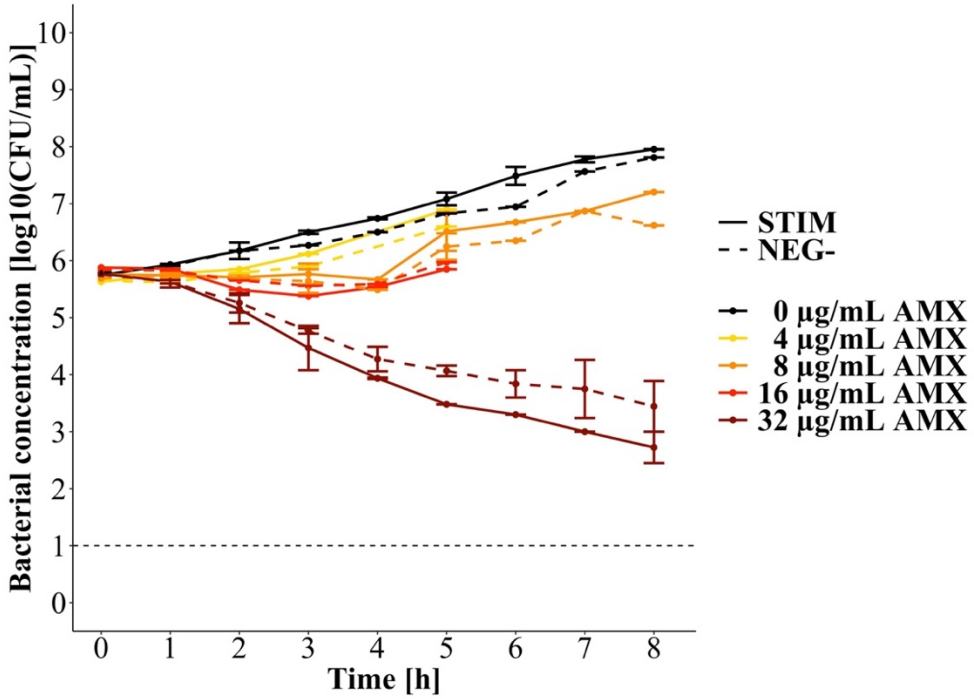

Figure 3.9: Bacterial growth of *Streptococcus pneumoniae* serotype 1 versus time on a semi-logarithmic scale in either NEG- or STIM of batch 2 each with different concentrations of AMX (0-32 µg/mL; $n_{experiment}$=1-2 with 1-2 replicates each.).The median with minimum and maximum bacterial concentrations of the median of single experiments as error bar is depicted for each studied case; LLOQ=1 log10 CFU/mL. Abbreviations: AMX: Amoxicillin; CFU: Colony forming units; LLOQ: Lower limit of quantification; MPLA: Monophosphoryl lipid A; NEG-: Negative control of not-stimulated supernatant; STIM: MPLA-stimulated supernatant.

3.2 Bioanalytical quantification of amoxicillin in serum

An LC-MS/MS assay was successfully developed, validated and applied to mouse serum samples. In the present chapters, the results of the bioanalytical quantification of amoxicillin in murine serum are presented.

3.2.1 Development of the bioanalytical LC-MS/MS assay

3.2.1.1 Sample pretreatment

Purification of thawed serum samples from matrix constituents was best with chilled MeOH. Other investigated organic precipitation agents (acetone, ACN and EtOH (Chapter 2.3.1.2)), did not improve protein precipitation and AMX recovery. They revealed a less intense detector response with maximum 60% of the response of a MeOH sample. The detector response was not enhanced by subsequent evaporation of the organic solvent. Also, a direct injection of the supernatant of the precipitated sample into the LC-MS/MS system did not ameliorate the detector response. Serious signal deteriorations occurred, especially when analysing samples over several hours. Dissolved salts being originally part of the serum were not separated from the injected sample and contaminated the MS source over time. Subsequently, ionisation was suppressed and resulted in the need for complex cleaning procedures and ultimately a reduction in detector sensitivity [89]. As a consequence, the supernatant was diluted 1:10 (v/v) with MilliQ® water. As additional protection of the MS ion source from matrix constituents, the eluent was directed into the triple quadrupole MS detector only for a short time period, in which AMX elution response was expected. Hence, the eluents reached the MS only between 2 and 3.5 min instead of being directly led into the waste.

3.2.1.2 Instrumentation and LC-MS/MS instrument setup

A final gradient profile of an aqueous (UP water with 0.1% (v/v) formic acid (mobile phase A)) and an organic eluent (ACN with 0.1% (v/v) formic acid (mobile phase B)) at a constant flow rate revealed best separation of matrix constituents and AMX compared to other gradient profiles with higher/lower proportions of mobile phase B at earlier/later time points (Figure 3.10). For the first 0.5 min, the proportion of mobile phase B was kept at 2% (v/v) and subsequently steadily increased to 30% (v/v) at 1.25 min. Then, the proportion was further increased to 95% (v/v) at 4 min and kept at 95% (v/v) for 1 min. Ultimately, the proportion of the aqueous mobile phase A was increased back to 98% (v/v) at 6 min and kept constant for 1.5 min for re-equilibration of the system. Hence, the analytical run time totalled up to 7.5 min.

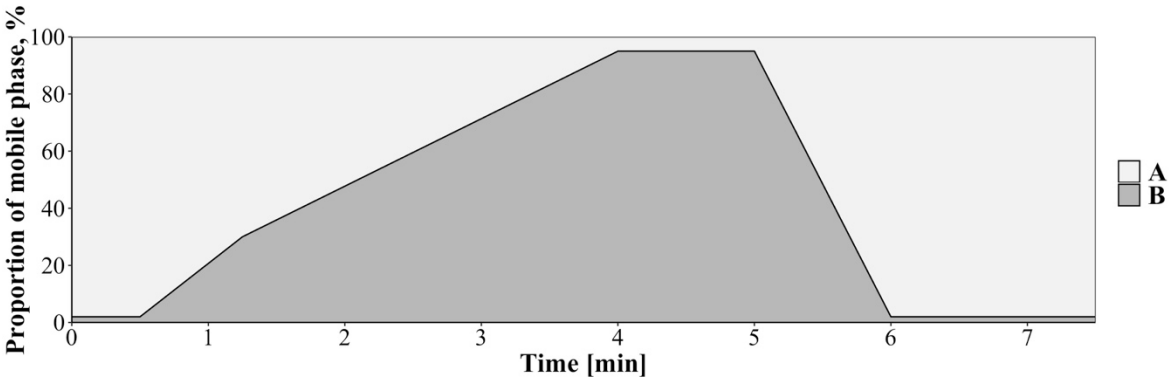

Figure 3.10: Gradient elution for quantification of amoxicillin in mouse serum. Mobile phase A consisted of ultra-pure water and mobile phase B of acetonitrile, both containing 0.1% (v/v) formic acid.

Optimised and final source parameters with respect to detection of AMX with highest intensity were: Capillary voltage of 4500 V, nebuliser gas pressure of 30 psi, gas and sheath gas flow of 20 L/min and 12 L/min, gas and sheath gas temperature of 150 °C and 300 °C, respectively. Final mass transitions with respective settings of the triple quadrupole MS/MS detector are shown in Table 3.4.

Table 3.4: Mass spectrometric parameters of the LC-MS/MS assay to quantify amoxicillin in mouse serum [179].

m/z (Precursor ion)	*m/z* (Product ion)	Fragmentor voltage [V]	Collision energy [V]	Cell accelerator voltage [V]	Polarity
366.11	349	380	5	5	Positive
366.11	208	380	8	5	Positive
366.11	114	380	16	5	Positive

Abbreviations: LC-MS/MS: Liquid chromatography-tandem mass spectrometry; *m/z*: Mass-to-charge ratio.

The fragments *m/z* 349 and *m/z* 208 were chosen as qualifier ions of the method due to relatively high noise at the retention time of AMX. Contrarily, for fragment *m/z* 114, a clear, sharp and intense detector response and low noise were observed and fragment *m/z* 114 was defined as quantifier. AMX eluted constantly after 2.47 min with a clear and sharp detector response and acceptable qualifier ratios with deviations of maximum ±20% indicating that AMX was reliably identifiable (Figure 3.11).

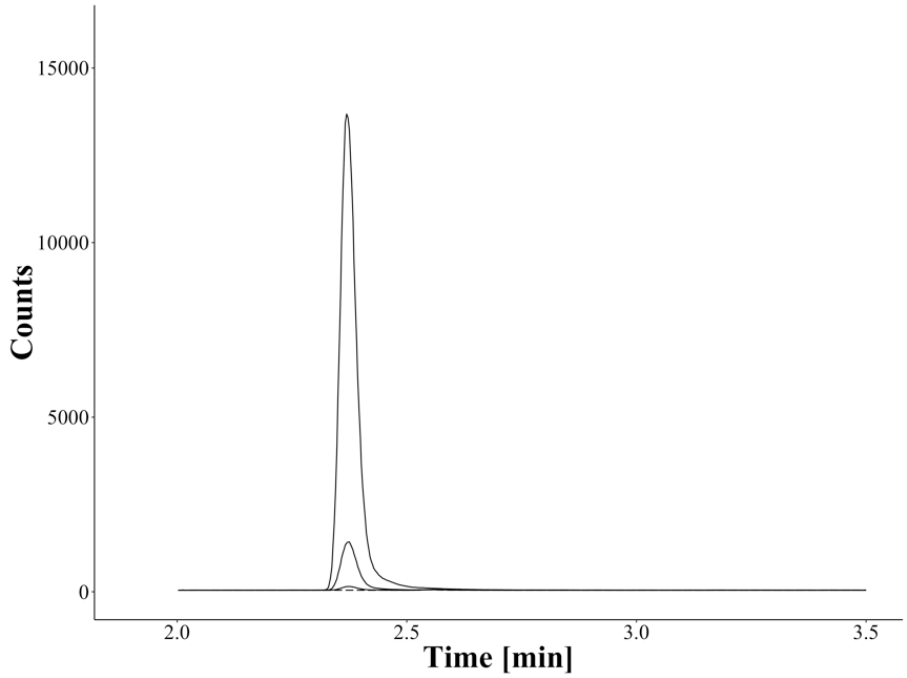

Figure 3.11: Representative multiple reaction monitoring chromatogram for the product ion *m/z* 114 of spiked serum with amoxicillin at 0.01, 0.1 and 1 µg/mL (solid lines) and blank serum (dashed line) in the time frame that was monitored by the triple quadrupole mass spectrometry detector [179].

3.2.2 Validation of the bioanalytical LC-MS/MS assay

The developed LC-MS/MS method was successfully validated according to the EMA guideline on bioanalytical method validation [121] as reported hereafter.

Selectivity. Due to the limitation of sufficient volume of serum in the conducted study (Chapter 3.3.1), alternative approaches for the routine preparation (pooled serum of individual study mice or commercial mouse serum (Chapter 2.3.2)) of CAL and QC samples were investigated. To assess the characteristics of these matrices, they were compared to serum of untreated individual study samples. Commercial serum did not result in a comparable baseline for matrix chromatograms. Pooled mouse serum had a comparable baseline to individual study samples and hence, was accepted as a matrix and used for preparation of CAL and QC samples. The pooled matrix met requirements of the guideline for selectivity with maximum 9.13% detector response compared to the LLOQ. Furthermore, study samples of 14 different individual mice without treatment also met requirements with ≤16.2% detector response.

Carry-over. Mandatory criteria for carry-over were fulfilled: Detector responses of blank samples, that followed CAL and QC samples with AMX concentrations ≥5 µg/mL, did not exceed 20% of the LLOQ for 84.4% of all studied samples (n_{sample}=32). Still, few samples (15.6%) did exceed the limit of 20% with maximum 32.9% of the detector response of a LLOQ sample. For this reason, injection of study samples was not randomised for analysis. To prevent any carry-over, additional blank samples of the

used solvent were included after samples of high concentrations. As a consequence, a carry-over effect was successfully prevented.

Lower limit of quantification. The lowest concentration being quantifiable with acceptable accuracy (90.7%-110%) and precision (≤7.69% CV) was 0.01 µg/mL. As already outlined for selectivity, the requirement of a ≥5 times higher detector response for LLOQ samples compared to blank and matrix samples was met. Calculating the LLOQ based on guidelines by the International Conference for Harmonisation (ICH) [123] resulted in a comparable LLOQ (mean calculated LLOQ: 0.00832 ± 0.00140 µg/mL). At an investigated concentration of 0.0025 µg/mL criteria were not fulfilled anymore. Finally, the concentration of 0.01 µg/mL was defined as LLOQ. Calculations led to a LOD of 0.003 µg/mL (mean calculated LOD: 0.00274 ± 0.000466 µg/mL).

Calibration range. On different days of the validation process calibration functions revealed acceptable coefficients of determination being >0.98 and typical calibration function parameters leading to a linear calibration relation over the entire studied range of 0.01-10 µg/mL (Table 3.5).

Table 3.5: Calibration function parameters (intercept, slope and R^2) including mean values and standard deviation of calibrator samples ($n_{replicate}$=3 per concentration level each on three consecutive days [179]).

Day	Intercept Mean ± SD	Slope Mean ± SD	R^2
1	16.7 ± 76.0	62.6 ± 1.86	0.992
2	28.7 ± 112	66.0 ± 5.83	0.988
3	12.2 ± 89.6	87.0 ± 7.43	0.990

Abbreviations: R^2: Coefficient of determination; SD: Standard deviation.

The back calculated concentrations of the CAL samples were accurate for 92.1% of all calibration samples (n_{CAL}=63, Figure 3.12) measured on the three consecutive days. Determined accuracies of mean concentrations of the CAL samples were within the mandatory limits of the relative error of ±15% (93.3%-112%, Table 7.1). In total, all requirements for CAL samples were met.

Accuracy and precision. Demanded requirements for within-run and between-run accuracies and their precision were successfully met. Deviating from the guidelines, QC samples were more evenly distributed across the entire concentration range at LLOQ, and 1%, 10% and 50% of the ULOQ. The reason for that adjustment was the broad concentration range with more concentrations being expected in the lower range. The mean concentrations of QC samples revealed accuracy values in a range of 104%-114% (Figure 3.12, Table 7.2). Moreover, the quantification of AMX QC samples was precise with a CV ≤13.8%. Of all studied QC samples (n_{QC}=63) only 13.3% of individual QC sample concentrations were outside the required limit of the relative error of ±15%.

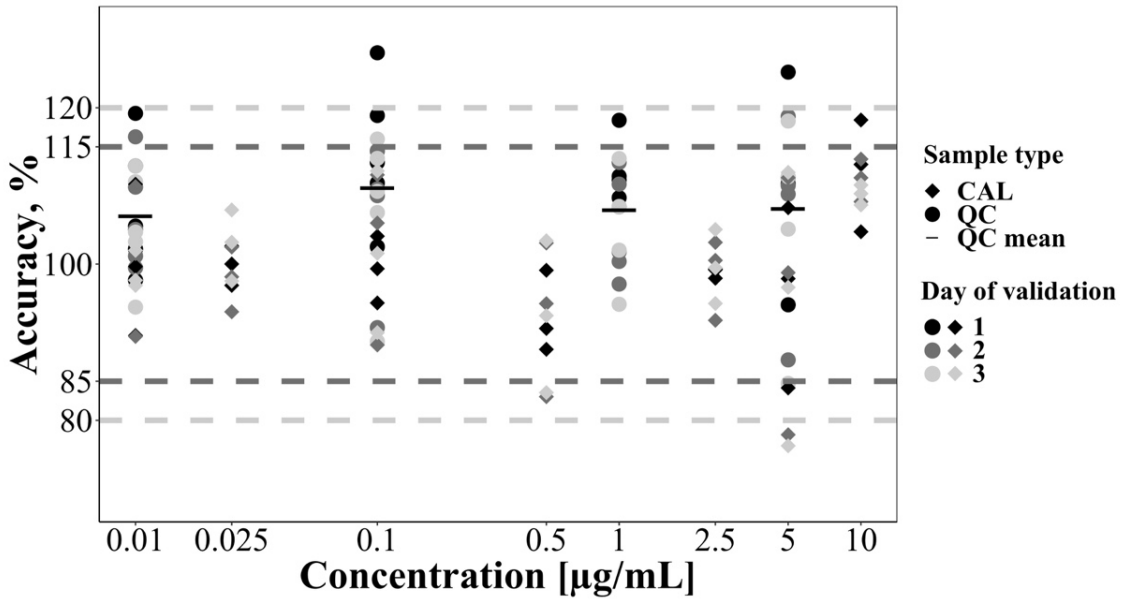

Figure 3.12: Accuracy of calibrator (CAL) and quality control (QC) samples on three consecutive days during the validation process. Allowed limits for accuracy are depicted as dashed lines for ±15% and ±20% for concentrations at the lower limit of quantification. Symbols refer to types of individual or overall mean samples, differentiation in colour refers to the day of validation [179].

Matrix effect. Matrix as well as aqueous samples spiked with AMX were processed identically including sample preparation with protein precipitation using MeOH, which enabled to solely elucidate the effect of the matrix. Although matrix of individual mice was requested to be investigated according to the EMA guideline [121], pooled mouse serum was used as matrix due to the lack of sufficient individual samples and already described comparable characteristics. The matrix factor was calculated reliably with adequate precision of 7.94% CV and 7.83% CV at a concentration of 0.025 µg/mL ($n_{replicate}$=9) and 1 µg/mL ($n_{replicate}$=7), respectively. The matrix factor itself was very high with a value of >90% (94.7% at 0.025 µg/mL; 98.5% at 1 µg/mL) displaying no significant influence of the presence of matrix on the detector response of AMX.

Stability. Overall, AMX was considered stable under the investigated conditions that were relevant for application of the bioanalytical method to quantify AMX in study samples of mouse serum. Autosampler (4 concentration levels, each $n_{replicate}$=3), long-term (4 concentration levels, each $n_{replicate}$=2-3) and freeze-thaw stability (2 concentration levels, each $n_{replicate}$=2) met the specific requirements of the EMA guideline (Table 3.6). Investigated QC samples revealed mean recoveries of 94.2% to 104% and were determined precisely (≤8.69% CV). Short-term stability at room temperature was investigated over 20 h. A mean loss of 20.2% for serum samples ($n_{replicate}$=6) and 5.87% for processed samples ($n_{replicate}$=6) confirmed stability of AMX especially in processed samples. Nevertheless, samples were processed immediately after thawing to prevent degradation of AMX in serum over time.

Table 3.6: Mean recovery and precision of amoxicillin at four quality control tiers under specified conditions (Autosampler stability ($n_{replicate}$=3 per concentration level), long-term stability ($n_{replicate}$=2-3 per concentration level), 3 cycles of freeze-thaw stability ($n_{replicate}$=2 per concentration level), [179])

C_{AMX} [µg/mL]	Autosampler stability 4 °C, t=20 h		Long-term stability -80 °C, 6 months		Freeze-thaw stability -80 °C, 3 cycles	
	Recovery, %	CV, %	Recovery, %	CV, %	Recovery, %	CV, %
0.01	103	7.41	95.2	6.89	97.8	3.74
0.1	103	5.72	100	2.02	94.2	6.59
1	104	3.41	97.8	8.69		
5	102	4.72	97.5	0.89		

Abbreviations: C_{AMX}: Concentration of amoxicillin; CV: Coefficient of variation.

3.2.3 Application of the bioanalytical LC-MS/MS assay

Application of the developed bioanalytical method to study samples adhered to determined time frames and temperatures of the validation process (Chapter 3.2.2) to prevent instability of AMX. Study samples obtained from three different experimental setups of a PK study in Swiss mice (Chapter 2.4.1) were analysed in two different parts.

As demanded by the EMA guideline [121], an in-study validation was performed successfully. Freshly prepared CAL samples were prepared in pooled mouse serum in a concentration range of 0.01-10 µg/mL with 7 tiers for each respective part of the analysis. AMX concentrations were calculated based on the described quadratic weighing function (Chapter 2.3.2) with acceptable calibration function parameters for the respective studies (Table 3.7).

Table 3.7: Calibration function parameters (intercept, slope and R^2) including mean values of calibrator samples ($n_{replicate}$=1 per concentration level for each part) of independently performed analyses of pharmacokinetic study samples of mice being treated with amoxicillin.

Part	Intercept Mean	Slope Mean	R^2
1	-28.8	72.6	0.999
2	-58.0	44.2	0.994

Abbreviations: R^2: Coefficient of determination.

The back calculated concentrations of all CAL samples and concomitant mean accuracy values (91.5%-111%, Figure 3.13, Table 7.3) fulfilled the criteria of the EMA guideline being within 15% of nominal concentrations. As demanded, individual accuracy values of ≥67% of studied QC samples were within the range of ±15% or ±20% at the LLOQ. Also, mean accuracy values of QC samples did not exceed

the required limits as well as overall precision (CV≤15%) was compliant with the EMA guideline for almost all samples, except for QC samples at the LLOQ investigated in part 2 of the analysis with 30.3% CV (Figure 3.13, Table 7.4).

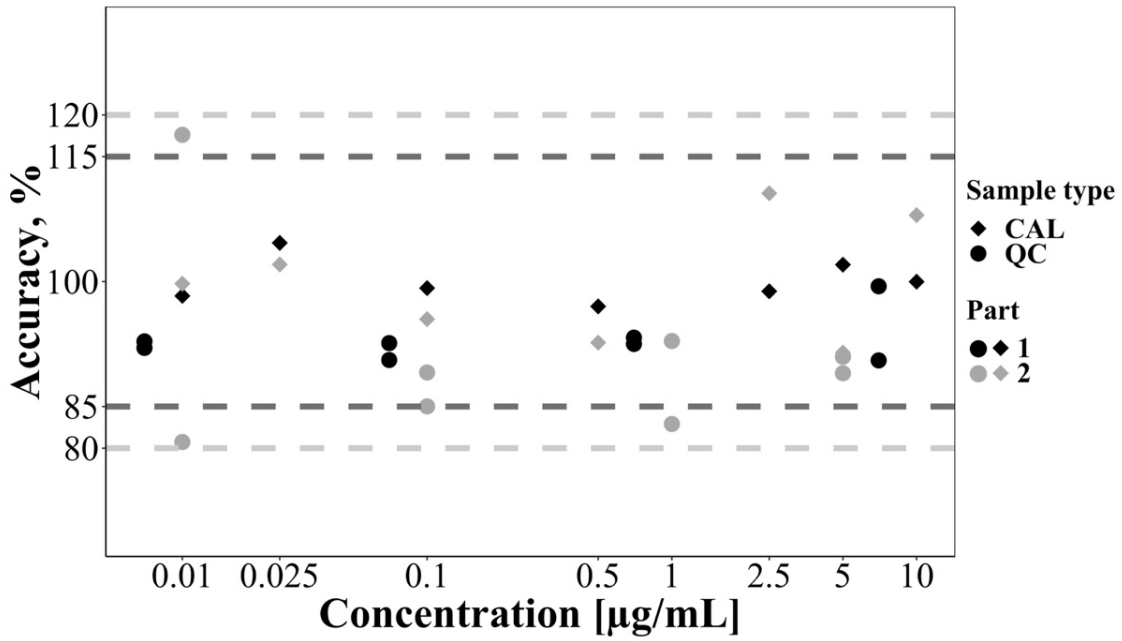

Figure 3.13: Accuracy of calibrator (CAL) and quality control (QC) samples for the two different part during the application of the liquid chromatography-tandem mass spectrometry method to serum study samples. Allowed limits for accuracy are depicted as dashed lines for ±15% and ±20% for concentrations at the lower limit of quantification. Symbols refer to types of individual samples, differentiation in colour to the part of the application of the method.

3.3 Animal infection model

In the present chapters, results of *in vivo* studies, that had been performed at the Institut Pasteur de Lille, France, and had partly been analysed [124], will be presented. In detail, results of PK of AMX, bacterial growth kinetics and the survival study will be reported. Additionally, a short overview of performed experiments to assess the body weight profile, gene expression of markers of the immune system, cytokine kinetics in serum, histopathology in lung of markers of the immune system and recruitment of immune system-related cells in mice will be given.

3.3.1 Pharmacokinetics of amoxicillin *in vivo*

In a first step, sampling time points were determined based on literature. Due to a considerably short half-life of AMX of approximately 30 min [180], a comparable early time-point was determined for the first sample at 12.167 h after infection. Additional sampling time points with a denser sampling schedule were defined to be at 12.5, 13, 14, 15, 18 and 24 h.

Study samples were quantified by the validated LC-MS/MS method (Chapter 3.2.2) and an in-study validation was performed successfully (Chapter 3.2.3). In total, 132 study samples of 108 individual mice obtained from three different PK studies were analysed including 26 samples of untreated mice as control, 66 samples of AMX treated mice and 40 samples of mice treated with the combination of AMX and MPLA (Figure 3.14).

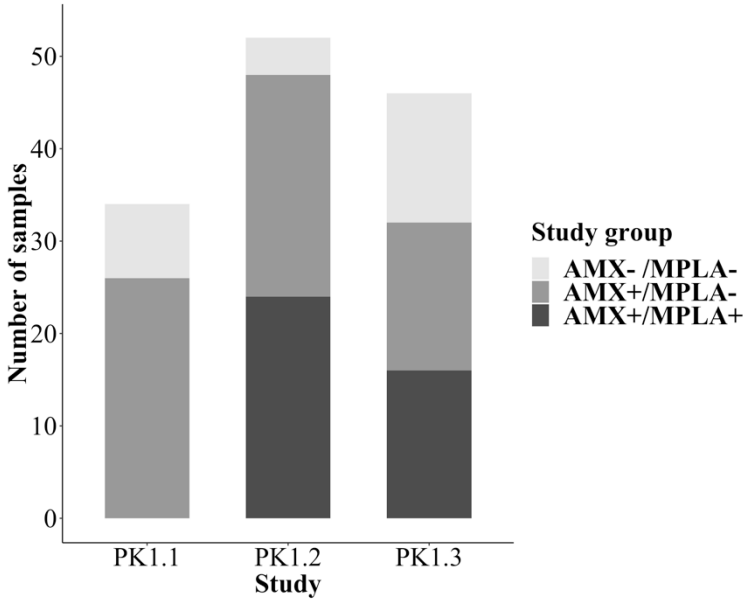

Figure 3.14: Number of study samples of three pharmacokinetic studies (PK1.1, PK1.2, PK1.3) in mice stratified into the three study groups: Untreated mice as control (AMX-/MPLA-), mice treated with AMX (AMX+/MPLA-) or a combination of AMX and MPLA (AMX+/MPLA+). Abbreviations: AMX: Amoxicillin (14.0 mg/kg for PK1.1 and PK1.2, 0.4 mg/kg for PK1.3); MPLA: Monophosphoryl lipid A (2.00 mg/kg for PK1.1-1.3); PK: Pharmacokinetics; +: Treatment with respective drug; -: No treatment with respective drug.

As expected, control samples of mice not being treated (study group: AMX-/MPLA-) led to AMX concentrations below the LLOQ for 100% (n_{sample}=26). Of mice being treated with AMX in monotherapy (study group: AMX+/MPLA-) or by using a combined treatment with MPLA (study group: AMX+/MPLA+), 15.1% of 106 individual samples were below the LLOQ of 0.01 µg/mL. Hence, 84.9% of samples of mice being treated with AMX hat quantifiable AMX concentrations. Samples being below the LLOQ mainly occurred at the end of the observation period. An overview of respective mean AMX concentrations per study group and time as well as AMX concentrations per individual mouse is displayed in Table 7.5 and Figure 7.4, respectively. For visualisation of obtained results, AMX concentrations being even below the LOD were included into the graphical representation to display and not neglect these values. In further performed analyses, these concentrations were treated as values below the LLOQ (Chapter 3.4.1.1).

After oral administration of the antibiotic, the concentration-time profile of AMX in mice showed plausible serum concentrations (Figure 3.15). A rapid increase of serum concentrations until achieving maximum concentrations C_{max} of 5.84 µg/mL at the highest studied AMX dose in the study group of

infected and combined treated mice (study group: SP1+/AMX+/MPLA+) and a subsequently pronounced decline were observed. In addition, the concentration-time profiles showed differences between monotherapy and combined treatment. For the combined treatment (study group: SP1+/AMX+/MPLA+), maximum serum concentrations were reached at a time t_{max} of 30 min after drug administration compared to 10 min for monotherapy with AMX (study groups: AMX+/MPLA-) and a less steep decrease of the concentrations after C_{max} occurred. A comparison of the low dose study to higher doses of AMX revealed similarities in the concentration-time profiles. As already described, t_{max} was shifted from 10 min in monotherapy to 30 min for the combined treatment. For monotherapy, the C_{max} value was approximately 35.2 times higher at highest dose (14 mg/kg) being in line with a 35-fold increase of the dose compared to the lowest studied dose (0.40 mg/kg). In contrast, the factor was increased to a value of 41.3 for the combined treatment. In addition to these observations, determined concentrations revealed differences of almost 10 times between individual samples of respective study groups and at specific time points. This variability must be taken into account when interpreting the obtained results.

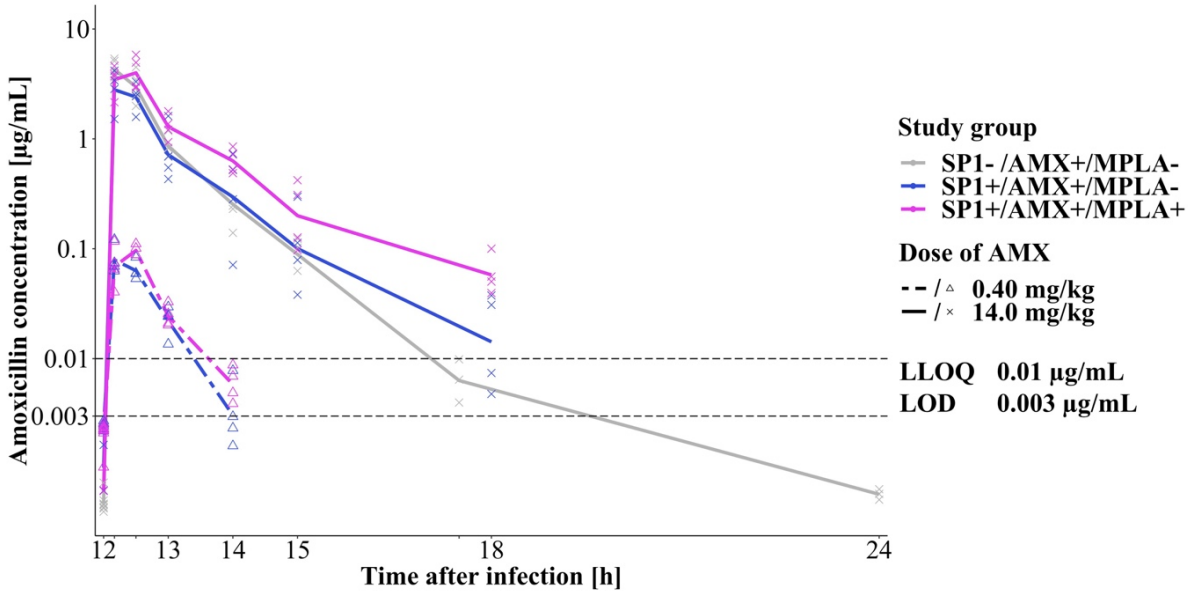

Figure 3.15: AMX concentrations in serum of 132 study samples at a low and a high dose of AMX (0.40 and 14 mg/kg, respectively) on a semi-logarithmic scale. A pharmacokinetic study in mice being non-infected or infected with SP1 (SP1- or SP1+, respectively) and treated with either AMX in monotherapy (AMX+/MPLA-) or in combination with MPLA (AMX+/MPLA+) was performed. Line: Geometric mean of each respective study group; Symbols: Individual observations of the measured samples; LLOQ=0.01 µg/mL; LOD = 0.003 µg/mL. Abbreviations: AMX: Amoxicillin, LLOQ: Lower limit of quantification (0.01 µg/mL); LOD: Limit of detection (0.003 µg/mL); MPLA: Monophosphoryl lipid A; SP1: *Streptococcus pneumoniae* serotype 1; +: Treatment with respective drug; -: No treatment with respective drug.

3.3.2 Bacterial growth kinetics

To assess bacterial growth kinetics, bacterial numbers of *S. pneumoniae* serotype 1 were quantified in eight different study groups over in total 48 h. One lung and one spleen sample were collected from altogether 634 individual mice adding up to 1268 samples in the entire study (Figure 3.16). 28.4% of these mice were not treated at all as control group (study group: AMX-/MPLA-). 24.3% and 23.0% received monotherapy of different doses of AMX (study groups: AMX0.2/MPLA- (0.2 mg/kg), AMX0.4/MPLA- (0.4 mg/kg) and AMX1.2/MPLA- (1.2 mg/kg)) or a standard dose of MPLA (study group: AMX-/MPLA+ (2.0 mg/kg)), respectively. The combination of a different dose of AMX and the standard dose of MPLA was studied in 24.3% (study groups: AMX0.2/MPLA+, AMX0.4/MPLA+ and AMX1.2/MPLA+). To investigate the influence of the used mouse type, 17.4% and 82.6% of the samples were collected from Balb/cJ or Swiss mice, respectively. In total, 7 samples, which were nearly evenly distributed between lung and spleen samples, were missing (e.g. deceased mice at an unexpected time point, wrongly handled sample). The bacterial numbers were not calculated due to numbers being below the LLOQ of 1.22 log10 CFU/organ in 26.2% of all 1268 samples. In a few cases, where the LLOQ value deviated from the reported one, it was reported and set to this LLOQ independently. The proportion of samples <LLOQ was significantly higher for spleen with 24.3% of all lung and spleen samples together (51.9% of all samples in spleen) compared to lung samples with 1.89% (4.01% of all samples in lung). Especially for spleen samples, the number of samples being <LLOQ was clearly differentiating between the study groups with a high proportion of samples <LLOQ for combined treated mice (Figure 7.5). Comparing the number of mice being treated in the respective study groups revealed that only 12 mice each (1.89% of all mice) were studied at an AMX dose of 0.20 mg/kg administered in monotherapy or as combination with MPLA, respectively. Contrarily, other study groups consisted of at least 64 mice. Also, not each mouse strain was investigated for all study groups. Here, the dose of 0.2 mg/kg AMX was not studied in Swiss mice, whereas the dose of 1.2 mg/kg was excluded for Balb/cJ mice.

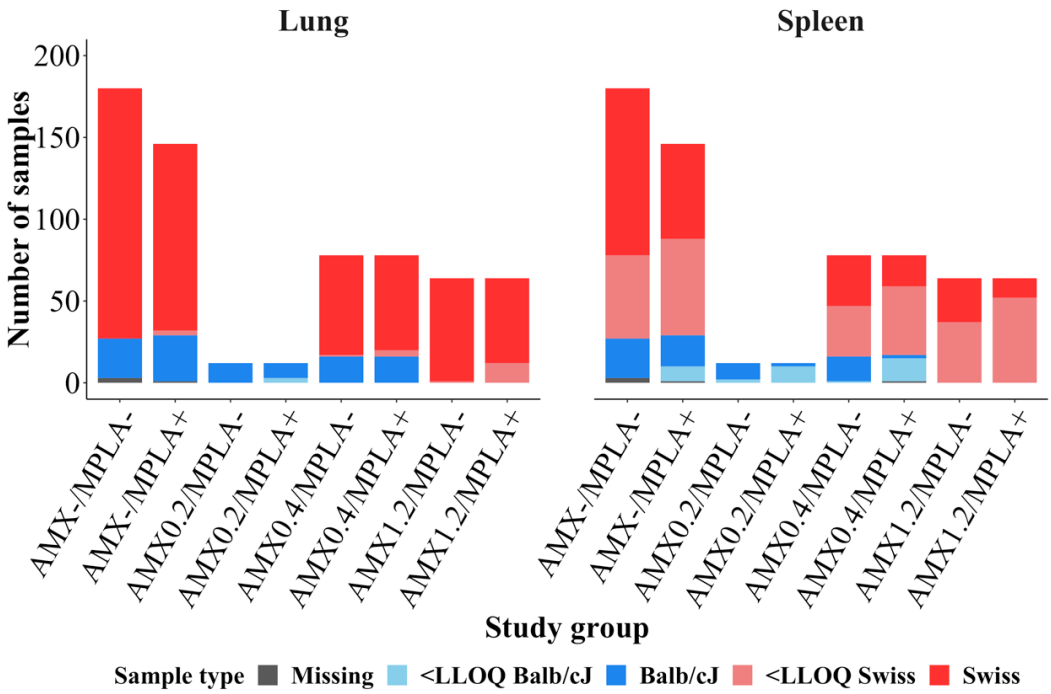

Figure 3.16: Distribution of study samples in lung and spleen of different study groups of a study investigating the effect of AMX and MPLA mono- or coadministration on *Streptococcus pneumoniae* serotype 1 in mice. Samples are allocated into planned, but not evaluated samples (Missing, e.g. due to deceased mice), samples of BALB/cJ mice being below the LLOQ (<LLOQ Balb/cJ), samples of Balb/cJ above the LLOQ (Balb/cJ), samples of Swiss mice being below the LLOQ (<LLOQ Swiss) and samples of Swiss mice above the LLOQ (Swiss). Abbreviations: AMX: Amoxicillin (0.20 mg/kg, 0.40 mg/kg or 1.20 mg/kg); Balb/cJ: Inbred Balb/cJRj mouse strain; LLOQ: Lower limit of quantification; MPLA: Monophosphoryl lipid A (2.00 mg/kg); Swiss: Outbred RjOrl:Swiss (CD-1) mouse strain; +: Treatment with respective drug; -: No treatment with respective drug.

As depicted in Figure 3.17, bacterial numbers were quantified at 4, 8, 12, 13, 14, 18, 24, 30, 36 and 48 h after infection. To assess a typical growth curve of *S. pneumoniae* serotype 1 in mice, samples of untreated Swiss mice were collected across the entire time interval with ≥6 individual mice per time point. In all other study groups of Swiss mice, sampling started after drug administration at 13 h. A relatively rich data situation was obtained for Swiss mice being treated with MPLA, 0.4 mg/kg AMX or the combination of both with 6 studied time points compared to only 4 studied time points later than 24 h after infection at an AMX dose of 1.2 mg/kg. Compared to Swiss mice, samples of Balb/cJ mice were less intensely collected with bacterial numbers being determined only at 24 h and 48 h.

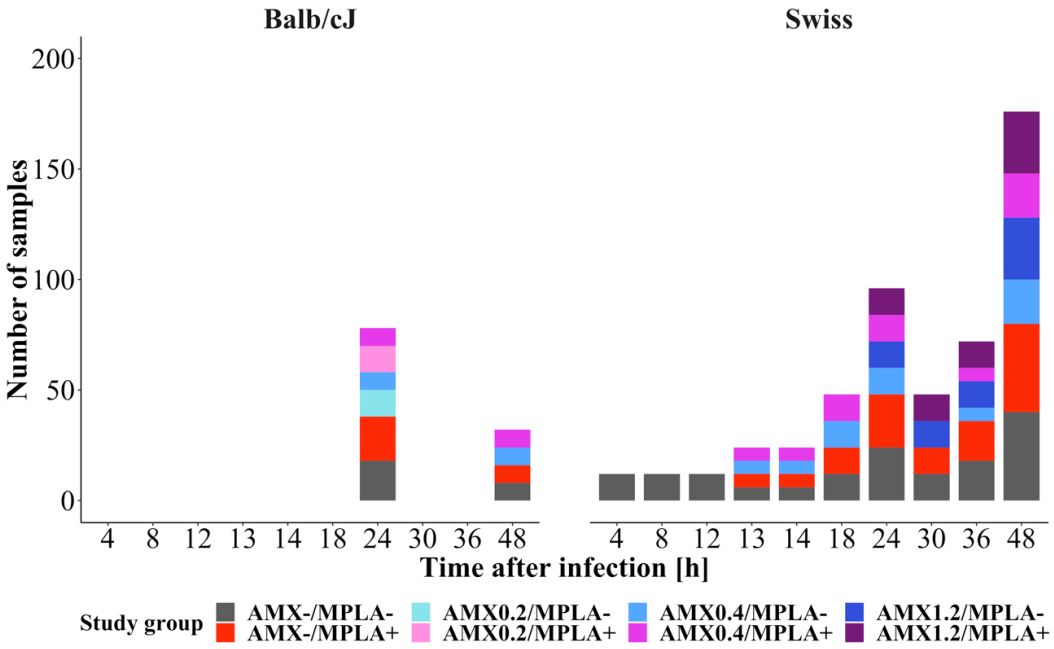

Figure 3.17: Study sample distribution mice (Balb/cJ, Swiss) versus time of a study investigating the effect of AMX and MPLA mono- and coadministration on *Streptococcus pneumoniae* serotype 1. Different study groups are displayed: Untreated mice (AMX-/MPLA-), mice treated with AMX (AMX+/MPLA-) or a combination of AMX and MPLA (AMX+/MPLA+). Abbreviations: AMX: Amoxicillin (0.20 mg/kg, 0.40 mg/kg or 1.20 mg/kg); Balb/cJ: Inbred Balb/cJRj mouse strain; MPLA: Monophosphoryl lipid A (2.00 mg/kg); Swiss: Outbred RjOrl:Swiss (CD-1) mouse strain; +: Treatment with respective drug; -: No treatment with respective drug.

In addition, it was important to consider for the data analysis that several experiments ($n_{experiment}$=11) were performed on different days and in different time periods over more than a year (Table 7.6). Here, not all study groups were investigated during a single experiment at the same time.

In a next step, the bacterial numbers in lung and spleen will be presented separately. For a better understanding of the following graphical representations of obtained results, it is mandatory to mention that bacterial numbers being below the LLOQ were set to the respective LLOQ value and bacterial numbers at a dose of 0.2 mg/kg AMX were only evaluated at 24 h.

Lung. Being infected with an initial inoculum of 1-4 log10 CFU/mouse, bacterial numbers in lung of untreated animals decreased from the first determined median number of 5.76 log10 CFU/lung at 4 h to 5.04 log10 CFU/lung at 12 h after infection (Figure 3.18). Next, a stationary phase was reached with median bacterial numbers being constant between 12 h and 24 h. After that stationary phase, bacterial numbers increased to 7.55 log10 CFU/lung at 48 h. Compared to untreated animals, bacterial numbers of mice being treated with a monotherapy of MPLA 12 h after infection were within a range of 0.05 log10 CFU/lung and reduced by 3.09 log10 CFU/lung at 13 h and 48 h, respectively. Here, the bacterial number-time profile led to a decrease up to 24 h (4.41 log10 CFU/lung), followed by increasing numbers until 36 h (5.31 log10 CFU/lung) that were finally reduced again. For mice solely treated with 0.2 mg/kg AMX, a reduction of bacterial numbers within the first hours turned into an

increase at 36 h. At the highest dose of AMX, bacterial numbers were constant after 36 h. In general, a trend of lower bacterial numbers occurred for increasing concentrations of AMX. Apart from that trend, a reverse observation was made at 24 h indicating bacterial numbers of 4.14, 4.23 and 4.53 log10 CFU/lung for the AMX doses of 0.20, 0.40 and 1.20 mg/kg, respectively. At 48 h, bacterial numbers reached their maximum with 6.37 and 3.49 log10 CFU/lung for doses of 0.4 and 1.2 mg/kg, respectively. Combining AMX and MPLA lead to continuously decreasing bacterial numbers over time. These bacterial numbers were lower as compared to single treatment of either AMX or MPLA. Comparing monotherapy to a combined treatment at the highest dose of AMX, bacterial numbers were reduced by 18.5% at 24 h, 16.4% at 36 h and 36.4% at 48 h. No regrowth occurred and minimal bacterial numbers of 2.90 and 2.22 log10 CFU/lung at 48 h for 0.40 and 1.20 mg/kg AMX in a combined treatment, respectively, were determined. The particular study groups also showed a higher variability with bacterial numbers ranging e.g. from 3.69 to 6.63 log10 CFU/lung or 4.46 to 7.95 log10 CFU/lung for untreated mice at 24 h or MPLA treated mice at 48 h, respectively (Figure 7.6).

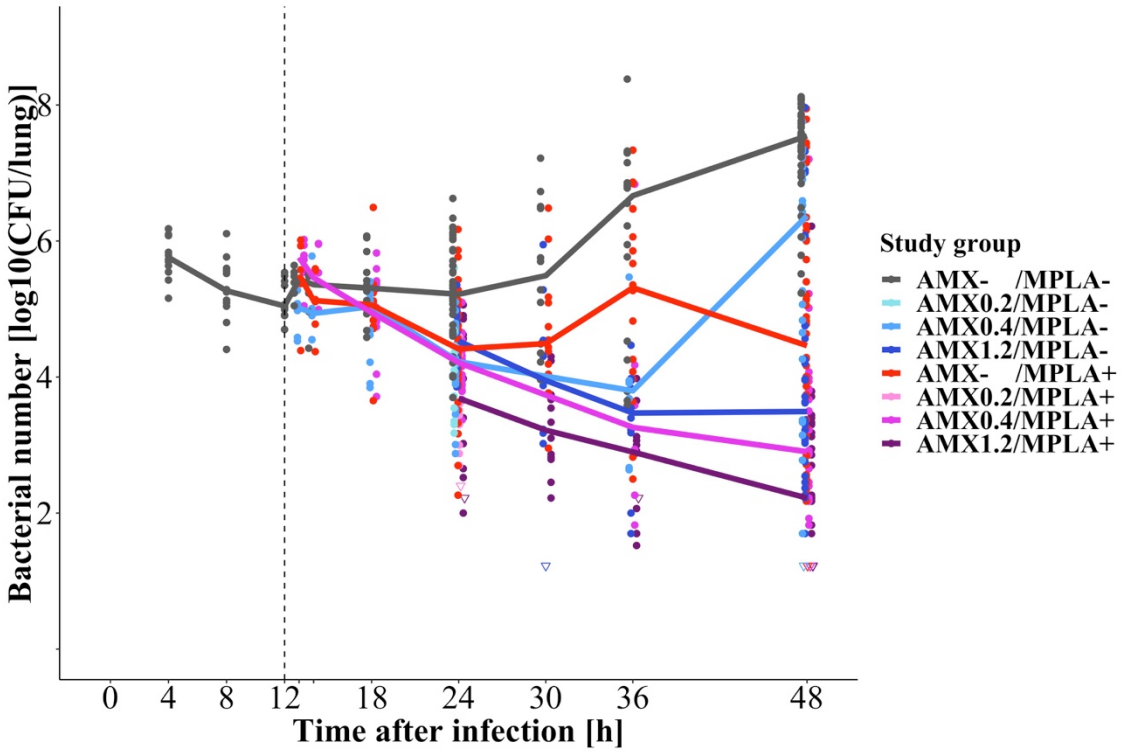

Figure 3.18: Bacterial numbers of *Streptococcus pneumoniae* serotype 1 in lung after intranasal infection at 0 h and drug administration of AMX and/or MPLA at 12 h (dashed line). Different study groups were investigated (untreated mice (AMX-/MPLA-), mice treated with AMX (AMX0.2/MPLA-, AMX0.4/MPLA-, AMX1.2/MPLA-), MPLA (AMX-/MPLA+) or a combination of AMX and MPLA (AMX0.2/MPLA+, AMX0.4/MPLA+, AMX1.2/MPLA+)) and individual observations (symbols: Points: Individual numbers above the LLOQ; Triangles: Individual numbers below the LLOQ) as well as the median of n_{obs}=6-39 observations per study group and time point are depicted (lines). Abbreviations: AMX: Amoxicillin (0.20 mg/kg, 0.40 mg/kg or 1.20 mg/kg); CFU: Colony forming units; LLOQ: Lower limit of quantification (1.22-2.40 log10 CFU/lung); MPLA: Monophosphoryl lipid A (2.00 mg/kg); +: Treatment with respective drug; -: No treatment with respective drug.

Spleen. Analysis of bacterial numbers in spleen resulted in analogous trends compared to the results in lung and within the study groups (Figure 3.19). Bacteria were not detectable in spleen within the first 13 h. Afterwards, bacterial numbers started to increase constantly up to a median maximum number of 6.27 log10 CFU/spleen at 48 h for untreated animals. Compared to untreated mice, administration of AMX in monotherapy led to a less steep increase of bacterial numbers that was also dependent on the dose: The higher the AMX concentration, the lower the bacterial numbers. After 48 h, bacterial numbers were reduced by 18.7% and 75.8% after administration of 0.40 or 1.20 mg/kg AMX, respectively, compared to untreated mice. At 24 h, the trend of less bacterial growth in spleen for higher AMX concentrations was confirmed with bacterial numbers of 2.32, 1.52 log10 CFU/spleen and numbers <LLOQ for 0.20, 0.40 and 1.20 mg/kg, respectively. Administration of MPLA in monotherapy showed highest bacterial numbers at 36 h (4.61 log10 CFU/spleen). After this increase with its maximum at 36 h, bacterial numbers were reduced subsequently to 2.50 log10 CFU/spleen. A comparable trend was shown for the combination of AMX at a dose of 0.40 mg/kg and MPLA with 2.21 log10 CFU/spleen and numbers <LLOQ at 36 and 48 h, respectively. At the highest dose of AMX combined with MPLA, almost no bacterial growth occurred with most numbers (61.9% at 48 h) being below the LLOQ of 1.22 log10 CFU/spleen. The already described high variability in lung samples was also shown for spleen samples with bacterial numbers ranging e.g. from being <LLOQ to 7.03 log10 CFU/spleen for AMX treated mice (0.40 mg/kg) at 48 h (Figure 7.7).

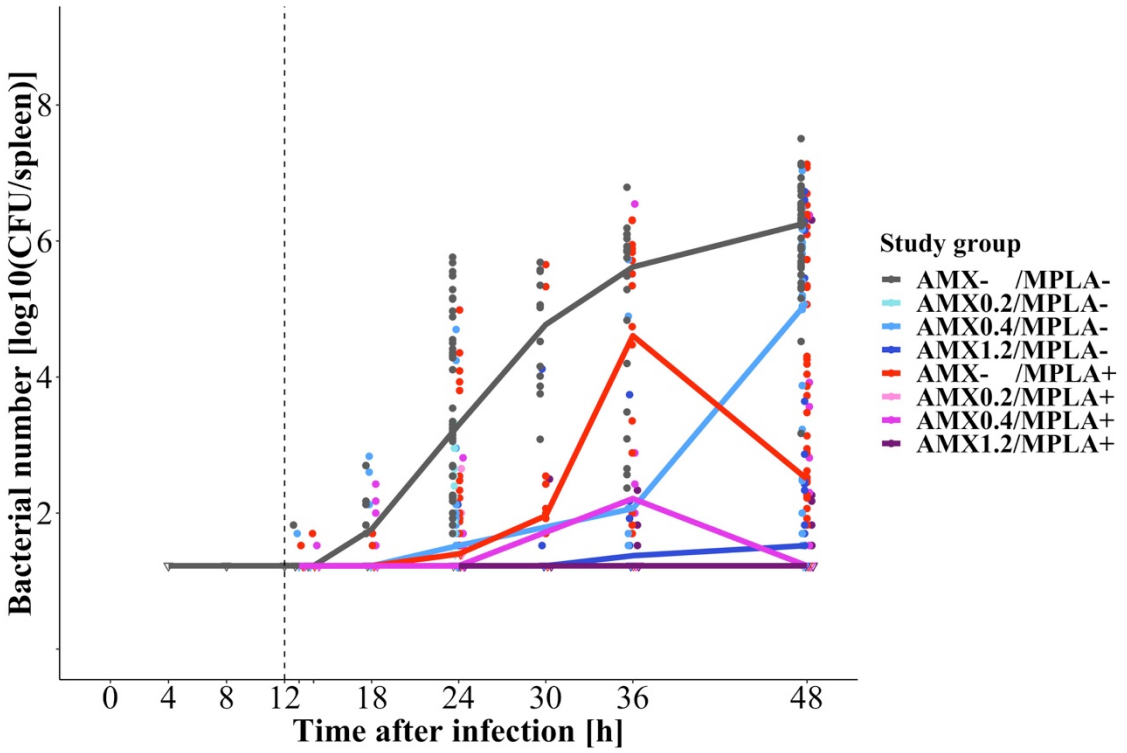

Figure 3.19: Bacterial numbers of *Streptococcus pneumoniae* serotype 1 in spleen after intranasal infection at 0 h and drug administration of AMX or MPLA at 12 h (dashed line). Different study groups were investigated (untreated mice as control (AMX-/MPLA-), mice treated with AMX (AMX0.2/MPLA-, AMX0.4/MPLA-, AMX1.2/MPLA-), MPLA (AMX-/MPLA+) or a combination of AMX and MPLA (AMX0.2/MPLA+, AMX0.4/MPLA+, AMX1.2/MPLA+)) and individual observations (points: Individual numbers above the LLOQ; Triangles: Individual numbers below the LLOQ) as well as the median of n_{obs}=6-39 observations per study group and time point are depicted (lines). Abbreviations: AMX: Amoxicillin (0.20 mg/kg, 0.40 mg/kg or 1.20 mg/kg); CFU: Colony forming units; LLOQ: Lower limit of quantification (1.22-1.40 log10 CFU/lung); MPLA: Monophosphoryl lipid A (2.00 mg/kg); +: Treatment with respective drug; -: No treatment with respective drug.

Various specific study characteristics that had been investigated (the type of mouse strain, administration of a dummy drug or interexperimental variability) were further analysed in a next step. Here, it had to be considered that these study characteristics were not studied exclusively, but rather also influenced each other when e.g. the type of mouse was studied in two independent experiments. Due to that reason, only major trends will be analysed in this part.

Regarding the type of mouse, a comparison of the entire bacterial number-time profile was not possible due to the lack of samples at different time points for Balb/cJ mice. Comparing bacterial numbers at 24 h and 48 h in lung, the general trend was mainly in line for Swiss and Balb/cJ mice indicating comparable numbers for both types of mice (Figure 3.20). This trend was also confirmed for bacterial numbers in spleen. The already mentioned increased variability at 48 h compared to 24 h was even more distinct illustrated in Figure 3.20 compared to other graphical representations. Here, the variability of

Swiss mice also revealed higher variability compared to Balb/cJ mice probably biased due to the fact, that more samples were generated for Swiss mice.

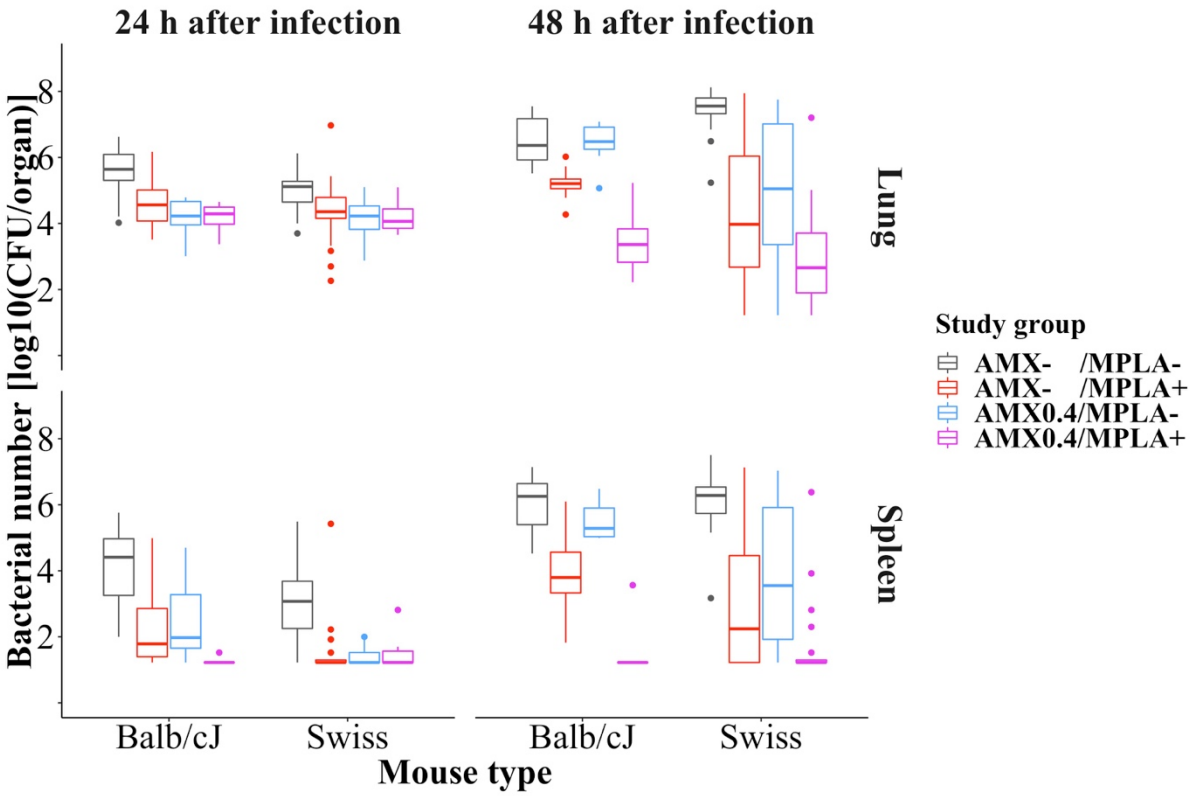

Figure 3.20: Distribution of bacterial numbers of *Streptococcus pneumoniae* serotype 1 per mouse type in lung and spleen after intranasal infection at 0 h and drug administration of AMX and/or MPLA at 12 h. Different study groups (untreated mice as control (AMX-/MPLA-), mice treated with AMX (AMX0.4/MPLA-), with MPLA (AMX-/MPLA+) or a combination of AMX and MPLA (AMX0.4/MPLA+)) are stratified into time after infection (24 h; 48 h) and the sampled organ (lung; spleen). Bacterial numbers are displayed as median, 25th (Q1) and 75th (Q3) percentile (lower and upper hinge), Q1-1.5×IQR (lower whisker), Q1+1.5×IQR (upper whisker) and outliers (points). Abbreviations: AMX: Amoxicillin (0.40 mg/kg); Balb/cJ: Inbred Balb/cJRj mouse strain; CFU: Colony forming units; IQR: Interquartile range; LLOQ: Lower limit of quantification (1.22 log10 CFU/lung); MPLA: Monophosphoryl lipid A (2.00 mg/kg); Swiss: Outbred RjOrl:Swiss (CD-1) mouse strain; +: Treatment with respective drug; -: No treatment with respective drug.

The assignment of the data to the different single experiments showed various findings depending on the aspects that had been investigated in the respective experiments. In general, a comparable variability was present within one experiment and between several experiments across all study groups in lung and spleen at 24 h and 48 h independent of the study characteristics (Figure 7.8, Figure 7.9). Specific experiments investigated the influence of the administration of a dummy solution of the respective other drug (experiment codes FC-018 and FC-047), when a drug in monotherapy was studied. In this setting, no clear trend that was differentiating from the reported interexperimental variability was detected with respect to bacterial numbers in lung and spleen at 24 h and 48 h. The studied type of mouse in specific

experiments (experiment codes FC-018, FC-020 and FC-084) was Balb/cJ. Here, no significant differences compared to Swiss mice in respective other experiments were observed at 24 h and 48 h. Especially considering the interexperimental variability, bacterial numbers were comparable.

3.3.3 Survival study

To assess survival, Swiss mice were monitored for ≤14 days with n_{ID}=6-43 mice investigated per study group (Figure 3.21). Analysing the reported survival, it was important to consider that only 6 individual mice were studied at an AMX dose of 0.80 mg/kg each, alone or in combination with MPLA within one single experiment. Other study groups consisted of up to 43 mice being investigated in 2-4 experiments.

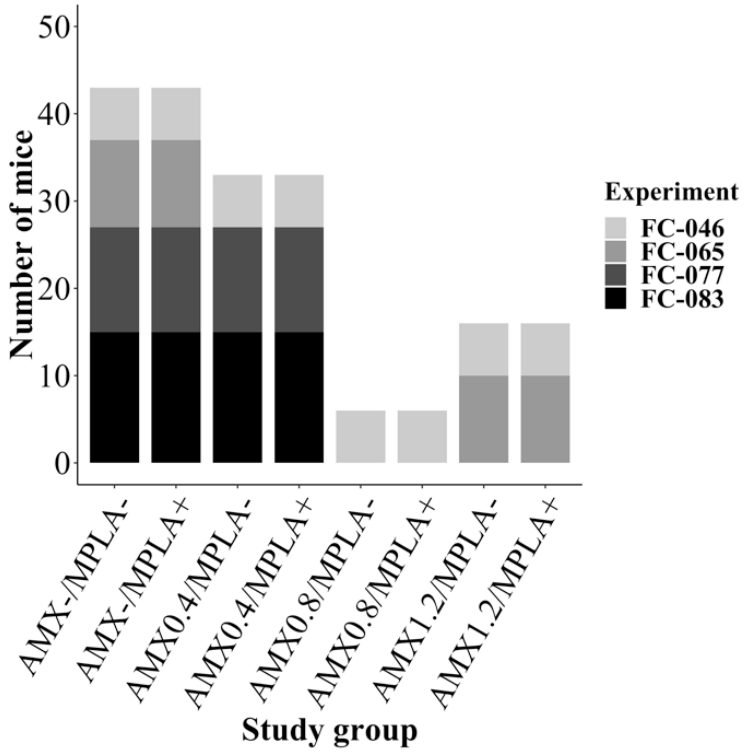

Figure 3.21: Distribution of Swiss mice of different study groups of a study investigating the survival of mice being untreated (AMX-/MPLA-), treated with AMX (AMX0.4/MPLA-, AMX0.8/MPLA-, AMX1.2/MPLA-) or MPLA (AMX-/MPLA+) in monotherapy or in a combined treatment (AMX0.4/MPLA+, AMX0.8/MPLA+, AMX1.2/MPLA+) after infection with *Streptococcus pneumoniae* serotype 1. Mice are allocated into the specific experiments (FC-046, FC-065, FC-077, FC-083). Abbreviations: AMX: Amoxicillin (0.40 mg/kg, 0.80 mg/kg or 1.20 mg/kg); FC: Code of experiment performed by Fiordiligie Casilag (Institut Pasteur de Lille, France); MPLA: Monophosphoryl lipid A (2.00 mg/kg); Swiss: Outbred RjOrl:Swiss (CD-1) mouse strain; +: Treatment with respective drug; -: No treatment with respective drug.

Survival of infected mice supported the already described trend of bacterial numbers (Chapter 3.3.2) that indicated less infection for a combined treatment and, hence, longer survival (Figure 3.22). Study groups investigated over >7 days showed constant survival rates after day 8. Hence, analysis of obtained results focussed on day 7 and the time course of survival itself. Survival investigations of Swiss mice

being not treated at all (n_{ID}=43) resulted in a relatively high mortality with 9.30% being alive after 7 d. Most mice (81.4%) died after day 1 and before day 5. In contrast, the proportion of dead mice was comparably low in the beginning as well as from day 5 onwards. This tendency was also present for all other study groups. Monotherapy of MPLA (n_{ID}=43) resulted in survival of 39.5% after 7 d. Treatment of mice with a combination of AMX and MPLA was superior to single treatment with AMX with an increase in survival of +54.5% and +18.7% after 7 d for 0.40 (n_{ID}=33) and 1.20 mg/kg (n_{ID}=16), respectively. Increasing concentrations of AMX in monotherapy also were in line with expectations of higher survival rates of 27.3% and 68.8% for 0.40 and 1.20 mg/kg, respectively. Here, MPLA in monotherapy increased survival rates more than the lowest dose of AMX in monotherapy. Contradictory to these results, an AMX dose of 0.80 mg/kg resulted in high survival rates in combined treatment (83.3% after 7 d) and even higher survival of 100% in monotherapy. However, as already highlighted, only 6 mice were studied in these dosing groups in a single experiment and, hence, these results had to be interpreted with caution.

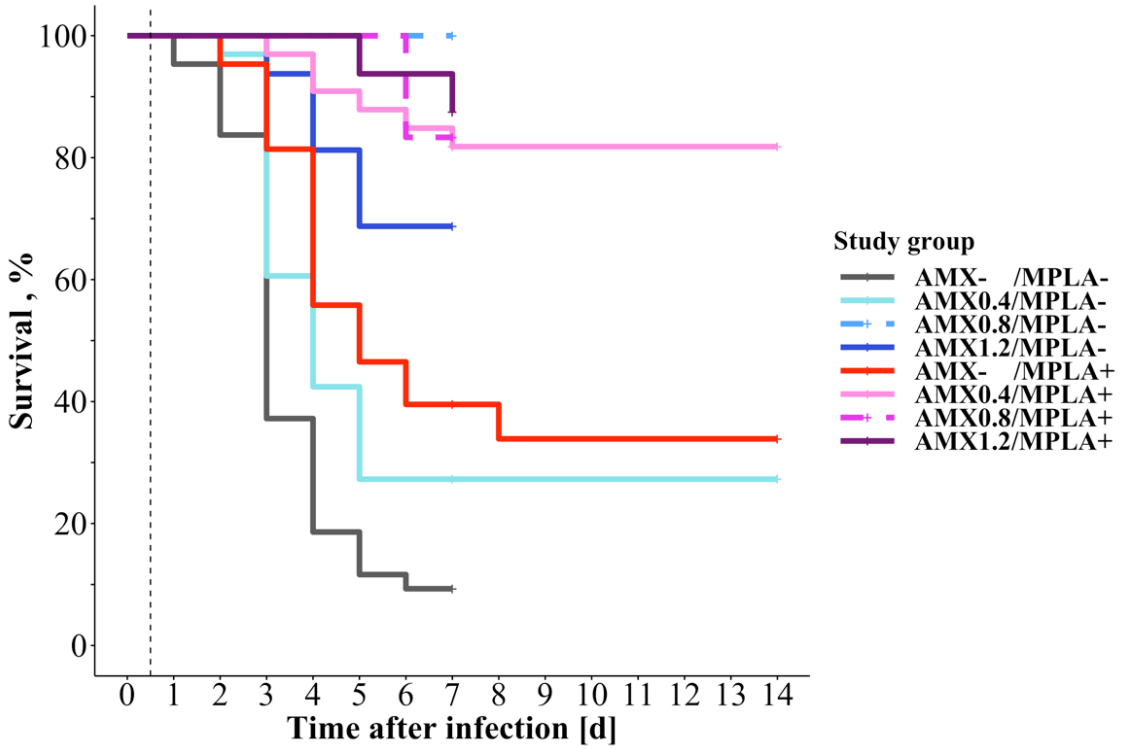

Figure 3.22: Kaplan-Meier plot for survival analysis of outbred RjOrl:Swiss (CD-1) mice being infected with *Streptococcus pneumoniae* serotype 1 at day 0 and drug administration at 12 h (dashed line) over 14 d stratified into the different study groups: Mice untreated (AMX-/MPLA-), treated with AMX (AMX0.4/MPLA-, AMX0.8/MPLA-, AMX1.2/MPLA-) or MPLA (AMX-/MPLA+) in monotherapy or in a combined treatment (AMX0.4/MPLA+, AMX0.8/MPLA+, AMX1.2/MPLA+). Abbreviations: AMX: Amoxicillin (0.40 mg/kg, 0.80 mg/kg or 1.20 mg/kg); MPLA: Monophosphoryl lipid A (2.00 mg/kg); +: Treatment with respective drug; -: No treatment with respective drug.

Based on a log-rank test (Chapter 2.6.2), statistical differences between single groups were analysed after 7 d. Significant improvement in survival was revealed for all treatment groups compared to untreated mice ($p<0.0095$, $\alpha=0.05$). The reported differences between monotherapy of MPLA, low doses and high doses of AMX (0.40 mg/kg and 1.20 mg/kg) were not statistically significant ($p>0.051$, $\alpha=0.05$). Contrarily, combined treatment with AMX and MPLA resulted in significantly higher survival compared to a low dose of AMX or MPLA in monotherapy, respectively ($p<0.00140$, $\alpha=0.05$). Differences between the highest studied dose of AMX in monotherapy and combined treated animals were not statistically significant in this analysis ($p>0.280$, $\alpha=0.05$).

3.3.4 Parameters related to the physical condition and immune system of the animal

A brief overview of the results of additionally investigated parameters will be presented in this chapter to identify general trends and finally relate them to already reported results.

3.3.4.1 Body weight profile

Body weight of individual study mice was assessed in eight study groups simultaneously with survival (Chapter 3.3.3) and, thus, resulted in the same number of studied mice in four different experiments (Figure 3.21). Obvious differences in median body weight between mice that either survived or not survived were obtained. Independent of the received treatment, finally surviving mice showed a continuous increase of body weight over time, except for some study groups on the first day (Figure 3.23). In contrast, dead mice at one of the first days showed a substantial decrease of their body weight. Evaluating the respective dosing groups, differences between MPLA treated and not-treated animals were observed. In animals surviving the infection and being treated with MPLA, an initial decrease in body weight was recorded, followed by a subsequent increase in body weight. This tendency was not present for mice not treated with MPLA. However, in mice that finally did not survive a comparable profile was observed on the first two days. Afterwards, body weight decreased again and was in line with respective other study groups.

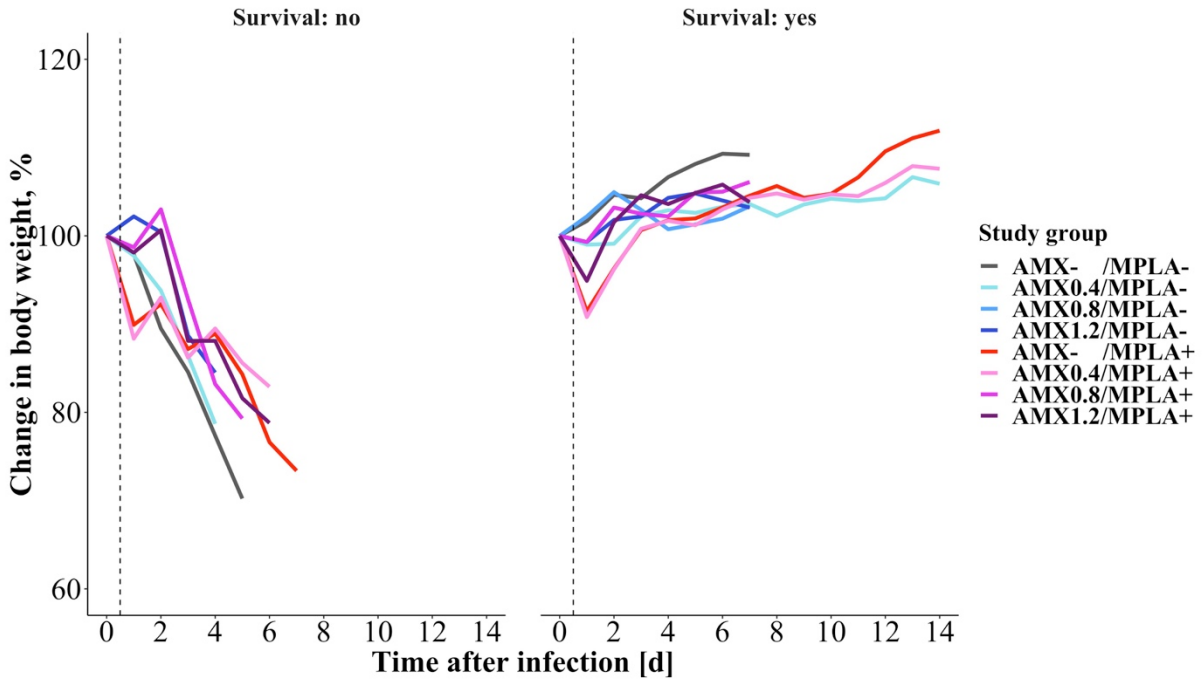

Figure 3.23: Body weight of outbred RjOrl:Swiss (CD-1) mice being infected with *Streptococcus pneumoniae* serotype 1 at day 0 and drug administration at 12 h (dashed line) over 14 d stratified by survival and differentiated into the different study groups: Mice untreated (AMX-/MPLA-), treated with AMX (AMX0.4/MPLA-, AMX0.8/MPLA-, AMX1.2/MPLA-) or MPLA (AMX-/MPLA+) in monotherapy or in a combined treatment (AMX0.4/MPLA+, AMX0.8/MPLA+, AMX1.2/MPLA+). Median body weight of different study groups was reported as percentage compared to initial body weight. Abbreviations: AMX: Amoxicillin (0.40 mg/kg, 0.80 mg/kg or 1.20 mg/kg); MPLA: Monophosphoryl lipid A (2.00 mg/kg); +: Treatment with respective drug; -: No treatment with respective drug.

3.3.4.2 Gene expression of markers of the immune system

The motivation of evaluating relative expression of specific genes was to assess characteristic immune system-related markers describing the effect of MPLA on the immune system in lung. Several of these markers represented the activity of the immune system, e.g. IL-1β as important modulator of the inflammatory process or CCL20 being strongly chemotactic for lymphocytes and neutrophils.

Within each of the six study groups, 3-6 samples were taken with one individual sample per mouse at 4 different time points. For most markers (10 of 15), a general tendency in relative gene expression was revealed (Figure 7.10). The respective study groups consisting of (a) PD4.2, (b) PD4.3 and PD4.4, and (c) PD4.5 and 4.6 (Table 2.4) were best suitable to analyse the data by allocating them into these three groups. With onset of infection in group b (infected and untreated or AMX-treated mice), the markers cAMP, CCL2, FKBP5, ITGB2L, IL-4i1, MMP8, NGP, PROK2, S100A9 and ZBTB16 had a relatively slight increase of relative gene expression over time in common. In contrast, MPLA treatment after onset of infection (c) revealed higher gene expression within the first few hours achieving baseline concentrations subsequently. Treating non-infected mice with MPLA (a) indicated a delayed onset in

the increase of gene expression compared to infected and MPLA treated mice (c). A distinct effect of MPLA and the bacterial infection was shown for these parameters being independent of AMX treatment. Analysis of the markers CCL20, CXCL2, IL-12 and IL-1β resulted only in minor differences between the investigated study groups showing initially higher gene expression that decreased fast within a few hours. These markers did not show any dependency on MPLA treatment and seemed to be more influenced by the infection itself. The marker IL-6 was not completely in line with other markers, but still supported the general trend of differences between MPLA treated mice (c) and not MPLA treated mice (b). In total, the pattern of the differently expressed markers over time in lung showed a characteristic influence of MPLA and the infection itself being highly pronounced right in the beginning.

3.3.4.3 Cytokine kinetics in serum

To further gather information about the effect of MPLA and the infection caused by *S. pneumoniae* serotype 1, cytokine kinetics of four different proinflammatory cytokines were studied over time in serum (Chapter 2.4.4.3). At specific time points (n_{time}=13), serum samples were collected with n_{sample}=6-59 samples per time point and cytokine concentrations were assessed. 24.7% of samples were collected from Balb/cJ mice and accordingly 75.3% from Swiss mice of in total n_{sample}=1057. Only 5.87% of all samples were taken from non-infected mice. In general, the number of samples was evenly distributed among the studied cytokines. However, especially for CCL2, IL-6 and TNFα approximately 30% of the determined concentrations were <LLOQ compared to only 1.47% for IL-6. These concentrations were set to the LLOQ in the graphical representation.

Non-infected or infected mice that received any treatment with MPLA (study groups PD5.3, PD5.4 and PD5.5) revealed median maximum concentrations of the respective cytokines within 16 h after infection and, subsequently, these concentrations decreased to baseline concentrations that were reached 24 h after infection (Figure 3.24). No significant differences between these three study groups were observed. Infected, untreated mice (PD5.1) and infected mice treated with AMX in monotherapy (PD5.2) did not show comparable profiles as the MPLA treated study groups. Here, no pronounced cytokine response was detected 24 h after infection. Afterwards, a moderate increase of cytokine concentrations occurred, which was mainly present for infected mice that had not been treated at all. Investigation of Swiss and Balb/cJ mice did not result in distinct differences in the pattern and magnitude of cytokine concentrations over time between the two studied mice. Here, the main tendency of an immediate response to MPLA was also seen.

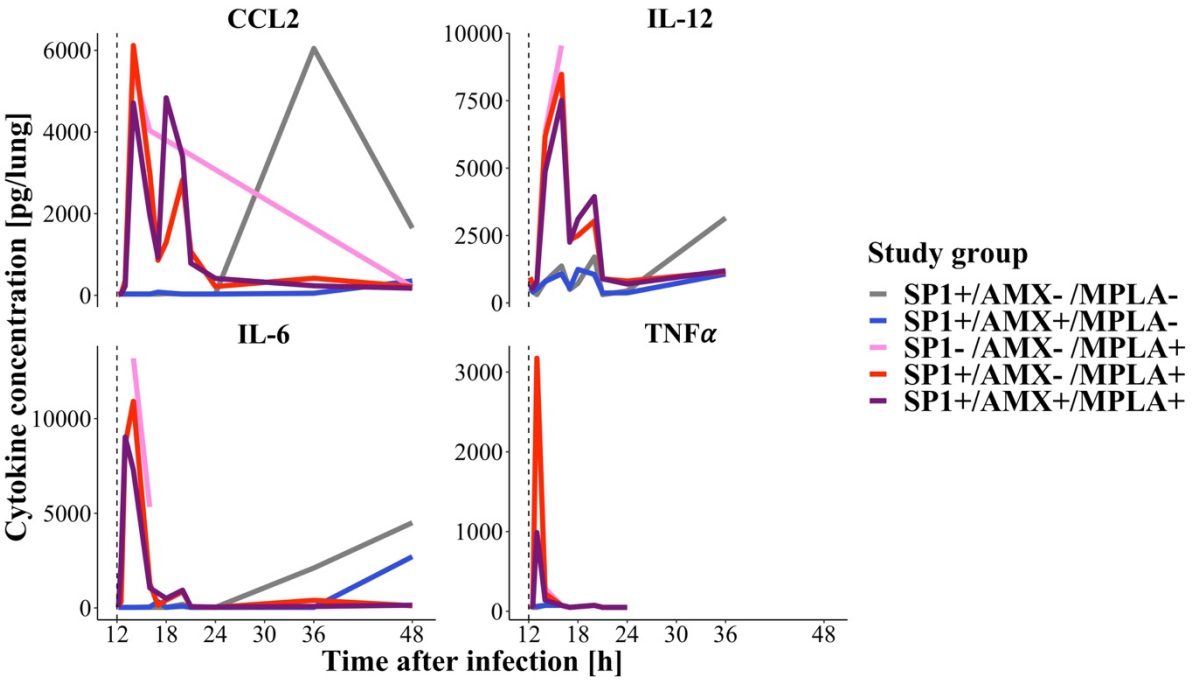

Figure 3.24: Cytokine concentrations of cytokines CCL2, IL-12, IL-6 and TNFα in serum of outbred RjOrl:Swiss (CD-1) and inbred Balb/cJRj mice being infected with SP1 at 0 h and drug administration at 12 h (dashed line) over in total 48 h, stratified by the respective cytokines. Median cytokine concentrations of different study groups (Infected and untreated (SP1+/AMX-/MPLA-), non-infected and treated with MPLA (SP1-/AMX-/MPLA+), infected and treated with AMX (SP1+/AMX+/MPLA-), MPLA (SP1+/AMX-/MPLA+) or the combination of both (SP1+/AMX+/MPLA+)) were reported. Abbreviations: AMX: Amoxicillin; CCL2: C-C-chemokine ligand 2; IL-6: Interleukin-6; IL-12: Interleukin-12; MPLA: Monophosphoryl lipid A; SP1: *Streptococcus pneumoniae* serotype 1; TNFα: Tumor necrosis factor α; +: Treatment with respective drug or bacteria; -: No treatment with respective drug or bacteria.

Another important fact to consider in this setup was that for one specific experiment, cytokine kinetics of CCL2, IL-12 and IL-6 in serum as well as bacterial numbers in lung and spleen were determined simultaneously for one individual mouse. Individual data were assessed for Swiss mice at 18 and 36 h after infection. Here, a clear dependency for each individual mouse was detected for all study groups (Figure 3.25). Higher bacterial numbers in lung were generally accompanied with higher cytokine concentrations. As shown, the treatment with MPLA did not affect the relation between bacterial numbers and cytokine concentrations and revealed a comparable slope to mice not treated with MPLA.

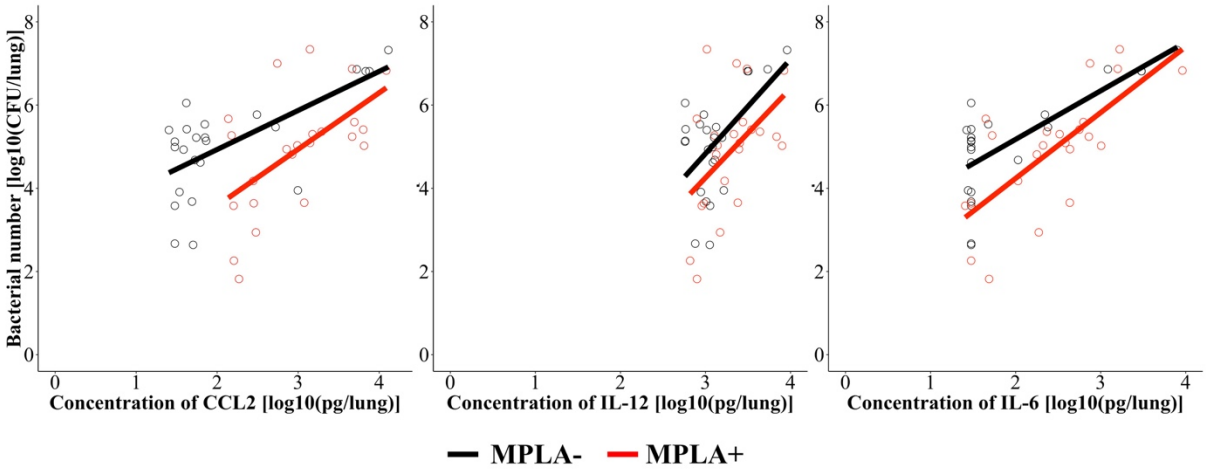

Figure 3.25: Simultaneous determination of bacterial numbers in lung in relation to cytokine concentrations of cytokines CCL2, IL-12 and IL-6 in serum at 18 h or 36 h after infection of individual outbred RjOrl:Swiss (CD-1) mice being infected with *Streptococcus pneumoniae* serotype 1. Individual data points as well as the trend in the population relating bacterial numbers to cytokine concentrations are represented depending on MPLA treatment (MPLA-: black; MPLA+: red). Abbreviations: CCL2: C-C-chemokine ligand 2; CFU: Colony forming units; IL-12: Interleukin-12; IL-6: Interleukin-6; MPLA: Monophosphoryl lipid A; +: Treatment with MPLA; -: No treatment with MPLA.

3.3.4.4 Histopathology in lung of markers of the immune system

Histopathology in lung of individual mice in different study groups (n_{ID}=4 per study group, Chapter 2.4.4.4) was assessed to gain information about the condition of the lung after being challenged by the infection or treated with AMX or MPLA. Here, stimulation of the immune system or severity of infection both being triggered by the infection itself or administration of the immunostimulatory drug MPLA was monitored by the different markers ((a) alveolar macrophages, (b) alveolar neutrophilic infiltration, (c) foreign body-related inflammation, (d) intraluminal neutrophils, (e) perivascular mixed inflammatory cells). Other markers, ((f) alveolar haemorrhage, (g) intravascular fibrinous thrombi, (h) microvascular/venular hyperaemia, (i) perivenous/periarterial oedema, (j) fibrin-leukocytic/suppurative pleuritis, (k) mesothelial pleura thickening) represented the influence on the general physical condition and associated medical conditions next to the effect on the immune system as a result of infection more in detail.

The total median histological score (Figure 7.11) revealed comparable scores of 6, 6.5 and 5.5 for MPLA treated and infected mice (PD6.3), AMX treated and infected mice at a curative dose of 14.0 mg/kg (PD6.6) and mice that were infected and treated with the combination of AMX and MPLA (PD6.4), respectively. These showed histological scores being in the same range as untreated and non-infected animals (4.7, PD6.1). Mice that were infected and either not treated (PD6.2) or received monotherapy of AMX at a low dose (0.40 mg/kg, PD6.5) resulted in total histological scores of 14 and 10.5, respectively, being approximately twice as high compared to other study groups. Between the two before

mentioned groups of markers representing either an influence on the immune system or the general physical condition, no significant tendency occurred indicated by comparable subscores of these groups. A comparison of the individually investigated parameters showed negligible histological score for markers b, c, d, g, j and k. Individual histological scores of the remaining markers confirmed the overall impression of the total median histological score.

3.3.4.5 Recruitment of immune system-related cells

As additional parameter to investigate the impact of infection with *S. pneumoniae* serotype 1 and treatment with AMX and/or MPLA on the immune system, the recruitment of specific cells of the immune system into the lung was monitored (Chapter 2.4.4.5). Here, no significant differences were observed between untreated mice and the respective other study groups (Figure 7.12). The number of cells of untreated and AMX treated animals was slightly higher compared to the other groups indicating an increased recruitment of cells of the immune system and, hence, a more severe infection to a certain extent. Nevertheless, also a relatively large variability had to be taken into account when interpreting these results with only 4 investigated mice per study group. When comparing median proportions of macrophages, monocytes and neutrophils compared to all CD45+ cells in BAL and lung, also no differences between the study groups were detected. In total, investigating cell recruitment did not reveal any significant trends that were able to explain differences between the study groups that had been seen in other performed studies.

3.4 *In silico* analysis of the combination of amoxicillin and monophosphoryl lipid A

The development of a semi-mechanistic PK/PD model aimed to describe the effect of the combination of AMX and MPLA administered to mice being infected with *S. pneumoniae* serotype 1. The analysis of this combination was based on the comprehensive pooled *in vivo* studies that was extensively analysed beforehand (Chapter 3.3). In this chapter, the developed PK/PD model will be introduced, evaluated stepwise and further explored and applied in different simulation and translation studies.

3.4.1 Pharmacokinetic/pharmacodynamic model of the combination of amoxicillin and monophosphoryl lipid A

Based on the introduced modelling strategy (Chapter 2.5.3.2), a semi-mechanistic PK/PD model was developed (Figure 3.26). Briefly, the separately developed PK, bacterial disease, effect compartment, disease and treatment and TTE submodels were combined and optimised.

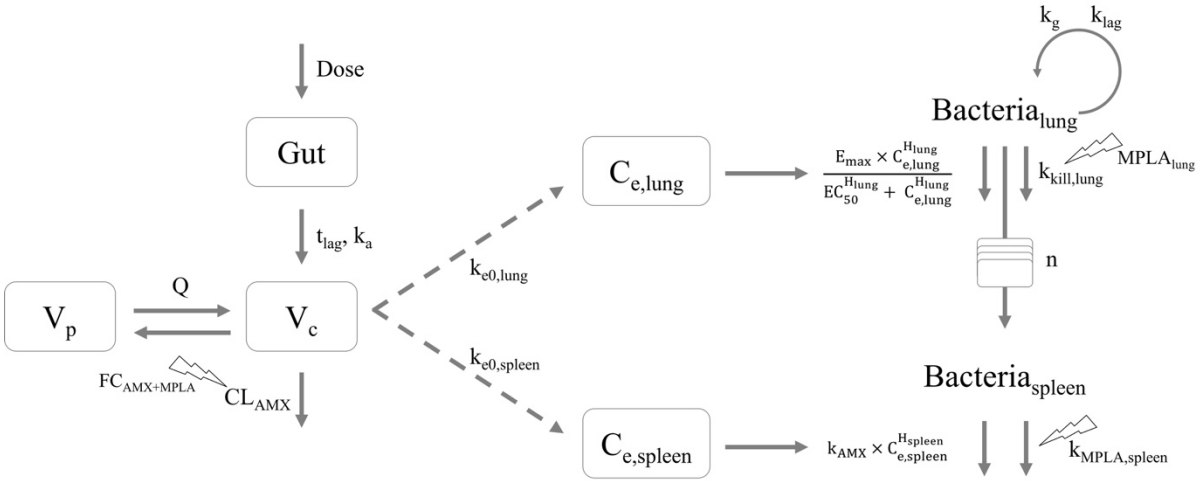

Figure 3.26: Schematic illustration of the semi-mechanistic nonlinear mixed-effects pharmacokinetic/pharmacodynamic model for AMX with coadministration of MPLA of mice infected with *Streptococcus pneumoniae* serotype 1, comprising a two-compartment PK submodel (left), an effect compartment as PK/PD link submodel (middle) and a bacterial disease and treatment submodel including unrelated killing and natural death effects as well as killing effects of the immune system, AMX and MPLA (right).
Abbreviations: AMX: Amoxicillin; $Bacteria_{lung}$: Number of bacteria in lung; $Bacteria_{spleen}$: Number of bacteria in spleen; $C_{e,lung}$: AMX concentration in lung effect compartment; $C_{e,spleen}$: AMX concentration in spleen effect compartment; CL_{AMX}: Clearance of AMX monotherapy without MPLA interaction; Dose: Administered dose of AMX by oral gavage; EC_{50}: Concentration of AMX to achieve half maximum killing effect; E_{max}: Maximum killing effect of AMX; $FC_{AMX+MPLA}$: Fractional change of CL_{AMX} in presence of MPLA depending on the AMX dose implemented as covariate; Gut: Organ of administration; H_{lung}: Hill factor for lung; H_{spleen}: Hill factor for spleen; k_a: First-order absorption rate constant; k_{AMX}: First-order killing rate constant of AMX in spleen representing the slope of the effect compartment concentration and effect relationship; $k_{e0,lung}$: First-order rate constant for effect delay in lung; $k_{e0,spleen}$: First-order rate constant for effect delay in spleen; k_g: First-order growth rate constant in lung; $k_{kill,lung}$: First-order rate constant for treatment-unrelated killing and natural death effects in lung; k_{lag}: First-order rate constant for delay in onset of bacterial growth in lung; $k_{MPLA,spleen}$: First-order killing rate constant for killing effect in spleen only in presence of MPLA; MPLA: Monophosphoryl lipid A; $MPLA_{lung}$: Fractional change of $k_{kill,lung}$ in presence of MPLA; n: Number of transit compartments; Q: Intercompartmental clearance; t_{lag}: Lag time; V_c: Central volume of distribution; V_p: Peripheral volume of distribution.

To introduce a time delay between serum concentrations of AMX and the antibacterial effect, the PK submodel of AMX concentrations in serum (Figure 3.26 (left)) and bacterial growth submodel of bacterial numbers in lung and spleen (Figure 3.26 (right)) were linked by separate effect compartment submodels for lung and spleen with concentrations $C_{e,\,lung}$ and $C_{e,\,spleen}$, respectively (Figure 3.26 (middle)). An extension to a disease and treatment submodel was performed by including PD effects of AMX and MPLA. In the upcoming section, the entire semi-mechanistic PK/PD model structure with its single submodel components will be presented in detail. Here, the developed PK submodel will be considered on its own and separately presented and evaluated in a first step. Afterwards, a link to the PD data will be established.

3.4.1.1 Pharmacokinetic submodel

Neither a one- nor a three-compartment model better described the data compared to a two-compartment model as indicated by the underlying data. Nonlinear absorption and elimination kinetics in terms of Michaelis Menten did not improve the model performance and plausibility. A Michaelis Menten constant, indicating the substrate concentration, at which the reaction rate is half of the maximum [101], was already higher than maximum observed concentrations. Hence, application of first-order absorption and elimination kinetics was supported. Inclusion of a lag time t_{lag} improved the OFV in a LRT significantly (p=0.0133, df=1, α=0.05). Accordingly, the final structural PK submodel for AMX concentrations in serum consisted of a two-compartment model with first-order absorption kinetics including a lag time as well as first-order elimination kinetics and a combined RUV model.

Fixing the final parameter estimate of the first-order absorption rate constant k_a to the predicted parameter estimate of 5.04 h^{-1} stabilised the model convergence and reduced RSEs substantially without influencing other parameter estimates. Due to the relatively high proportion of samples of 15.1% below the LLOQ of 0.01 µg/mL, usage of the so-called M3-method was justified to estimate the likelihood that a concentration was below the LLOQ (Chapter 2.5.1.4) to not influence the structural model and to not disregard these samples. IIV was ultimately included on CL and Q reducing the OFV significantly (p=$1.37 \cdot 10^{-6}$, df=2, α=0.05). Additional implementations of IIV on other model parameters were less stable and did not allow successful minimisation of the estimation step and were also not supported due to the sparse study design with only partly two samples per individual. Integration of coadministration of MPLA on CL_{AMX} depending on the AMX dose ($FC_{AMX+MPLA}$) as covariate significantly increased the predictive performance of the PK submodel and better described the data compared to implementation on other parameters (Figure 3.27). For Q, no influence of any covariates was determined. Measurements at 24 h after infection were not included in this graphical representation due to the fact that serum was sampled only three times in one study group with AMX concentrations being below the LLOQ. In the combination of MPLA with the highest dose of AMX (14.0 mg/kg), the CL_{AMX} was decreased by 40.9% compared to monotherapy. At a low dose of AMX (0.4 mg/kg), this effect was negligible with a reduction of 1.17%. Additional covariates (e.g. the infection status of the mice) or a implementation of the covariates on other parameters did not have an impact on the model performance and, hence, were not included.

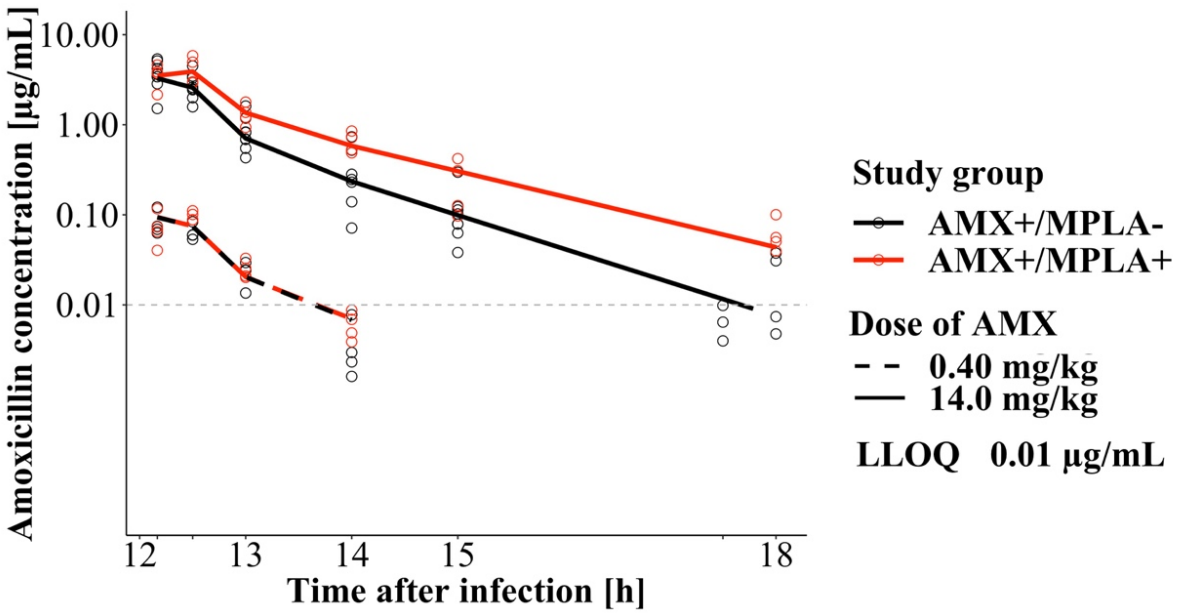

Figure 3.27: Measured (circles, n_{sample}=106 with 15.1% below the LLOQ of 0.01 µg/mL) and median of model-predicted (line) AMX concentrations of the pharmacokinetic submodel after administration of 0.40 mg/kg (dashed) or 14.0 mg/kg (solid) AMX without (AMX+/MPLA-, black) or with (AMX+/MPLA+, red) MPLA coadministration. Abbreviations: AMX: Amoxicillin; LLOQ: Lower limit of quantification; MPLA: Monophosphoryl lipid A.

The final PK submodel was parameterised in terms of CL_{AMX}, Q, V_c and V_p, in addition to the lag time t_{lag} and a first-order absorption rate constant k_a with a proportional RUV model, IIV on CL_{AMX} and Q and MPLA influencing the clearance of AMX as depicted in Figure 3.26 (left). Final parameter estimates of the PK submodel are displayed in Table 3.8.

Table 3.8: Model-predicted parameter estimates including bootstrap results of the pharmacokinetic submodel of amoxicillin and monophosphoryl lipid A.

Parameter	Parameter estimate	Bootstrap	
[unit]	(RSE, %)	Median	95% CI
Structural model			
k_a [h^{-1}]	5.04*	5.04*	-
t_{lag} [h]	0.125 (10.0)	0.116	0.0400 - 0.156
V_c [mL]	15.4 (25.5)	17.5	4.41 - 37.0
V_p [mL]	50.7 (10.1)	50.4	38.3 - 60.6
Q [mL/h]	71.9 (17.4)	66.2	33.3 - 132
CL_{AMX} [mL/h]	124 (5.90)	122	108 - 139
$FC_{AMX+MPLA}$ [mL/h/µg]	-0.145 (18.1)	-0.138	-0.186 - (-0.0958)
Interindividual variability			
CL, %CV	23.4 (14.3)	21.7	14.9 - 28.4
Q, %CV	25.7 (43.2)	39.2	8.60 - 87.1
Residual unexplained variability			
Proportional, %CV	28.2	26.5	15.2 - 33.0

Abbreviations: CI: Confidence interval; CV: Coefficient of variation; CL_{AMX}: Clearance of amoxicillin (AMX) monotherapy without monophosphoryl lipid A (MPLA) interaction; $FC_{AMX+MPLA}$: Fractional change of clearance of AMX in presence of MPLA depending on the AMX dose; k_a: First-order absorption rate constant; Q: Intercompartmental clearance; RSE: Relative standard error; t_{lag}: Lag time; V_c: Central volume of distribution; V_p: Peripheral volume of distribution; *Fixed parameter estimate based on model development process (sensitivity analysis, log-likelihood profiling and bootstrap results) due to stability reasons.

Parameter estimates were predicted with acceptable RSEs and RUV (<25.5% and 28.2% CV, respectively, Table 3.8). In general, the overall PK submodel performance showed good prediction of the serum AMX concentrations. Model evaluation itself did not only focus on typical GOF plots, since a relative high proportion of samples below the LLOQ is typically not adequately depicted in these representations. However, typical GOF plots were evaluated for AMX concentrations above the LLOQ (Figure 7.13) of observations, individual and population predictions and weighed residuals. The data were evenly distributed around the lines of identity. At higher concentrations, the estimation was less precise due to a higher variation in the data, but still equally distributed.

In case of lower concentrations, a pcVPC was more meaningful due to consideration of data below the LLOQ. In general, the pcVPC plots displayed a good predictive performance of the PK submodel over the entire investigated time and captured the fraction of samples being above and below the LLOQ (general trend, variability and fraction, respectively (Figure 3.28)). Here, observations at 24 h after

infection were included to illustrate the predictive performance for the fraction of samples below the LLOQ at later time points. A logarithmic representation of the pcVPC focussed on lower concentrations between 12 and 18 h after infection with samples above and below the LLOQ at same time points (Figure 7.14). The observed trend of good model performance was confirmed, but, still, higher variability was observed at higher concentrations between 12 and 12.5 h after infection. Particularly, this trend can be observed by evaluating VPCs stratified into the different study groups (Figure 7.15). At a high dose of 14.0 mg/kg AMX, predictions met observations. Contrarily, at a low dose of 0.40 mg/kg AMX, the PK submodel was not able to capture the observations within 0.5 h after drug administration (i.e. 12.5 h after infection). Other additional implementations of the covariate MPLA did not improve this trend that was also caused by the sparse data situation in these study groups. Hence, the presented PK submodel was accepted. A performed bootstrap analysis supported the generated results with a convergence rate of 86.5% and parameter estimates and concomitant 95% CIs being not substantially different to original parameter estimates (Table 3.8).

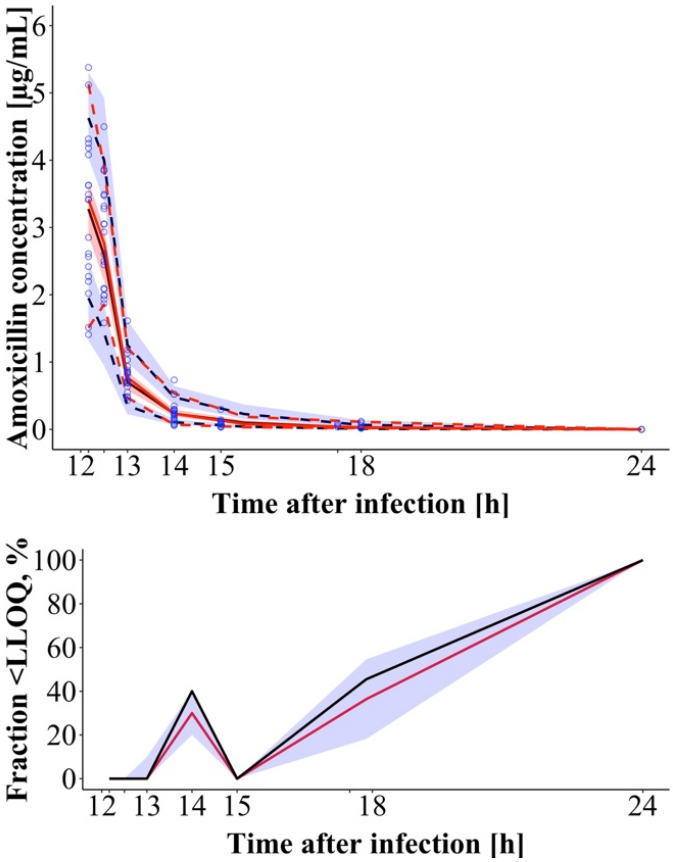

Figure 3.28: Prediction-corrected visual predictive check (n=1000 simulations incl. interindividual variability and unexplained variability) of the developed pharmacokinetic submodel for amoxicillin concentrations in mouse serum with or without MPLA coadministration and fraction of samples being below the LLOQ: Circles: Measurements; Lines: 50th percentile (solid), 5th and 95th percentile (dashed) of measured (red) and simulated (black) amoxicillin concentrations; Shaded area: 90% confidence interval around simulated percentiles. Abbreviations: LLOQ: Lower limit of quantification; MPLA: Monophosphoryl lipid A.

3.4.1.2 Semi-mechanistic pharmacokinetic/pharmacodynamic model

Based on the developed PK submodel (Chapter 3.4.1.1), the PD submodel was developed sequentially. Final parameter estimates of the PK submodel were fixed and used as input to assess the influence of AMX concentrations with MPLA coadministration on the AMX effect on *S. pneumoniae* serotype 1. Allowing PK parameter estimates to change in a simultaneous estimation of PK and PD was not successful and destabilised the PK/PD model. Since PK and PD observations originated from different individual mice and, accordingly, were not directly connected, the sequential modelling approach was selected to reliably estimate the link between PK and PD.

Next, the developed PK/PD model will be comprehensively presented. To better understand and summarise the developed PK/PD model, its single components with their respective single processes will be evaluated stepwise and general trends within the population will be evaluated.

Bacterial disease submodel. The proposed bacterial disease submodel (Figure 3.26, right) was able to capture bacterial growth in lung and spleen. As part of this submodel, the initial number of bacteria in lung ($N_{bacteria,\ t=0}$) characterised the bacterial input and was fixed to a bacterial amount of 6.12 log10 CFU/lung during the model development process due to a reliable and precise estimation with increased stability. Estimation of $N_{bacteria,\ t=0}$ during the model development process did not change PD parameter estimates substantially and destabilised the estimation process. In addition, the bacterial disease submodel consisted of the first-order growth rate constant k_g (0.477 h^{-1}) depending on a delay in onset of bacterial growth characterised by k_{lag} (0.0595 h^{-1}), and the first-order rate constant $k_{kill,\ lung}$ (0.274 h^{-1}) capturing natural bacterial elimination processes in lung that mainly consisted of treatment-unrelated effects in terms of natural bacterial death as well as effects of the immune system. Higher uncertainty was especially shown for k_{lag} (46.2% RSE) being also supported by a relatively large 95%CI in the performed bootstrap analysis (Table 3.9). Here, a simultaneous and at the same time reliable estimation of k_{lag} along with k_g was challenging during the entire development process of the PK/PD model. Hence, other approaches were investigated to estimate k_g and k_{lag} with increased stability. Neither a simplification to k_{net} nor introducing prebacterial compartments (ΔAIC=+50.9) did improve parameter precision during the model development process. As a consequence, the original parametrisations of k_{lag} was maintained. Given the underlying data of the bacterial growth submodel, simplifications were not possible without neglecting important trends of initial killing or delayed growth in the data. All parameters were essential to characterise the bacterial growth kinetics sufficiently and, hence, a higher uncertainty was accepted. Defining $k_{kill,\ lung}$ mathematically in a different way as e.g. E_{max} model or with an additional exponential term to allow variation over time (Chapter 2.5.3.2) was also not beneficial compared to the original implementation. As expected, limiting bacterial growth to a maximum value did not improve the model performance (ΔAIC≥+2.00) and led to an estimated maximum bacterial number of 15.2 log10 CFU/lung (121% RSE), that was not reached in the investigated time period of 48 h. A first-order growth rate constant k_g of 0.477 h^{-1} in lung corresponded to a mean generation time

(MGT) of 1.45 h indicating an average time required for doubling of a bacterial culture of 87.2 min. In this setting, the MGT was not incorporating any killing effects, either by the immune system or by natural death [101,181]. Inclusion of the delay term for bacterial growth and natural bacterial elimination processes in lung caused a time-varying MGT of *S. pneumoniae* serotype 1. Here, the MGT was relatively high in the beginning and finally reduced to 3.95 h at 48 h after infection. Considering bacterial growth and neglecting any bacterial elimination effects in the bacterial disease submodel showed a typical bacterial growth curve over time (Figure 7.16). Due to the implemented parameter k_{lag}, a delay in onset of bacterial growth was successfully characterised. Addition of natural bacterial elimination in terms of the first-order killing rate constant $k_{kill,\ lung}$, that was estimated to be in a comparable range as k_g (Figure 3.32), decreased bacterial numbers substantially (Figure 7.16). Considering the delay term for bacterial growth, the constant effect $k_{kill,\ lung}$ reduced bacterial numbers in the simple disease submodel up to 14.4 h after infection. Afterwards, bacterial growth overtook initial killing processes. Over the investigated time frame of 48 h, a net increase of bacterial numbers in lung was observed as long as the effects of AMX and MPLA were not considered.

To allow the transition of bacteria from lung to spleen, estimation of the exact number of transit compartments was superior compared to other introduced methods adding e.g. a specific number of compartments in a stepwise fashion as indicated by an increase in AIC values ($\Delta AIC \geq +108$). The transition was reliably described by 23.0 transit compartments (13.1% RSE) leading to a *MTT* of 40.8 h (4.30% RSE). Due to the marked delay in transition from lung to spleen with bacteria determined in spleen about 15 h after infection, a high number of compartments (n=23.0) as well as the concomitant high *MTT* (40.8 h) were plausible, especially considering the different barriers that bacteria had to overcome to transit from lung to spleen. In spleen, the increase in bacterial numbers was only driven by the inflow from lung leading to accumulation of bacteria. The reliable estimation of bacterial growth $k_{g,\ spleen}$ as well as natural death and treatment-unrelating killing effects as a first-order killing rate constant $k_{kill,\ spleen}$ was not supported by the underlying data. Hence, an increase in bacterial numbers in spleen was completely driven by the transition of bacteria from lung and bacteria reducing effects only occurred in presence of at least one drug. Implementation of one of the parameters reduced the model precision substantially and was not statistically significant in a LRT. As a result, these approaches were not considered. This trend was also already seen in the underlying data indicating no clear initial killing processes as in lung (Chapter 3.3.2).

Effect compartment submodel. Two separate effect compartments with first-order in- and outflow kinetics allowed the transfer of AMX into lung and spleen. Both estimated first-order rate constants $k_{e0,\ lung}$ and $k_{e0,\ spleen}$ that characterised the effect delay in lung and spleen were estimated reliably (19.7% and 17.7% RSE, respectively) and showed relatively low parameter estimates indicating a slow equilibration of the central and the respective effect compartments. Still, estimated parameter values of $k_{e0,\ lung}$ and $k_{e0,\ spleen}$ were in one order of magnitude (0.125 h^{-1} ($t_{1/2,lung}$=5.54 h) and 0.0435 h^{-1}

($t_{1/2,spleen}$=15.9 h), respectively). Hence, a simplification of both first-order rate constants to one single rate constant and, thus, only one effect compartment for lung and spleen, was considered, but finally disregarded due to numerical stability issues of the estimation and less plausibility.

Based on the two effect compartments, a typical concentration-time profile was obtained for serum concentrations of AMX with comparatively low concentrations in lung and spleen (Figure 7.17). As a consequence, a delayed increase of AMX concentrations and a slower elimination compared to serum concentrations were visible as especially observed in a semi-logarithmic representation of the different investigated study groups (Figure 3.29). This trend was more prominent in spleen indicating an even slower equilibration between serum and spleen. The determined PK interaction of MPLA on CL_{AMX} was less noticeable in this setting, since only comparably small doses of AMX were studied.

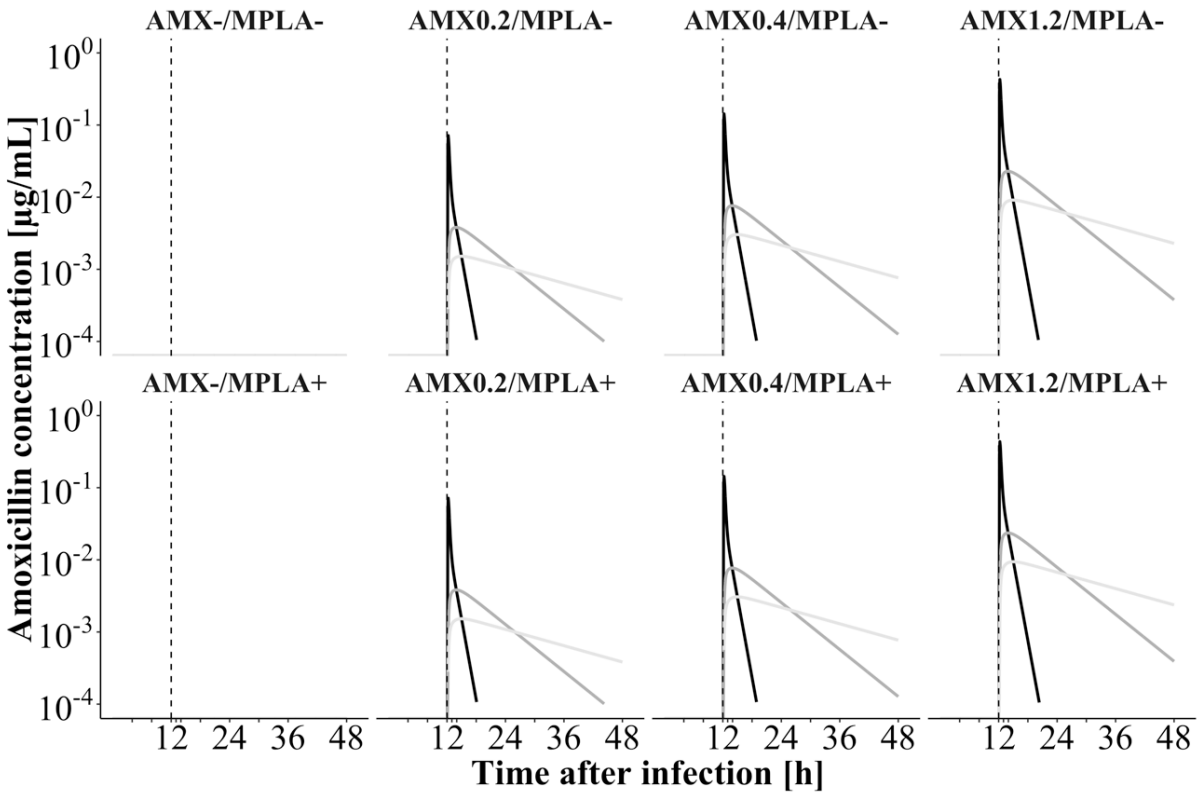

Figure 3.29: Population-predicted AMX concentrations in the central compartment (black), and respective effect compartments in lung (dark grey) and spleen (light grey) over 48 h after infection with *Streptococcus pneumoniae* serotype 1 in mice with drug administration at 12 h (dashed vertical line). Different study groups are displayed: Mice untreated (AMX-/MPLA-), treated with AMX (AMX0.2/MPLA-, AMX0.4/MPLA-, AMX1.2/MPLA-) or MPLA (AMX-/MPLA+) in monotherapy or in a combined treatment (AMX0.2/MPLA+, AMX0.4/MPLA+, AMX1.2/MPLA+). Abbreviations: AMX: Amoxicillin (0.20 mg/kg, 0.40 mg/kg or 1.20 mg/kg); MPLA: Monophosphoryl lipid A (2.00 mg/kg); +: Treatment with respective drug; -: No treatment with respective drug.

Disease and treatment submodel. The effect of AMX on *S. pneumoniae* serotype 1 in lung was best characterised by a sigmoidal E_{max} model as drug-dependent bacterial killing process that was superior to simple linear models (ΔAIC=+70.6), a power model (ΔAIC=+11.5), an E_{max} model (ΔAIC=+19.9) or the Richards model (ΔAIC=+10.7). The concentration-effect relationship was very steep indicated by the estimated very high Hill factor, which was not quantifiable with high precision (H_{lung}=105; 37.8% RSE; 95% CI of LLP 1.96-105). Nevertheless, H was significantly higher than 1 as indicated by a performed LLP and, hence, its use was justified to describe the steep concentration-effect relationship. To increase the model precision, the parameter H_{lung} was subsequently fixed to 20 [104]. Since the sigmoidal E_{max} model was implemented enhancing bacterial killing as parallel pathway to growth and natural bacterial elimination kinetics in an additive way, E_{max} (E_{max}=0.255 h^{-1}) was the maximum achievable bacterial killing rate constant being within one order of magnitude as other treatment-unrelated killing and natural death effects ($k_{kill,\ lung}$=0.274 h^{-1}) or k_g (k_g=0.477 h^{-1}). Implementing the effect of AMX on respective first-order rate constants k_g or $k_{kill,\ lung}$, allowing AMX to either reduce growth or enhance natural bacterial elimination separately, did not improve the model performance. The EC_{50} value (EC_{50}=0.00109 µg/mL) was approximately within one order of magnitude compared to present AMX concentrations in lung with $C_{max,\ lung}$ of 0.0236 µg/mL altogether justifying the use of a sigmoidal E_{max} model (Figure 3.30).

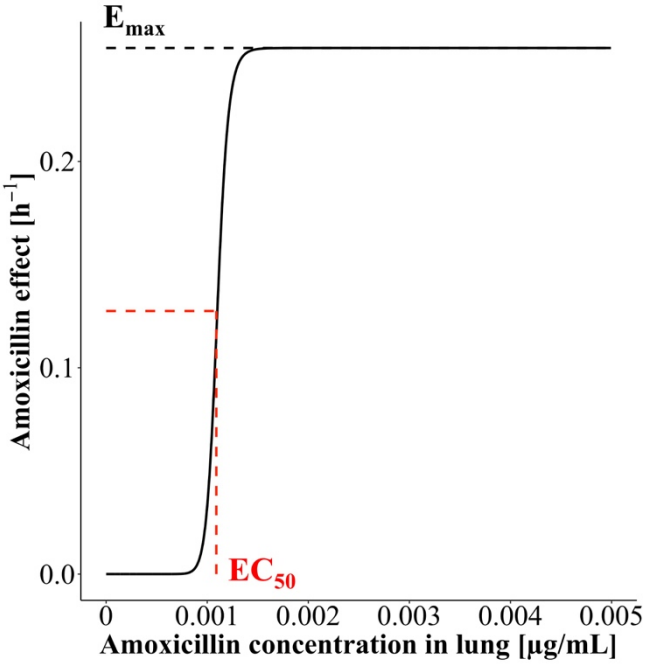

Figure 3.30: The effect of AMX in terms of a sigmoidal E_{max} model (EC_{50}=0.00109 µg/mL (red dashed line); E_{max}=0.255 h^{-1} (black dashed line)) depending on AMX concentrations in lung of mice infected with *Streptococcus pneumoniae* serotype 1 and treated with AMX. Abbreviations: AMX: Amoxicillin; EC_{50}: Concentration of AMX to achieve half maximum killing effect; E_{max}: Maximum killing effect of AMX; MPLA: Monophosphoryl lipid A.

The sigmoidal E_{max} model characterised by a relatively high Hill factor of 20 led to the assumption that the effect of AMX was only present as long as AMX concentrations were above a certain threshold in lung (Figure 7.18), in this case the EC_{50}, comparable to an on/off switch of the effect.

As expected, AMX in monotherapy had a dose dependent effect. With an increasing dose of AMX, the effect lasted over a longer time period up to approximately 40 h after infection for 1.20 mg/kg AMX (Figure 3.32). Neglecting bacterial elimination effects in terms of $k_{kill,\ lung}$ revealed that AMX alone was not able to reduce bacterial numbers in a sustained manner (Figure 7.16). AMX was only able to keep bacterial numbers more or less constant as long as AMX concentrations were above the EC_{50}. Addition of bacterial elimination effects lead to final bacterial numbers observed in lung for AMX monotherapy.

In spleen, a simplified slope model with the killing rate constant k_{AMX} with a separate Hill factor H_{spleen} representing the slope of the AMX effect compartment concentration and effect relationship was most stable and best captured killing effects. More complex implementations of the AMX effect in spleen, e.g. a simple linear model (ΔAIC=+17.2) or a sigmoidal E_{max} model (ΔAIC=+2.00), did not improve the model performance and were less precise. Compared to lung, a relatively high Hill factor of 5.06 in spleen also indicated steep killing kinetics depending on AMX concentrations in spleen (Figure 3.31). At the lowest investigated dose of AMX of 0.2 mg/kg, a $C_{max,\ spleen}$ value of 0.00152 µg/mL was determined indicating only a very minor effect of AMX on bacteria compared to higher AMX concentrations with $C_{max,\ spleen}$ of 0.00941 µg/mL at a dose of 1.2 mg/kg with a substantially higher AMX effect (Figure 7.19).

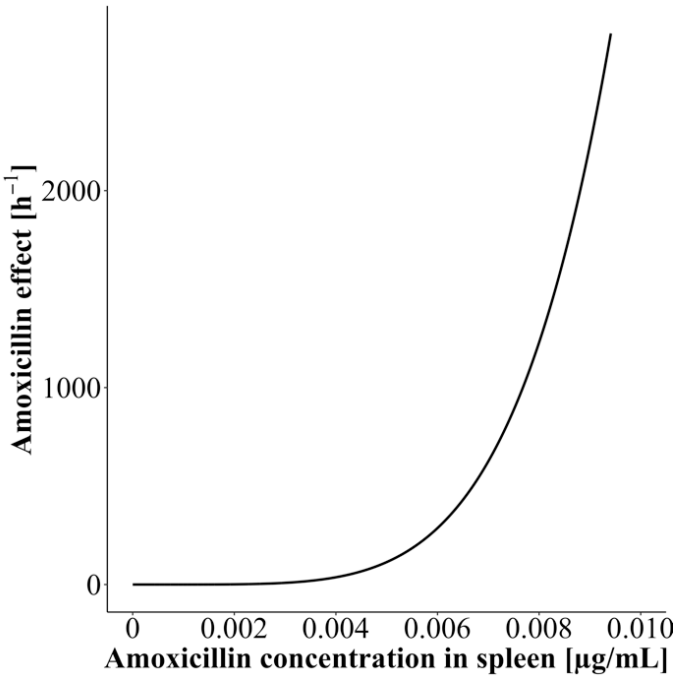

Figure 3.31: The effect of AMX in terms of a linear effect model with Hill factor depending on AMX concentrations in spleen of mice infected with *Streptococcus pneumoniae* serotype 1 and treated with AMX. Abbreviations: AMX: Amoxicillin; MPLA: Monophosphoryl lipid A.

In lung, the effect of MPLA on bacteria was best implemented as its ability to enhance the efficacy of the treatment-unrelated killing effects on bacteria $k_{kill,lung}$ after administration at 12 h (Figure 3.32). Administration of MPLA in monotherapy at 12 h after infection affected $k_{kill,lung}$ and, hence, reduced bacterial numbers in mice treated with MPLA to numbers of 5.36 log10 CFU/lung at 48 h being below the initial inoculum (Figure 7.16). Next to the already described bacterial elimination effect of AMX, a clear boost on the immune system by MPLA was detected increasing the effect of the immune system 1.40-fold. Contrarily, a separate first-order killing rate constant $k_{MPLA,\ spleen}$ was estimated in spleen, only characterising an additional killing effect of the immune system in presence of MPLA and being independent of natural death and treatment-unrelated killing effects in spleen. In the latter case, a stable and precise estimation of a first-order rate constant describing the killing of the immune system without MPLA was not possible, since it was also not seen in the underlying observations and hence, it was disregarded. The effect of the immune system together with MPLA was estimated with acceptable stability and almost 10 times higher in spleen compared to lung ($k_{MPLA,\ lung}$=0.274 h^{-1} (20.3% RSE); $MPLA_{lung}$=1.40 (6.10% RSE); $k_{MPLA,\ spleen}$=3.71 h^{-1}(27.5% RSE)).

As depicted in Figure 3.32 and contrary to the effect of AMX, the effect of MPLA was constant over time. Administration of MPLA postponed the timepoint, at which the bacterial numbers in lung started to increase again, by 12.9 h to 27.3 h. Hence, MPLA was able to reduce bacterial numbers substantially. Especially the slope of the bacterial growth curve was decreased compared to monotherapy as soon as AMX concentrations in lung fall below the EC_{50} (Figure 7.16).

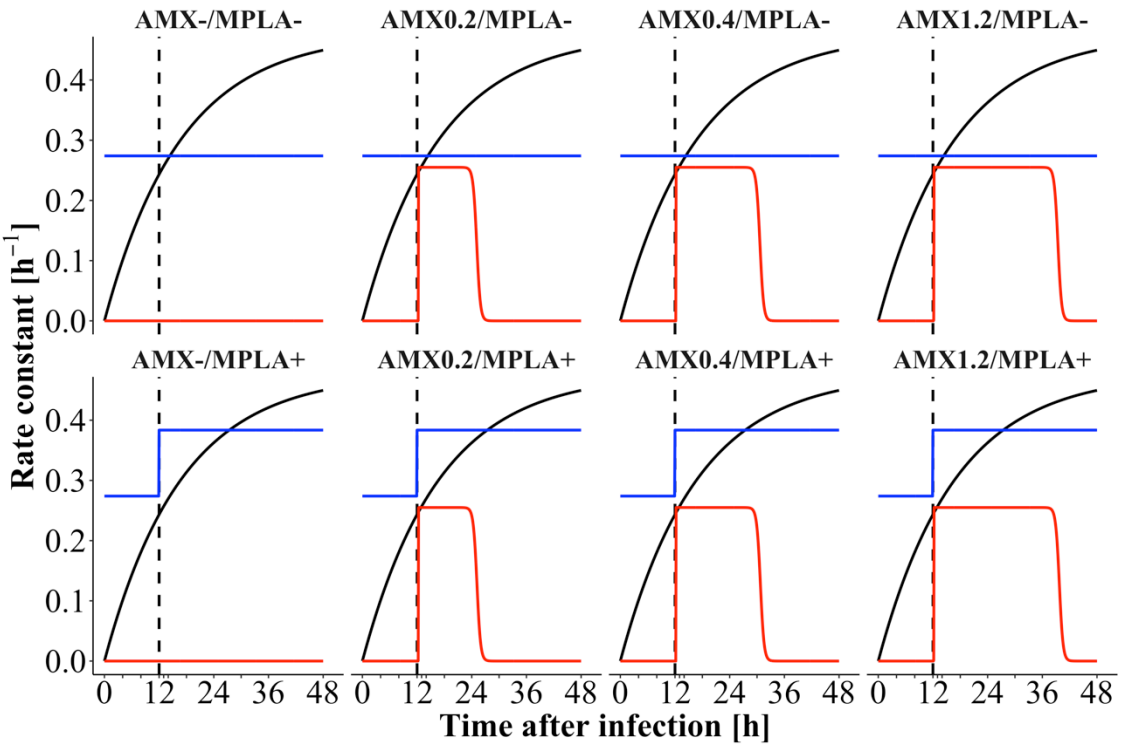

Figure 3.32: Comparison of respective rate constants of a pharmacokinetic/pharmacodynamic model defining bacterial growth of *Streptococcus pneumoniae* serotype 1 (black), natural bacterial elimination effects in absence or presence of MPLA (blue) and the effect of AMX depending on AMX concentrations (red) in lung with drug administration at 12 h (dashed line). Different study groups are displayed: Mice untreated (AMX-/MPLA-), treated with AMX (AMX0.2/MPLA-, AMX0.4/MPLA-, AMX1.2/MPLA-) or MPLA (AMX-/MPLA+) in monotherapy or in a combined treatment (AMX0.2/MPLA+, AMX0.4/MPLA+, AMX1.2/MPLA+). Abbreviations: AMX: Amoxicillin (0.20 mg/kg, 0.40 mg/kg or 1.20 mg/kg); MPLA: Monophosphoryl lipid A (2.00 mg/kg); +: Treatment with respective drug; -: No treatment with respective drug.

A potential interaction of AMX and MPLA was further analysed to define potential synergy or antagonism. Neither the implementation of MPLA as influence on the maximum effect of AMX (ΔE_{max}, p=0.944, df=1, α=0.05) nor on half the potency of AMX (ΔEC_{50}, p=0.272, df=1, α=0.05) led to a significant change of the OFV in a LRT. In addition, the 95% CI of a LLP included parameter estimates of 1 for ΔE_{max} (ΔE_{max} =1.01; 95% CI 0.875-1.16) and ΔEC_{50} (ΔEC_{50}=0.772; 95% CI 0.415-1.23), respectively, and no improvement in GOF plots was observed. These results clearly indicated an additive effect of AMX and MPLA and did not hint at any synergism or antagonism.

The already described relatively high variability in the data (Chapter 3.3.2) was captured by an additive RUV model on a logarithmic scale separating between RUV in lung and spleen. The final PK/PD model showed RUV of 1.12 and 1.81 log10 CFU/organ in lung and spleen, respectively, and was estimated reliably (3.90% and 4.40% RSE, respectively). Compared to determined LLOQ values of >1.22 log10 CFU/organ, reported RUV was in the same magnitude and, hence, was acceptable. Considering the underlying data indicating already a relatively high variability within each single study

group, the reported RUV was reasonable. These findings indicated already that administration of either AMX or MPLA in different study groups was a massive challenge for mice in context of the complex underlying processes and increased variability substantially indicating very different responses between individual mice.

Realisation of IIV was limited as already discussed due to the fact that only one sample was collected for quantification of bacteria from one individual mouse in lung and spleen (Chapter 2.5.3.2) and, hence, hampered the simultaneous estimation of RUV and IIV. To still get an impression of potential IIV, the determined RUV was modified. Evaluating RUV only within the first 12 h separated from other results revealed substantially decreased RUV in lung. Here, only bacterial numbers of mice that were infected but did not receive any treatment yet were assessed and resulted in a RUV of 0.302 log10 CFU/lung. To consider this value as well as reported LLOQ values, RUV was fixed to 1 in this case to characterise a fixed experimental variability. In this context, implementation of IIV caused an instable parameter estimation and not successful convergence of the estimation step. By investigating respective parts of the PK/PD model separately, estimation of IIV was partly possible. Given the still very sparse data situation, IIV was implemented on only one parameter. In the disease and treatment submodel for lung, the highest drop in the OFV was determined for the implementation of IIV on k_{lag} (IIV k_{lag}=48.0% (16.6% RSE); p=$5.53 \cdot 10^{-38}$, df=1, α=0.05). To further evaluate the included IIV on k_{lag}, its impact on possible covariates was analysed in detail. For that reason, the individual k_{lag} values of different study groups were investigated against respective covariates (Figure 7.20). Neither the type of mouse, the dummy administration of the respective other drug nor the study groups itself revealed a significant trend on k_{lag}. Addition of fixed IIV of either k_{lag} or the determined IIV of the PK submodel did not stabilise the estimation of the entire PK/PD model. Hence, IIV was not included on the entire PK/PD model.

In total, the PK/PD model reflected the observed data and important processes reliably and with plausible parameter estimates (Table 3.9) and the overall model performance revealed good prediction of underlying processes, especially given the sparse data situation with only one sample in lung and spleen being present per individual mouse. A bootstrap analysis with a convergence rate of 99.7% was in agreement with model-predicted parameter estimates (Table 3.9).

Table 3.9: Parameter estimates incl. bootstrap results of the semi-mechanistic PK/PD model of mice infected with *Streptococcus pneumoniae* serotype 1 being untreated or treated with AMX and/or MPLA.

Parameter	Parameter estimate	Bootstrap	
[unit]	(RSE, %)	Median	95% CI
Pharmacokinetic submodel			
k_a [h^{-1}]	5.04*	5.04*	-
t_{lag} [h]	0.125*	0.125*	-
V_c [mL]	15.4*	15.4*	-
V_p [mL]	50.7*	50.7*	-
Q [mL/h]	71.9*	71.9*	-
CL_{AMX} [mL/h]	124*	124*	-
$FC_{AMX+MPLA}$ [mL/h/µg]	-0.145*	-0.145*	-
Effect compartment submodel			
$k_{e0,\ lung}$ [h^{-1}]	0.125 (19.7)	0.125	0.0830 - 0.247
$k_{e0,\ spleen}$ [h^{-1}]	0.0435 (17.7)	0.0435	0.0287 - 0.0635
Bacterial disease submodel			
$N_{bacteria,\ t=0}$ [log10(CFU/lung)]	6.12**	6.12**	-
k_g [h^{-1}]	0.477 (7.00)	0.504	0.439 - 1.12
k_{lag} [h^{-1}]	0.0595 (46.2)	0.0555	0.0111 - 0.108
$k_{kill,\ lung}$ [h^{-1}]	0.274 (20.3)	0.270	0.199 - 0.382
n	23.0 (13.1)	23.3	18.0 - 31.4
MTT [h]	40.8 (4.30)	40.5	37.2 - 44.5
Disease and treatment submodel			
$MPLA_{lung}$	1.40 (6.10)	1.41	1.29 - 1.61
E_{max} [h^{-1}]	0.255 (6.00)	0.253	0.220 - 0.283-
EC_{50} [µg/mL]	0.00109 (29.4)	0.00109	0.000134 - 0.00146
H_{lung}	20**	20**	-
$k_{MPLA,\ spleen}$ [h^{-1}]	3.71 (27.5)	3.50	2.05 - 6.12
k_{AMX} [log10(h^{-1})]	13.7 (22.1)	14.0	9.05 - 24.2
H_{spleen}	5.06 (23.9)	5.14	3.22 - 9.26
Residual unexplained variability***			
Lung [log10(CFU/lung)]	1.12 (3.90)	1.12	1.03 - 1.21
Spleen [log10(CFU/spleen)]	1.81 (4.40)	1.79	1.65 - 1.95

Abbreviations: AMX: Amoxicillin; CFU: Colony forming units; CI: Confidence interval; CL_{AMX}: Clearance of AMX monotherapy without MPLA interaction; EC_{50}: Concentration of AMX to achieve half maximum killing effect; E_{max}: Maximum killing effect of AMX; $FC_{AMX+MPLA}$: Fractional change of CL_{AMX} in presence of MPLA depending on the AMX dose implemented as covariate; H_{lung}: Hill factor in lung; H_{spleen}: Hill factor in spleen; k_a: First-order absorption rate constant; k_{AMX}: First-order killing rate constant of AMX in spleen representing the slope of the effect compartment concentration and effect relationship; $k_{e0,lung}$: First-order rate constant for effect delay in lung; $k_{e0,spleen}$: First-order rate constant for effect delay in spleen; k_g: First-order growth rate constant of bacteria in lung; $k_{kill,lung}$: First-order rate constant for treatment-unrelated killing and natural death effects in lung; k_{lag}: First-order rate constant for delay in onset of bacterial growth in lung; $k_{MPLA,spleen}$: First-order killing rate constant for killing effect in spleen only in presence of MPLA; MPLA: Monophosphoryl lipid A; $MPLA_{lung}$: Fractional change of $k_{kill,lung}$ in presence of MPLA; MTT: Mean transition time; n: Number of transit compartments; $N_{bacteria,\ t=0}$: Initial number of bacteria in lung at 0 h; PD: Pharmacodynamic; PK: Pharmacokinetic; Q: Intercompartmental clearance; RSE: Relative standard error; t_{lag}: Lag time; V_c: Central volume of distribution; V_p: Peripheral volume of distribution; *Fixed parameter estimates of developed PK submodel; **Fixed parameter estimate based on model development process (sensitivity analysis, log-likelihood profiling and bootstrap results) due to stability and plausibility; ***Residual unexplained variability estimated on standard deviation scale.

Evaluation of GOF plots required the omission of bacterial numbers below the LLOQ for the graphical representation. For bacterial numbers in lung, GOF plots were generated to observe general trends in the data (Figure 7.21). Hence, especially at lower numbers, a bias that might be created due to omission of bacterial numbers below the LLOQ was accepted and considered for evaluation. For these GOF plots, individual predictions were equal to population predictions as no IIV was included in the final PK/PD model. Evaluating observations against population predictions led to an equal distribution of the bacterial numbers around the line of identity with a relatively high variability. This variability was confirmed by investigation of weighted residuals against population predictions and against time after infection and revealed an increase in variability over time. A comparable trend was already described for the raw data (Chapter 3.3.2). Still, residuals were evenly scattered around the line of identity. In spleen, evaluation of GOF plots was not reasonable due to the high proportion of samples <LLOQ of 51.9%. Hence, VPCs were analysed in detail to consider all bacterial numbers. In general, comparable trends were also well captured in VPCs of the model for bacterial numbers in lung (Figure 3.33) and spleen (Figure 3.34) stratified into the different dosing groups and supported described findings. Here, the study groups receiving 0.20 mg/kg AMX were not displayed since only a few samples were present at only one time point. Still, an overall high variability was observed in the data.

In lung, bacterial numbers being <LLOQ were adequately captured in all study groups and, hence, complemented described findings of GOF plots. The VPCs itself showed that the median simulated numbers followed same trends as median observations. Over the entire study period, minor deviations between observations and simulations occurred. Nevertheless, no significant trends in these deviations were detected and each study group revealed deviations at different time points. At 48 h these differences were further analysed, since this time point was used to characterise bacterial numbers at the

end of the study period. Here, observations were either under- or overpredicted by the developed PK/PD model. However, these trends were not associated with certain study characteristics, such as coadministration of MPLA. In addition to the described trends, a relatively high variability was also present in the VPCs and plausible given the imprecision of the underlying data and the fact that no IIV was implemented in the final PK/PD model.

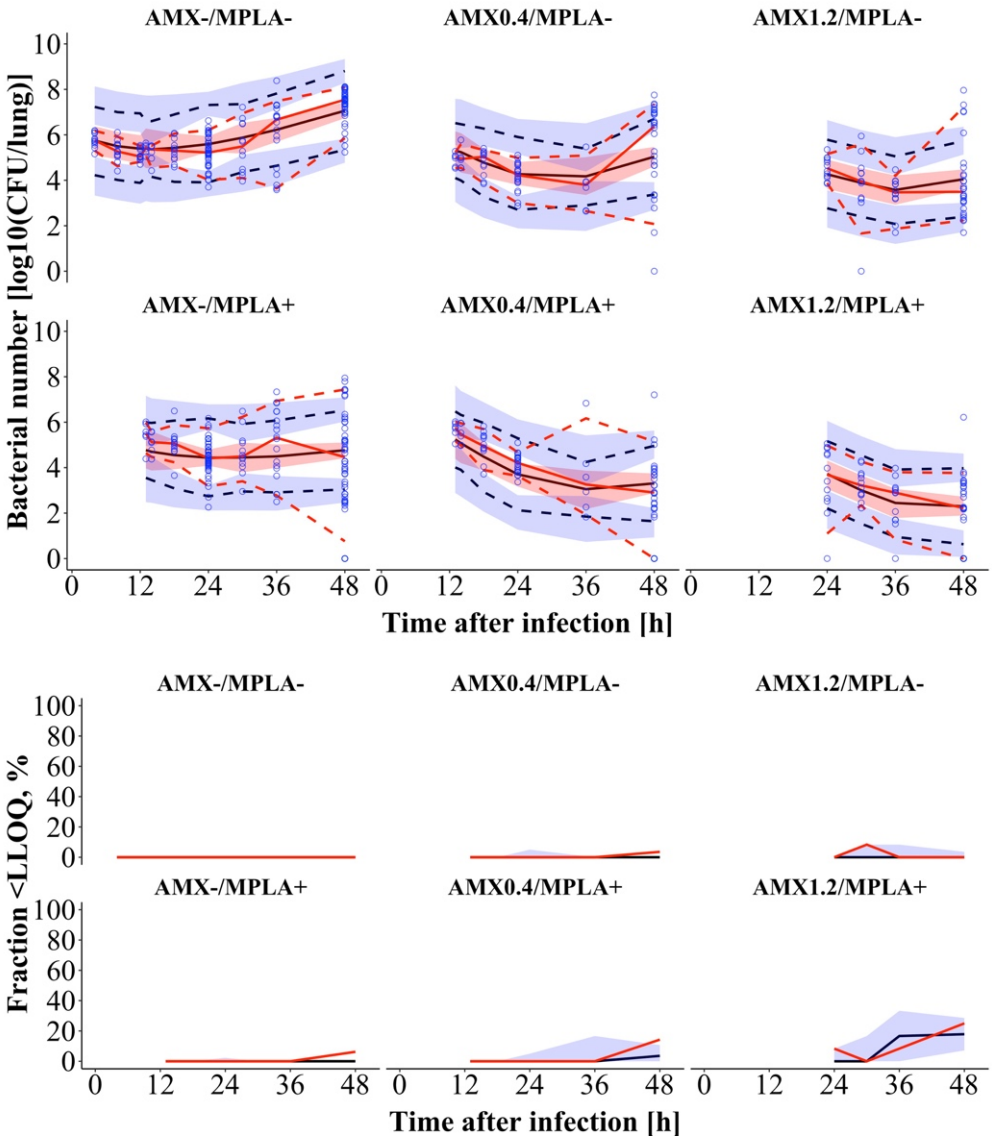

Figure 3.33: Visual predictive check (n=1000 simulations incl. residual unexplained variability) of the developed PK/PD model for bacterial numbers in lung of mice being untreated (AMX-/MPLA-), treated with AMX without (AMX0.4/MPLA-, AMX1.2/MPLA-) or with (AMX0.4/MPLA+, AMX1.2/MPLA+) MPLA coadministration or treated with MPLA (AMX-/MPLA+) and fraction of samples being below the LLOQ: Circles: Measurements; Lines: 50th percentile (solid), 5th and 95th percentile (dashed) of measured (red) and simulated (black) bacterial numbers; Shaded area: 90% confidence interval around simulated percentiles. Abbreviations: AMX: Amoxicillin (0.40 mg/kg or 1.20 mg/kg); CFU: Colony forming units; LLOQ: Lower limit of quantification; MPLA: Monophosphoryl lipid A (2.00 mg/kg); PD: Pharmacodynamic; PK: Pharmacokinetic; +: Treatment with respective drug; -: No treatment with respective drug.

In spleen, evaluation of bacterial numbers being <LLOQ was particularly important due to the high proportion of these samples. As depicted in Figure 3.34, the fraction of samples being <LLOQ was adequately captured in all study groups. The VPCs itself also showed that the developed PK/PD model was able to reflect the underlying processes. Except for only a few cases, the median simulated numbers followed same trends as median observations. Especially bacterial numbers of MPLA treated animals in monotherapy or in combination with 0.40 mg/kg AMX were not completely described by the PK/PD model. The PK/PD model was not able to capture the increase and subsequent decrease of bacterial numbers in spleen at 36 h. However, over the entire study period, only minor deviations between observations and simulations occurred in general without showing any significant trends between the different study groups. At 48 h, minor under- or overprediction of observations by the developed PK/PD model occurred. Given the high variability of the bacterial numbers and the dependence of bacterial numbers in spleen to those in lung, a good predictive performance in spleen was shown.

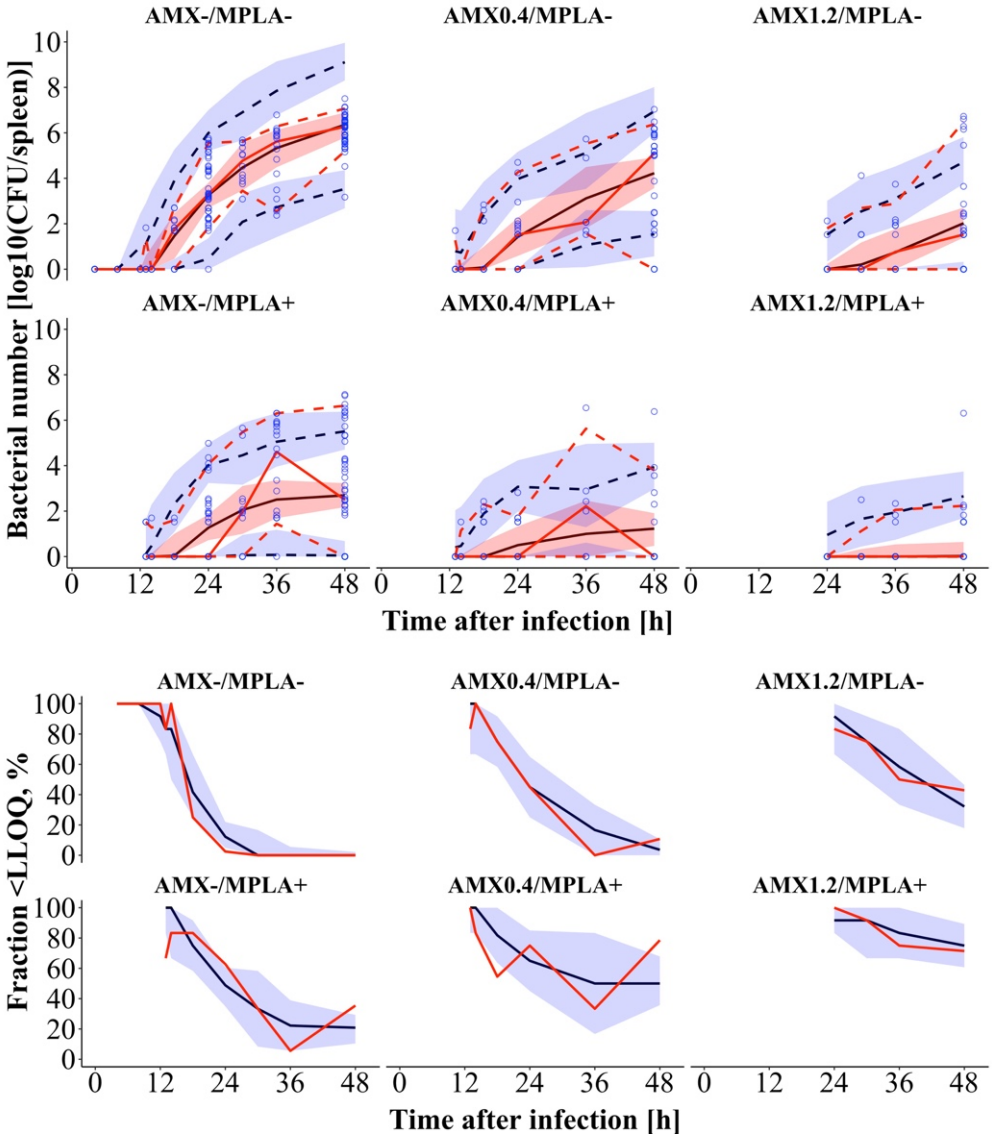

Figure 3.34: Visual predictive check (n=1000 simulations incl. residual unexplained variability) of the developed PK/PD model for bacterial numbers in spleen of mice being untreated (AMX-/MPLA-), treated with AMX without (AMX0.4/MPLA-, AMX1.2/MPLA-) or with (AMX0.4/MPLA+, AMX1.2/MPLA+) MPLA coadministration or treated with MPLA (AMX-/MPLA+) and fraction of samples being below the LLOQ: Circles: Measurements; Lines: 50th percentile (solid), 5th and 95th percentile (dashed) of measured (red) and simulated (black) bacterial numbers; Shaded area: 90% confidence interval around simulated percentiles. Abbreviations: AMX: Amoxicillin (0.20 mg/kg, 0.40 mg/kg or 1.20 mg/kg); CFU: Colony forming units; LLOQ: Lower limit of quantification; MPLA: Monophosphoryl lipid A (2.00 mg/kg); PD: Pharmacodynamic; PK: Pharmacokinetic; +: Treatment with respective drug; -: No treatment with respective drug.

Especially given the data situation and huge variability in data, the entire PK/PD model was able to adequately describe the data, reflect underlying processes and, hence, a subsequent use for further analyses was justified and did allow the connection to survival data.

As next evaluation step, the effect of the drugs in monotherapy as well as in combination was comprehensively studied at 48 h in lung to evaluate the effect of the combination at the end of the study. To directly assess the efficacy of the investigated combination, reduction in bacterial numbers in the respective study groups compared to bacterial numbers of untreated mice was studied (Figure 3.35). Here, a higher effect occurred with increasing doses of AMX. In comparison of the respective study groups only receiving AMX with combined treated animals, an even higher effect was observed for the combined treatment. In case of AMX monotherapy, the effect increased constantly to a specific time point that was mainly depending on the AMX dose and stopped afterwards. Contrarily to these characteristics, MPLA was in combination with AMX able to increase the killing effect to an even higher extent and continued after the AMX effect stopped.

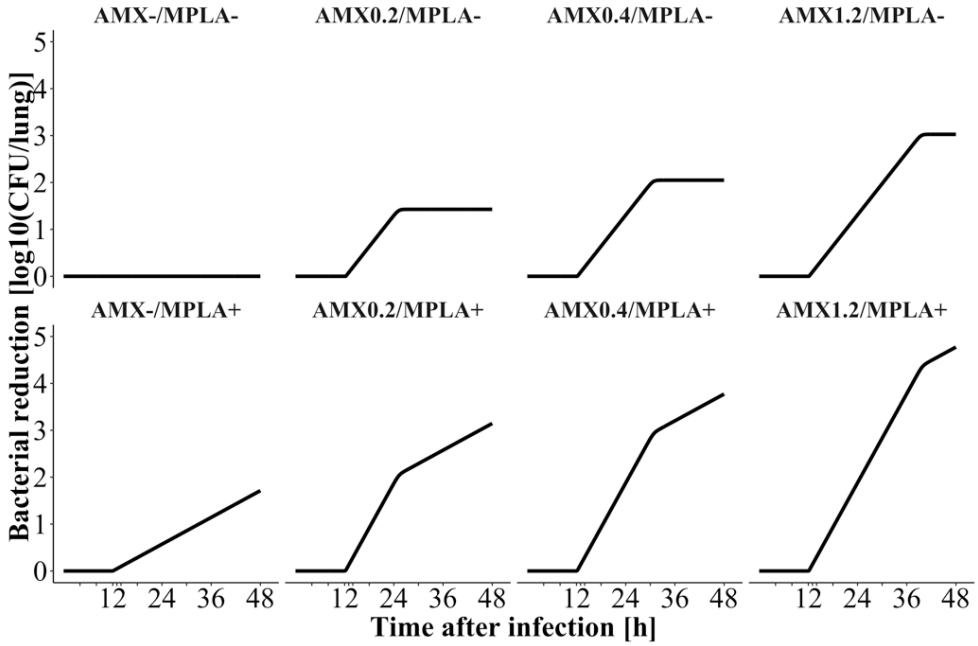

Figure 3.35: Model-predicted bacterial reduction of bacterial numbers of *Streptococcus pneumoniae* serotype 1 in lung of mice being untreated (AMX-/MPLA-), treated with AMX without (AMX0.2/MPLA-, AMX0.4/MPLA-, AMX1.2/MPLA-) or with (AMX0.2/MPLA+, AMX0.4/MPLA+, AMX1.2/MPLA+) MPLA coadministration or treated with MPLA (AMX-/MPLA+) compared to bacterial numbers of untreated mice versus time. Abbreviations: AMX: Amoxicillin (0.20 mg/kg, 0.40 mg/kg or 1.20 mg/kg); MPLA: Monophosphoryl lipid A (2.00 mg/kg); +: Treatment with respective drug; -: No treatment with respective drug.

This effect of MPLA was also observed by evaluating the bacterial reduction against the AMX dose differentiated by monotherapy or combined treatment (Figure 3.36). AMX as monotherapy at the highest investigated dose (1.2 mg/kg) reduced bacterial numbers in lung by 3.03 log10 CFU/lung as reduction compared to natural growth at 48 h. MPLA alone augmented the estimated treatment-unrelated bacterial elimination by 1.40-fold leading to a reduction of 1.71 log10 CFU/lung. In combination, a killing of 4.77 log10 CFU/lung resulted in an enhancement of AMX efficacy by 57.7%. 24 h after infection this effect was less prominent with comparable bacterial numbers of mice treated

with AMX alone and enhancing monotherapy by only 43.6%. In spleen, comparable characteristics were observed. Here, the maximum effect in bacterial reduction was determined for doses of 0.4 and 1.2 mg/kg AMX with MPLA coadministration.

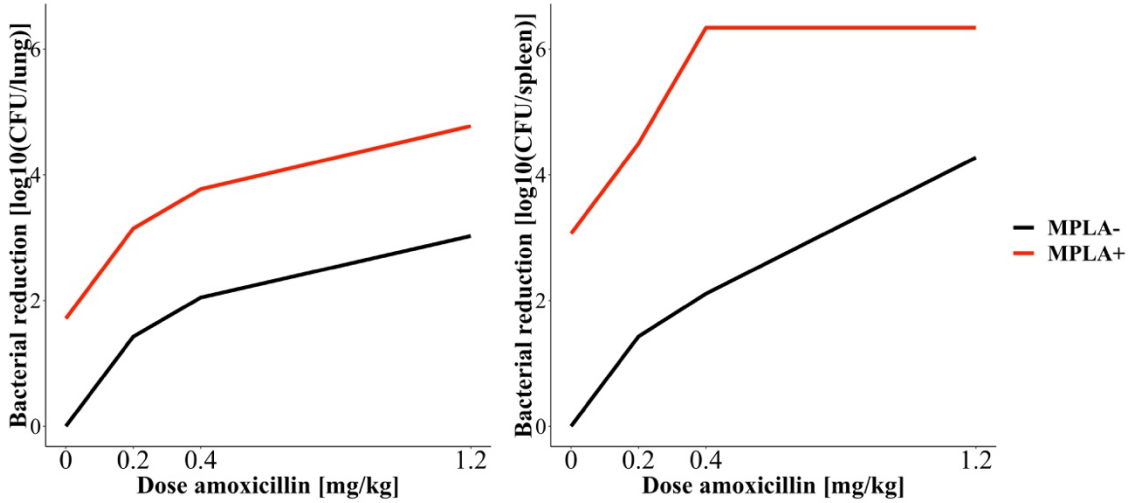

Figure 3.36: Model-predicted bacterial reduction of bacterial numbers of *Streptococcus pneumoniae* serotype 1 in lung and spleen of mice treated with AMX with (red) or without (black) MPLA coadministration compared to bacterial numbers of untreated mice against studied doses of AMX. Abbreviations: AMX: Amoxicillin (0.20 mg/kg, 0.40 mg/kg or 1.20 mg/kg); MPLA: Monophosphoryl lipid A (2.00 mg/kg); +: Treatment with MPLA; -: No treatment with MPLA.

Linking the PD effect, bacterial reduction, to the PK of AMX in lung revealed an hysteresis curve (Figure 7.22). With increasing concentrations of AMX in the lung, the effect only slowly escalated. Highest PD effects were achieved at lowest AMX concentrations. Nevertheless displayed concentrations were estimated at target site, an effect delay was observed, since the effect of the immune system itself cannot be considered in this setting.

3.4.1.3 Time-to-event analysis

Evaluation of the investigated study groups considered by its own in a base model revealed best correlation of observed survival data (Chapter 3.3.3) and model-predicted survival by using the surge-function as hazard base model. During model development (Chapter 2.5.3.2), this distribution function was superior to all other investigated distribution functions in OFVs and VPCs. As depicted in the Kaplan-Meier VPCs of Figure 3.37, survival was adequately described for all study groups in a single analysis of each study group alone. As already presented, mice treated with 0.80 mg/kg AMX were not included in the analysis in the first place due to their inconsistent results and only a few number of mice being investigated without any groups for comparison within the same study (Chapter 3.3.3). Variability of the predicted survival was in line with the number of mice investigated in each study group: With increasing doses of AMX, less mice were investigated resulting in higher variability.

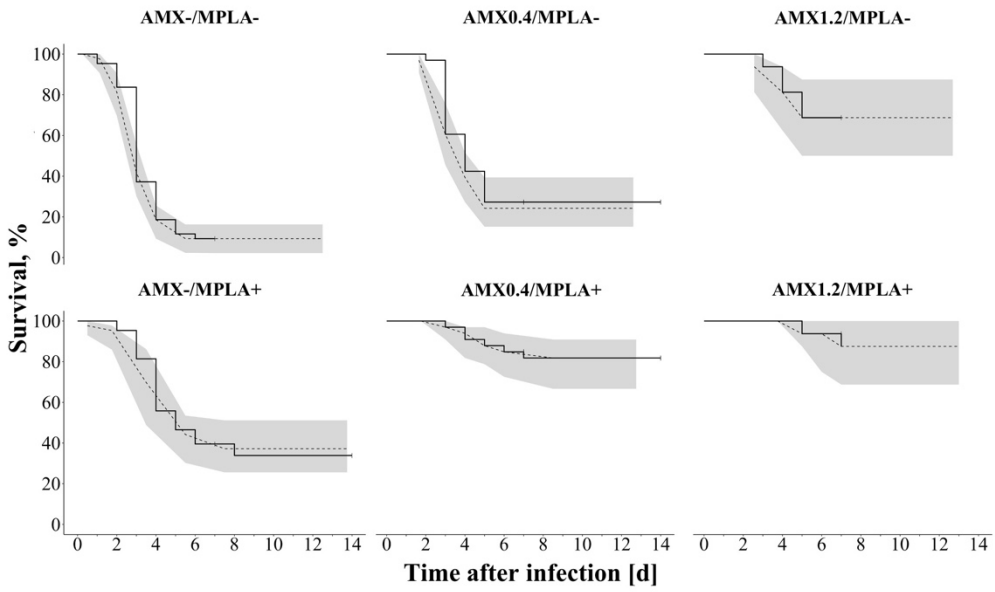

Figure 3.37: Kaplan-Meier visual predictive checks (n=100 simulations) of a surge function hazard model for each study group of mice infected with *Streptococcus pneumoniae* serotype 1 and being untreated (AMX-/MPLA-), treated with AMX without (AMX0.4/MPLA-, AMX1.2/MPLA-) or with (AMX0.4/MPLA+, AMX1.2/MPLA+) MPLA coadministration or treated with MPLA (AMX-/MPLA+). Solid lines: Observed survival; Dashed lines: Simulated median survival; Shaded area: 90% confidence interval around simulated survival. Abbreviations: AMX: Amoxicillin (0.40 mg/kg or 1.20 mg/kg); MPLA: Monophosphoryl lipid A (2.00 mg/kg); +: Treatment with respective drug; -: No treatment with respective drug.

By further analysing the respective study groups separately, the maximum hazard *SA* was identified as the parameter of the surge function that mainly differed between the respective study groups (Table 3.10) indicating the highest hazard for untreated animals (AMX-/MPLA-, *SA*=0.0356 h^{-1}) and the lowest hazard for combined treated animals (AMX1.2/MPLA+, *SA*=0.00190 h^{-1}). The maximum hazard of untreated mice was 2.68-fold higher than for MPLA treated mice (AMX-/MPLA+, *SA*=0.0133 h^{-1}). In addition, the effectiveness of MPLA was indicated by comparing maximum AMX doses without (AMX1.2/MPLA-, *SA*=0.00660 h^{-1}) and with MPLA coadministration revealing a 3.47-fold increase in maximum hazard for AMX monotherapy. However, MPLA monotherapy was not superior to maximum doses of AMX in monotherapy indicated by a 2.00-fold higher maximum hazard. Minor trends within the study groups were present for model parameters *SW*, *PT* and γ (Table 3.10). Thus, the hazard was present over a similar time period of approximately 3 d indicating the time mice are challenged by the infection with occurrence of the maximum hazard at comparable time points. Nevertheless, with increasing doses of AMX, the time point of maximum hazard was delayed from 81.4 h (AMX-/MPLA-) to 134 h (AMX1.2/MPLA+). This especially occurred for mice treated in a combination of AMX and MPLA. In addition, the shape parameter γ was relatively high for all treatment groups and even substantially higher for AMX treated mice. To increase model stability, γ was fixed to a value indicating a steep increase and subsequent decrease in hazard for AMX treated mice. Here, the

hazard occurred and disappeared rather fast. Accordingly, at the time periods of maximum hazard almost all death cases occurred reliably.

Table 3.10: Parameter estimates of a developed survival model using a surge function for each single study group of mice being infected with *Streptococcus pneumoniae* serotype 1 and being either untreated or treated with different doses of AMX and/or MPLA.

Study group	SA [h^{-1}]	SW [h]	y	PT [h]
AMX-/MPLA-	0.0356	31.8	2.17	81.4
AMX0.4/MPLA-	0.0182	35.8	20*	82.3
AMX1.2/MPLA-	0.00660	28.1	20*	90.4
AMX-/MPLA+	0.0133	33.1	1.70	94.0
AMX0.4/MPLA+	0.00190	53.6	20*	109
AMX1.2/MPLA+	0.00190	37.3	20*	134

Abbreviations: AMX: Amoxicillin (0.40 mg/kg or 1.20 mg/kg); γ: Shape parameter: MPLA: Monophosphoryl lipid A (2.00 mg/kg); *PT*: Peak time; *SA*: Surge amplitude; *SW*: Surge width at half maximum intensity; +: Treatment with respective drug; -: No treatment with respective drug; *Fixed parameter estimate based on model development due to stability reasons.

A joint survival analysis of all study groups also showed the best predictive performance of the survival data by usage of the surge function (ΔAIC≥-79.3) compared to other investigated distributions (Chapter 2.5.1.6). Covariates, included by a proportional hazard model, showed best relation between PK, PD and survival, when the $T_{>MIC}$ in serum and coadministration with MPLA were combined, compared to other potential covariates. On a PK level, no other covariates improved the relationship to survival (ΔAIC≥+0.450). Usage of other covariates on a PD level, like the bacterial number at 48 h in spleen or the AUC of bacterial numbers in spleen, revealed slightly better AIC values compared to $T_{>MIC}$ and MPLA coadministration (ΔAIC≥-1.30), but were excluded due to a worse overall predictive performance. Here, especially bacterial numbers at 48 h in spleen were a good predictive covariate for survival but were disregarded for plausibility reasons: Using a specific marker that was determined at 48 h to predict events that are able to already occur at 24 h was considered as implausible. VPCs as well as a bootstrap analysis with a convergence rate of 100% supported the adequacy of the surge function-based hazard model with stable parameter estimates (Table 3.11).

Table 3.11: Survival model parameter estimates incl. bootstrap results of the time-to-event analysis of survival data of mice infected with *Streptococcus pneumoniae* serotype 1 and being either untreated or treated with different doses of AMX and/or MPLA.

Parameter	Parameter estimate	Bootstrap	
[unit]	(RSE, %)	Median	95% CI
Structural model			
SA [h^{-1}]	0.0404 (20.9)	0.0413	0.0263 - 0.0676
SW [h]	35.7 (17.3)	36.0	23.5 - 67.1
y	2.24 (26.0)	2.36	1.38 - 7.39
PT [h]	89.2 (4.80)	89.4	81.6 - 110
Covariate model			
$T_{>MIC}$	-0.926 (16.7)	-0.940	-1.28 - (-0.654)
$MPLA_{TTE}$	-1.32 (16.6)	-1.33	-1.82 - (-0.878)

Abbreviations: AMX: Amoxicillin; CI: Confidence interval; *γ*: Shape parameter: $MPLA_{TTE}$: Covariate effect of coadministration of monophosphoryl lipid A (MPLA) on overall survival; *PT*: Peak time; *SA*: Surge amplitude; *SW*: Surge width at half maximum intensity; $T_{>MIC}$: Covariate effect of the time period of total AMX concentrations in serum above the minimal inhibitory concentration (MIC).

The VPC of the overall survival model stratified into the different study groups underlined the good predictive performance of the model (Figure 3.38). In almost all study groups, survival was predicted reliably. Solely survival of mice treated with MPLA only (AMX-/MPLA+) or 0.4 mg/kg AMX with MPLA coadministration (AMX0.4/MPLA+) were slightly over- and underestimated, respectively. A comparison of the last-mentioned study group to mice treated with the highest dose of AMX in combination with MPLA (AMX1.2/MPLA+) showed that the TTE model was not completely able to distinguish these two study groups.

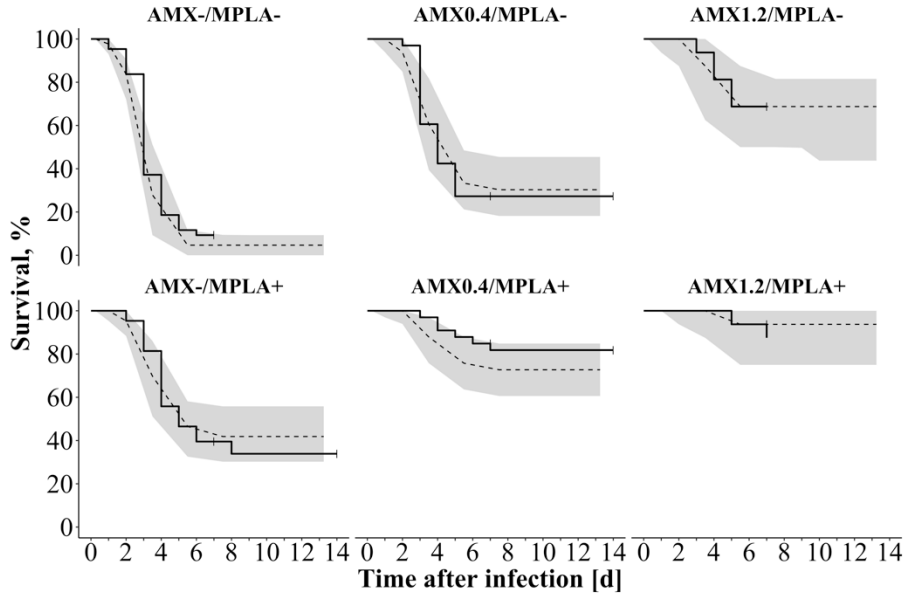

Figure 3.38: Kaplan-Meier visual predictive checks (n=1000 simulations) of the surge function hazard model for all study groups of mice infected with *S. pneumoniae* serotype 1 and being untreated (AMX-/MPLA-), treated with AMX without (AMX0.4/MPLA-, AMX1.2/MPLA-) or with (AMX0.4/MPLA+, AMX1.2/MPLA+) MPLA coadministration or treated with MPLA (AMX-/MPLA+). Solid lines: Observed survival; Dashed lines: Simulated survival; Shaded area: 90% confidence interval around simulated survival. Abbreviations: AMX: Amoxicillin (0.40 mg/kg or 1.20 mg/kg); MPLA: Monophosphoryl lipid A (2.00 mg/kg); +: Treatment with respective drug; -: No treatment with respective drug.

An alternative approach to investigate the covariate effect and further improve the TTE model was to add potential covariates directly to single model parameters instead of addition to the entire hazard model. In a graphical analysis, potential covariates, that displayed a certain trend with respect to a single model parameter, were selected. The most affected model parameter *SA* describing the maximum hazard differed mainly depending on the bacterial number in spleen at 48 h. The peak time was primarily influenced by AMX concentrations in lung in terms of $C_{max,\,lung}$ or AUC_{lung} both depending on MPLA coadministration. For other TTE model parameters, no clear trends were observed. Addition of those covariates to the respective TTE model parameters in an either linear, piece-wise linear or exponential parametrisation slightly decreased the AIC values ($\Delta AIC \geq -6.55$). However, due to a worse predictive performance in VPCs, relatively high RSE for the covariate effects, unstable bootstrap results with a convergence rate of only 78.6% and impaired plausibility, the original implementation of $T_{>MIC}$ and MPLA coadministration was accepted.

A larger $T_{>MIC}$ as wells as presence of MPLA decreased the overall hazard and thereby increased survival. As depicted in Figure 3.39, increased hazard was primarily present between day 1 and 6 with highest maximum hazard between day 3 and 5 justifying a surge function.

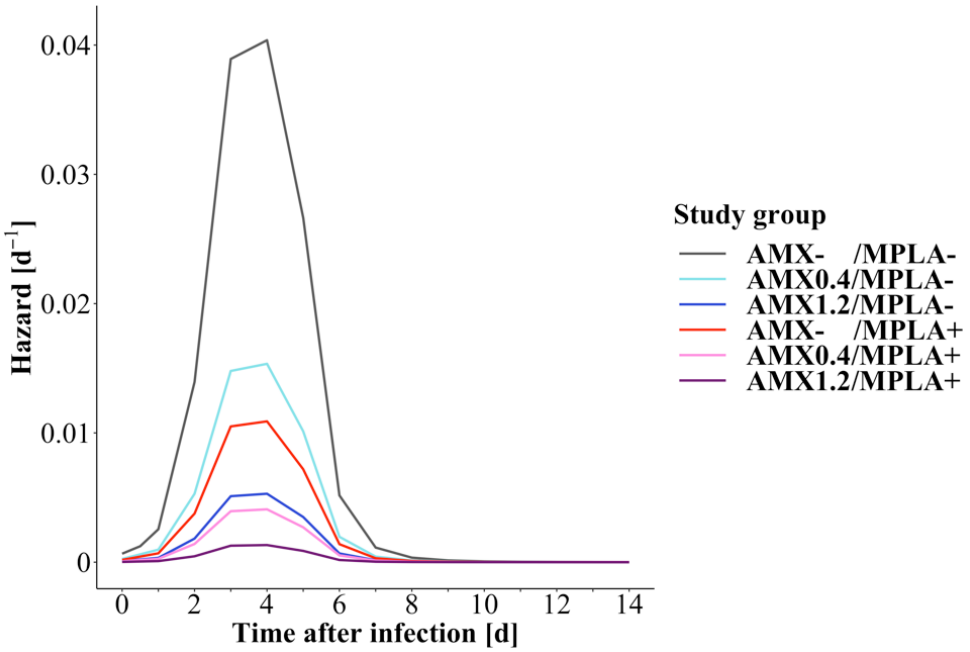

Figure 3.39: Model-predicted hazard in mice being infected with *Streptococcus pneumoniae* serotype 1 and being untreated (AMX-/MPLA-), treated with AMX without (AMX0.4/MPLA-, AMX1.2/MPLA-) or with (AMX0.4/MPLA+, AMX1.2/MPLA+) MPLA coadministration or treated with MPLA (AMX-/MPLA+) administered at 12 h from a time-to-event analysis using a surge function hazard model. Abbreviations: AMX: Amoxicillin (0.40 mg/kg or 1.20 mg/kg); MPLA: Monophosphoryl lipid A (2.00 mg/kg); +: Treatment with respective drug; -: No treatment with respective drug.

The maximum hazard of untreated mice (AMX-/MPLA-, *SA*=0.0404 h^{-1}) was 3.71-fold higher than for MPLA treated mice (AMX-/MPLA+, *SA*=0.0109 h^{-1}). Most important, cotreatment with MPLA was able to reduce the hazard of AMX treated mice at maximum dose by a factor of 4.00 (AMX1.2/MPLA-, *SA*=0.00530 h^{-1} vs. AMX1.2/MPLA+, *SA*=0.00133 h^{-1}). Comparison of both monotherapies led to an almost 2 times higher hazard for MPLA monotherapy (AMX-/MPLA+, *SA*=0. 0109 h^{-1} vs. AMX1.2/MPLA-, *SA*=0. 00530 h^{-1}). After 7 d, survival was increased by 23.6% from 66.7% for AMX monotherapy at highest dose to 90.3% in a combined treatment approach.

3.4.1.4 Simulations: Exploration of the pharmacokinetic/pharmacodynamic model

Deterministic simulation studies were performed (Chapter 2.5.1.7) to gain more detailed information about the performance of the semi-mechanistic PK/PD model.

Longer time period. In a first step, bacterial numbers in lung were investigated over in total 7 d to assess the drug effects for longer study periods (Figure 3.40). Latest with end of the observation period after 48 h, bacterial numbers continuously increased to numbers >10 log10 CFU/lung. Especially without the additional effect of MPLA, bacterial numbers in lung increased substantially without present effects of AMX. The semi-mechanistic PK/PD model was not predictive for a longer time period as long as only single doses of AMX were studied. As depicted in Figure 3.32, bacterial growth exceeded any

killing effects, either by AMX or MPLA, leading to constantly increasing bacterial numbers after latest 2 d. Still, the boosting effects of MPLA were distinctly shown with in total lower bacterial numbers and a reduced increase of bacterial numbers after the end of the observation period.

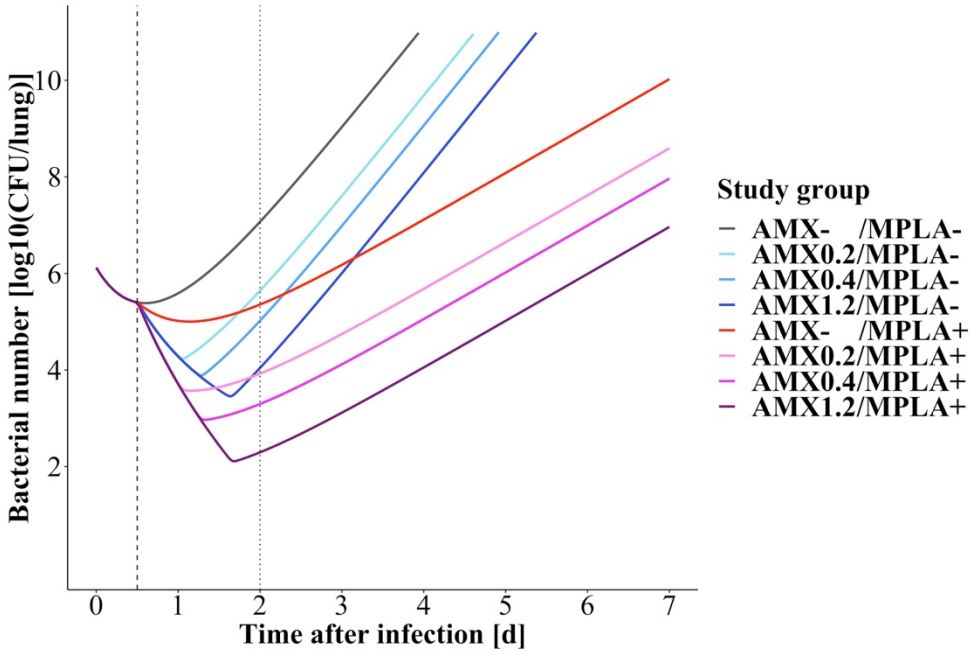

Figure 3.40: Bacterial numbers of *Streptococcus pneumoniae* serotype 1 in lung after intranasal infection at 0 h, with drug administration at 12 h (dashed line) and the end of the observation period at 2 d (dotted line) of a deterministic simulation study for an extended study time of 7 d for eight study groups: Mice untreated (AMX-/MPLA-), treated with AMX (AMX0.2/MPLA-, AMX0.4/MPLA-, AMX1.2/MPLA-) or MPLA (AMX-/MPLA+) in monotherapy or in a combined treatment (AMX0.2/MPLA+, AMX0.4/MPLA+, AMX1.2/MPLA+). Abbreviations: AMX: Amoxicillin (0.20 mg/kg, 0.40 mg/kg or 1.20 mg/kg); CFU: Colony forming units; MPLA: Monophosphoryl lipid A (2.00 mg/kg); +: Treatment with respective drug; -: No treatment with respective drug.

Dose fractionation study. To evaluate different dosing regimens, a dose fractionation study was performed. Administered total doses of AMX were evaluated in a broad dosing range up to 30 mg/kg. On basis of the developed PK submodel (Chapter 3.4.1.1), AMX concentrations increased due to a reduced clearance with MPLA coadministration depending on the AMX dose. Here, the MPLA effect on CL_{AMX} was of negligible relevance at lower doses ≤10 mg/kg of AMX (Figure 7.23). Overall, higher AMX doses led to a higher exposure of AMX in serum, lung and spleen. For a total dose of 1.00 mg/kg AMX, C_{max} in one of the respective compartments, e.g. serum, was highest for a single administration (C_{max}=0.357 µg/mL) and was reduced with increased numbers dosing events (C_{max}=0.178 µg/mL and C_{max}=0.119 µg/mL for twice and thrice administration, respectively). As already described, the time point of maximum concentrations, e.g. in case of single administration, in lung (t_{max}=13.9 h) and spleen (t_{max}=15.0 h) was delayed compared to t_{max} in serum (t_{max}=12.2 h). A typical concentration-time profile for AMX concentrations in serum, lung and spleen is presented exemplarily for the total dose of 1.00 mg/kg, where no distinct PK interaction was observed, in Figure 3.41. In case of a thrice

administration, the C_{max} value increased from 0.00635 to 0.00841 µg/mL and from 0.00253 to 0.00510 µg/mL comparing maximum concentrations after first and third administration in lung and spleen, respectively. Due to a lack of accumulation in serum, C_{max} after first and last administration was equal.

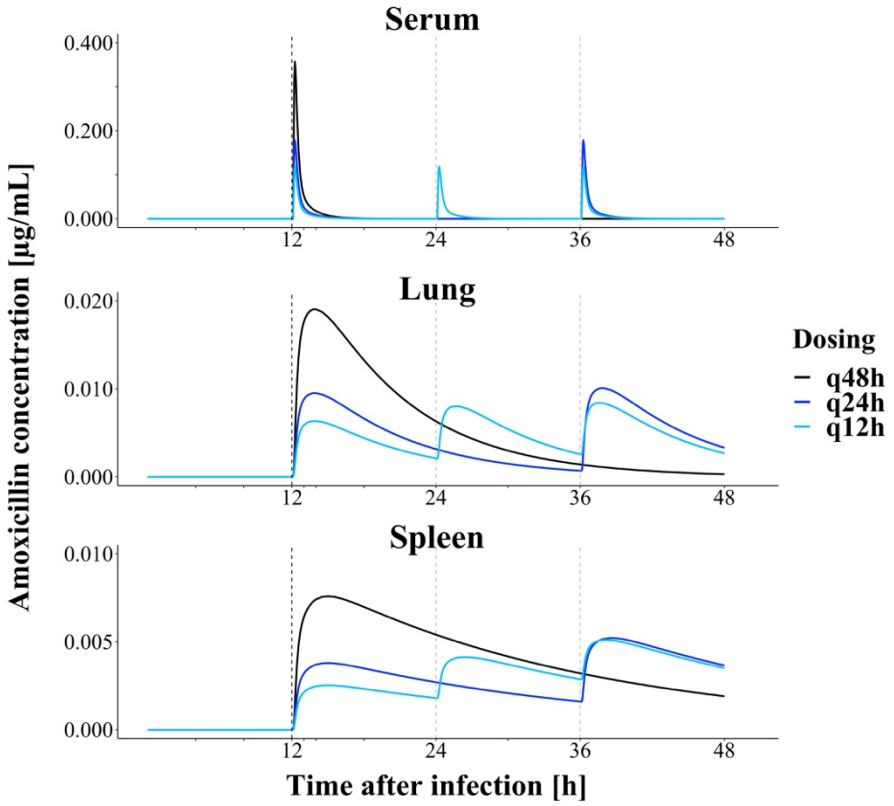

Figure 3.41: Simulated AMX concentrations in serum (top), lung (middle) and spleen (bottom) of mice infected with *Streptococcus pneumoniae* serotype 1 at 0 h and treated with a total dose of 1.00 mg/kg AMX in different dosing regimens. Abbreviations: AMX: Amoxicillin; q12h: Three times AMX administration every 12 h at 12, 24 and 36 h; q24h: Twice AMX administration every 24 h at 12 and 36 h; q48h: Single AMX administration at 12 h.

Bacterial numbers of the investigated strain *S. pneumoniae* serotype 1 with an MIC of 0.016 mg/L in lung are depicted in Figure 3.42 for different investigated total doses and dosing regimens. In this scenario, untreated mice and solely MPLA-treated mice were used as controls without any AMX treatment. Maximum effects in AMX monotherapy with single drug administration were reached with total AMX doses >3.00 mg/kg. In combination with MPLA, the maximum effect expressed as lowest bacterial numbers was even higher. Up to doses <0.10 mg/kg, no effect at all occurred in mono- and combination therapy. At total AMX doses between 0.10 and 3.00 mg/kg, different bacterial number-time profiles were observed depending on the number of administered doses. Splitting the total AMX dose into two or three different doses, maximum effects were assessed with lower total doses compared to single administration: Especially with a thrice administration, highest efficacy of AMX was obtained already with a total AMX dose of 0.60 mg/kg. Administering AMX twice reduced the total dose to

observe maximum effects from 3.50 mg/kg to 1.50 mg/kg. Contrarily, at the lowest effective dose of 0.10 mg/kg, only the single AMX administration was effective, since only here AMX concentrations exceeded already determined thresholds. However, with reasonable AMX doses, highest effects were already achieved in combination with MPLA indicating the strong boosting effects of MPLA. At highest efficacies of AMX (total doses >3.00 mg/kg), MPLA was able to boost the AMX efficacy 2.24-fold from 3.10 to 1.38 log10 CFU/lung.

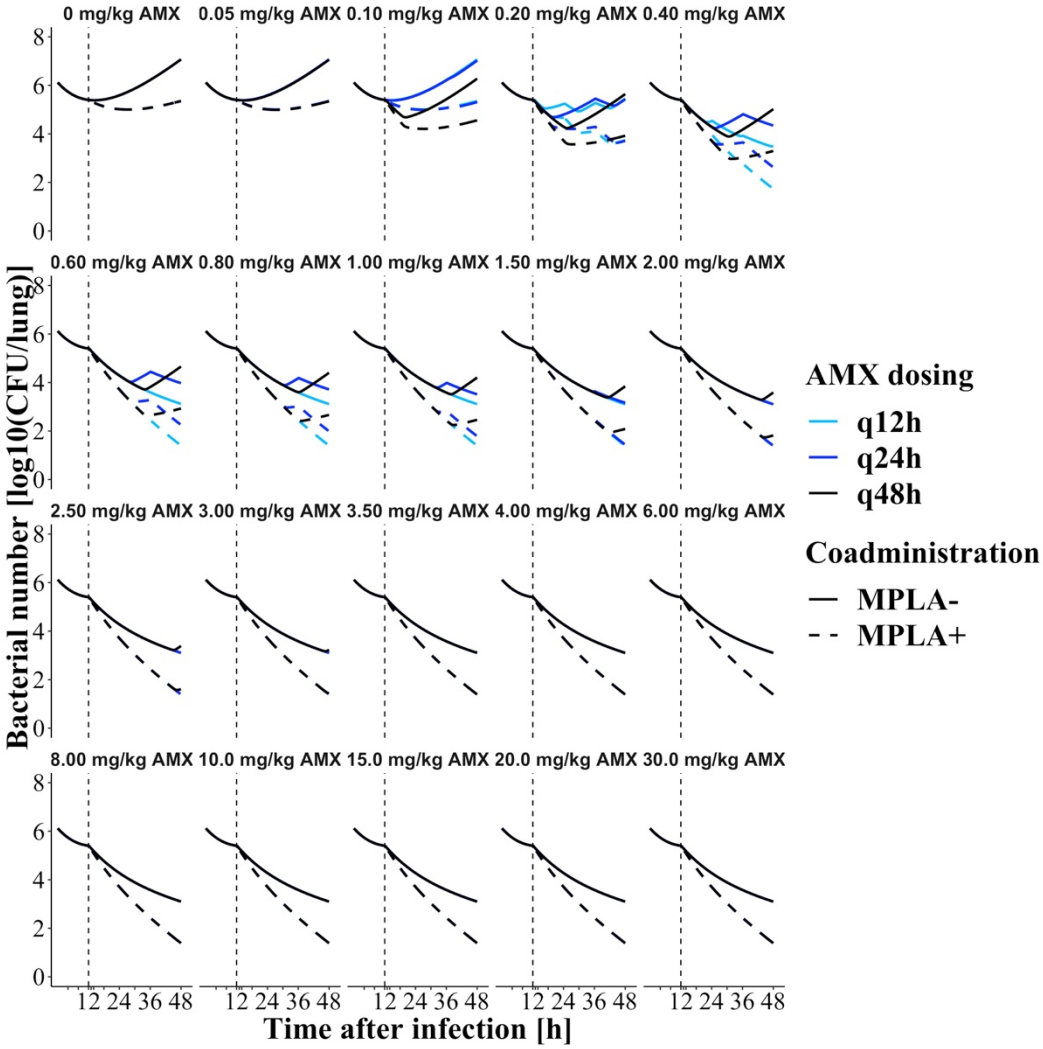

Figure 3.42: Simulated bacterial numbers in lung of mice being infected with *Streptococcus pneumoniae* serotype 1 at 0 h and being either untreated or treated with different doses of AMX in different dosing regimen at 12 h without or with MPLA coadministration. Abbreviations: AMX: Amoxicillin; CFU: Colony forming units; MPLA: Monophosphoryl lipid A; q12h: Three times AMX administration every 12 h at 12, 24 and 36 h; q24h: Twice AMX administration every 24 h at 12 and 36 h; q48h: Single AMX administration at 12 h; +: Treatment with MPLA; -: No treatment with MPLA.

Susceptibility study. To additionally consider bacterial strains with resistant characteristics, the influence of MIC values up to 8 mg/L was studied in a next step. In this setting, the PK of AMX itself was not influenced. Due to scaling of EC_{50} with the MIC of *S. pneumoniae* (Chapter 2.5.4), the efficacy

of the applied treatment regimen was inferior with increase in the resistance of the bacterial strain (Figure 3.43). Higher AMX total doses at higher MIC values were necessary to achieve effects comparable to the reference MIC of 0.016 mg/L. As outlined, total AMX dose >3.00 mg/kg assessed maximum effects at an MIC value of 0.016 mg/L. Already at a MIC value of 0.5 mg/L, maximum effects were only detected with a thrice administration at total doses >15.0 mg/kg. Moreover, the AMX dose showing first effects on the bacterial numbers was increased from 0.10 mg/kg at an MIC value of 0.016 mg/L to 2.00 mg/kg at an MIC value of 0.5 mg/L and even 20.0 mg/kg at an MIC value of 8 mg/L. In these scenarios, coadministration of MPLA was also able to boost the AMX efficacy. At highest MIC of 8 mg/L and dose of 30 mg/kg, bacterial numbers were reduced by 4.31 log10 CFU/lung from 6.88 log10 CFU/lung for solely AMX treated mice to 2.57 log10 CFU/lung mice treated with AMX and boosted by MPLA. Here, in addition to the PD interaction, the $T_{>MIC}$ was prolonged from 0.216 to 0.977 h due to the underlying PK interaction given the administered high dose of AMX. In all investigated MIC values and AMX doses, a reduction in bacterial numbers compared to growth control by at least 4 log10 CFU/lung was only observed for mice treated with a combination of AMX and MPLA. Partly, a reduction of at least 3 log10 CFU/lung occurred for mice treated in monotherapy for $T_{>MIC} \geq 1.49$ h or treated in combination with MPLA for $T_{>MIC} \geq 0.605$ h. At reasonable doses of AMX for mice, that are typically too low to show any PK interaction, comparable trends were determined.

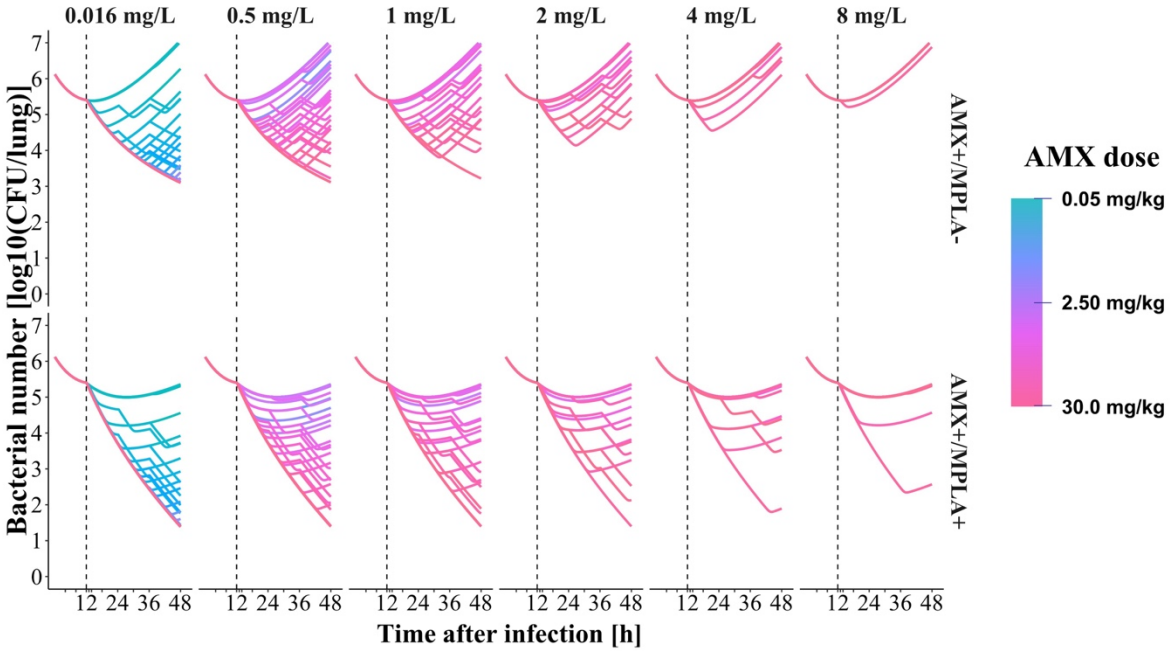

Figure 3.43: Simulated bacterial numbers in lung of mice being infected with *Streptococcus pneumoniae* serotype 1 at 0 h and being either untreated or treated with different doses of AMX in different dosing regimen at 12 h without or with MPLA coadministration depending on different susceptibility of the bacterial strain (MIC values ranging from 0.016 to 8 mg/L). Abbreviations: AMX: Amoxicillin (Total doses ranging from 0.05 to 30.0 mg/kg administered at one dose or split into two or three doses); CFU: Colony forming units; MPLA: Monophosphoryl lipid A; +: Treatment with respective drug; -: No treatment with respective drug.

Prediction of PK/PD indices. Based on the simulated data of the introduced dose fractionation and susceptibility studies, PK/PD indices were further evaluated to assess the PK/PD index of AMX with MPLA coadministration in mice, which was most predictive of reduction of bacterial numbers. For this purpose, the most commonly reported PK/PD indices $T_{>MIC}$, C_{max}/MIC and AUC/MIC were chosen and plotted in relation to the bacterial numbers in lung at the end of the study at 48 h. These graphical representations displayed that the PK/PD index $T_{>MIC}$ best described the AMX characteristics based on the developed semi-mechanistic PK/PD model with the largest R^2 value of 0.992 and 0.988 for mono- and combination therapy, respectively (Figure 3.44). Contrarily, for C_{max}/MIC and AUC/MIC no comparable trend and lower R^2 values (C_{max}/MIC: 0.908 (AMX+/MPLA-), 0.921 (AMX+/MPLA+); AUC/MIC: 0.975 (AMX+/MPLA-), 0.977 (AMX+/MPLA+)) were observed (Figure 7.24 and Figure 7.25, respectively). In this graphical presentation, the boosting effects of MPLA are also shown. Based on the performed nonlinear regression analysis, bacterial numbers were reduced to maximum 3.01 log10 CFU/lung for AMX monotherapy compared to 1.732 log10 CFU/lung for the combined treatment approach. A reduction of >5.00 log10 CFU/lung was observed for values of the $T_{>MIC}$ of the entire dosing period of>5.46% for the combination with MPLA, whereas in AMX monotherapy a value of >5.44% reduced bacterial numbers only by 3.37 log10 CFU/lung.

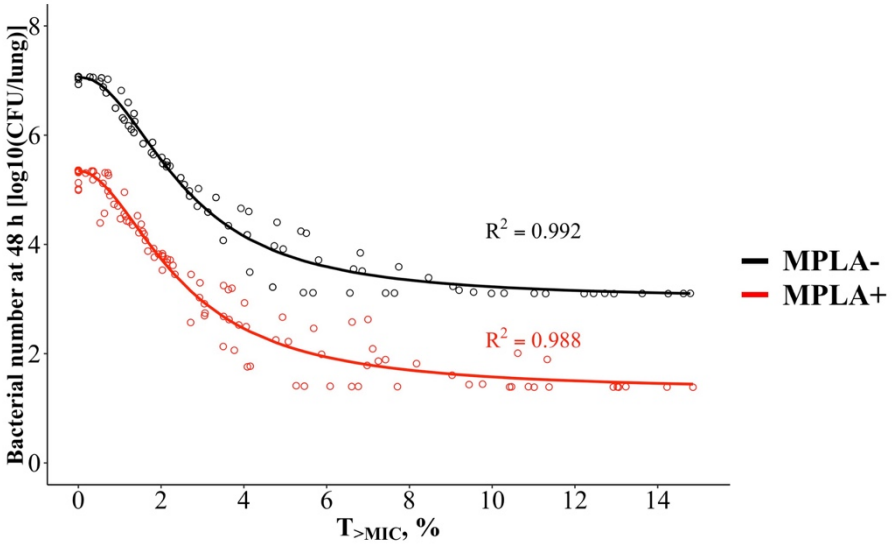

Figure 3.44: Simulated bacterial numbers at 48 h in lung of mice infected with *Streptococcus pneumoniae* with different susceptibility (MIC values ranging from 0.016 to 8 mg/L) against the $T_{>MIC}$ in serum expressed as percentage of the dosing time period of 36 h. Mice were either untreated, treated with AMX monotherapy (black) or a combined treatment of AMX and MPLA (red) in single to thrice administration. Abbreviations: AMX: Amoxicillin (Total doses ranging from 0.05 to 30.0 mg/kg administered at one dose or split into two or three doses within 36 h); CFU: Colony forming units; MPLA: Monophosphoryl lipid A; $T_{>MIC}$: Time period of total AMX concentrations in serum above the minimal inhibitory concentration; +: Treatment with MPLA; -: No treatment with MPLA.

Evaluation of the determined PK/PD index $T_{>MIC}$ in context of the survival data also clearly indicated the difference between AMX monotherapy and the combined treatment with MPLA at the end of the study period at day 14 (Figure 3.45). MPLA in monotherapy already improved survival from 4.43% to 43.1%. Survival increased with increasing $T_{>MIC}$ of AMX. Survival rates >95% were determined at $T_{>MIC}$ values of >3.05 h (9.03% of the entire dosing period) and >4.48 h (12.5% of the entire dosing period) for the combined treatment and AMX monotherapy, respectively. Coadministration of MPLA reduced the required $T_{>MIC}$ to reach survival >95% by 1.43 h.

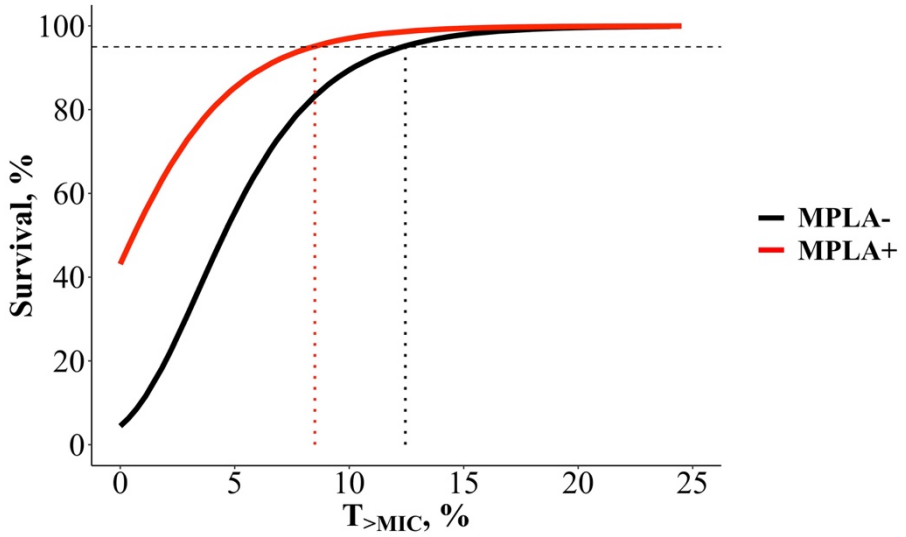

Figure 3.45: Simulated survival of mice being infected with *Streptococcus pneumoniae* and untreated or treated with AMX with (red, solid line) or without (black, solid line) MPLA coadministration in different dosing regimens depending on the determined $T_{>MIC}$ expressed as percentage of the entire dosing period of 36 h with 95% survival (black, dashed line), $T_{>MIC}$ for 95% survival of AMX monotherapy (black, dotted line) and $T_{>MIC}$ for 95% survival of the combined treatment (red, dotted line).Abbreviations: AMX: Amoxicillin; MPLA: Monophosphoryl lipid A; $T_{>MIC}$: Time period of total AMX concentrations in serum above the minimal inhibitory concentration; +: Treatment with MPLA; -: No treatment with MPLA.

3.4.2 Translational approaches: From mouse to human

Aiming to translate the preclinical results of the comprehensive *in silico* analysis (Chapter 3.4.1) into a clinical setting, different translational approaches were investigated (Chapter 2.5.5). In a first step, determined PK parameters CL_{AMX}, Q, V_c and V_p were extrapolated based on the basic allometric scaling approach assuming 25 g mice and 70 kg humans. Original mouse as well as scaled human parameters are displayed in Table 3.12.

Table 3.12: Original and extrapolated values of pharmacokinetic parameters of mice and humans based on a basic allometric scaling approach in comparison to literature reported values [29,30,105,182,183].

Parameter	Mouse	Human	
		Extrapolated	Literature
CL_{AMX} [L/h]	0.124	47.7	10.0 - 27.2
Q [L/h]	0.0719	27.7	1.70 - 20.8
V_c [L]	0.0154	43.1	10.1 - 28.9
V_p [L]	0.0507	142	3.03 - 13.7

Abbreviations: CL_{AMX}: Clearance of amoxicillin (AMX) monotherapy without monophosphoryl lipid A interaction; Q: Intercompartmental clearance; V_c: Central volume of distribution; V_p: Peripheral volume of distribution.

In literature, five different studies had been reported analysing the PK of AMX in humans [29,30,105,182,183] in non-infected or infected patients with subject numbers ranging from 8 to 28 individuals studied. The studies are characterised by different routes of administration with varying dosing regimens leading to PK models assuming either an one or two compartment model structure with multiple absorption and first-order elimination kinetics. In general, extrapolated AMX PK parameters were within a 2-fold range (except V_p) compared to reported values in literature. Evaluating the concentration-time profiles using the extrapolated parameters from mice and the parameters reported in literature by in this case Carlier et al. [29] revealed that the profile using extrapolated parameters showed lower concentrations of AMX over time (Figure 7.26). For comprehensive comparison and discussion of obtained parameters, the underlying assumptions of the respective studies in literature have to be considered. An extension of the basic allometric approach for the PK parameter *CL* based on considering the kidney function in mouse and human and led to a correction factor of 7.96 and an adjusted CL_{AMX} of 6.00 L/h corresponding to a weight adjusted CL_{AMX} of 0.0857 L/h/kg. In literature, CL_{AMX} values of 10.0 L/h [29], 21.3 L/h [182], 12.4 L/h [105], 13.1 L/h [30] and 27.2 L/h [183] had been reported and, hence, were only slightly higher compared to the extrapolated and adjusted CL_{AMX} of 6.00 L/h. The extrapolated value of the parameter Q was slightly higher but also still in line with reported values in literature (15.6 L/h [29], 1.70 L/h [182], 11.1 L/h [105] and 20.8 L/h [30]). Moreover, the translated volume for the central compartment was 14.2 L higher than the reported maximum central volumes of 28.9 L [183]. The volume of the peripheral compartment was even higher with an 10.4-fold increase compared to maximum reported volumes of 13.7 L [29]. In this context, higher extrapolated values were obtained especially for volumes that were only scaled on body weight. However, considering the different assumptions made, the developed PK submodel in mice seemed to allow translation to humans by applying allometric scaling approaches.

Nevertheless allometric scaling of certain parameters of the developed PK submodel revealed plausible parameter estimates, the reported PK model of Carlier et al. [29] was selected as basis for subsequent translation into a clinical setting for a better comparison to published data in humans. Here, overall 104 blood samples of 13 intensive care unit patients with pulmonary infections were analysed. The study population itself consisted mainly of males (85%) and showed no other noticeable challenges. It was characterised by a median age of 62 years and median body weight of 75 kg with a median body mass index of 24. Patients were treated with AMX and clavulanic acid, which had no influence on the PK of AMX, in a dose of 1000 mg and 200 mg, respectively, that were administered as 30 min infusion four times daily and three times daily for patients with normal and impaired renal function, respectively. AMX concentrations were determined at steady state. A PK analysis showed that the underlying data was best described by a two-compartment model with zero-order input and first-order linear elimination kinetics with IIV included on CL and V_c. The determined results of Carlier et al. had been confirmed by Spyker at al. investigating non-infected humans after oral administration of AMX [184] and only expanding the PK model by first-order absorption with time delay.

To connect the chosen PK models in humans to the developed PD model in mice and to allow translation into a clinical setting, different assumptions had to be made. For reason of simplicity, the analysis was limited to bacterial numbers in the lung as a first step. The covariate effect of MPLA on CL_{AMX} was not implemented. An insignificant effect was expected in humans due to probably very low doses that were so far administered to humans. For aimed deterministic simulations, the determined RUV, IIV as well as a covariate effect of the creatinine clearance by Carlier et al. were neglected. In addition, the coadministration of clavulanic acid was not further considered as no PK interaction was reported. Subsequently, certain parameters of the bacterial disease and treatment submodel were adjusted. Considering the bacterial growth submodel, bacteria specific parameters (k_g and k_{lag}), and the natural bacterial elimination rate constant $k_{kill,\ lung}$ were not extrapolated to humans. Since the initial number of bacteria $N_{bacteria,\ t=0}$ in mice was estimated as CFU/lung, the parameter was scaled to humans, Assuming an organ weight in lung of 0.166 g and 1000 g in Swiss mice [185] and humans [122], respectively, an initial bacterial number in lung for humans was set to 9.90 log10 CFU/lung. The first-order rate constant $k_{eo,\ lung}$ of the effect compartment submodel was extrapolated according to basic allometric scaling approaches to a value of 0.0172 h^{-1}. This parameter was neither drug- nor bacteria-specific and most likely changed from mouse to human. PD parameters of the disease and treatment submodel were not extrapolated. AMX related parameters of the sigmoidal E_{max} model were drug-specific and as a consequence independent of the species. The influence of MPLA on the bacterial elimination effects was also not considered to be different in humans primarily.

Deterministic simulations of the described PK submodel capturing AMX concentrations in humans showed important differences in comparison to an AMX concentration-time profile in mice (Figure 7.27). Based on a single standard dose of 1000 mg AMX, corresponding to 14.3 mg/kg in humans

assuming a body weight of 70 kg, the $T_{>MIC}$ in serum was increased by 19.1 h to 24.2 h in comparison to a similar dose of 15.0 mg/kg AMX in mice. C_{max} as well as the AUC (route independent) were increased 9.27- and 33.1-fold, respectively. Due to the different routes of administration, this comparison has to be analysed with caution. However, a slower elimination was detected with maximum concentrations being determined later according to a 30 min infusion. Evaluating AMX concentrations in lung based on the scaled first-order transit rate $k_{eo,\ lung}$ from serum to the effect compartment led to an even slower elimination from the effect compartment leading to higher time periods with AMX concentrations above the EC_{50}. As a consequence, the AMX effect was longer present compared to mice.

In a next step, a dose fractionation and susceptibility study was performed based on the extrapolated PK/PD model for humans, comparable to already presented results in mice (Chapter 3.4.1.4). Here, too, the PK/PD index $T_{>MIC}$ was most predictive to capture the effect of AMX (Figure 3.46). Bactericidal effects characterised by a bacterial reduction of ≥2 log10 CFU/lung were achieved by $\%T_{>MIC}$ >5%. The accompanying dose of AMX to e.g. achieve bactericidal killing corresponded to a single dose of 2 mg per human assuming a susceptible bacterial strain with an MIC of 0.016 mg/L. In combination with MPLA, this dose was reduced to 1 mg. With declining susceptibility of the bacterial strain, a single dose of AMX of 500 mg with MPLA coadministration was already sufficient for bactericidal killing at a MIC of 8 mg/L indicating that the investigated therapy was effective against even highly resistant bacterial strains in this simulation scenario.

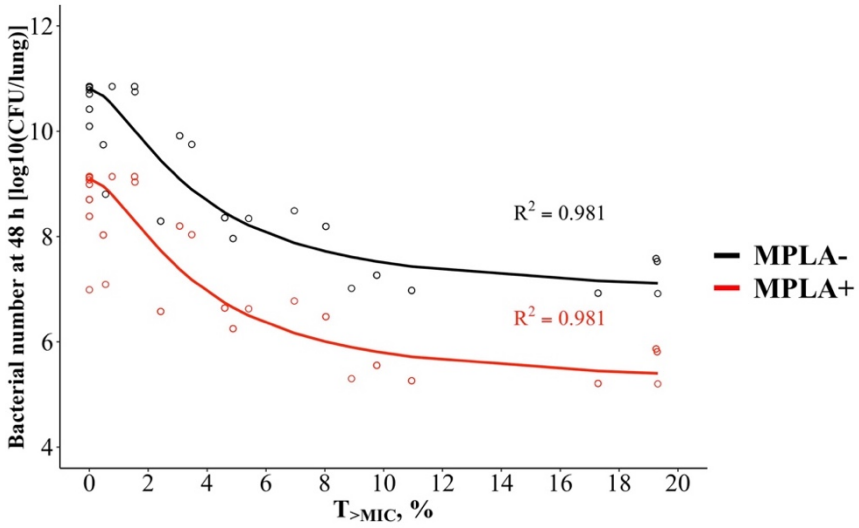

Figure 3.46: Simulated bacterial numbers at 48 h in human lungs infected with *Streptococcus pneumoniae* with different susceptibility (MIC values ranging from 0.016 to 8 mg/L) versus the $T_{>MIC}$ in serum expressed as percentage of the dosing time period of 36 h. Simulated patients were either untreated, treated with AMX monotherapy (black) or a combined treatment of AMX and MPLA (red) in single to thrice administration. Abbreviations: AMX: Amoxicillin (Total doses ranging from 0.1 to 6000 mg administered at one dose or split up to 6 doses within 36 h); CFU: Colony forming units; MPLA: Monophosphoryl lipid A; $\%T_{>MIC}$: Time period of total AMX concentrations in serum above the minimal inhibitory concentration in relation to dosing period; +: Treatment with MPLA; -: No treatment with MPLA.

4 Discussion

The present thesis provides an enhanced quantitative understanding of the investigated innovative combination regimen of antibiotics and immunostimulatory drugs by deploying *in vitro*, *in vivo* and *in silico* approaches. Thereby, a contribution to the restriction of the emergence of bacterial resistance and improvement of therapeutic effectiveness was fostered. The upcoming chapters present the critical discussion of the introduced approaches, the generated results and the conducted pharmacometric analysis. Introduced antibiotic and immunostimulatory drugs were characterised *in vitro* and, subsequently, appropriate combination partners for comprehensive preclinical *in vivo* studies were selected. Based on the preclinical data, the drug exposure and bacterial response relationship was in detail characterised *in silico* aiming for a translation into a clinical setting.

4.1 Selection of appropriate combination partners

This part of the thesis aimed to select appropriate antibiotic and immunostimulatory drug candidates showing potentially useful interactions, such as additive effects or synergy, *in vitro* that may be of benefit for subsequent *in vivo* investigations. For that purpose, required experimental considerations were evaluated and bacterial strains and antibiotic and immunostimulatory drugs were classified according to their MIC, before possible interaction and time-kill curve studies were conducted to determine drug- and modulator-mediated antibacterial effects in more detail.

4.1.1 Susceptibility of bacterial strains and antimicrobial drugs

Four different bacterial species potentially causing pneumonia and various antibiotic and immunostimulatory drugs were investigated *in vitro* regarding their specific experimental requirements as basis for a subsequent analysis of the bacterial susceptibility.

Experimental conditions allowing reliable characterisation of bacterial susceptibility. In context of all performed *in vitro* experiments, reproducible and standardised conditions were strictly aimed for to enable comparison of generated results within one laboratory, but also between different consortium sites. For that purpose, specific requirements of drugs and bacteria were studied intensively and defined as basis for all experiments (Chapters 2.2.1, 2.1.5, 3.1.1 and 3.1.2.1). Within the ABIMMUNE consortium, *K. pneumoniae*, *P. aeruginosa*, *S. aureus* and *S. pneumoniae* were identified as key pathogens. The selected strains of these species were able to represent the intended standardised conditions being either laboratory ATCC strains in case of *K. pneumoniae* or *P. aeruginosa* or well-characterised and commonly used clinical isolates in case of *S. aureus* [186] or *S. pneumoniae* [187]. Growth conditions were defined for each investigated bacterial strain separately to assure reproducible results. Selection of appropriate solid and liquid media according to international guidelines [91,112] facilitated handling and counting of bacteria as CFU. Here, it has to be considered that CFU itself are only an estimate of the approximate number of bacterial cells, since a colony can arise from several

hundred bacterial cells that are able to grow at the present conditions [188]. The process of counting is time- and material-consuming, especially with slow-growing bacteria. Different methods are present to count bacteria mainly distinguishable into typical quantification on agar plates or turbidity-based methods. The latter ones have the advantage of being rapid and inexpensive, in case an appropriate microplate ultraviolet spectrometer is present [189]. Nevertheless, disadvantages predominate in context of this thesis: The presence of extracellular products and the size or shape of bacteria led to a higher variability, since measured absorbance is very sensitive to these factors [190]. In addition, turbidity-based methods do typically not differ between dead and living bacteria, which was mandatory for these experiments, and have a quantification limit of $1 \cdot 10^7$ CFU/mL [190,191]. Various additional test kits are available, making use of e.g. the enzyme luciferase or specific dies, that are able to render bacteria visible also at smaller concentrations by photometric analyses. Nevertheless, these specific kits are relatively cost-intensive compared to quantification on agar plates. Due to these reasons, commonly performed plate counting methods were preferred being able to distinguish dead and living bacteria. By the standardised growth and counting methods, control was gained of specific growth characteristics of certain strains in terms of zoned colony shapes, such as for *K. pneumoniae* being known for producing mucous and sticky colonies on inappropriate agar plates [14]. The fastidious *S. pneumoniae* typically produces hydrogen peroxide by species-specific pyruvate oxidases [12]. This could be beneficial *in vivo* allowing to potentially affect competitive bacterial strains or the host virulently [12], but rather hampered bacterial growth *in vitro* due to autolysis in consequence of the peroxide production [10]. Sheep blood or LHB added to solid or liquid growth media, respectively, served as nutritious supplement and reduced the growth-inhibiting effects of peroxides due to the presence of catalases with antioxidative effects in the blood [192]. The growth medium supplemented with LHB, being characterised by the lysis of horse blood cells especially leading to a release of catalase enzymes, showed an increased activity against peroxides [193]. Additional supplementation with antioxidative agents was disregarded as not mentioned in respective guidelines [91,112] and to adhere to standardised conditions. Nevertheless, finally used conditions led to a decline in the bacterial population after 8 h and, hence, limited the maximum observation time period to 8 h (Figure 7.3). These findings also caused challenging storage conditions and required a specific handling of *S. pneumoniae* serotype 1 in comparison to the other bacterial strains. Here, fresh overnight cultures had to be prepared with bacteria stored at -80 °C for each single experiment. Furthermore, *S. pneumoniae* serotype 1 showed relatively low bacterial concentrations of approximately $1.20 \cdot 10^7$ CFU/mL at 0.5 McF compared to the intended concentration of 10^8 CFU/mL (Chapter 3.1.1.1). Hence, an exact determination of bacterial concentrations at the start of the experiment was required to assure targeted initial concentrations. Already a minor increase of the aimed inocula has been reported to significantly increase the MIC, introduced as inoculum effect in literature, that especially occurs for beta-lactam antibiotics [194]. In this context, limitations in bacterial counting as CFU also have to be considered. Since CFU themselves are only an estimate of the approximate number of bacterial cells, they are highly variable being influenced by the experimentalist

her-/himself or the colony morphology and colony density on the used agar [188]. In addition, the growth state of bacteria being in lag- or log-phase at start of the experiment can influence bacterial *in vitro* investigations due to varying susceptibility in the growth states being characterised as resting or replicating bacteria, respectively [195]. In this thesis, experiments were performed using lag-phase bacteria as demanded by guidelines and since only general antibacterial characteristics were studied in a first place.

Regarding the *in vitro* utilised drugs, also certain requirements were met. Whereas AMX, streptomycin, metformin and MPLA did not require any supplements, other drugs needed to be handled differently. Due to the mechanism of action of fosfomycin, G6P was added to the medium for susceptibility testing as widely accepted and defined in guidelines [13]. Due to the water-insoluble characteristics of pioglitazone, DMSO was chosen as alternative solvent. At DMSO concentrations >5% (v/v), the water-miscible DMSO seemed to remove fatty acids from bacterial membranes [196] and may have caused bacterial death as a consequence (Figure 3.1). Hence, addition of DMSO was limited to final concentration of 5% (v/v) being even below 10% (v/v) DMSO as proposed by several other studies [197-199]. For colistin, a loss of up to 100% especially at relatively low concentrations ≤2 mg/L due to adhesion to plastics has been reported for microplates commonly used for MIC investigations [119,200,201]. Since addition of polysorbate 80 did not change the MIC of colistin (Chapter 3.1.2.1) and according to guidelines [92], polysorbate 80 was not added to prevent the adhesion.

Minimal inhibitory concentration as tool to determine bacterial susceptibility. Based on these determined bacteria- and drug-specific characteristics, a broth dilution setting was applied for susceptibility testing [91,112]. Almost all investigated combinations of bacterial strains and antibiotics were classified as susceptible according to EUCAST breakpoint tables [92] as discussed in the following. However, these results (Chapter 3.1.2.2) have to be analysed with caution. The MIC value is only determined visually at a single point of time after 16-20 h neglecting any growth and killing effects over time. Furthermore, the MIC depends on certain light conditions, the experimentalist with a specific experimental experience and many other factors, such as the inoculum, the type of growth medium, an exact incubation time, the temperature or inoculation preparation methods [90]. In addition, only twofold dilution steps are investigated without considering any concentrations in between. Due to these complex requirements, variations of MIC values for same combinations of drug and strain have been reported to vary 8-fold even at standardised conditions [202]. Yet, the MIC value is still widely used for classification and dosing adjustment in the clinics [203]. In context of the present thesis, which aimed to avoid the use of any resistant bacteria, it was intended to primarily mimic patients being infected with susceptible bacteria and to potentially show that the development of bacterial resistance and reduced therapeutic success can be prevented *in vivo* by the applied treatment. Hence, the limitations in determination of a MIC value were acceptable.

In case of the antibiotic AMX, only rarely breakpoints have been reported. Typically, susceptible strains against one drug of the class of beta-lactams are also susceptible against other beta-lactams. Hence, e.g. ampicillin can be used as class representative for breakpoint values [13]. Here, *S. pneumoniae* serotype 1 was determined as susceptible (Chapter 3.1.2.2) being in line with results of Casilag et al. [124] and general findings indicating susceptibility to beta-lactamase labile antibiotics [28]. In general, most strains of *S. aureus* are resistant to beta-lactamase labile antibiotics like AMX due to production of beta-lactamases [13,92]. The used strain *S. aureus* Newman was classified as susceptible with an MIC value of 0.25 mg/L being in line with reported values of other susceptible standard control strains of *S. aureus* in literature [204] or by the MIC distribution by EUCAST for *S. aureus* and ampicillin [92]. A MIC determination in RPMI1640 with 10% (v/v) FBS for the case example of *S. aureus* Newman did only reduce the MIC value by one dilution step indicating comparable susceptibility in the less nutritious medium and being plausible due to the more challenging growth conditions easily affecting bacteria. For colistin, susceptibility against Gram-negative bacteria was shown. Determined MIC values against *K. pneumoniae* and *P. aeruginosa* were comparable to values reported in literature that have investigated more than 150 clinical isolates or the ATCC strain PAO1, respectively [118,205]. The determined susceptibility of fosfomycin was also confirmed by values reported in literature for laboratory strains of *S. aureus* [206] and patient isolates of *K. pneumoniae* [43]. In case of *P. aeruginosa*, the strain PAO1 was determined to be resistant against fosfomycin in this project. However, inconsistent results were observed in these investigations due to the following reason: It was assumed that the inconsistency was caused by *P. aeruginosa* specific growth conditions and the specific requirements of fosfomycin not being recommended for broth dilution methods. Still, the obtained results were used for further considerations due to the exploratory stage of the investigations. In context of streptomycin, no breakpoint values have been reported due to the neglected use during the last decades and, hence, breakpoint values of aminoglycosides in general and reported MIC values in literature were considered for classification being in line for strains of *K. pneumoniae* [207], *P. aeruginosa* [208] and *S. aureus* [209]. By these assumptions, bacterial strains were allowed to be characterised as rather susceptible than resistant in terms of streptomycin.

Evaluation of immunostimulatory drugs in a susceptibility testing revealed no direct antibacterial effects in the investigated concentration ranges (Chapter 3.1.2.2). Although antibacterial efficacy has been reported with MIC values of 62.5 mg/L for pioglitazone against *K. pneumoniae* and *P. aeruginosa* in an agar plate dilution method [77], these effects were not confirmed. Hence, studied bacterial strains were assumed to be resistant at investigated concentrations ranges against metformin and pioglitazone. Concentrations of metformin and pioglitazone being in range of C_{max} in patients in serum after oral administration were used for subsequent checkerboard studies. In case of MPLA, growth was as well observed in bacterial growth medium. Hence, MPLA concentrations were set to concentrations being used for stimulation of macrophages for better comparison of direct and indirect effects in a next step.

These first exploratory experiments allowed to gain extensive knowledge about characteristics of drugs and bacterial strains and allowed to classify bacteria according to their MIC. The aim to mainly use susceptible bacterial strains was achieved qualifying all investigated strains to be further investigated in checkerboard assays. Nevertheless, limitations of certain discussed aspects have to be considered for upcoming analyses.

4.1.2 Quantification of drug-mediated antibiotic and immunostimulatory effects in interaction studies *in vitro*

The investigated antibiotics and immunostimulatory drugs qualified for checkerboard experiments to assess potential interactions of antibiotics and the direct effect of the immunostimulatory drugs. Compared to prior susceptibility investigations (Chapter 3.1.2.2), conventional static checkerboard assays display the same limitations. Mainly, results are only assessed as a single time point neglecting any dynamic effects. Nevertheless, quantification of bacteria at this time point enables going one step further compared to common turbidity-based evaluation indicating visible growth or no visible growth. Now, also bacteria below the experimentally defined visual detection limit of approximately $5 \cdot 10^7$ CFU/mL are assessed.

In this setting, no PD interactions based on direct effects were observed, i.e. the immunostimulatory drugs metformin and pioglitazone did not show any drug-mediated killing effects alone as well as in combination (Chapter 3.1.3). These findings were also in line with reported mechanisms of action of the immunostimulatory drugs not showing any known drug-mediated antibacterial effects (Chapter 1.3.2). Hence, direct effects of metformin and pioglitazone were excluded based on checkerboard investigations and no further interaction analysis in terms of response surface modelling was performed. Nevertheless, limitations of these assays not quantifying any dynamic kill kinetics and effects of the immune systems have to be considered. Hence, assessment of indirect effects was mandatory.

4.1.3 Modulator-mediated immunostimulatory effects *in vitro*

Distinguishing direct, i.e. drug-mediated, and indirect, i.e. modulator-mediated, effects is of key importance for further analysis of immunostimulatory drugs and potential description of underlying mechanisms *in vivo*. Assessment of indirect effects was limited due to the lack of an appropriate representation of the immune system in the *in vitro* investigations of this thesis. Hence, alternative approaches to assess immunostimulatory effects *in vitro* needed to be addressed. To comprehensively assess possible drug-drug interactions and detailed information about bacterial growth and kill behaviour over time, time-kill curve studies were performed having the advantage of evaluating growth and kill kinetics over time compared to common MIC or checkerboard investigations.

One approach to incorporate effects of the immune system included the stimulation of macrophages with immunostimulatory drugs in cell growth medium RPMI1640 with 10% (v/v) FBS (Chapter 3.1.4).

Harvesting the supernatant of such experiments, as done at collaboration partners at the Institut Pasteur de Lille, France, generated media consisting of the original cell growth medium, the immunostimulatory drug of interest and any natural or stimulation-derived products of macrophages. For investigations of these indirect effects on bacteria, the availability of pretreated cell growth media after stimulation of macrophages was limited due to relatively small volumes of only a few mL. To still allow an appropriate analysis in time-kill curve studies with quantification of bacteria by using the droplet plate assay (Chapter 2.2.1.5), the total volume within one replicate was reduced to 1 mL compared to volumes of at least 5 mL in common time-kill curve studies [93,162,210-212]. This newly developed miniaturised setting enabled reproducible bacterial quantification and investigation of indirect effects and was beneficial compared to the common practice of time-kill curve analysis.

Bacterial growth in cell growth medium as prerequisite. One prerequisite of the innovative assay was to prove that bacterial growth is possible in such a less nutrient cell growth medium compared to standard bacterial growth media (Chapter 3.1.4.1). The cell growth medium was based on RPMI1640 supplemented with glutaMAX^{TM} and 10% (v/v) FBS, commonly used for growth of cell lines [213]. The medium consisted among several others of amino acids, vitamins, inorganic salts, glucose, growth factors, glutathione and phenol red, but lacks the complex organic materials that are present in conventional bacterial growth media [214]. Within these investigations, the bacterial strains of *K. pneumoniae* and *P. aeruginosa*, that were challenging to handle *in vitro*, were excluded. *S. aureus* and *S. pneumoniae* revealed reproducible results in prior *in vitro* investigations and were also known as easily to investigate *in vivo*. In these cell growth media, *S. aureus* and *S. pneumoniae* showed visible and quantifiable growth (Figure 3.5 and Figure 3.6, respectively). In comparison to the standardised bacterial growth conditions, growth in media used to investigate indirect effects was more challenging and revealed substantially reduced maximum bacterial concentrations and growth rates for *S. aureus* and *S. pneumoniae*. The observed delay in passing over into the exponential growth phase after 4 h in cell growth medium has also been reported by Meduri et al. [214] by monitoring bacterial growth of *S. aureus*. Baldoni et al. have also described that maximum bacterial concentrations have already been reached after 8 h [215]. In addition, a positive effect of FBS on bacterial growth was shown for *S. pneumoniae*. With increasing concentrations of FBS to 10% (v/v), bacterial death was reduced leading to higher bacterial concentrations. FBS may influence bacterial growth and stabilise bacterial concentrations in the stationary phase. These limited growth characteristics indicated an exhausted usage of essential nutrients. In particular for *S. pneumoniae* being known as very fastidious organism, these characteristics were plausible. In addition, a shift in the pH value to more acidic conditions below a pH value of 6.6 occurred. This shift was more prominent with increasing concentrations of FBS indicating a specific mechanism affecting the pH value of the medium and could e.g. be caused by any ingredients of FBS that were converted into acidic products by bacteria. Bacterial growth itself may also be affected by the pH shift, since optimal bacterial growth conditions typically also include a defined

pH value [216]. Hence, reduced bacterial growth in cell growth medium was probably caused by the combination of a lack of appropriate nutrients and the varying pH value.

Considering these findings and the discussed limitations, the cell growth medium, composed of RPMI1640, glutaMAX^{TM}, FBS and, if applicable, macrophages pretreated with MPLA, was shown to be appropriate for further investigations with stimulated media. However, these findings also showed that assessment of the actual course of bacterial growth over time is mandatory for detailed investigations and to differentiate bacterial growth in cell growth medium from growth in pretreated media.

Modulator-mediated effects of MPLA. Based on performed studies investigating characteristics of bacteria and drugs (Chapter 3.1.3), certain antibiotic and immunostimulatory drugs were selected for analysis of indirect effects. As immunostimulatory drug, MPLA was chosen as strongest known activator of macrophages compared to metformin and pioglitazone and providing the possibility of a valid comparison to LPS [69]. Based on prior studies by Casilag et al. [124], the MPLA concentration was set to 1 µg/mL for these investigations. Stimulation of macrophages caused among others production of cytokines, such as IL-6 or IL-12 [124]. As expected, investigation of indirect effects of MPLA in an experimental susceptibility setting with increasing concentrations of STIM up to 89% clearly indicated that the maximum possible amount of STIM and an investigation in a time-kill curve setting were required to detect any indirect effects (Chapter 3.1.4.3). Accordingly, assessment of direct effects in NEG+ and growth in the control medium NEG- was mandatory for meaningful conclusions. In general, no clear trends in bacterial growth were observed and, hence, no indirect effects of MPLA were detected. However, over time, *S. aureus* and *S. pneumoniae* revealed diverse growth behavior in the pretreated medium. *S. aureus* showed increased growth in NEG- being in line with expectations of enhanced growth inhibition in STIM due to present indirect effects (Figure 3.7). Nevertheless, only minor differences in bacterial growth of *S. aureus* in STIM and NEG- were obvious. Addition of MPLA to NEG- led to a minor increase in bacterial growth indicating a beneficial effect of MPLA. One potential cause might be the use of MPLA as nutritional factor by bacteria, which was only observable in a time-kill curve setting. However, considering the relative huge variability in the data and only minor differences between the different media, no indirect effects of MPLA were shown for *S. aureus*. The challenge of a relatively high variability was even more pronounced for *S. pneumoniae* that was investigated in two different batches of pretreated cell growth medium (Figure 3.8). The exact composition of the pretreated cell growth medium might have had a significant effect on bacterial growth and, hence, has to be considered carefully for future investigations that should aim at use of one unique batch. In addition, growth inhibition was less in STIM. Due to existing cytokines harming bacteria, lower bacterial concentrations were expected. This behavior might be best explained by the fastidious characteristics of the bacterial strain. Present MPLA, potential residuals of destroyed macrophages or even cytokines may be used by *S. pneumoniae* as additional nutritional source. To

exclude MPLA being causative for these observations, direct effects of MPLA were investigated by using NEG+. In this case, bacterial growth was nearly identical to growth in stimulated supernatant. As already observed for *S. aureus*, both bacterial strains seemed to be able to utilise MPLA as additional nutritional source in the current *in vitro* setting. Still, these effects were defined as not statistically significant and negligible in comparison to the discussed high variability and, hence, a use for further investigations of combinatorial effects with antibiotics were justified. Conclusively, indirect effects of MPLA were excluded based on the investigated *in vitro* approach.

Immunostimulatory effects combined with antibiotics *in vitro*. For the assessment of those combinatorial effects, AMX was chosen as drug of choice for several reasons. At the moment, AMX is the most important antibiotic for treatment of LRTI [4]. In addition, so far discussed results and antibacterial efficacy against tested strains were reproducible. Colistin and fosfomycin were excluded due to their discussed inconsistent *in vitro* results that might have hindered an appropriate evaluation of indirect effects. In addition, colistin may interact with the potential combination partner MPLA due to its affinity to the comparable structure of LPS that is typically targeted by colistin [217]. Streptomycin as aminoglycoside often provokes the generation of small colony variants being characterised by a slow growth rate and atypical colony morphology [218]. This observation was also made within these experiments for streptomycin and limits the translation to *in vivo*, where small colony variants are only rarely observed [5]. The killing behaviour of AMX in NEG- and STIM in the miniaturised time-kill curve analysis revealed reasonable characteristics with higher bacterial killing for increasing concentrations of AMX. Contrarily, growth inhibition was less pronounced at concentrations below the MIC and equal to or higher the MIC of AMX for STIM and NEG-, respectively (Figure 3.9). At higher AMX concentrations, one can hypothesize that bacteria may be more weakened due to enhanced AMX treatment and facilitate acting of indirect effects of present cytokines. In addition, bacteria did not seem to reach the exponential growth phase and grew rather slowly. Hence, AMX may not affect all bacteria in a replicating state. Still, a relatively high variability occurred limiting the validity in dissecting effects in NEG- and STIM.

Recapitulatory, a new and promising approach was presented to investigate the indirect effects of immunostimulatory drugs enabling observations of differences in growth in various media. Neither drug- nor modulator-mediated effects of MPLA were determined *in vitro* in mono- and combination treatment. The used approach to assess modulator-mediated effects as a result of cytokine production was not able to reflect *in vivo* conditions in terms of the immune system entirely. Degradation of produced cytokines at a storage temperature of -80 °C might be a reason for lacking indirect effects, but at least stability at short-term storage over a few weeks at -80 °C was excluded by Casilag et al. [124]. Substantial direct effects of MPLA were excluded at investigated static concentrations in a time-kill curve setting. To also assess any indirect effects as result of macrophage activity and exclude potential degradation in long-term storage over month of cytokines, an alternative may be to simultaneously

investigate macrophages and bacteria within one assay comparable to a few assays reported in literature [219,220]. Several other assays have been described trying to mimic the even more complex situation of the infected lung *in vitro* that might also be of potential use for future investigations [221,222]. Furthermore, only static AMX concentrations were investigated in these exploratory analyses, instead of considering the dynamic concentration-time profile of AMX concentrations *in vivo* in a dynamic *in vitro* infection model [223]. In addition, the time period of one experiment may be prolonged to expose bacteria over more than 24 h to the different antimicrobial effects. In a next step, this promising approach could be extended by combining the assessment of drug-, modulator- and macrophage-mediated antibacterial effects with varying AMX concentrations over time to comprehensively characterise the combination of antibiotics and immunostimulatory drugs from all sides. Due to various limitations and a lack in appropriate reflection of the immune system *in vitro*, the several performed investigations did not reveal any favourable combinations of antibiotics, immunostimulatory drugs and bacterial strains showing beneficial interaction mechanisms for subsequent analysis *in vivo*. Nevertheless, conducted experiments excluded drug- and modulator-mediated immunostimulatory effects and contributed to an enhanced understanding of the interplay of antibiotics, immunostimulatory drugs and bacteria.

4.2 Boosting the innate immune response in combination with antibiotics

Based on the generated *in vitro* data and literature-based knowledge, *in vivo* studies were designed in collaboration with and conducted at the Institut Pasteur de Lille, France. *In vivo* models are excellent tools to investigate combinations in a preclinical setting being beneficial over *in vitro* studies due to implemented effects of the immune system, dynamic PK and the possibility to assess PD over time at target site. A subsequent analysis leveraging knowledge from *in vitro* and *in vivo* by using pharmacometric approaches provided a better quantitative understanding of the investigated combination and supported the generated findings discussed in this chapter. Performing semi-mechanistic modelling enabled the continuous and simultaneous evaluation of PK and PD with description of its manifold processes and potential interactions. Here, the *in vivo* analysis focussed on treatment of pneumonia caused by *S. pneumoniae* and assessing PK and PD of the combination of AMX and MPLA.

Specification of the bacterial strain and the antibiotic and immunostimulatory combination partners. *S. pneumoniae* as most relevant bacterial species causing LRTI [8] and despite its fastidious characteristics with reliable and reproducible results *in vitro* was selected as bacterial species. The chosen serotype 1 represented an AMX-susceptible strain allowing to replicate typical clinical conditions and not assuming resistant characteristics. As appropriate drug combination partners, AMX and MPLA were chosen for following reasons: AMX as current standard treatment option for LRTI needs to be protected against the emergence of resistance and is well-characterised *in vivo*. Hence, the drug AMX serves as excellent option to provide a basis for analysis of immunostimulatory drugs in

combination. Relatively low doses of AMX were defined to allow characterisation of additional beneficial effects in combination with the immunostimulatory drug. Providing an established preclinical basis with reliable and well-characterised results for subsequent translation into a clinical setting may allow to exchange AMX by discussed neglected drugs in follow-up studies. AMX was combined with the host-directed TLR4 agonist MPLA. Contrarily to the pleiotropic mechanisms of action of metformin and pioglitazone, the immunostimulatory characteristics of MPLA are characterised in more detail. By activating TLR4, signalling cascades leading to production of various chemokines and antibacterial compounds are promoted. Current literature dealing with MPLA indicates continued interest in further applications of MPLA in addition to its use as supplement to vaccines and, so far, have mainly focussed on a prophylactic treatment with MPLA before a bacterial infection [224-227]. Administering MPLA post-infection to *P. aeruginosa* infected mice having a burn injury already indicated increased bacterial reduction [227] and served as promising approach being investigated within this combination partners. Establishing an infection prior to treatment mimics a more clinical situation with treatment starting after diagnosis and allows to also capture immune responses in consequence of an infection. Based on these effects on the immune system, the additional effect of MPLA on the immune system was evaluated. A single dose of 50 µg/mouse (2.00 mg/kg) was administered based on *in vitro* and *in vivo* satellite experiments by Casilag et al. [124] and was in line with other studies reported in literature using MPLA doses of typically 20 to 50 µg/mouse [73,74,224,226,228,229].

Selection of a murine model as appropriate animal model. The mouse as selected animal model offered several advantages over other species: Mice are the most-closest related mammalians to humans with overall biologic similarities and comparatively immunological characteristics [230-232]. They are easy to handle with relatively low maintenance costs, are usually not aggressive, show rapid reproductive rates and are not stressed by everyday events being important among others for long-term survival studies [231]. Due to the differentiation in inbred and outbred mice, cohorts being characterised as genetically identical or as heterogenous can be studied in exploratory studies or as representation of variations within a population like humans, respectively [233]. In case of AMX, the drug administration via oral gavage was applied displaying certain advantages: The technique is attributed with a relatively low variability related to drug administration compared to other methods, such as addition to drinking water, due to a direct transport of the drug into the gastrointestinal tract. It is known as a highly accurate and reliable method enabling fast absorption of the drug [234]. Contrarily to AMX, MPLA was administered intraperitoneally allowing an efficient and easy systemic application of MPLA [235]. As recommended, ≥3 measurements per study group and time point were evaluated and allowed to reliably assess trends and characteristics of the data [5].

4.2.1 Pharmacokinetics as basis for pharmacodynamic effects

Generation of high-quality PK data and a comprehensive PK analysis of potential combination partners are crucial tools as basis for understanding PD effects, to gain detailed information of potential drug interactions and allow deeper insights of the investigated combinations compared to studies not considering PK.

Appropriate preclinical study design as prerequisite for assessment of reliable pharmacokinetic characteristics. An appropriate study design with its various study-specific aspects is essential to assess the pursued aims and has to be discussed intensively. The reported advantages of the mouse as exemplary animal model for preclinical studies face a few drawbacks with regard to PK studies. The challenges associated with such studies in mice are low sampling volumes, a typically low dose with subsequently low serum concentrations and usually only a single PK sample per mouse [236]. In addition, mouse kinetics differ from human PK especially in a shorter half-life and possible different elimination processes [237]. Based on these needs, usage of appropriate sampling techniques and the development of a reliable bioanalytical method to meet the requirements of multiple blood sampling after low dose administration in mice with limited access to the sample matrix were pursued. Guidelines of the National Centre for the Replacement, Refinement and Reduction of Animal Research (NC3R^S) have recommended to not collect more than 10% of the murine total blood volume of approximately 1.80 mL for a 25 g mouse every two weeks [235]. For repeated bleeds at short intervals within 24 h only 1% is suggested to reduce stress for each mouse. For that reason, blood of mice was typically collected only once, and mice were commonly sacrificed for sampling. This destructive sampling design is in particular critical in case of an inappropriate choice of sampling times and urgently required a well-deliberate study design to assess C_{max} and differences between study groups. Here, the accelerated kinetics in mice compared to humans have to be considered in addition to the drugs PK characteristics.

Challenges in quantification of MPLA in serum. In an optimised setting, PK of both partners of a combination study is assessed. Here, one major limitation of this thesis emerged. Quantification of MPLA in mouse serum and concomitant assessment of MPLA's PK was not feasible for several reasons: The low administered dose of only 50 µg/mouse in combination with low sampling volumes required the application of a very sensitive and reliable bioanalytical quantification method. In simplified terms, considering the extravascular administration, metabolism, degradation and distribution processes and assuming a still relatively high bioavailability, a total blood volume of 1.8 mL and a final sample volume for analysis of 10 µL, a concentration of only a few µg would ensue indicating mandatory LLOQ values of only a few ng/mL. Furthermore, the heterogenic composition of MPLA differing between suppliers and depending on the occurrence of different metabolic processes lead to challenging conditions in terms of reproducibility and reliability of reference standards. Various bioanalytical methods have been reported in literature during the last decades. Biological assays, such as the limulus amoebocyte lysate test [238] or enzymatic tests [239], were beneficial due to low LLOQ values, but were not successfully

implemented due to missing sensitivity for *in vivo* samples by the collaboration partner. In addition, time-consuming and more challenging chromatographic-based assays with mass- or UV-spectrometric detection have been reported mostly based on LPS. Here, either not applicable concentration ranges [67,68,240,241] or time-consuming and not easily realisable chemical derivatisations [239] limited the use of these methods. Hence, assessing the concentration-time course of MPLA by a direct measurement was not feasible. Another potential approach was to assess the PK of MPLA indirectly as response of the immune system in terms of cytokine concentrations by collaboration partners at the Institut Pasteur de Lille, France. Nevertheless, this approach was dismissed as discussed within this chapter. Considering these limitations, a quantification of MPLA in mouse serum would not have been meaningful. To assess any information about the PK of MPLA, characteristics reported in literature for other species were considered. Studies in rabbits and dogs treated with 300 µg/kg as bolus injection revealed dose-independent distribution and elimination kinetics with a distribution half-life of 4.0 and 5.2 min, a terminal elimination half-life of 7.6 and 3.5 h, clearance values of 4.4 and 17.1 mL/min/kg and volumes of distribution of 2.9 and 5.2 L/kg, respectively [64].

Development of a sensitive, rapid and economic quantification assay of AMX in serum. To capture the PK characteristics of AMX, a bioanalytical quantification method was developed (Chapter 3.2.1). Knowledge gained from a performed literature research on different sample preparation methods as well as on drug quantification techniques was linked to personal expertise to fulfill the necessary requirements. The targeted small doses of AMX in conjunction with the presumed rapid elimination required quantification of very low concentrations of AMX. Furthermore, the very low blood volume of mice and limited blood sampling possibilities due to ethic regulations and limited sampling sites, led to sampling of only small volumes. For quantification of AMX in different matrices, several methods have been published. Here, sample preparation mainly consisted of solid-phase extraction [242] or simple protein precipitation with EtOH [243], MeOH [26,244] or ACN [29,32,245-251] followed by either subsequent back-extraction with dichloromethane [29,32,246,248,250,251], filtration [249] or evaporation [245,247]. As quantification methods, High-performance liquid chromatography (HPLC) coupled to UV detection [26,32,182,242,243,246,247,250] or LC coupled to MS [29,31,244,245,248,249,251] were used. Only a few assays have been reported for mouse serum [27,180,243,246,252-255], mostly using an agar well diffusion assay with high LLOQ values [27,252-255]. Based on the defined requirements and literature-based information, a LC-MS/MS assay was successfully developed and validated according to European guidelines [121] allowing the reliable and sensitive quantification of AMX in mouse serum. Here, pooled mouse serum of untreated mice of the PK studies was used allowing to develop the method in original serum and excluding unforeseen matrix effects.

The sample pretreatment was designed aiming for simplicity and usage of only small volumes of serum. The applied protein precipitation with MeOH and subsequent dilution with MilliQ® water represents a

simple, rapid and economic sample preparation. It can be easily conducted in any laboratory compared to other described solid-phase or liquid-liquid extraction methods and showed highest recovery of AMX. As a consequence of using simple protein precipitation, the total concentration of AMX in a sample was quantified and AMX being bound to proteins was neglected. Considering the comparably low and linear PPB of AMX of 15%-20% in humans that has been reported to be comparable in mice [243], this simplification was justified in face of the other advantages of the reported sample preparation. Due to the dilution step, only a small amount of 10 µL serum was required and was typically substantially lower than reported other sampling volumes of >50 µL [26,32,242,245-247,249,250,256]. The total run time of the assay was in the same range as already introduced other HPLC-based studies with reported run times ranging from 3 to 15 min [32,244-246,248-250,256,257] and overall rather short with 7.5 min. By reducing the time interval of samples being led to the triple quadrupole MS detector, challenging contamination of the ion source and, hence, reduced sensitivity was successfully avoided and allowed analysis of samples continuously for >24 h within one experimental run. Consequently, selectivity of the developed assay was reproducible within demanded limits despite the used small volume, the simplified protein precipitation and the high number of samples.

Successful validation of the bioanalytical assay. In face of a wide AMX concentration range, that was considered especially important for the application of the bioanalytical assay, carry-over was a critical aspect of this analysis. However, implementation of additional MeOH samples successfully avoided carry-over and contributed to the accurate and precise quantification of very low concentrations. Compared to literature, various authors have reported LLOQ values in mouse serum of 0.1 µg/mL [180,252,253] using a microbial assay, 0.5 µg/mL [243] or 0.2 µg/mL [246] using HPLC coupled to UV-detection or 0.001 µg/mL using LC-MS/MS [249]. Indeed, the assay by Marx et al. reported a very low LLOQ of 0.001 µg/mL but requires 50 µL of mouse serum for quantification as opposed to 10 µL in the present project. Due to the fact that the calibrator samples covered a broad calibration range of 10^3, a wide range in the detector signal arose. Accordingly, a larger absolute deviation in the detector response at higher concentrations resulted in a higher impact on the calibration function than deviations at smaller concentrations. This known heteroscedasticity in the data recommended to apply a weighing function of $1/(\text{concentration})^2$ in the linear regression analysis to higher weight especially the lower concentration range leading to increased accuracy. The developed method was accurate and precise over the entire concentration range (Figure 3.12). Nevertheless, a differentiation in the slopes of the calibration (values: 62.6, 66.0, 87.0) was noticeable. The spread in the slope of the regression function is not uncommon for LC-MS/MS analyses due to the very sensitive conditions in the ion source of the MS system, especially compared to HPLC using UV detection, in which calibration functions are more constant and typically very reproducible [89]. Still, variability in the slopes of the calibration is not listed as quality criterion by the EMA guideline on bioanalytical method development and all requirements regarding accuracy and precision were fully met. Stability investigations of the developed LC-MS/MS

method demonstrated appropriate stability of AMX under tested conditions being in agreement with previously published studies [31,242,256]. Autosampler stability up to 20 h, long-term stability up to 6 months, freeze-thaw stability up to 3 cycles and stability at room temperature up to 20 h were indicated by the QC samples (Table 3.6). Comparable stability of AMX has been reported in literature under similar conditions compared to the here presented assay. AMX fulfilled long-term stability criteria in human and sheep plasma for at least 4 weeks and was stable after three freeze-thaw cycles at -80 °C [31,242,256]. In addition, stability of an aqueous stock solution at 8 °C for more than one month [242] as well as stability in mouse serum for ≥6 h has been reported [246]. Another important fact to consider was the reported instability of AMX in MeOH, as it was used in the present experiments for protein precipitation. Indeed, under specific conditions AMX and MeOH are able to form an adduct [258]. This adduct was also detected in the present project, but only in solution of AMX in pure MeOH. Due to the amount of water in the serum sample itself, a rapid processing and the subsequent addition of MilliQ® water (20% (v/v) MeOH), no adduct was detected in the samples. Moreover, various authors reported the use of MeOH in stock solutions or as mobile phase without describing any instabilities [31,32,259]. In total, the stability of AMX in the samples promotes the simple pretreatment of samples during analysis and storage at -80 °C for a long time period of at least 6 months. Applying the developed method to study samples adhered determined time frames and temperatures and, hence, avoided instability of AMX.

Until now, at the best of the author's knowledge, no assay had been established which is at the same time rapid, simple and highly sensitive for quantification of small amounts of AMX in a low volume of mouse serum. The assay combines a simple sample preparation with various other advantages being simultaneously timesaving and cost-effective. The simplicity of separating AMX from serum constituents allows for the use of only 10 µL serum, which was a 5-fold reduction compared to reported assays with a comparable LLOQ. Furthermore, it allows an easy transfer to other laboratories not equipped with high-cost materials as e.g. solid-phase extraction. In addition, this small volume enables analyses of fully characterise PK by covering very low concentrations at later time points after drug administration. Additionally, for the bioanalytical part of a therapy optimisation study in vulnerable patients, such as neonates or in *in vitro* settings in a miniaturised format, the assay might be used as a starting point.

Pharmacokinetic interaction as potential explanation for pharmacodynamic effects. The developed and validated LC-MS/MS method was successfully applied to serum study samples of mice treated with AMX in monotherapy or the combination with MPLA (Chapter 3.2.3). Studies reported in literature and conducted with mice reported total doses ranging from 2.5-1280 mg/kg orally administered up to six times daily [27,246,254,255]. In this thesis, two dose levels of AMX were investigated over maximum 12 h. To ensure quantifiable AMX concentrations, a relatively high dose of 14.0 mg/kg was selected for first studies in non-infected and infected mice. Based on the obtained

results, the AMX dose was reduced to targeted doses of 0.40 mg/kg of the PD studies. Assuming linear PK, the resulting samples were estimated to be within the wide calibration range of the LC-MS/MS assay. Sampling time points were chosen based on a study conducted by Moine et al. reporting a short-elimination half-life of 0.41 h for mice [260] with more dense sampling directly after drug administration. Due to the small volume of serum required for quantification of AMX using the present assay, it was also possible to take two blood samples from selected individual mice and the required number of mice was thus reduced compared to traditional one-sample investigations. As a consequence, the burden for each individual mouse was limited by reducing the finally required volume of serum and estimation of IIV was possible. Compared to common analyses with AMX in mice [27,180,243,246,252-255], the assay in combination with the study design proved and quantification of AMX in serum with low administered doses, and the required number of mice for a study was reduced by up to 50%. Still, reported variability in the *in vivo* data has to be considered for analysis of obtained results and may have various reasons: One potential explanation might be the administration route of AMX. Next to already discussed advantages, also limitations have to be noticed. Oesophageal trauma or struggle caused by injection into the lung are possible and also increased blood pressure, heart rate and serum corticosterone concentrations are reported [234,261,262]. Here, variability between samples of different mice may occur, since each mouse reacts different and the administration of a drug can cause a specific stress level resulting in such symptoms [234]. Potential actions to reduce these characteristics were not studied within this thesis. E.g., sugar has been reported to show analgesic properties and calm the mouse. Acidic solutions seem to enhance swallowing, since it activates the process of swallowing and hereby helps the mouse to swallow the catheter and reduce the stress level [234]. Furthermore, the blood sampling technique of retroorbital bleeding may increase variability due to challenging handling procedures. The alternative and more beneficial sampling technique of capillary microsampling was not used within this experiments due to technical limitations. Here, sampling of small and exact volumes would have allowed assessment of a full PK profile with up to six sampling time points in one individual mouse [236]. To support the estimation of the transfer of the AMX from the serum to the infection site and gain advanced knowledge, future studies, in particular in a clinical setting, should consider assessing AMX concentrations in lung by applying e.g. the minimal invasive sampling technique of microdialysis that already has been studied to determine lung concentrations [263].

Despite these reported limitations but also due to the advantages of a well-structured study design with two samples per individual for study PK 1.2, the developed PK submodel on basis of the generated *in vivo* data had the ability to differentiate IIV and RUV reliably and characterise the PK of AMX (Chapter 3.4.1.1). The concentrations of AMX in mouse serum after oral administration of the antibiotic displayed a plausible time course (Figure 3.15). These findings were confirmed by the conducted pharmacometric analysis in comparison to state-of-the-art knowledge in literature. An analogous pharmacometric

analysis in mice has been performed by Moine et al. with subcutaneous administration of AMX [180]. A two-compartment model with linear first-order elimination kinetics has been established as best model being identical to findings of this thesis. Contrarily, Woodnutt et al. have recommended to use a one-compartment model with linear absorption after oral administration in rats [27]. However, the design of the study with its sampling time points and administered doses, and the differentiating species might justify the defiant compartment model and still confirmed first-order absorption kinetics. Compared to human profiles of orally administered AMX [31-33,182,250], a faster absorption of AMX was identified decreasing t_{max} from 1 to 2 h in humans to 10-30 min in mice being in agreement with previous studies conducted in mice [27,246,253-255]. As indicated by the already discussed more rapid rate of various processes in mice and drug administration of a solution directly into the gut, a fast absorption in mice compared to humans was plausible being even more shortened due to the implemented lag time in the PK submodel. Maximum serum concentrations (C_{max}=5.84 mg/L) were also comparable to values of 2.5-12 mg/L reported in literature [27,246,252,253,255]. Volumes of the central compartment (V_c=15.4 mL; 0.616 L/kg) were in line with reported parameters in literature for mice of approximately 16.3 mL (0.740 L/kg [180]) and were physiologically plausible in comparison to a body weight of approximately 25 g. The population *CL* of AMX monotherapy was 124 mL/h, corresponding to 2.07 mL/min. Moine et al. have reported a CL_{AMX} of 0.7 mL/min in infected mice after s.c. injection of different doses by using a two-compartment model with linear first-order elimination from the central compartment [180]. Creatinine clearance values of 0.255 mL/min and 0.329 mL/min in C57BL/6J mice have been reported by Dunn et al. and Takahashi et al., respectively [264,265]. As barely non-renal elimination has been reported [26], the clearance values indicated tubular secretion of AMX, most probably by renal organic anion transporters (OAT, [183]).

Still, visual differences between non-infected and infected mice as well as mice treated with AMX or a combination of AMX and MPLA were shown. In particular, combination-treated mice had higher maximum concentrations at a later time point and showed delayed uptake with also higher serum concentrations over the entire study period. Simultaneous administration of MPLA indicated a longer and increased exposure of AMX changing PK of AMX into a beneficial direction. To evaluate the significance of these differences in the respective PK profiles, NLME modelling was able to give more mechanistic and quantitative insights into the PK. Here, a PK interaction between AMX and MPLA was revealed affecting the clearance of AMX. In this PK study, only two doses were studied hampering the detection of non-linearity and, hence, the determined interaction of AMX and MPLA could not be completely characterised. Due to this limitation, the effect of MPLA on the clearance of AMX was included linearly depending on the administered dose of AMX in a simplified relationship. Elimination of MPLA has been reported to be renally to a certain extent and might also occur via renal OATs and influence the tubular secretion of AMX [64]. A competitive mechanism for the elimination of both drugs could arise being only present in case of high AMX concentrations at high administered doses.

Furthermore, the missing administration of a dummy drug in case of monotherapy could induce additional stress for the mice leading to a reduction in elimination compared to combined treated animals. Accordingly, the varying stress level may substantially influence the elimination processes. It has to be considered that mice are very sensitive to stress and already the administration of a second drug might increase the stress level of a mouse and influence PK of AMX [261].

The determined interaction of AMX and MPLA on a PK level illustrates the importance of a comprehensive analysis of the PK over time. It may serve as potential explanation for any further detected interactions. Not considering the PK, potential interactions on a PD level could be wrongly classified as e.g. synergistic due to the mechanism of action, although underlying PK is the main driver of the interaction.

4.2.2 MPLA boosting the immune system in combination with amoxicillin

A comprehensive PD study was performed to determine the effect of AMX in combination with MPLA. As result, not only the overall PD effect was described extensively considering various aspects, but also important knowledge of the time course of infection and antibacterial therapy were assessed. As main PD outcome, bacterial numbers and survival were studied (Chapters 3.3.2 and 3.3.3, respectively). The advantage of this project assessing PD in mice was to characterise bacterial numbers at site of infection over time and, hence, in detail describe bacterial growth. Next to the lung as site of infection for pneumonia, bacterial numbers in spleen were determined reflecting potential sepsis [266]. In addition, survival analysis enabled to assess long-term effects of the studied combination regimen. The analysis of these main PD outcomes was supported by several additional markers allowing to characterise the stimulation of the immune system and general physical condition of the mice (Chapter 3.3.4).

Aiming to exploit the exposure-response relationship of this innovative treatment option and to highlight the necessity to go beyond commonly used approaches, i.e. also consider effects over time, the combination treatment was investigated by the use of semi-mechanistic PK/PD modelling and subsequent survival analysis being useful tools to support and further quantitatively interpret experimentally defined outcomes of *in vivo* studies and to evaluate the effectiveness of the proposed combination comprehensively. Indeed, the grade of pneumonia, represented as the bacterial burden in lung, as well as sepsis, defined by bacterial burden in spleen, were investigated simultaneously and subsequently linked to survival.

The following sections aim to discuss relevant aspects of the performed analysis and, subsequently, amalgamate *in vivo* and *in silico* generated knowledge on top of the mechanistic insights from the *in vitro* analysis. To successfully characterise the investigated combination, certain limitations and considerations of the thesis must be discussed. In this context, it was of highest relevance, that most of the generated data were studied in different experiments and accordingly different mice. Hence, a direct link of two different investigated read-outs, such as bacterial number and AMX serum concentration,

within one individual mouse was typically not possible. Only survival and body weight were assessed within one study and could be related to each other. Also, bacterial numbers in lung and spleen were quantified in the same individual mouse. Due to quantification of bacteria or other markers only once for one individual mouse, no IIV was assessed. Investigated methodological approaches to allow separation of IIV and RUV within the PK/PD model, such as fixing the RUV to the assay variability, were not successful and, accordingly, the two hierarchical levels of IIV and RUV were not separated. To consider this issue, the same conditions between the different PD studies and the PK study in the *in vivo* lung infection model were adhered to minimise variability. Due to the high number of investigated animals in studies evaluating bacterial numbers and survival, a profound basis for subsequent *in silico* analysis was given. Nevertheless, high variability in particular in bacterial numbers was observed, although mice have been reported to typically show less variability compared to humans as most controlled *in vivo* system [267]. Inter-animal variability may still differ 10-fold as reported by Mizgerd et al. [233] and was also observed within these experiments. Here, different treatment groups were evaluated in different experiments at different time points in different mice with varying numbers of mice per study group. Intranasal inoculation may already cause a variable bacterial deposition in lung and potentially introduced variability in the initial bacterial burden between animals. As described for the inoculum *in vitro*, that can also have a substantial impact on generated results *in vivo* [268]. Certainly, the already discussed variability in the PK of AMX also contributed to the described variability in the PD data. Another drawback was that typically no dummy drug was administered in monotherapy substituting either AMX or MPLA for most study groups. Still, administration of a dummy drug was partly investigated for bacterial numbers and significant effects were excluded considering the overall high variability. Another fact to consider with regards to the PK study is, that PK were studied over a broad AMX dose range from 0.4 to 14 mg/kg with only two investigated doses and an effect of MPLA on the clearance of AMX was detected depending on the administered AMX dose in a linear relationship. Particularly, when differentiating between monotherapy and combined treatment, this might have an effect or result in an explanation for findings revealed by PK/PD modelling. However, due to the low doses of AMX in the PD studies being in a small range, the PK interaction was rather expected to be negligible. Despite these discussed limitations, quantitative insights into the combination and plausible parameters estimates (Table 3.9) were obtained and the combination of AMX and MPLA was characterised successfully.

Evaluating the results of the *in vivo* performed studies (Chapter 3.3), MPLA in combination with AMX was superior to monotherapy of either AMX or MPLA and MPLA was able to boost the processes allocated to the innate immune response. A single administration of MPLA was associated with substantially lower bacterial numbers in lung (Figure 3.18) and spleen (Figure 3.19) and indicated higher survival rates (Figure 3.22) compared to untreated animals. In context of histopathology in lung, MPLA had the ability to be as effective as a curative dose of AMX and did not lead to severe lung inflammation

(Chapter 3.3.4.4). Here, already the potential ability of MPLA to function as therapeutic agent in context of LRTI was shown. Monotherapy with AMX also decreased bacterial numbers and improved survival. Early after treatment, bacterial numbers were reduced, and a dose-dependent regrowth occurred. The comparably low AMX dose of 0.40 mg/kg revealed a similar survival outcome as MPLA monotherapy but ultimately led to lung tissue damage over time with increased histopathological scores. The typically observed loss of alveolar architecture after a few days [269] has also been shown in this project for not at all or not sufficiently treated animals at a low dose of 0.40 mg/kg. In the combination regimen, the minor efficacy of a low dose of AMX was potentiated and showed histological scores closest to non-infected animals, i.e. the burden for the lung was reduced to a minimal level, no long-lasting lung toxicity occurred, and tissue recovery was promoted. In addition, pneumonia in terms of bacterial numbers in lung was substantially reduced and sepsis in spleen almost completely avoided resulting in enhanced survival with almost no death occurring. Evaluation of the developed semi-mechanistic PK/PD model with the PK, bacterial disease, effect compartment and bacterial disease and treatment submodels clearly confirmed the substantial boosting effect of MPLA and the benefits of administering AMX in combination with MPLA as discussed next.

Progression of the bacterial infection in untreated mice. After transmission of droplets via the air and physical contact, infection with *S. pneumoniae* typically occurs intranasally by oropharyngeal aspiration with subsequent invasion into the lung [233]. Successfully, mice were inoculated intranasally reflecting the natural route of infection, although Moine et al. have reported of failures to induce pneumonia in immunocompetent mice [260]. The bacterial number of *S. pneumoniae* serotype 1 of approximately 6.00-6.60 log10 CFU/mouse was in line with the model-estimated initial number of bacteria of 6.12 log10 CFU/lung and, hence, the applied bacterial suspension seemed to enter the lung entirely indicating plausible initial bacterial numbers. The bacterial population was assumed to be homogenous with all bacteria having the same growth rate constant k_g (0.477 h^{-1} ,Figure 3.32). This simplification was justified due to the fact that a well-characterised and standardised bacterial strain, i.e. an isogenic strain being genetically identical, was used instead of a patient isolate [105,270]. However, differentiation into a more genetically heterogenous strain might occur over time due to genetic variations as a result of the strain being challenged by the specific circumstances as the presence of AMX. This scenario was not considered in the developed PK/PD model as it was not investigated in terms of e.g. whole genome sequencing and not indicated by the underlying data. Following the inoculation with a pathogenic respiratory strain, bacteria typically are getting used to the new environment being initially challenged by the immune system. Due to release of pneumolysin by *S. pneumoniae* and its recognition via the TLR4, the innate immune response is activated [10]. Hereafter, the activation leads to partial but ineffective bacterial elimination among others by alveolar macrophages [269]. Furthermore, natural death of bacteria e.g. due to a lack in nutrients occurs. The growth behaviour is characterised by an almost not present growth directly after the infection indicating that bacteria need

time to familiarise to the for bacteria challenging conditions in immunocompetent mice. Over time, improved growth occurs. Bacteria become adjusted and growth is facilitated. This described profile was also observed in this project with reduced bacterial numbers in untreated animals right after infection. As long as no treatment was initiated, bacterial growth typically occurred as observed in growth control data of untreated mice. The delay in growth could be interpreted as bacterial lag phase of bacteria being typically in a range of 1 h for *S. pneumoniae in vitro* [271]. The proposed theoretical considerations of how to describe the data were plausible and successfully implemented into the pharmacometric model. The description of bacterial growth including the described lag phase of untreated animals was allowed given the exponential term with k_{lag} (0.0595 h^{-1}) and was only affected by a first-order kill-rate constant ($k_{kill,\ lung}$=0.274 h^{-1}). This constant amalgamates treatment-unrelated killing in terms of effects of the immune system and natural bacterial death. A differentiation into these two separate processes was not possible without having any incidence on the single effects of the immune system, e.g. compared to mice lacking active TLR4. Using immunodeficient or TLR4 lacking mice in *in vivo* studies would also have the advantage of less variability due to the missing manifold effects of the immune system. Still, a separation of growth and killing kinetics was possible without simplification to a net growth rate in lung. Bacterial growth outperformed killing processes over time leading to a higher bacterial burden and, subsequently, reduced survival rates. The bacterial fitness of the utilised strain, i.e. the ability to replicate in a given organism [101] and corresponding to bacterial growth, was evaluated in comparison to literature: The simplified MGT neglecting any killing effects of 87.2 min was in line with reported MGT of 30-45 min for *S. pneumoniae* considering that the latter ones were determined under optimal conditions *in vitro* [271]. The twice as high MGT in mice was at least in the same range and seemed to be plausible given the fact that completely different conditions were present *in vivo*. Considering treatment-unrelated killing effects, the determined MGT of 3.95 h was also comparable to reported values *in vivo*, e.g. in rat with a MGT of 2.83 h [271]. Given the species differences and that a different strain was used, the values were plausible.

With inefficient treatment due to a too low dosing regimen or emergence of resistance, a transit of bacteria to spleen was observed indicating a progression of the infection possibly leading to sepsis which was determined by bacterial quantification in spleen. Typically, sepsis is developed secondary to intranasally induced pneumonia. In particular in spleen, a high number of samples below the LLOQ indicating less sepsis was shown in this thesis (Figure 3.16). However, bacteria in spleen occurred only at later time points and seemed to be successfully avoided in multiple treatment groups, and, hence, justified the high proportion of samples being below the LLOQ in spleen. Accordingly, the bacteria appearing in spleen only arose from lung and made a relatively long transit reasonable. The mechanistic implementation into the PK/PD model allowed a characterisation of the bacterial transit in terms of transit models pathophysiologically describing the transit of bacteria, although the kinetics of the transition from lung can usually not be controlled experimentally due to the various involved processes

[272]. The high number of 23.0 transit compartments supported the already discussed time-consuming (*MTT*=40.8 h) and highly variable process of the bacterial transit. In this transit manifold process are involved: A physiological transit through multiple barriers has to be accomplished. Bacteria needed to be transferred into blood and distributed within the body to ultimately reach spleen. In spleen, bacterial growth kinetics were characterised simplified in comparison to growth in lung. First-order processes of the bacterial transit from the transit compartments to the spleen compartment described bacterial numbers in spleen at subtherapeutic dose levels only as arrival in spleen and no additional growth or kill rate was required. At sufficient dose levels, bacteria were not reaching spleen at all, which was in line with the observations. Here, the assumption was justifiable that a certain net growth in spleen was negligible with growth and killing processes compensating each other.

On-off killing kinetics of amoxicillin. The implemented natural bacterial elimination into the PK/PD model contained not only natural death of bacteria, but also killing effects of the immune system that are present consistently over time. In case of AMX, bacterial elimination as well as survival was increased depending on the dose of AMX. The difference in infection-site and serum concentration-time profiles, with maximum concentrations being delayed at infection site (Figure 3.29), led to an antibiotic effect lasting longer than AMX was actually above the MIC in serum. In face of the short presence of AMX in serum and observed PD effects until 48 h after infection, the estimation of a prolonged infection-site concentration was plausible being mechanistically implemented by effect compartments ($k_{e0,\ lung}$=0.125 h^{-1}, $k_{e0,\ spleen}$=0.0435 h^{-1}). In the lung, the bacterial killing of AMX was best described by on-off kinetics with AMX exerting antibacterial effects as long as the AMX concentrations were above the EC_{50} in lung (EC_{50}=0.00109 g/mL, E_{max}=0.255 h^{-1}, H_{lung}=20, Figure 3.30). The differently introduced effects of AMX and MPLA in the spleen as well as the slower equilibrium formation with serum led to longer lasting AMX effects in the spleen (k_{AMX}=13.7 log10(h^{-1})) compared to the lung. Comparison of the AMX efficacy in lung and spleen did not only reveal that different mathematical implementations were better able to capture the effect of AMX in the respective compartments, but also that the killing effect was substantially increased in spleen. Although the effect was rather expected to be drug- than organ-specific, this trend was explainable due to the very low AMX concentrations in spleen that still had a significant effect. In addition, no other killing effects were present within the structure of the PK/PD model in case of AMX monotherapy. The model-described efficacy of AMX in lung being associated with on-off kinetics depending on high $T_{>EC50}$ correlates well with the $T_{>MIC}$, the main PK/PD parameter used for beta-lactams [273].

Constant immunostimulatory effect of MPLA. As discussed, administration of a single dose of MPLA revealed reduced bacterial numbers and enhanced survival. Analysing the semi-mechanistic PK/PD model, the effect of MPLA was successfully characterised being constant over time as indicated by a proportionality factor affecting the natural kill kinetics in lung over time ($MPLA_{lung}$=1.40). MPLA could also have mechanistically affected bacterial growth directly or the efficacy of AMX, but due to

the mechanism of action of MPLA, a strong relation to treatment-unrelated killing in terms of the immune system was most plausible and showed best predictability in the pharmacometric model. Accordingly, MPLA was able to boost the treatment-unrelated killing 1.40-fold. In comparison to the *in vivo* data, this parametrisation reflected the observed long-lasting effects of MPLA as also discussed in the upcoming sections. In addition, the spleen as important organ of the immune system played a crucial role in the conducted study due to the fact that the effect of MPLA as immunostimulant was studied. One can hypothesize that the highly more effective killing rate ($k_{MPLA,\ spleen}$=3.71 h^{-1}), being 9.66-fold higher in spleen compared to lung, was caused by more pronounced immunostimulatory effects in spleen. A further simplification or other implementation of any MPLA effects was not successful due to most bacterial numbers being below the LLOQ. This lack in insufficient characterisation of the MPLA effects in spleen supported the proposed findings. In total, the effect of MPLA was characterised successfully by the semi-mechanistic PK/PD model with respect to the following considerations: A fast response in gene expression in lung of several markers after administration of MPLA occurred in the *in vivo* study (Chapter 3.3.4.2). The upregulated genes were in close context to various functions of the immune system, such as the neutrophil function. The response to an infection by *S. pneumoniae* was among others obviously caused by pneumolysin acting via TLR4-specific pathways [187] and, hence, showing comparable characteristics as MPLA. This behaviour was confirmed by the mechanistic implementation of the MPLA effect depending on treatment-unrelated killing in the PK/PD model. A prior stimulation of the TLR4 on basis of pneumolysin may be the reason for MPLA to amplify the initial effect of the infection-related stimulation of the immune system as a delayed and less pronounced effect was shown for non-infected animals treated with MPLA. In general, the effect of MPLA on gene expression in lung was immediate, transient and finally leading to an enhanced immune response through activation of LPS dependent pathways via TLR4. Importantly, the immune system was affected by MPLA and the bacterial infection at the same time. Evaluating cytokine kinetics over time indicated, that higher cytokine concentrations were mostly driven by higher bacterial numbers and there is a clear dependency between both of these investigated PD parameters next to the impact of MPLA on both. In this context, the already introduced approach to use cytokine concentrations in serum as surrogate of MPLA concentrations in serum was limited considering the complex interconnections of the immune system and obtained results. Next to the fact that the cytokine concentrations were only assessed for a very minor percentage together with bacterial numbers, a clear simultaneous effect of MPLA as well as bacterial numbers on the cytokine concentration was shown. Using these now as a surrogate for MPLA serum concentrations was not implemented into the pharmacometric analysis as bacterial numbers were also influencing them to a higher extent and cannot be neglected. In future, studies should aim at assessing cytokine concentration and bacterial numbers simultaneously in non-infected and infected mice to more detailed distinguish between effects on the immune system of the infection itself and MPLA.

Combinatorial approach enhancing treatment success. As discussed, MPLA increased the killing effects constantly over time, showing highest mortality in combination with AMX. Here, a clear boosting effect was visible (Figure 3.36). Unfortunately, no enhanced response-surface analysis was possible to investigate the combination comprehensively for any synergistic interactions on a PD level due to the lack of any information on the MPLA concentrations over time. However, based on the performed interaction analyses, a PK interaction was quantified being ultimately not able to alone explain PD benefits. Also, no PD interactions were determined by the semi-mechanistic PK/PD model considering the presence of MPLA potentially affecting the efficacy of AMX in terms of the EC_{50} or E_{max}. Hence, the boost of the immune system by MPLA in combination with the effects of AMX mainly conducted to a successful treatment with increased survival.

Analysing the various PK and PD outcomes thoroughly over time based on the *in vivo* data and the performed pharmacometric analysis, a clear trend became visible indicating time-dependent antibacterial characteristics that differed between AMX and MPLA. Whereas the AMX effect was rather short-termed and mainly affected by the PK of AMX as indicated by revealed on-off kinetics, MPLA showed long-lasting effects characterised as being constant over time. As discussed, studies in other species hinted to a rapid distribution of MPLA and a relatively short presence in serum [64]. Accordingly, MPLA seemed to initially activate the immune system leading to a persistent effect probably due to an initiated expression of important genes of the immune response that may take time. Evaluating bacterial numbers in lung and spleen, regrowth after MPLA treatment was only shown for a short time frame. These findings supported the proposed more long-lasting effects of MPLA compared to in particular low doses of AMX. Being in line with these finding, the combination therapy revealed high initial killing with an additional minor reduction afterwards. As discussed, the extent of response by the immune system was strongly affected by the absence or presence of an infection and the impact of MPLA. *In vivo* determined cytokine concentrations indicated a rapid response to MPLA administration as evidenced by the systemic determination of proinflammatory markers (Chapter 3.3.4.3). An ongoing infection with increasing bacterial burden over time led to a late increase in cytokine concentrations clearly indicating a distinct effect on the immune system. It was also obvious that mice mainly died only within a particular time frame between day 1 and 5. In the beginning, an infection was established and as indicated by bacterial numbers in spleen, sepsis occurred after >36 h being in line with first observed cases of death after the first day. Interestingly, the survival analysis showed that the length of a certain period with occurrence of most cases of death was not depending on the treatment itself and only the time point of appearance and most importantly the survival rate was affected by the efficacy of the respective treatment (Chapter 3.4.1.3). After leaving a critical phase until approximately day 5 to 8 behind, the survival rate was constant being in line with the length of the time period reported in studies conducted by Moine et al. evaluating survival of neutropenic mice infected with *S. pneumoniae* and treated with AMX [180]. The mice and accordingly their immune system

adjusted to the infection and in combination with the administered treatment, mice overcame the infection. As long as the mice outperformed the challenges of the first days, probability of survival was high. Reduced body weight in the beginning due to the infection already weakened mice substantially and resulted in even more vulnerable animals. AMX treated mice did not show that body weight reduction indicating an immediate effect of AMX. In case of MPLA treatment, a reduction in body weight occurred due to the additional challenge for the immune system next to the bacterial infection. However, mice had the ability to withstand this challenge in case of MPLA treatment compared to no treatment. Again, the MPLA effect seemed to be rather delayed and in combination therapy benefits of the rather immediate response of AMX.

Comparison to current state-of-the-art knowledge. Due to the lack of appropriate and comparable studies in literature, a comparison of generated results to state-of-the-art knowledge was challenging. Although studies investigating bacterial growth of *S. pneumoniae* in mice have been published, a generic comparison to the conducted study was not possible due to differently administered doses of AMX, immunodeficient mice, different types of infection or mainly varying bacterial strains that substantially influenced bacterial fitness as expected [180,243,252,253,255]. Still, general trends of bacterial numbers and survival were in line with the results of this thesis. Indeed, usage of the semi-mechanistic PK/PD model allowed further evaluation of the data and an integration into current knowledge. In particular, the generation of exposure-response in contrast to commonly assessed dose-response characteristics was beneficial. In general, bacteria in spleen as sign of sepsis are a strong indicator of death. The conducted survival analysis also clearly indicated a relation between survival and the bacterial burden in spleen (Chapter 3.4.1.3). Since the bacterial burden at 48 h was most predictive, but death already occurred before, the chosen parameter in favour of a good predictability was the $T_{>MIC}$ of AMX in serum concomitant with the presence of MPLA. Thereby, the immediate effect of AMX together with the long-lasting effects of MPLA was illustrated. The $T_{>MIC}$ as best predictive parameter for survival was not only confirmed by performed dose fractionation and susceptibility studies (Chapter 3.4.1.4) but also by literature-based studies dealing with AMX [27,252]. By performing these studies *in silico* to identify an appropriate PK/PD index, additional *in vivo* studies and usage of even more mice were avoided. In the dose fractionation and susceptibility studies, the varying bacterial characteristics in terms of the MIC were directly related to the efficacy of AMX in terms of the EC_{50}. Allowing for variation of these characteristics in terms of bacterial growth or treatment-unrelated killing kinetics was not plausible, since no concrete information about a varying bacterial fitness was present and the MIC was typically more correlated to AMX. As expected for AMX, the pharmacometric analysis revealed that the PK/PD index $T_{>MIC}$ characterising time-dependent killing was superior to the indices AUC/MIC and C_{max}/MIC. With $\%T_{>MIC}$ values of 9.03% and 12.9% for the combined treatment and AMX monotherapy, respectively, leading to survival rates >95%, rather small values were revealed indicating a highly efficient therapy (Figure 3.45). Andes et al. have published highest survival rates for mice with AMX

concentrations exceeding the MIC for 40% in neutropenic mice [252] that were confirmed by Woodnutt et al. [27]. A potential reason for the varying values might be the usage of immunodeficient mice. Here, the beneficial effects of the immune system are able to substantially increase the efficacy of an applied treatment as generally shown by a 7-fold reduction of bacterial numbers in immunocompetent in comparison to neutropenic Swiss mice infected with *S. pneumoniae* and treated with ceftobiprole [274]. It also has to be kept in mind, that the MIC as *in vitro* determined marker only is a single time-point measurement with certain already discussed limitations and, hence, may hamper the significance of conventional MIC-based PK/PD indices. Here, dynamic effects of bacterial growth and effects of the immune system *in vivo* are not considered [203]. Additional tools proposed by Seeger et al. [223] may be able to consider the dynamic effects of bacterial growth. Still, an easily accessible MIC-based PK/PD index, being commonly used in clinics as tool to set specific targets and judge the efficacy of a treatment, was selected and determined as appropriate to predict survival of mice.

So far, the developed PK/PD model was able to characterise the underlying processes and interactions, especially considering the various discussed limitations. Next to the determined efficacy of AMX, a clear boost on the immune system by MPLA was detected and quantified. The PK interaction of MPLA on AMX clearance did not affect the PD effects and cannot be used as explanation for any interaction on the PD level. With the $T_{>MIC}$ as easily accessible clinical parameter in addition to simple binary MPLA implementation, a PK/PD index was predictive to capture survival of mice after infection. The herein outlined approach contributes to reducing the use of animals in preclinical studies in future, since various changes in the study, e.g. different dosing regimens, can be simulated.

4.3 Translation into a clinical setting

The performed pharmacometric analysis of the preclinical data provided insights into the underlying mechanisms of the combination of AMX and MPLA. In a next step, the developed PK/PD and TTE model could be translated into a clinical setting bringing this promising combination therapy closer to patients. Aiming to integrate knowledge of the preclinical data including effects of the immune system should allow the intended translation and prediction of an appropriate dose to achieve the desired efficacy in humans. For that purpose, a comprehensive analysis of the preclinical disease model in comparison to humans is mandatory as basis for prediction of an outcome in humans. Here, not only the disease progression but also manifold aspects on a PK and on a PD level have to be considered. Ultimately, the success of the performed pharmacometric analysis in context of the predictive power in comparison to state-of-the-art knowledge can be judged. In this way, the preclinical data might be able to provide important information for clinical studies, such as dose selection or efficacy in humans.

To achieve a powerful translation into clinics, standardised methods and appropriate models for the respective indication have to be used, sources of variability have to be known, appropriate endpoints have to be defined, and the relevance of the immune status needs to be considered [5]. The murine lung

infection model is known as a highly reliable system to preclinically mimic pneumonia. It is well-characterised and standardised conditions have been proposed in literature [5] that were also adhered within this thesis. Nevertheless, these standardised settings did not allow to completely reduce variability to a minimum as already discussed. However, the semi-mechanistic PK/PD model was not only able to capture the variability, but also to characterise the innovative treatment approach.

Murine infection model mimicking human pneumonia. Accordingly, the well-captured disease progression in mice needs also to be adequately represented in humans. In case of infectious diseases, PD effects of antibiotics are rather exerted to tackle bacteria instead directly affecting the human. This direct interaction of drug and bacteria allows in the first place a rather good predictability from mouse to human. In general, mouse and humans share >90% of the same genes and have been reported to be one of the human closest mammalian relatives [230]. Considering general physiological characteristics of mouse and human, a comparability between both species is given. Humans are characterised by genetic heterogenicity within the population not being common in mice to this extent. This study paid attention to this issue and extended the study by investigating to two different type of mice, i.e. one inbred and one outbred strain with the outbred strain generally already showing more genetic heterogenicity. Typically, pneumonia is caused by pathogenic bacteria entering the lung intranasally. Here, anatomic differences have to be evaluated. Mice are breathing obligate via the nose with higher complexity, surface area and respiratory rate compared to humans [275]. Their marked olfactory sense typically leads to an easier colonisation with more bacteria staying in nose and throat region. To allow a better comparability to humans, this behaviour was minimised in the *in vivo* study by inoculating mice intranasally directly into the lung. A successful implementation was confirmed by determined bacterial numbers and the estimated bacterial initial number in lung being in line with the administered number of bacteria. The human lung is arranged into five pulmonary lobes being partitioned into three and two lobes for the right and left lung, respectively, and displays a symmetric branching of bronchioles. Contrarily, the murine lung is constructed in a monopodial bronchial branching with five pulmonary lobes apportioned into four and one for the right and left lung, respectively [276], and generally fewer branches and bronchioles [277]. The asymmetric structure of the murine lung may cause an uneven distribution of particles and needs to be considered when comparing distribution of bacteria in mouse and human. However, these differences do not translate in substantial differences in alveolar distribution [275] and lung capacity is at least in a similar range with 0.04 and 0.08 L/kg in mouse and human, respectively [276]. The barrier between air and blood has been reported to be less pronounced in mice leading to a potential easier invasion of bacteria into the bloodstream and distribution within the body among others to spleen [276]. Indeed, the way of bacteria from lung to spleen certainly offers various differences between mouse and human but this issue will not be discussed in this setting. Contrarily, in spleen a comparable structure with minor functional differences for mouse and human have been

proposed [278] with organ weights representing 0.35% and 0.26% of the total body weight in mouse and human, respectively [279].

As already introduced, an appropriate endpoint has to be defined to enable a reliable translation. Bulitta et al. have proposed to use PK/PD indices as efficacy endpoint of mouse models [5]. In this thesis, the PK/PD index $T_{>MIC}$ displayed best predictability of the generated *in vivo* data and was evaluated in a clinical setting requiring to appropriately capture PK and PD. To enable a successful translation of the PK from mice to humans, certain assumptions and characteristics have to be considered with respect to the PK. The introduced technique of allometric scaling (Chapter 2.5.5) unites most assumptions and allows a simplified comparison. One major difference between both species is the already discussed higher metabolism mice are generally showing [230]. That may also substantially affect the PK characteristics. e.g. a much faster elimination in mouse is reasonable [86,237,280]. These increased rates in physiological process is typically considered by the varying exponents used in allometric scaling. Nevertheless, these exponents are still subject of lots of debates, since the exponent of a certain estimated parameter can still vary vastly depending on the drug or the investigated animal [281].

Studying a combination of antibiotics and immunostimulatory drugs outside a clinical setting requires the discussion of potential differences related to the immune system between both species. In particular in this project, the comparability is of highest importance to enable a prediction of the boosting effect of MPLA on the innate immune response in humans. Indeed, difference in immune responses are obvious [230]. In context of this project evaluating antibacterial effects only over a short time frame, it was crucial to examine the innate immune response rather than the adaptive immune response not being of main interest here. In general, the murine immune system is well characterised [275] and similarities as well as differences to humans can be detected. The progression and immune response of pneumonia has been reported to be overall comparable in mouse and human [232]. Still, certain limitations can be found that may hamper the comparability between the two species and challenge the intended translation. Within the complexity of the immune system, only a few examples shall further be elucidated focussing on the TLR4 and consequences of its activation. The balance of lymphocytes varies throughout the species: Whereas human blood is neutrophil rich, in mice lymphocytes are dominating [232]. The relative number and volume of macrophages in lung is higher in humans compared to mice [275]. However, direct consequences of these shifts are not completely clear [232]. TLRs as early warning system in terms of the innate immune response may also differ between both species. TLR10 or TLR8 are not expressed or non-functional, respectively, in mice, whereas for other receptors presence has been reported [282]. Still, specificity or expression may vary between both species [233]. In context of *S. pneumoniae* releasing pneumolysin and the immunostimulatory drug MPLA, processes involving the TLR4 are of main interest. Mice are proposed to be extremely resistant to endotoxins while humans are way more sensitive [283]. One mechanism seemed to be that murine TLR4 more generally recognise e.g. the structure of LPS without differentiation between deviant structures of the lipid A part [233]. The

activity also seems to depend on the chain length of the fatty acids [284]. It has been proposed, that mice rather fight, whereas humans rather tolerate infections with respect to TLR4-depending pathways [285]. It can be assumed that the response to LPS is related to MPLA as lipid A is the main part binding the receptor. These characteristics lead to distinct consequences in terms of MPLA. Administered doses in mice were manifold higher than common doses in humans. For licensed vaccines Cervarix® and Fendrix®, 50 µg/human are administered compared to 50 µg/mouse leading to an approximately 2800-fold higher exposure in mice [65,66]. In addition, toxicity is substantially increased in humans. Lethal doses of LPS of 15 µg/kg compared to 25 mg/kg have been reported for humans and mouse, respectively [286]. A LPS concentration of 2 to 4 ng/kg has already been sufficient to induce fever in humans [283,287] resulting in a narrow therapeutic window of LPS in humans. This may cause the fact that humans are proposed to be more sensitive to endotoxins by factor 10^5. MPLA has been infused into humans with a concentration of 5 µg/kg without displaying any significant toxicity [224]. Still, the increased toxicity of MPLA in humans compared to mice has to be considered for the intended translation and may have an impact on dose prediction.

Taken the discussed anatomic and immune system-related characteristics together, the murine pneumonia model is still considered as best option to translate preclinical results into a clinical setting [267,272] and using the mouse within this thesis was justified as animal models typically are able to forecast drug efficacy in patients [5] and similarities outweigh differences [233].

The immune system as a challenge for a successful translation. Translation to clinics of comparable approaches based on immune stimulation and antibiotics has already been proposed [18]. The safe use of MPLA in humans and the augmented innate antimicrobial immunity establish a basis for a successful translation as adjunct therapy to conventional antibiotic treatments.

Considering the PK of AMX, the translation was successful with respect to the comparability to reported studies in literature (Chapter 3.4.2). Adapting the determined PK parameters to humans by allometric scaling revealed plausible parameter estimates being comparable to human estimates. By making use of allometric scaling, the different shapes of concentration-time profiles in mouse and human were approximated and a first step to humanised PK was achieved being reasonable as AMX, a drug with 60% renal excretion, is potentially suited for allometric scaling [172]. However, the exact exponent of the allometric scaling equation cannot be determined by only studying a single animal species and may also be in the range of 0.65 and 0.7 [172]. An exponent of e.g. 0.65 would substantially reduce e.g. the intercompartmental clearance by >50%. Hence, extrapolated PK parameters of allometric approaches considering only one species are commonly approximated. Accordingly, to assure a closeness to humans and mask uncertainties of allometric scaling due to the lack of multiple investigated species, the human PK model proposed by Carlier et al. [29] was chosen and human PK profiles of different dosing regimens were successfully simulated. The determined PK interaction influencing the clearance of AMX in presence of MPLA and depending on the dose of AMX was not included for the translation.

The discussed mechanism of the interaction involving OATs may be plausible to translate from mouse to human, since these transporters are present in mice and humans [288]. Only the localisation within a nephron may vary and, hence, exert different effects. Still, these differences have been reported to not be profound [288]. The main reason for excluding the interaction was the presumably administered human dose of MPLA (<0.005 mg/kg , [224]) being significantly lower compared to mice (2.00 mg/kg). In particular, since the interaction was depending on the administered dose of AMX and the study aimed use rather low AMX doses, this assumption was reasonable.

In context of the efficacy of the combination, the translation was more challenging. As discussed, mainly the pathogen and the antibiotic drug are involved with the host mainly affecting the PK of AMX and the PD in terms of the immune system. Indeed, this scenario was also investigated within this thesis in case of AMX monotherapy. Considering the exposure of AMX in terms of human data in dependence on the MIC, the developed semi-mechanistic PK/PD model in mice seemed to be not predictive for humans, since already very low single AMX doses reduced bacterial numbers of highly resistant bacterial strains significantly. Bacteria- and drug-specific parameters were not altered considering the specificity and interaction that should typically not vary between different species. Given the technique quantifying the total bacterial number in the whole lung allowed a linear extrapolation of the bacterial amount from the murine to the human lung considering the analogous structure. Hence, only the parameter characterising the treatment-unrelated killing and, accordingly, effects of the innate immune response seemed to be not adequately transferable. Limitations of translating immunostimulatory effects from mouse to human have already been mentioned. The determined $T_{>MIC}$ of 5% leading already to bactericidal killing of ≥2 log10 CFU/lung (Figure 3.46) was significantly deviating from reported values for beta-lactams targeting at least 40% for sufficient bacterial efficacy in humans [289]. Given the performed translation, a single dose of 500 mg AMX would have already been sufficient for bactericidal killing of a highly resistant bacterial strain. Adjusting the treatment-unrelated killing effects without further knowledge to receive a reasonable PK/PD index deemed adequate. As a consequence of the already implausible translation of the innate immune response, a translation of MPLA effects that are based on the treatment-unrelated killing was hampered. Adjusting the study design to additionally investigate TLR4-deficient or immunodeficient mice might allow to dissect the treatment-unrelated killing effects into natural bacterial death and effects of the immune system and simplify a translation. Here, the effects of the immune system are captured by their own. Furthermore, the MPLA effect could be translated by adjusting the proportionality factor with respect to the increased receptor response.

Still, the performed translation from mouse to human revealed valuable insights into the semi-mechanistic PK/PD model and the interactions of bacteria, drugs and the host. The murine PK of AMX was in line with reported PK in humans. The greatest challenge of the translation process was that human and mouse developed comparable, but not equal strategies during evolution to combat infections, in particular in context of an activation of the TLR4.

5 Conclusions and perspectives

The current thesis aimed at developing novel therapeutic approaches against LRTI to overcome the challenges associated with the emergence of bacterial resistance and to ultimately minimise treatment failures. The innovative combination regimen of an antibiotic drug and an immunostimulatory drug improved treatment efficacy against LRTI caused by *S. pneumoniae*. The most prominent result was the substantial boost of the assumed innate immune response by MPLA that allowed sufficient therapeutic success in combination with the beta-lactam antibiotic AMX. Amalgamating knowledge of *in vitro*, *in vivo* and *in silico* approaches enhanced the understanding of the investigated novel treatment approach and allowed mechanistic and quantitative insights into the nature of interactions.

The screening for appropriate bacterial and drug candidates within the *in vitro* investigations confirmed the usage of susceptible bacterial strains and allowed a detailed characterisation of the drugs and the bacteria. The applied approach of a miniaturised time-kill curve setting in a cell-pretreated medium represents a methodological advancement being able to distinguish drug-and modulator-mediated effects of immunostimulatory drugs. This thesis underlines the value of *in vitro* investigations allowing such mechanistic insights. Here, drug-mediated effects were excluded, and no distinct modulator-mediated effects were revealed. Still, the elaborated approaches were not able to mimic *in vivo* conditions entirely. Any effects directly exerted by stimulated immune cells, such as macrophages, were not considered and reflected the known difficulties to incorporate the immune system *in vitro*. Future studies should comprise investigations of bacteria, drug and immune cells within one dynamic time-kill curve setting to additionally allow determination of cell-mediated effects and changing drug concentrations over time.

Based on the *in vitro* and state-of-the-art knowledge, a combination regimen was selected displaying promising results *in vivo* in experiments performed at the Institut Pasteur de Lille, France. Whereas the *in vitro* systems enabled knowledge about the mechanism of the drugs, the *in vivo* system allowed to learn about effects of the innate immune response more comprehensively and revealed the dynamic interplay of the drug, the pathogen and the host, that was characterised *in silico* in a next step. This thesis clearly demonstrates that a systemic and carefully-considered preclinical study enables quantitative insights on the exposure-response relationship of antibiotics combined with immunostimulatory drugs, when linked to pharmacometric modelling.

Determination of the exposure of AMX was enabled by the successfully developed and validated LC-MS/MS assay being rapid, simple and highly sensitive at the same time. The method was proven to be applicable to quantify AMX in mouse serum over a broad concentration range and was demonstrated to be accurate and precise according to the European guideline on bioanalytical method validation. In face of the simplicity of sample preparation and stability of AMX under applied conditions, the developed assay allows very sensitive quantification of AMX to fully characterise the PK. Additionally, for future

bioanalytical questions in challenging settings, such as a therapy optimisation study in vulnerable patients, e.g. neonates, or in *in vitro* settings in a miniaturised format, the assay might be used as a starting point. The limitation of not being able to quantify MPLA concentrations was at least partly compensated by the comprehensive assessment of the innate immune response *in vivo* characterising time-dependent effects. Still, future studies should aim at quantification of drug concentrations of both combination partners to enable a comprehensive response-surface analysis. Furthermore, the quantification of unbound drug concentrations at the infection site by microdialysis and assessment of a concentration-profile of one individual mouse by the technique of capillary microsampling potentially provides additional insights.

The elaborated highly effective experimental treatment option against pneumococcal pneumonia in a murine infection model was proven to be successful *in vivo* with respect to the PD outcomes bacterial burden as sign of pneumonia and assumed sepsis as well as survival. Already a single, sub-curative dose of AMX combined with the boosting effects of MPLA reduced the bacterial burden and improved survival substantially. The innate immune response simultaneously affected by the bacterial strain as well as the immunostimulatory effects of MPLA was comprehensively characterised.

Aiming to exploit the PK/PD relationship of this innovative treatment option and to highlight the necessity to go beyond commonly used approaches, pharmacometric analyses were performed. This work adds weight to the use of semi-mechanistic PK/PD modelling and subsequent survival analysis being useful tools to support and further quantitatively interpret experimentally defined outcomes of *in vivo* studies and to evaluate the effectiveness of the proposed combination comprehensively.

Here, quantitative and mechanistic insights into the novel treatment option revealing a PD interaction on top of a PK interaction and boosting of AMX activity by MPLA were provided. A stepwise workflow allowing reliable estimation of PK/PD relationships was developed and led to the prediction of change in overall survival based on easily accessible clinical parameters. The *in vivo* observations, indicating that the innate immune response was simultaneously affected by the bacterial strain as well as the immunostimulatory effects of MPLA, supported the model-informed characteristics of MPLA being consistently present over time compared to rather short-term exerted effects of AMX. The boost of the innate immune response by MPLA shows the potential of MPLA to function as therapeutic agent, in particular as combination partner of antibiotics.

Thereby, the efficacy of the combination was fully characterised. The used *in vivo* model potentially serves as exemplary model for future investigations of novel combination approaches providing an excellent *in vivo* infection environment and valuable insights into combinatorial effects by *in silico* analyses. Furthermore, AMX could be exchanged by neglected and disused antibiotics and, additionally, the emergence of bacterial resistance could be assessed by studying resistance mechanisms genetically in terms of whole genome sequencing. Also, resistant bacterial strains or clinical isolates could be

investigated to judge the potential of the combination therapy. A prerequisite for such additional studies is the successful translation into a clinical setting. Here, the intended translation of the preclinical data was hampered by the incomplete characterisation of the innate immune response. A translation of the murine PK to humans was successful and valuable insights into interactions of bacteria, drugs and the host were gathered. The comparison to immunodeficiency may allow further information about contributions of the immune system to drug efficacy, e.g. by the use of neutropenic or TLR4-deficient mice. As a consequence, a translation of immunostimulatory effects of MPLA and the efficacy of AMX may also be enabled.

This thesis allowed mechanistic and quantitative insights into a novel treatment option combining antibiotics with immunostimulatory drugs by making use of *in vitro*, *in vivo* and *in silico* knowledge. Boosting the innate immune response enhances not only the efficacy of the antibiotic drug but may also serve as promising approach to ultimately avoid a post-antibiotic era, in which antibiotics would not be effective anymore due to the continuing emergence of bacterial resistance.

6 Bibliography

[1] R. Cantón, J.P. Horcajada, A. Oliver, P.R. Garbajosa, J. Vila. Inappropriate use of antibiotics in hospitals: The complex relationship between antibiotic use and antimicrobial resistance. Enferm. Infecc. Microbiol. Clin. 31: 3–11 (2013).

[2] P.C. Collignon, J.M. Conly, A. Andremont, S.A. McEwen, A. Aidara-Kane, P.M. Griffin, Y. Agerso, T. Dang Ninh, P. Donado-Godoy, P. Fedorka-Cray, H. Fernandez, M. Galas, R. Irwin, B. Karp, G. Matar, P. McDermott, E. Mitema, R. Reid-Smith, H.M. Scott, R. Singh, C.S. Dewaal, J. Stelling, M. Toleman, H. Watanabe, G.J. Woo. World Health Organization ranking of antimicrobials according to their importance in human medicine: A critical step for developing risk management strategies to control antimicrobial resistance from food animal production. Clin. Infect. Dis. 63: 1087–1093 (2016).

[3] J.W. Mouton, P.G. Ambrose, R. Canton, G.L. Drusano, S. Harbarth, A. MacGowan, U. Theuretzbacher, J. Turnidge. Conserving antibiotics for the future: New ways to use old and new drugs from a pharmacokinetic and pharmacodynamic perspective. Drug Resist. Updat. 14: 107–117 (2011).

[4] Paul-Ehrlich-Gesellschaft für Chemotherapie e.V. S2k Leitlinie: Kalkulierte parenterale Initialtherapie bakterieller Erkrankungen bei Erwachsenen – Update 2018. (2019). https://www.awmf.org/uploads/tx_szleitlinien/082-006l_S2k_Parenterale_Antibiotika_2019-08.pdf (last access 03 Mar 2020).

[5] J.B. Bulitta, W. Hope, A.E. Eakin, T. Guina, V.H. Tam, A. Louie, G.L. Drusano, J.L. Hoover. Generating robust and informative nonclinical in vitro and in vivo bacterial infection model efficacy data to support translation to humans. Antimicrob. Agents Chemother. 63: e02307-18 (2019).

[6] Center for Disease Dynamics, Economics & Policy. The state of the world's antibiotics, 2015. (2015).

[7] L.C. Balsalobre, M. Dropa, M.H. Matté. An overview of antimicrobial resistance and its public health significance. Brazilian J. Microbiol. 45: 1–5 (2014).

[8] GBD 2016 Lower Respiratory Infections Collaborators. Estimates of global, regional, and national morbidity, mortality, and aetiologies of diarrhoeal diseases: A systematic analysis for the global burden of disease study 2015. Lancet Infect. Dis. 18: 1191–210 (2018).

[9] C. Duarte, O. Sanabria, J. Moreno. Molecular characterization of Streptococcus pneumoniae serotype 1 invasive isolates in Colombia. Rev. Panam. salud publica 33: 422–6 (2013).

[10] B. Henriques-Normark, E.I. Tuomanen. The pneumococcus: Epidemiology, microbiology, and pathogenesis. Cold Spring Harb. Perspect. Med. 3: a010215 (2013).

[11] N. Williams-Bouyer, A. Hernandez, B.S. Reisner. Predicting susceptibility of Streptococcus pneumoniae to ceftriaxone and cefotaxime by cefuroxime and ceftizoxime disk diffusion testing. J. Clin. Microbiol. 37: 3707–3710 (1999).

[12] P. Rai, M. Parrish, I.J.J. Tay, N. Li, S. Ackerman, F. He, J. Kwang, V.T. Chow, B.P. Engelward. Streptococcus pneumoniae secretes hydrogen peroxide leading to DNA damage and apoptosis in lung cells. Proc. Natl. Acad. Sci. 112: E3421–E3430 (2015).

[13] Clinical and Laboratory Standards Institute. Performance standards for antimicrobial susceptibility testing: Twenty-first informational supplement. CLSI document M100-S21. (2011).

[14] X. Nassif, J.M. Fournier, J. Arondel, P.J. Sansonetti. Mucoid phenotype of Klebsiella pneumoniae is a plasmid-encoded virulence factor. Infect. Immun. 57: 546–552 (1989).

[15] C. Stein, O. Makarewicz, J.A. Bohnert, Y. Pfeifer, M. Kesselmeier, S. Hagel, M.W. Pletz. Three dimensional checkerboard synergy analysis of colistin, meropenem, tigecycline against

multidrug-resistant clinical Klebsiella pneumonia isolates. PLoS One 10: e0126479 (2015).

[16] A.F. Mohamed, A.N. Kristoffersson, M. Karvanen, E.I. Nielsen, O. Cars, L.E. Friberg. Dynamic interaction of colistin and meropenem on a WT and a resistant strain of Pseudomonas aeruginosa as quantified in a PK/PD model. J. Antimicrob. Chemother. 71: 1279–1290 (2016).

[17] World Health Organization. Global priority list of antibiotic-resistant bacteria to guide research, discovery, and development of new antibiotics. (2017). https://www.who.int/medicines/publications/WHO-PPL-Short_Summary_25Feb-ET_NM_WHO.pdf (last access 05 May 2017).

[18] L. Czaplewski, R. Bax, M. Clokie, M. Dawson, H. Fairhead, V.A. Fischetti, S. Foster, B.F. Gilmore, R.E.W. Hancock, D. Harper, I.R. Henderson, K. Hilpert, B. V. Jones, A. Kadioglu, D. Knowles, S. Ólafsdóttir, D. Payne, S. Projan, S. Shaunak, J. Silverman, C.M. Thomas, T.J. Trust, P. Warn, J.H. Rex. Alternatives to antibiotics: A pipeline portfolio review. Lancet Infect. Dis. 16: 239–251 (2016).

[19] N. Cassir, J.M. Rolain, P. Brouqui. A new strategy to fight antimicrobial resistance: The revival of old antibiotics. Front. Microbiol. 5: 551 (2014).

[20] P. Hamill, K. Brown, H. Jenssen, R.E. Hancock. Novel anti-infectives: Is host defence the answer? Curr. Opin. Biotechnol. 19: 628–636 (2008).

[21] U. Theuretzbacher, F.V. Van Bambeke, R. Cantón, C.G. Giske, J.W. Mouton, R.L. Nation, M. Paul, J.D. Turnidge, G. Kahlmeter. Reviving old antibiotics. J. Antimicrob. Chemother. 70: 2177–2181 (2015).

[22] World Health Organization. Model list of essential medicines: 20th edition. (2017).

[23] Aristo Pharma GmbH. Summary of product characteristics of amoxicillin Aristo® 500 mg / 1000 mg Filmtabletten. (2015). http://fachinformation.srz.de/pdf/aristo/amoxicillinaristo500mg1000mgfilmtabletten.pdf (last access 02 Feb 2017).

[24] B. Aparecida de Marco, J.S.H. Natori, S. Fanelli, E.G. Tótoli, H.R.N. Salgado. Characteristics, properties and analytical methods of amoxicillin: A review with green approach. Crit. Rev. Anal. Chem. 47: 267–277 (2017).

[25] D. Thambavita, P. Galappatthy, U. Mannapperuma, L. Jayakody, R. Cristofoletti, B. Abrahamsson, D.W. Groot, P. Langguth, M. Mehta, A. Parr, J.E. Polli, V.P. Shah, J. Dressman. Biowaiver monograph for immediate-release solid oral dosage forms: Amoxicillin trihydrate. J. Pharm. Sci. 106: 2930–2945 (2017).

[26] L.R. Pires de Abreu, R.M. Ortiz, S.C. de Castro, J. Pedrazzoli. HPLC determination of amoxicillin comparative bioavailability in healthy volunteers after a single dose administration. J. Pharm. Pharm. Sci. 6: 223–30 (2003).

[27] G. Woodnutt, V. Berry. Two pharmacodynamic models for assessing the efficacy of amoxicillin-clavulanate against experimental respiratory tract infections caused by strains of Streptococcus pneumoniae. Antimicrob. Agents Chemother. 43: 29–34 (1999).

[28] The European Committee on Antimicrobial Susceptibility Testing. Amoxicillin: Rationale for the EUCAST clinical breakpoints. (2010). http://www.eucast.org (last access 14 Aug 2017).

[29] M. Carlier, M. Noë, J.J. De Waele, V. Stove, A.G. Verstraete, J. Lipman, J.A. Roberts. Population pharmacokinetics and dosing simulations of amoxicillin/clavulanic acid in critically ill patients. J. Antimicrob. Chemother. 68: 2600–2608 (2013).

[30] A. Fournier, S. Goutelle, Y.-A. Que, P. Eggimann, O. Pantet, F. Sadeghipour, P. Voirol, C. Csajka. Population pharmacokinetic study of amoxicillin-treated burn patients hospitalized at a Swiss tertiary-care center. Antimicrob. Agents Chemother. 62: e00505-18 (2018).

[31] M. Szultka, R. Krzeminski, J. Walczak, M. Jackowski, B. Buszewski. Pharmacokinetic study of

amoxicillin in human plasma by solid-phase microextraction followed by high-performance liquid chromatography-triple quadrupole mass spectrometry. Biomed. Chromatogr. 28: 255–264 (2014).

[32] S.M. Foroutan, A. Zarghi, A. Shafaati, A. Khoddam, H. Movahed. Simultaneous determination of amoxicillin and clavulanic acid in human plasma by isocratic reversed-phase HPLC using UV detection. J. Pharm. Biomed. Anal. 45: 531–534 (2007).

[33] P. Ball. The clinical development and launch of amoxicillin/clavulanate for the treatment of a range of community-acquired infections. Int. J. Antimicrob. Agents 30S: S113–S117 (2007).

[34] W. Dong, Z. Hou, X. Jiang, Y. Jiang. A simple sample preparation method for measuring amoxicillin in human plasma by hollow fiber centrifugal ultrafiltration. J. Chromatogr. Sci. 51: 181–186 (2012).

[35] L.M. Lim, N. Ly, D. Anderson, J.C. Yang, L. Macander, A. Jarkowski, A. Forrest, J.B. Bulitta, B.T. Tsuji. Resurgence of colistin: A review of resistance, toxicity, pharmacodynamics, and dosing. Pharmacotherapy 30: 1279–91 (2010).

[36] M.E. Falagas, S.K. Kasiakou. Colistin: The revival of polymyxins for the management of multidrug-resistant Gram-negative bacterial infections. Clin. Infect. Dis. 40: 1333–1341 (2005).

[37] J. Li, J. Turnidge, R. Milne, R.L. Nation. In vitro pharmacodynamic properties of colistin and colistin methanesulfonate against Pseudomonas aeruginosa isolates from patients with cystic fibrosis. Antimicrob. Agents Chemother. 45: 781–785 (2001).

[38] J. Li, K. Coulthard, R. Milne, R.L. Nation, S. Conway, D. Peckham, C. Etherington, J. Turnidge. Steady-state pharmacokinetics of intravenous colistin methanesulphonate in patients with cystic fibrosis. J. Antimicrob. Chemother. 52: 987–992 (2003).

[39] Grünenthal GmbH. Summary of product characteristics of colistin: Trockenstechampullen mit Lösungsmittel. (2010). https://nanopdf.com/download/zusammenfassung-der-merkmale-des-4_pdf#modals (last access 16 Sep 2019).

[40] J. Li, R.L. Nation, R.W. Milne, J.D. Turnidge, K. Coulthard. Evaluation of colistin as an agent against multi-resistant Gram-negative bacteria. Int. J. Antimicrob. Agents 25: 11–25 (2005).

[41] D. Yahav, L. Farbman, L. Leibovici, M. Paul. Colistin: New lessons on an old antibiotic. Clin. Microbiol. Infect. 18: 18–29 (2012).

[42] F. Docobo-Pérez, G.L. Drusano, A. Johnson, J. Goodwin, S. Whalley, V. Ramos-Martín, M. Ballestero-Tellez, J.M. Rodriguez-Martinez, M.C. Conejo, M. Van Guilder, J. Rodríguez-Baño, A. Pascual, W.W. Hope. Pharmacodynamics of fosfomycin: Insights into clinical use for antimicrobial resistance. Antimicrob. Agents Chemother. 59: 5602–5610 (2015).

[43] M. de Cueto, J.R. Hernández, L. López-Cerero, C. Morillo, A. Pascual. In vitro activity of fosfomycin against extended-spectrum-beta-lactamase-producing Escherichia coli and Klebsiella pneumoniae: Comparison of susceptibility testing procedures. Antimicrob. Agents Chemother. 50: 368–370 (2006).

[44] A.S. Michalopoulos, I.G. Livaditis, V. Gougoutas. The revival of fosfomycin. Int. J. Infect. Dis. 15: e732–e739 (2011).

[45] M.E. Falagas, K.P. Giannopoulou, G.N. Kokolakis, P.I. Rafailidis. Fosfomycin: Use beyond urinary tract and gastrointestinal infections. Clin. Infect. Dis. 46: 1069–1077 (2008).

[46] N. Roussos, D.E. Karageorgopoulos, G. Samonis, M.E. Falagas. Clinical significance of the pharmacokinetic and pharmacodynamic characteristics of fosfomycin for the treatment of patients with systemic infections. Int. J. Antimicrob. Agents 34: 506–515 (2009).

[47] M.S. Albur, A. Noel, K. Bowker, A. MacGowan. The combination of colistin and fosfomycin is synergistic against NDM-1-producing Enterobacteriaceae in in vitro pharmacokinetic/ pharmacodynamic model experiments. Int. J. Antimicrob. Agents 46: 560–567 (2015).

[48] C.C. Walsh, M.P. McIntosh, A.Y. Peleg, C.M. Kirkpatrick, P.J. Bergen. In vitro pharmacodynamics of fosfomycin against clinical isolates of Pseudomonas aeruginosa. J. Antimicrob. Chemother. 70: 3042–3050 (2015).

[49] Sandoz. Summary of product characteristics of fosfomycin: Trockensubstanz zur Infusionszubereitung. (2015). https://studylibde.com/doc/9744501/1.3.1-fachinformation--zusammenfassung-der---ami-info (last access 03 Jan 2017).

[50] S.L. Parker, F. Frantzeskaki, S.C. Wallis, C. Diakaki, H. Giamarellou, D. Koulenti, I. Karaiskos, J. Lipman, G. Dimopoulos, J.A. Roberts. Population pharmacokinetics of fosfomycin in critically ill patients. Antimicrob. Agents Chemother. 59: 6471–6476 (2015).

[51] S. Sastry, Y. Doi. Fosfomycin: Resurgence of an old companion. J. Infect. Chemother. 22: 273–280 (2016).

[52] G.L. Drusano, A. Louie. Optimization of aminoglycoside therapy. Antimicrob. Agents Chemother. 55: 2528–2531 (2011).

[53] M. Zhu, W.J. Burman, G.S. Jaresko, S.E. Berning, R.W. Jelliffe, C.A. Peloquin. Population pharmacokinetics of intravenous and intramuscular streptomycin in patients with tuberculosis. Pharmacotherapy 21: 1037–1045 (2001).

[54] B. Springer, Y.G. Kidan, K. Ellrott, E.C. Böttger, T. Prammananan, E.C. Bo. Mechanisms of streptomycin resistance: Selection of mutations in the 16S rRNA gene conferring. Antimicrob. Agents Chemother. 45: 2877–2884 (2001).

[55] R.E.W. Hancock, A. Nijnik, D.J. Philpott. Modulating immunity as a therapy for bacterial infections. Nat. Rev. Microbiol. 10: 243–254 (2012).

[56] R. Pryor, F. Cabreiro. Repurposing metformin: An old drug with new tricks in its binding pockets. Biochem. J. 471: 307–322 (2015).

[57] W.R.A. Patkee, G. Carr, E.H. Baker, D.L. Baines, J.P. Garnett. Metformin prevents the effects of Pseudomonas aeruginosa on airway epithelial tight junctions and restricts hyperglycaemia-induced bacterial growth. J. Cell. Mol. Med. 20: 758–764 (2016).

[58] J.P. Garnett, E.H. Baker, S. Naik, J.A. Lindsay, G.M. Knight, S. Gill, J.S. Tregoning, D.L. Baines. Metformin reduces airway glucose permeability and hyperglycaemia-induced Staphylococcus aureus load independently of effects on blood glucose. Thorax 68: 835–45 (2013).

[59] E.L. Pearce, M.C. Walsh, P.J. Cejas, G.M. Harms, H. Shen, S. Wang, R.G. Jones, Y. Choi. Enhancing CD8 T cell memory by modulating fatty acid metabolism. Nature 460: 103–107 (2010).

[60] K. Araki, A.P. Turner, V.O. Shaffer, S. Gangappa, S.A. Keller, M.F. Bachmann, C.P. Larsen, R. Ahmed. mTOR regulates memory CD8 T-cell differentiation. Nature 460: 108–12 (2009).

[61] Y. Nakamaru, Y. Hayashi, M. Davies, H.J. Heuer, N. Hisanaga, K. Akimoto. Investigation of potential pharmacokinetic interactions between teneligliptin and metformin in steady-state conditions in healthy adults. Clin. Ther. 37: 2007–2018 (2015).

[62] J. Zack, J. Berg, A. Juan, N. Pannacciulli, M. Allard, M. Gottwald, H. Zhang, Y. Shao, O. Ben-Yehuda, P. Jochelson. Pharmacokinetic drug-drug interaction study of ranolazine and metformin in subjects with type 2 diabetes mellitus. Clin. Pharmacol. Drug Dev. 4: 121–129 (2015).

[63] Merck Serono GmbH. Summary of product characteristics of Glucophage® 500 mg / 850 mg / 1000 mg. (2015). https://www.fachinfo.de/pdf/000959 (last access 02 Aug 2016).

[64] P. Baldrick, D. Richardson, G. Elliott, A.W. Wheeler. Safety evaluation of monophosphoryl lipid A (MPL): An immunostimulatory adjuvant. Regul. Toxicol. Pharmacol. 35: 398–413 (2002).

[65] GlaxoSmithKline. Summary of product characteristics of Fendrix®. (2014). https://www.fachinfo.de/api/fachinfo/pdf/013154 (last access 13 Apr 2020).

[66] GlaxoSmithKline. Summary of product characteristics of Cervarix®. (2019). https://www.fachinfo.de/api/fachinfo/pdf/010508 (last access 13 Apr 2020).

[67] S. Hamdy, A. Haddadi, V. Somayaji, D. Ruan, J. Samuel. Pharmaceutical analysis of synthetic lipid A-based vaccine adjuvants in poly (d,l-lactic-co-glycolic acid) nanoparticle formulations. J. Pharm. Biomed. Anal. 44: 914–923 (2007).

[68] A. Kilar, A. Dörnyei, B. Kocsis. Structural characterization of bacterial lipopolysaccharides with mass spectrometry and on- and off-line separation techniques. Mass Spectrom. Rev. 32: 90–117 (2013).

[69] J.K. Bohannon, A. Hernandez, P. Enkhbaatar, W.L. Adams. The immunobiology of TLR4 agonists: From endotoxin tolerance to immunoadjuvants. Shock 40: 451–462 (2013).

[70] C.R. Casella, T.C. Mitchell. Putting endotoxin to work for us: Monophosphoryl lipid A as a safe and effective vaccine adjuvant. Cell. Mol. Life Sci. 65: 3231–3240 (2008).

[71] C.R.H. Raetz, T.A. Garrett, C.M. Reynolds, W.A. Shaw, J.D. Moore, D.C. Smith, A.A. Ribeiro, R.C. Murphy, R.J. Ulevitch, C. Fearns, D. Reichart, C.K. Glass, C. Benner, S. Subramaniam, R. Harkewicz, R.C. Bowers-Gentry, M.W. Buczynski, J.A. Cooper, R.A. Deems, E.A. Dennis. Kdo2-Lipid A of Escherichia coli, a defined endotoxin that activates macrophages via TLR-4. J. Lipid Res. 47: 1097–1111 (2006).

[72] B. Wang, Y. Han, Y. Li, Y. Li, X. Wang. Immuno-stimulatory activity of Escherichia coli mutants producing Kdo2-monophosphoryl-lipid A or Kdo2-pentaacyl-monophosphoryl-lipid A. PLoS One 10: e0144714 (2015).

[73] A. Hernandez, J.K. Bohannon, L. Luan, B.A. Fensterheim, Y. Guo, N.K. Patil, C. McAdams, J. Wang, E.R. Sherwood. The role of MyD88- and TRIF-dependent signaling in monophosphoryl lipid A-induced expansion and recruitment of innate immunocytes. J. Leukoc. Biol. 100: 1311–1322 (2016).

[74] V. Mata-Haro, C. Cekic, M. Martin, P.M. Chilton, C.R. Casella, T.C. Mitchell. The vaccine adjuvant monophosphoryl lipid A as a TRIF-biased agonist of TLR4. Science 316: 1628–1633 (2007).

[75] P.M. Chilton, C.A. Embry, T.C. Mitchell. Effects of differences in lipid A structure on TLR4 pro-inflammatory signaling and inflammasome activation. Front. Immunol. 3: 154 (2012).

[76] D. Liu, B.X. Zeng, S.H. Zhang, S.L. Yao. Rosiglitazone, an agonist of peroxisome proliferator-activated receptor γ, reduces pulmonary inflammatory response in a rat model of endotoxemia. Inflamm. Res. 54: 464–470 (2005).

[77] M.M. Masadeh, N.M. Mhaidat, S.I. Al-Azzam, K.H. Alzoubi. Investigation of the antibacterial activity of pioglitazone. Drug Des. Devel. Ther. 5: 421–425 (2011).

[78] C. Mueller, V. Weaver, J.P. Vanden Heuvel, A. August, M.T. Cantorna. Peroxisome proliferator-activated receptor y ligands attenuate immunological symptoms of experimental allergic asthma. Arch. Biochem. Biophys. 418: 186–196 (2003).

[79] R.C. Reddy, V.G. Keshamouni, S.H. Jaigirdar, X. Zeng, T. Leff, V.J. Thannickal, T.J. Standiford. Deactivation of murine alveolar macrophages by peroxisome proliferator-activated receptor-y ligands. Am. J. Physiol. Lung Cell. Mol. Physiol. 286: L613–L619 (2004).

[80] R.F. Fernandez-Boyanapalli, S.C. Frasch, S.M. Thomas, K.C. Malcolm, M. Nicks, R.J. Harbeck, C. V. Jakubzick, R. Nemenoff, P.M. Henson, S.M. Holland, D.L. Bratton. Pioglitazone restores phagocyte mitochondrial oxidants and bactericidal capacity in chronic granulomatous disease. J. Allergy Clin. Immunol. 135: 517–527 (2015).

[81] K. Katayama, R. Kumagai, M. Isono, K. Fujihara, H. Yagyu, G. Ohara, K. Kagohashi, H. Satoh. Pioglitazone-induced pulmonary injury in a very elderly patient. Intern. Med. 55: 1779–1782 (2016).

[82] J.M.G. Wearn, M. V. Crisman, J.L. Davis, R.J. Geor, D.R. Hodgson, J.K. Suagee, M. Ashraf-Khorassani, L.J. McCutcheon. Pharmacokinetics of pioglitazone after multiple oral dose administration in horses. J. Vet. Pharmacol. Ther. 34: 252–258 (2011).

[83] K. Budde, H.-H. Neumayer, L. Fritsche, W. Sulowicz, T. Stompôr, D. Eckland. The pharmacokinetics of pioglitazone in patients with impaired renal function. Br. J. Clin. Pharmacol. 55: 368–74 (2003).

[84] M.L. Christensen, B. Meibohm, E.V. Capparelli, P. Velasquez-Mieyer, G.A. Burghen, W.V. Tamborlane. Single- and multiple-dose pharmacokinetics of pioglitazone in adolescents with type 2 diabetes. J. Clin. Pharmacol. 45: 1137–1144 (2005).

[85] European Medicines Agency. Guideline on the use of pharmacokinetics and pharmacodynamics in the development of antibacterial medicinal products. (2016). https://www.ema.europa.eu/en/documents/scientific-guideline/guideline-use-pharmacokinetics-pharmacodynamics-development-antimicrobial-medicinal-products_en.pdf (last access 07 Apr 2020).

[86] M. Zhao, A.J. Lepak, D.R. Andes. Animal models in the pharmacokinetic/pharmacodynamic evaluation of antimicrobial agents. Bioorganic Med. Chem. 24: 6390–6400 (2016).

[87] Janvier Labs. Price catalogue. (2017). http://www.janvier-labs.com (last access 07 Mar 2019).

[88] Joel Owen, Jill Fiedler-Kelly (eds.). Introduction to population pharmacokinetic/pharmacodynamic analysis with nonlinear mixed effects models. John Wiley & Sons, Inc, Hoboken, 1st ed. (2014).

[89] Stavros Kromidas (ed.). Das HPLC-MS-Buch für Anwender. Wiley-VCH Verlag GmbH & Co. KGaA, Weinheim, 1st ed. (2017).

[90] M. Balouiri, M. Sadiki, S.K. Ibnsouda. Methods for in vitro evaluating antimicrobial activity: A review. J. Pharm. Anal. 6: 71–79 (2016).

[91] Clinical and Laboratory Standards Institute. Methods for dilution antimicrobial susceptibility tests for bacteria that grow aerobically: Approved standard-ninth edition. M07-A9. CLSI Doc. M07-A9 (2012).

[92] The European Committee on Antimicrobial Susceptibility Testing. Breakpoint tables for interpretation of MICs and zone diameters. Version 10.0. (2020). http://www.eucast.org (last access 22 Feb 2020).

[93] S.G. Wicha, M.G. Kees, J. Kuss, C. Kloft. Pharmacodynamic and response surface analysis of linezolid or vancomycin combined with meropenem against Staphylococcus aureus. Pharm. Res. 32: 2410–2418 (2015).

[94] M. Müller, A. Dela Peña, H. Derendorf. Issues in pharmacokinetics and pharmacodynamics of anti-infective agents: Kill curves versus MIC. Antimicrob. Agents Chemother. 48: 369–377 (2004).

[95] F. de Velde, J.W. Mouton, B.C.M. de Winter, T. van Gelder, B.C.P. Koch. Clinical applications of population pharmacokinetic models of antibiotics: Challenges and perspectives. Pharmacol. Res. 134: 280–288 (2018).

[96] J.W. Mouton, M.N. Dudley, O. Cars, H. Derendorf, G.L. Drusano. Standardization of pharmacokinetic/pharmacodynamic (PK/PD) terminology for anti-infective drugs: An update. J. Antimicrob. Chemother. 55: 601–607 (2005).

[97] C. Rathi, R.E. Lee, B. Meibohm. Translational PK/PD of anti-infective therapeutics. Drug Discov Today Technol. 21–22: 41–49 (2016).

[98] S.G. Wicha, C. Chen, O. Clewe, U.S.H. Simonsson. A general pharmacodynamic interaction model identifies perpetrators and victims in drug interactions. Nat. Commun. 8: 2129 (2017).

[99] M. Danhof, E.C.M. de Lange, O.E. Della Pasqua, B.A. Ploeger, R.A. Voskuyl. Mechanism-

based pharmacokinetic-pharmacodynamic (PK-PD) modeling in translational drug research. Trends Pharmacol. Sci. 29: 186–191 (2008).

[100] D.D. Khan, P. Lagerbäck, S. Cao, U. Lustig, E.I. Nielsen, O. Cars, D. Hughes, D.I. Andersson, L.E. Friberg. A mechanism-based pharmacokinetic/pharmacodynamic model allows prediction of antibiotic killing from MIC values for WT and mutants. J. Antimicrob. Chemother. 70: 3051–3060 (2015).

[101] E.I. Nielsen, L.E. Friberg. Pharmacokinetic-pharmacodynamic modeling of antibacterial drugs. Pharmacol. Rev. 65: 1053–1090 (2013).

[102] E.I. Nielsen, O. Cars, L.E. Friberg. Pharmacokinetic/pharmacodynamic (PK/PD) indices of antibiotics predicted by a semimechanistic PKPD model: A step toward model-based dose optimization. Antimicrob. Agents Chemother. 55: 4619–4630 (2011).

[103] C. Kloft, M.N. Trame, C.A. Ritter. Systems pharmacology in drug development and therapeutic use - A forthcoming paradigm shift. Eur. J. Pharm. Sci. 94: 1–3 (2016).

[104] S.G. Wicha, W. Huisinga, C. Kloft. Translational pharmacometric evaluation of typical antibiotic broad-spectrum combination therapies against Staphylococcus aureus exploiting in vitro information. CPT Pharmacometrics Syst. Pharmacol. 6: 515–522 (2017).

[105] C.B. Landersdorfer, M. Kinzig, J.B. Bulitta, F.F. Hennig, U. Holzgrabe, F. Sörgel, J. Gusinde. Bone penetration of amoxicillin and clavulanic acid evaluated by population pharmacokinetics and Monte Carlo simulation. Antimicrob. Agents Chemother. 53: 2569–2578 (2009).

[106] Organisation for Economic Co-operation and Development. Guideline for the testing of chemicals. (2013). http://biotecnologiebt.com/guide/OECD_227.pdf (last access 20 Sep 2016).

[107] P.G. Engelkirk, J. Duben-Engelkirk (eds.). Burton's microbiology for the health sciences. Lippincott Williams & Wilkins, a Wolters Kluwer business, Baltimore, 9th ed. (2011).

[108] R.J. Keizer, M. van Benten, J.H. Beijnen, J.H.M. Schellens, A.D.R. Huitema. Pirana and PCluster: A modeling environment and cluster infrastructure for NONMEM. Comput. Methods Programs Biomed. 101: 72–79 (2011).

[109] L. Lindbom, P. Pihlgren, N. Jonsson. PsN-Toolkit - A collection of computer intensive statistical methods for non-linear mixed effect modeling using NONMEM. Comput. Methods Programs Biomed. 79: 241–257 (2005).

[110] S.G. Wicha. Integrated in vitro and in silico studies for optimisation of broad-spectrum antibiotic combination therapy. Freie Universität Berlin. (2015).

[111] E.O. King, M.K. Ward, D.E. Raney. Two simple media for the demonstration of pyocyanin and fluorescin. J. Lab. Clin. Med. 44: 301–307 (1954).

[112] The European Committee on Antimicrobial Susceptibility Testing. Media preparation for EUCAST disk diffusion testing and for determination of MIC values by the broth microdilution method. (2014). http://www.eucast.org (last access 05 Oct 2016).

[113] G. Fejer, M.D. Wegner, I. Györy, I. Cohen, P. Engelhard, E. Voronov, T. Manke, Z. Ruzsics, L. Dölken, O. Prazeres da Costa, N. Branzk, M. Huber, A. Prasse, R. Schneider, R.N. Apte, C. Galanos, M.A. Freudenberg. Nontransformed, GM-CSF-dependent macrophage lines are a unique model to study tissue macrophage functions. Proc. Natl. Acad. Sci. 110: E2191-8 (2013).

[114] B. Herigstad, M. Hamilton, J. Heersink. How to optimize the drop plate method for enumerating bacteria. J. Microbiol. Methods 44: 121–129 (2001).

[115] H. Naghili, H. Tajik, K. Mardani, S.M. Razavi Rouhani, A. Ehsani, P. Zare. Validation of drop plate technique for bacterial enumeration by parametric and nonparametric tests. Vet. Res. Forum 4: 179–183 (2013).

[116] H. Grimm. In vitro investigations with fosfomycin on Mueller-Hinton agar with and without glucose-6-phosphate. Infection 7: 256–259 (1979).

[117] M. Tao, J.K. Wang, Y. Wang. Solubilities of pioglitazone hydrochloride in different solvents. J. Chem. Eng. Data 56: 2710–2713 (2011).

[118] C.A. Sutherland, D.P. Nicolau. To add or not to add polysorbate 80: Impact on colistin MICs for clinical strains of Enterobacteriaceae and Pseudomonas aeruginosa and quality controls. J. Clin. Microbiol. 52: 3810 (2014).

[119] M. Karvanen. Optimization of colistin dosage in the treatment of multiresistant Gram-negative infections. Uppsala Universitet. (2013).

[120] G.M. Eliopoulos, C.T. Eliopoulos. Antibiotic combinations : Should they be tested? Clin. Microbiol. Rev. 1: 139–156 (1988).

[121] European Medicines Agency. Guideline on bioanalytical method validation. (2011). https://www.ema.europa.eu/en/documents/scientific-guideline/guideline-bioanalytical-method-validation_en.pdf (last access 28 Oct 2016).

[122] B. Davies, T. Morris. Physiological parameters in laboratory animals and humans. Pharm. Res. 10: 1093–1095 (1993).

[123] International Conference on Harmonisation. ICH harmonised tripartite guideline - Validation of analytical procedures: Text and methodology Q2(R1). (2005). http://academy.gmp-compliance.org/guidemgr/files/Q2(R1).pdf. (last access 16 Jul 2018)

[124] F. Casilag, L. Matarazzo, S. Franck, M. Figeac, R. Michelet, C. Kloft, C. Carnoy, J.-C. Sirard. The biosynthetic monophosphoryl lipid A enhances the therapeutic outcome of antibiotic therapy in pneumococcal pneumonia. ACS Infect. Dis. doi: 10.1021/acsinfectdis.1c00176 (2021).

[125] S. Duwal, M. von Kleist. Top-down and bottom-up modeling in system pharmacology to understand clinical efficacy: An example with NRTIs of HIV-1. Eur. J. Pharm. Sci. 94: 72–83 (2016).

[126] Peter L. Bonate (ed.). Pharmacokinetic-pharmacodynamic modeling and simulation. Springer Science+Business Media, LLC, New York, 2nd ed. (2011).

[127] S.G. Wicha, C. Kloft. Quantitative systems pharmacology in model-informed drug development and therapeutic use. Curr. Opin. Syst. Biol. 10: 19–25 (2018).

[128] D.R. Mould, R.N. Upton. Basic concepts in population modeling, simulation, and model-based drug development. CPT Pharmacometrics Syst. Pharmacol. 1: e6 (2012).

[129] L.B. Sheiner, S.L. Beal. Evaluation of methods for estimating population pharmacokinetic parameters. I. Michaelis-menten model: Routine clinical pharmacokinetic data. J. Pharmacokinet. Biopharm. 8: 553–571 (1980).

[130] L.B. Sheiner, S.L. Beal. Evaluation of methods for estimating population pharmacokinetic parameters. II. Biexponential model and experimental pharmacokinetic data. J. Pharmacokinet. Biopharm. 9: 635–651 (1981).

[131] L.B. Sheiner, S.L. Beal. Evaluation of methods for estimating population pharmacokinetic parameters. III. Monoexponential model: Routine clinical pharmacokinetic data. J. Pharmacokinet. Biopharm. 11: 303–319 (1983).

[132] D.R. Mould, R.N. Upton. Basic concepts in population modeling, simulation, and model-based drug development - Part 2: Introduction to pharmacokinetic modeling methods. CPT Pharmacometrics Syst. Pharmacol. 2: e38 (2013).

[133] S.L. Beal, L.B. Sheiner, A.J. Boeckmann. NONMEM User's Guide, Part V. Introductory Guide. ICON Dev. Solut. Ellicott City, MD, USA. (2011).

[134] R.N. Upton, D.R. Mould. Basic concepts in population modeling, simulation, and model-based drug development - Part 3: Introduction to pharmacodynamic modeling methods. CPT Pharmacometrics Syst. Pharmacol. 3: e88 (2014).

[135] E.I. Ette, A.W. Kelman, C.A. Howie, B. Whiting. Analysis of animal pharmacokinetic data: Performance of the one point per animal design. J. Pharmacokinet. Biopharm. 23: 551–566 (1995).

[136] J.P. Hing, S.G. Woolfrey, D. Greenslade, P.M.C. Wright. Is mixed effects modeling or naive pooled data analysis preferred for the interpretation of single sample per subject toxicokinetic data? J. Pharmacokinet. Pharmacodyn. 28: 193–210 (2001).

[137] R.J. Bauer. NONMEM Tutorial Part II: Estimation Methods and Advanced Examples. CPT Pharmacometrics Syst. Pharmacol. 8: 538–556 (2019).

[138] K.-S. Bae, D.-S. Yim. R-based reproduction of the estimation process hidden behind NONMEM Part 2: First-order conditional estimation. Transl. Clin. Pharmacol. 24: 161–168 (2016).

[139] R.J. Bauer, S. Guzy, C. Ng. A survey of population analysis methods and software for complex pharmacokinetic and pharmacodynamic models with examples. AAPS J. 9: E60–E83 (2007).

[140] S.L. Beal. Ways to fit a PK model with some data below the quantification limit. J. Pharmacokinet. Pharmacodyn. 28: 481–504 (2001).

[141] M. Bergstrand, M.O. Karlsson. Handling data below the limit of quantification in mixed effect models. AAPS J. 11: 371–380 (2009).

[142] L.B. Sheiner, D.R. Stanski, S. Vozeh, R.D. Miller, J. Ham. Simultaneous modeling of pharmacokinetics and pharmacodynamics: Application to D-tubocurarine. Clin. Pharmacol. Ther. 25: 358–371 (1979).

[143] L. Zhang, S.L. Beal, L.B. Sheiner. Simultaneous vs. sequential analysis for population PK/PD data I: Best-case performance. J. Pharmacokinet. Pharmacodyn. 30: 387–404 (2003).

[144] P. Schober, T.R. Vetter. Survival analysis and interpretation of time-to-event data: The tortoise and the hare. Anesth. Analg. 127: 792–798 (2018).

[145] John P. Klein, Melvin L. Moeschberger (eds.). Survival analysis: Techniques for censored and truncated data. Springer-Verlag Inc., New York, 2nd ed. (2013).

[146] N. Holford. A time to event tutorial for pharmacometricians. CPT Pharmacometrics Syst. Pharmacol. 2: e43 (2013).

[147] K. Nurzyńska, R.P. Austin, P.M. Fischer, J. Booth, F. Gommer. Survival of the fittest: Time-to-event modeling of crystallization of amorphous poorly soluble drugs. J. Pharm. Sci. 105: 1858–1866 (2016).

[148] R.V. Juul, J. Nyberg, T.M. Lund, S. Rasmussen, M. Kreilgaard, L.L. Christrup, U.S.H. Simonsson. A pharmacokinetic-pharmacodynamic model of morphine exposure and subsequent morphine consumption in postoperative pain. Pharm. Res. 33: 1093–1103 (2016).

[149] E.K. Hansson, M.A. Amantea, P. Westwood, P.A. Milligan, B.E. Houk, J. French, M.O. Karlsson, L.E. Friberg. PKPD modeling of VEGF, sVEGFR-2, sVEGFR-3, and sKIT as predictors of tumor dynamics and overall survival following sunitinib treatment in GIST. CPT Pharmacometrics Syst. Pharmacol. 2: e84 (2013).

[150] David Collett (ed.). Modelling survival data in medical research. Chapman & Hall/crc, London, 2nd ed. (2003).

[151] Y. Wang, C. Sung, C. Dartois, R. Ramchandani, B.P. Booth, E. Rock, J. Gobburu. Elucidation of relationship between tumor size and survival in non-small-cell lung cancer patients can aid early decision making in clinical drug development. Clin. Pharmacol. Ther. 86: 167–174 (2009).

[152] P.J. Zufferey, E. Ollier, X. Delavenne, S. Laporte, P. Mismetti, S.B. Duffull. Incidence and risk factors of major bleeding following major orthopaedic surgery with fondaparinux thromboprophylaxis. A time-to-event analysis. Br. J. Clin. Pharmacol. 84: 2242–2251 (2018).

[153] E.L. Plan, G. Ma, M. Nagard, J. Jensen, M.O. Karlsson. Transient lower esophageal sphincter

relaxation pharmacokinetic-pharmacodynamic modeling: Count model and repeated time-to-event model. J. Pharmacol. Exp. Ther. 339: 878–885 (2011).

[154] E. Chigutsa, K. Patel, P. Denti, M. Visser, G. Maartens, C.M.J. Kirkpatrick, H. McIlleron, M.O. Karlsson. A time-to-event pharmacodynamic model describing treatment response in patients with pulmonary tuberculosis using days to positivity in automated liquid mycobacterial culture. Antimicrob. Agents Chemother. 57: 789–795 (2013).

[155] E. Schindler, M.A. Amantea, M.O. Karlsson, L.E. Friberg. PK-PD modeling of individual lesion FDG-PET response to predict overall survival in patients with sunitinib-treated gastrointestinal stromal tumor. CPT Pharmacometrics Syst. Pharmacol. 5: 173–181 (2016).

[156] A.K. Frobel, M.O. Karlsson, J.T. Backman, K. Hoppu, E. Qvist, P. Seikku, H. Jalanko, C. Holmberg, R.J. Keizer, S. Fanta, S. Jönsson. A time-to-event model for acute rejections in paediatric renal transplant recipients treated with ciclosporin A. Br. J. Clin. Pharmacol. 76: 603–615 (2013).

[157] H. Akaike. A new look at the statistical model identification. IEEE Trans. Automat. Contr. 19: 716–723 (1974).

[158] B. Efron, R. Tibshirani. Bootstrap methods for standard errors, confidence intervals, and other measures of statistical accuracy. Stat. Sci. 1: 54–77 (1986).

[159] T.H.T. Nguyen, M.S. Mouksassi, N. Holford, N. Al-Huniti, I. Freedman, A.C. Hooker, J. John, M.O. Karlsson, D.R. Mould, J.J. Perez Ruixo, E.L. Plan, R. Savic, J.G.C. Van Hasselt, B. Weber, C. Zhou, E. Comets, F. Mentre. Model evaluation of continuous data pharmacometric models: Metrics and graphics. CPT Pharmacometrics Syst. Pharmacol. 6: 87–109 (2017).

[160] R.J. Keizer, R.S. Jansen, H. Rosing, B. Thijssen, J.H. Beijnen, J.H.M. Schellens, A.D.R. Huitema. Incorporation of concentration data below the limit of quantification in population pharmacokinetic analyses. Pharmacol. Res. Perspect. 3: 1–15 (2015).

[161] M. Bergstrand, A.C. Hooker, J.E. Wallin, M.O. Karlsson. Prediction-corrected visual predictive checks for diagnosing nonlinear mixed-effects models. AAPS J. 13: 143–151 (2011).

[162] W. Treyaprasert, S. Schmidt, K.H. Rand, U. Suvanakoot, H. Derendorf. Pharmacokinetic/pharmacodynamic modeling of in vitro activity of azithromycin against four different bacterial strains. Int. J. Antimicrob. Agents 29: 263–270 (2007).

[163] K. Ozawa, H. Minami, H. Sato. Population pharmacokinetic and pharmacodynamic analysis for time courses of docetaxel-induced neutropenia in Japanese cancer patients. Cancer Sci. 98: 1985–1992 (2007).

[164] T. Sasaki, H. Takane, K. Ogawa, S. Isagawa, T. Hirota, S. Higuchi, T. Horii, K. Otsubo, I. Ieiri. Population pharmacokinetic and pharmacodynamic analysis of linezolid and a hematologic side effect, thrombocytopenia, in Japanese patients. Antimicrob. Agents Chemother. 55: 1867–1873 (2011).

[165] D.E. Mager, W.J. Jusko. Pharmacodynamic modeling of time-dependent transduction systems. Clin. Pharmacol. Ther. 70: 210–216 (2001).

[166] R.M. Savic, D.M. Jonker, T. Kerbusch, M.O. Karlsson. Implementation of a transit compartment model for describing drug absorption in pharmacokinetic studies. J. Pharmacokinet. Pharmacodyn. 34: 711–726 (2007).

[167] F.J. Richards. A flexible growth constant for empirical use. J. Exp. Bot. 10: 290–300 (1959).

[168] W.R. Greco, G. Bravo, J.C. Parsons. The search for synergy: A critical review from a response surface perspective. Pharmacol. Rev. 47: 332–385 (1995).

[169] S.G. Wicha, O. Clewe, R.J. Svensson, S.H. Gillespie, Y. Hu, A.R.M. Coates, U.S.H. Simonsson. Forecasting clinical dose–response from preclinical studies in tuberculosis research: Translational predictions with rifampicin. Clin. Pharmacol. Ther. 104: 1208–1218 (2018).

[170] I. Mahmood. Misconceptions and issues regarding allometric scaling during the drug development process. Expert Opin. Drug Metab. Toxicol. 14: 843–854 (2018).

[171] I. Mahmood, J.D. Balian. The pharmacokinetic principles behind scaling from preclinical results to phase I protocols. Clin. Pharmacokinet. 36: 1–11 (1999).

[172] Y. Huh, D.E. Smith, M. Rose Feng. Interspecies scaling and prediction of human clearance: Comparison of small- and macro-molecule drugs. Xenobiotica 41: 972–987 (2011).

[173] W. Huang, L. Geng, R. Deng, S. Lu, G. Ma, J. Yu, J. Zhang, W. Liu, T. Hou, X. Lu. Prediction of human clearance based on animal data and molecular properties. Chem. Biol. Drug Des. 86: 990–997 (2015).

[174] L. Kagan, A.K. Abraham, J.M. Harrold, D.E. Mager. Interspecies scaling of receptor-mediated pharmacokinetics and pharmacodynamics of type I interferons. Pharm. Res. 27: 920–932 (2010).

[175] S.W. Paine, K. Ménochet, R. Denton, D.F. McGinnity, R.J. Riley. Prediction of human renal clearance from preclinical species for a diverse set of drugs that exhibit both active secretion and net reabsorption. Drug Metab. Dispos. 39: 1008–1013 (2011).

[176] K.P. Zuideveld, P.H. Van Der Graaf, L.A. Peletier, M. Danhof. Allometric scaling of pharmacodynamic responses: Application to 5-HT 1A receptor mediated responses from rat to man. Pharm. Res. 24: 2031–2039 (2007).

[177] Q. Huang, J.E. Riviere. The application of allometric scaling principles to predict pharmacokinetic parameters across species. Expert Opin. Drug Metab. Toxicol. 10: 1241–1253 (2014).

[178] Jürgen Groß (ed.). Grundlegende Statistik mit R. Vieweg+Teubner Verlag, Springer, Berlin, 1st ed. (2010).

[179] S. Franck, T. Fuhrmann-Selter, J.F. Joseph, R. Michelet, F. Casilag, J.-C. Sirard, S.G. Wicha, C. Kloft. A rapid, simple and sensitive liquid chromatography tandem mass spectrometry assay to determine amoxicillin concentrations in biological matrix of little volume. Talanta 201: 253–258 (2019).

[180] P. Moine, J.X. Mazoit. Streptococcus pneumoniae pneumonia in mice: Optimal amoxicillin dosing predicted from a pharmacokinetic-pharmacodynamic model. J. Pharmacol. Exp. Ther. 291: 1086–1092 (1999).

[181] S.K.B. Sy, H. Derendorf. Pharmacometrics in bacterial infections. In: Stephan Schmidt, Hartmut Derendorf (eds.). Applied pharmacometrics. Springer, New York, 1st ed.: 229–258 (2014).

[182] F. de Velde, B.C.M. de Winter, B.C.P. Koch, T. van Gelder, J.W. Mouton. Non-linear absorption pharmacokinetics of amoxicillin: Consequences for dosing regimens and clinical breakpoints. J. Antimicrob. Chemother. 71: 2909–2917 (2016).

[183] M. Li, M.A. Andrew, J. Wang, D.H. Salinger, P. Vicini, R.W. Grady, B. Phillips, D.D. Shen, G.D. Anderson. Effects of cranberry juice on pharmacokinetics of β-lactam antibiotics following oral administration. Antimicrob. Agents Chemother. 53: 2725–2732 (2009).

[184] D.A. Spyker, R.J. Rugloski, R.L. Vann, W.M.O. Brien. Pharmacokinetics of amoxicillin: Dose dependence after intravenous, oral, and intramuscular administration. Antimicrob. Agents Chemother. 11: 132–141 (1977).

[185] S.H. Webster, E.J. Liljegren. Organ: Body-weight ratios for certain organs of laboratory animals - White Swiss mouse. Am. J. Anat. 97: 129–153 (1955).

[186] T. Baba, T. Bae, O. Schneewind, F. Takeuchi, K. Hiramatsu. Genome sequence of Staphylococcus aureus strain newman and comparative analysis of staphylococcal genomes: Polymorphism and evolution of two major pathogenicity islands. J. Bacteriol. 190: 300–310 (2008).

[187] L.A.S. Kirkham, J.M.C. Jefferies, A.R. Kerr, Y. Jing, S.C. Clarke, A. Smith, T.J. Mitchell.

Identification of invasive serotype 1 pneumococcal isolates that express nonhemolytic pneumolysin. J. Clin. Microbiol. 44: 151–159 (2006).

[188] S. Sutton. The limitations of CFU: Compliance to CGMP requires good science. J. GXP compliance 16: 74–80 (2012).

[189] S. Clais, G. Boulet, M. Van Kerckhoven, E. Lanckacker, P. Delputte, L. Maes, P. Cos. Comparison of viable plate count, turbidity measurement and real-time PCR for quantification of Porphyromonas gingivalis. Lett. Appl. Microbiol. 60: 79–84 (2015).

[190] R. Lindqvist. Estimation of Staphylococcus aureus growth parameters from turbidity data: Characterization of strain variation and comparison of methods. Appl. Environ. Microbiol. 72: 4862–4870 (2006).

[191] P. Dalgaard, K. Koutsoumanis. Comparison of maximum specific growth rates and lag times estimated from absorbance and viable count data by different mathematical models. J. Microbiol. Methods 43: 183–196 (2001).

[192] G. Regev-Yochay, K. Trzcinski, C.M. Thompson, M. Lipsitch, R. Malley. SpxB is a suicide gene of Streptococcus pneumoniae and confers a selective advantage in an in vivo competitive colonization model. J. Bacteriol. 189: 6532–6539 (2007).

[193] P. Nicholls. Activity of catalase in the red cell. Biochim. Biophys. Acta 99: 286–297 (1965).

[194] I. Brook. Inoculum effect. Rev. Infect. Dis. 11: 361–368 (1989).

[195] R.L. Bertrand. Lag phase is a dynamic, organized, adaptive, and evolvable period that prepares bacteria for cell division. J. Bacteriol. 201: e00697-18 (2019).

[196] B. Ghajar, A. Harmon. The Effect of DMSO on permeability of staphylococcus aureus. Biochem. Biophys. Res. Commun. 32: 940–944 (1968).

[197] G.E. Pottz, J.H. Rampey, F. Benjamin. The effect of dimethyl sulfoxide (DMSO) on antibiotic sensitivity of a group of medically important microorganisms: Preliminary report. Ann. N. Y. Acad. Sci. 141: 261–72 (1967).

[198] T. Wadhwani, K. Desai. Effect of various solvents on bacterial growth in context of determining MIC of various antimicrobials. Internet J. Microbiol. 7: 1–8 (2009).

[199] L.M. Koeth, J.M. DiFranco-Fisher, S. McCurdy. A reference broth microdilution method for dalbavancin in vitro: Susceptibility testing of bacteria that grow aerobically. J. Vis. Exp. 103: e53028 (2015).

[200] H.S. Sader, P.R. Rhomberg, R.K. Flamm, R.N. Jones. Use of a surfactant (polysorbate 80) to improve MIC susceptibility testing results for polymyxin B and colistin. Diagn. Microbiol. Infect. Dis. 74: 412–414 (2012).

[201] J.A. Hindler, R.M. Humphries. Colistin MIC variability by method for contemporary clinical isolates of multidrug-resistant Gram-negative bacilli. J. Clin. Microbiol. 51: 1678–1684 (2013).

[202] J.M. Schuurmans, A.S. Nuri Hayali, B.B. Koenders, B.H. ter Kuile. Variations in MIC value caused by differences in experimental protocol. J. Microbiol. Methods 79: 44–47 (2009).

[203] J.W. Mouton, A.E. Muller, R. Canton, C.G. Giske, G. Kahlmeter, J. Turnidge. MIC-based dose adjustment: Facts and fables. J. Antimicrob. Chemother. 73: 564–568 (2018).

[204] L.G. Reimer, C.W. Stratton, L.B. Reller. Minimum inhibitory and bactericidal concentrations of 44 antimicrobial agents against three standard control strains in broth with and without human serum. Antimicrob. Agents Chemother. 19: 1050–1055 (1981).

[205] P.J. Bergen, J.B. Bulitta, A. Forrest, B.T. Tsuji, J. Li, R.L. Nation. Pharmacokinetic/ pharmacodynamic investigation of colistin against Pseudomonas aeruginosa using an in vitro model. Antimicrob. Agents Chemother. 54: 3783–3789 (2010).

[206] B. Pfausler, H. Spiss, P. Dittrich, M. Zeitlinger, E. Schmutzhard, C. Joukhadar. Concentrations

of fosfomycin in the cerebrospinal fluid of neurointensive care patients with ventriculostomy-associated ventriculitis. J. Antimicrob. Chemother. 53: 848–852 (2004).

[207] R. Hamoud, J. Reichling, M. Wink. Synergistic antibacterial activity of the combination of the alkaloid sanguinarine with EDTA and the antibiotic streptomycin against multidrug resistant bacteria. J. Pharm. Pharmacol. 67: 264–273 (2015).

[208] R.J. Fass, J. Barnishan. Minimal inhibitory concentrations of 34 antimicrobial agents for control strains Escherichia coli ATCC 25922 and Pseudomonas aeruginosa ATCC 27853. Antimicrob. Agents Chemother. 16: 622–624 (1979).

[209] O. Olajuyigbe, M. Adeoye-Isijola, O. Adedayo. Synergistic potentials of benzylpenicillin, amoxicillin and streptomycin antibiotics against selected bacterial species. Life Sci. J. 13: 37–44 (2016).

[210] S. Schmidt, S.N. Sabarinath, A. Barbour, D. Abbanat, P. Manitpisitkul, S. Sha, H. Derendorf. Pharmacokinetic-pharmacodynamic modeling of the in vitro activities of oxazolidinone antimicrobial agents against methicillin-resistant Staphylococcus aureus. Antimicrob. Agents Chemother. 53: 5039–5045 (2009).

[211] B.E. Ferro, J. Van Ingen, M. Wattenberg, D. Van Soolingen, J.W. Mouton. Time-kill kinetics of antibiotics active against rapidly growing mycobacteria. J. Antimicrob. Chemother. 70: 811–817 (2015).

[212] A.F. Mohamed, O. Cars, L.E. Friberg. A pharmacokinetic/pharmacodynamic model developed for the effect of colistin on Pseudomonas aeruginosa in vitro with evaluation of population pharmacokinetic variability on simulated bacterial killing. J. Antimicrob. Chemother. 69: 1350–1361 (2014).

[213] Z. Yang, H.-R. Xiong. Culture conditions and types of growth media for mammalian cells. In: Luca Ceccherini-Nelli, Barbara Matteoli (eds.). Biomedical Tissue Culture. IntechOpen, London, 1st ed.: 3–18 (2012).

[214] G.U. Meduri, S. Kanangat, J. Stefan, E. Tolley, D. Schaberg. Cytokines IL-1b, IL-6, and TFNa enhance in vitro growth of bacteria. Am. J. Respir. Crit. Care Med. 160: 961–967 (1999).

[215] D. Baldoni, A. Steinhuber, W. Zimmerli, A. Trampuz. In vitro activity of gallium maltolate against Staphylococci in logarithmic, stationary and biofilm growth-phase: Comparison of conventional and calorimetric susceptibility testing methods. Antimicrob. Agents Chemother. 54: 157–163 (2009).

[216] P. Baudoux, N. Bles, S. Lemaire, M.P. Mingeot-Leclercq, P.M. Tulkens, F. Van Bambeke. Combined effect of pH and concentration on the activities of gentamicin and oxacillin against Staphylococcus aureus in pharmacodynamic models of extracellular and intracellular infections. J. Antimicrob. Chemother. 59: 246–253 (2007).

[217] M. Gough, R.E.W. Hancock, N.M. Kelly. Antiendotoxin activity of cationic peptide antimicrobial agents. Infect. Immun. 64: 4922–4927 (1996).

[218] L.G. Garcia, S. Lemaire, B.C. Kahl, K. Becker, R.A. Proctor, O. Denis, P.M. Tulkens, F. Van Bambeke. Antibiotic activity against small-colony variants of staphylococcus aureus: Review of in vitro, animal and clinical data. J. Antimicrob. Chemother. 68: 1455–1464 (2013).

[219] A. Dalhoff. Contribution of immunocompetence to the antibacterial activities of ciprofloxacin and moxifloxacin in an in vitro pharmacodynamic model. Infect. Suppl. 33: 44–49 (2005).

[220] S.E. Evans, B.L. Scott, C.G. Clement, D.T. Larson, D. Kontoyiannis, R.E. Lewis, P.R. Lasala, J. Pawlik, J.W. Peterson, A.K. Chopra, G. Klimpel, G. Bowden, M. Höök, Y. Xu, M.J. Tuvim, B.F. Dickey. Stimulated innate resistance of lung epithelium protects mice broadly against bacteria and fungi. Am. J. Respir. Cell Mol. Biol. 42: 40–50 (2010).

[221] A.J. Miller, J.R. Spence. In vitro models to study human lung development, disease and homeostasis. Physiology 32: 246–260 (2017).

[222] C.V. Montefusco-Pereira, C. de S. Carvalho-Wodarz, J. Seeger, C. Kloft, R. Michelet, C.-M. Lehr. Translating (patho-)physiology by advanced pulmonary cell cultures for the screening and development of new anti-infectives. Drug Discov. Today (2020).

[223] J. Seeger, S. Guenther, K. Schaufler, S.E. Heiden, R. Michelet, C. Kloft. Novel pharmacokinetic/pharmacodynamic parameters quantify the exposure-effect relationship of levofloxacin against fluoroquinolone-resistant Escherichia coli. Antibitotics 10: 615 (2021).

[224] J.K. Bohannon, L. Luan, A. Hernandez, A. Afzal, Y. Guo, N.K. Patil, B. Fensterheim, E.R. Sherwood. Role of G-CSF in monophosphoryl lipid A-mediated augmentation of neutrophil functions after burn injury. J. Leukoc. Biol. 99: 629–640 (2016).

[225] T. Hirano, S. Kodama, T. Kawano, K. Maeda, M. Suzuki. Monophosphoryl lipid A induced innate immune responses via TLR4 to enhance clearance of nontypeable Haemophilus influenzae and Moraxella catarrhalis from the nasopharynx in mice. FEMS Immunol. Med. Microbiol. 63: 407–417 (2011).

[226] A. Roquilly, L. Gautreau, J.P. Segain, P. de Coppet, V. Sebille, C. Jacqueline, J. Caillon, G. Potel, C. Lejus, R. Josien, K. Asehnoune. CpG-ODN and MPLA prevent mortality in a murine model of post-hemorrhage-Staphyloccocus aureus pneumonia. PLoS One 5: e13228 (2010).

[227] C.D. Romero, T.K. Varma, J.B. Hobbs, A. Reyes, B. Driver, E.R. Sherwood. The toll-like receptor 4 agonist monophosphoryl lipid a augments innate host resistance to systemic bacterial infection. Infect. Immun. 79: 3576–3587 (2011).

[228] T.N. Landgraf, F.F. Fernandes, G. Peron, A. Panunto-Castelo. Therapeutic effect of monophosphoryl lipid A administration on Paracoccidioides brasiliensis-infected mice. Med. Mycol. 55: 344–348 (2017).

[229] M.C. Leon-Garcia, E. Rios-Castro, E. Lopez-Romero, M. Cuellar-Cruz. Evaluation of cell wall damage by dimethyl sulfoxide in Candida species. Res. Microbiol. 168: 732–739 (2017).

[230] D. Masopust, C.P. Sivula, S.C. Jameson. Of mice, dirty mice, and men: Using mice to understand human immunology. J Immunol. 199: 383–388 (2017).

[231] E.R. Wickremsinhe, E.J. Perkins. Using dried blood spot sampling to improve data quality and reduce animal use in mouse pharmacokinetic studies. J. Am. Assoc. Lab. Anim. Sci. 54: 139–144 (2015).

[232] J. Mestas, C.C.W. Hughes. Of mice and not men: Differences between mouse and human immunology. J. Immunol. 172: 2731–2738 (2004).

[233] J. Mizgerd, S. Skerrett. Animal models of human pneumonia. Am J Physiol Lung Cell Mol Physiol 294: L387–L398 (2008).

[234] A.F. Hoggatt, J. Hoggatt, M. Honerlaw, L.M. Pelus. A spoonful of sugar helps the medicine go down: A novel technique to improve oral gavage in mice. J. Am. Assoc. Lab. Anim. Sci. 49: 329–334 (2010).

[235] K.-H. Diehl, R. Hull, D. Morton, R. Pfister, Y. Rabemampianina, D. Smith, J.-M. Vidal, C. Van De Vorstenbosch. A good practice guide to the administration of substances and removal of blood, including routes and volumes. J. Appl. Toxicol. 21: 15–23 (2001).

[236] F. Raynaud, J. Roberts, A.T. Henley, M. Richards, C. Thai. Capillary microsampling of mouse blood in early pre-clinical studies: A preferred alternative to dried blood spot sampling. J. Bioanal. Biomed. 8: 028–033 (2016).

[237] G.L. Drusano. Antimicrobial pharmacodynamics: Critical interactions of “bug and drug”. Nat. Rev. Microbiol. 2: 289–300 (2004).

[238] F. Sarti, G. Perera, F. Hintzen, K. Kotti, V. Karageorgiou, O. Kammona, C. Kiparissides, A. Bernkop-Schnürch. In vivo evidence of oral vaccination with PLGA nanoparticles containing the immunostimulant monophosphoryl lipid A. Biomaterials 32: 4052–4057 (2011).

[239] J.-P. Pais de Barros, T. Gautier, W. Sali, C. Adrie, H. Choubley, E. Charron, C. Lalande, N. Le Guern, V. Deckert, M. Monchi, J.-P. Quenot, L. Lagrost. Quantitative lipopolysaccharide analysis using HPLC/MS/MS and its combination with the limulus amebocyte lysate assay. J. Lipid Res. 56: 1363–1369 (2015).

[240] K. Vorauer-Uhl, D. Jeschek, G. Lhota, A. Wagner, S. Strobach, H. Katinger. Simultaneous quantification of complex phospholipid compositions containing monophosphoryl lipid-A by RP-HPLC. J. Liq. Chromatogr. Relat. Technol. 32: 2203–2215 (2009).

[241] S.R. Hagen, J.D. Thompson, D.S. Snyder, K.R. Myers. Analysis of a monophosphoryl lipid A immunostimulant preparation from Salmonella minnesota R595 by high-performance liquid chromatography. J. Chromatogr. A 767: 53–61 (1997).

[242] N. Lindegardh, T. Singtoroj, A. Annerberg, N.J. White, N.P.J. Day. Development and validation of a solid-phase extraction-liquid chromatographic method for determination of amoxicillin in plasma. Ther. Drug Monit. 27: 503–508 (2005).

[243] P. Abgueguen, E. Azoulay-Dupuis, V. Noel, P. Moine, V. Rieux, B. Fantin, J.P. Bedos. Amoxicillin is effective against penicillin-resistant Streptococcus pneumoniae strains in a mouse pneumonia model simulating human pharmacokinetics. Antimicrob. Agents Chemother. 51: 208–214 (2007).

[244] A. Wen, T. Hang, S. Chen, Z. Wang, L. Ding, Y. Tian, M. Zhang, X. Xu. Simultaneous determination of amoxicillin and ambroxol in human plasma by LC-MS/MS: Validation and application to pharmacokinetic study. J. Pharm. Biomed. Anal. 48: 829–834 (2008).

[245] M.J. Ahsman, E.D. Wildschut, D. Tibboel, R.A. Mathot. Microanalysis of β-lactam antibiotics and vancomycin in plasma for pharmacokinetic studies in neonates. Antimicrob. Agents Chemother. 53: 75–80 (2009).

[246] X. Du, C. Li, H.K. Sun, C.H. Nightingale, D.P. Nicolau. A sensitive assay of amoxicillin in mouse serum and broncho-alveolar lavage fluid by liquid-liquid extraction and reversed-phase HPLC. J. Pharm. Biomed. Anal. 39: 648–652 (2005).

[247] W. Li, F. Tan, K. Zhao. Simultaneous determination of amoxicillin and ranitidine in rat plasma by high-performance liquid chromatography. J. Pharm. Biomed. Anal. 41: 594–598 (2006).

[248] B. Lugoboni, T. Gazzotti, E. Zironi, A. Barbarossa, G. Pagliuca. Development and validation of a liquid chromatography/tandem mass spectrometry method for quantitative determination of amoxicillin in bovine muscle. J. Chromatogr. B 879: 1980–1986 (2011).

[249] J.O. Marx, D. Vudathala, L. Murphy, S. Rankin, F.C. Hankenson. Antibiotic administration in the drinking water of mice. J. Am. Assoc. Lab. Anim. Sci. 53: 301–306 (2014).

[250] Q. Pei, G.P. Yang, Z.J. Li, X.D. Peng, J.H. Fan, Z.Q. Liu. Simultaneous analysis of amoxicillin and sulbactam in human plasma by HPLC-DAD for assessment of bioequivalence. J. Chromatogr. B 879: 2000–2004 (2011).

[251] S. Zhang, F. Yang, B. Guo, Y. Chen, X. Wu, W. Liang, Y. Shi, J. Zhang. Development of an liquid chromatography–tandem mass spectrometry method for the determination of amoxicillin in broth medium and its application to an in vitro pharmacokinetic and pharmacodynamic model. J. Chromatogr. Sci. 54: 230–236 (2016).

[252] D. Andes, W.A. Craig. In vivo activities of amoxicillin and amoxicillin-clavulanate against Streptococcus pneumoniae: Application to breakpoint determinations. Antimicrob. Agents Chemother. 42: 2375–2379 (1998).

[253] E. Azoulay-Dupuis, P. Moine, J.P. Bedos, V. Rieux, E. Vallee. Amoxicillin dose-effect relationship with Streptococcus pneumoniae in a mouse pneumonia model and roles of in vitro penicillin susceptibilities, autolysis, and tolerance properties of the strains. Antimicrob. Agents Chemother. 40: 941–946 (1996).

[254] R.J. Boon, A.S. Beale. Response of Streptococcus pyogenes to therapy with amoxicillin or

amoxicillin-clavulanic acid in a mouse model of mixed infection caused by Staphylococcus aureus and Streptococcus pyogenes. Antimicrob. Agents Chemother. 31: 1204–1209 (1987).

[255] J. Gisby, B.J. Wightman, A.S. Beale. Comparative efficacies of ciprofloxacin, amoxicillin, amoxicillin-clavulanic acid, and cefaclor against experimental Streptococcus pneumoniae respiratory infections in mice. Antimicrob. Agents Chemother. 35: 831–836 (1991).

[256] G. Delis, G. Batzias, G. Kounenis, M. Koutsoviti-Papadopoulou. Application and validation of a LC/fluorescence method for the determination of amoxicillin in sheep serum and tissue cage fluid. J. Pharm. Biomed. Anal. 49: 375–380 (2009).

[257] M. Carlier, V. Stove, J.A. Roberts, E. Van De Velde, J.J. De Waele, A.G. Verstraete. Quantification of seven β-lactam antibiotics and two β-lactamase inhibitors in human plasma using a validated UPLC-MS/MS method. Int. J. Antimicrob. Agents 40: 416–422 (2012).

[258] S. Grujic, T. Vasiljevic, M. Lausevic, T. Ast. Study on the formation of an amoxicillin adduct with methanol using electrospray ion trap tandem mass spectrometry. Rapid Commun. mass Spectrom. 22: 67–74 (2008).

[259] J.I.D. Wibawa, D. Fowkes, P.N. Shaw, D.A. Barrett. Measurement of amoxicillin in plasma and gastric samples using high-performance liquid chromatography with fluorimetric detection. J. Chromatogr. B 774: 141–148 (2002).

[260] P. Moine, C. Sauve, E. Vallee, J.P. Bedos, E. Azoulay-Dupuis. In vivo efficacy of cefotaxime and amoxicillin against penicillin-susceptible, penicillin-resistant and penicillin-cephalosporin-resistant strains of Streptococcus pneumoniae in a mouse pneumonia model. Clin. Microbiol. Infect. 3: 608–615 (1997).

[261] M.K. Walker, J.R. Boberg, M.T. Walsh, V. Wolf, A. Trujillo, M.S. Duke, R. Palme, L.A. Felton. A less stressful alternative to oral gavage for pharmacological and toxicological studies in mice. Toxicol Appl Pharmacol 260: 65–69 (2012).

[262] C.P. Jones, K.L. Boyd, J.M. Wallace. Evaluation of mice undergoing serial oral gavage while awake or anesthetized. J. Am. Assoc. Lab. Anim. Sci. 55: 805–810 (2016).

[263] M. Zeitlinger, M. Müller, C. Joukhadar. Lung microdialysis - A powerful tool for the determination of exogenous and endogenous compounds in the lower respiratory tract. AAPS J. 7: E600–E608 (2005).

[264] N. Takahashi, G. Boysen, F. Li, Y. Li, J.A. Swenberg. Tandem mass spectrometry measurements of creatinine in mouse plasma and urine for determining glomerular filtration rate. Kidney Int. 71: 266–271 (2007).

[265] S.R. Dunn, Z. Qi, E.P. Bottinger, M.D. Breyer, K. Sharma. Utility of endogenous creatinine clearance as a measure of renal function in mice. Kidney Int. 65: 1959–1967 (2004).

[266] E.J. Brown, S.W. Hosea, M.M. Frank. The role of the spleen in experimental pneumococcal bacteremia. J. Clin. Invest. 67: 975–982 (1981).

[267] A.M. Burkhardt, A. Zlotnik. Translating translational research: Mouse models of human disease. Cell. Mol. Immunol. 10: 373–374 (2013).

[268] D.G. Lee, Y. Murakami, D.R. Andes, W.A. Craig. Inoculum effects of ceftobiprole, daptomycin, linezolid, and vancomycin with staphylococcus aureus and streptococcus pneumoniae at inocula of 10^5 and 10^7 CFU injected into opposite thighs of neutropenic mice. Antimicrob. Agents Chemother. 57: 1434–1441 (2013).

[269] E. Calbo, J. Garau. Of mice and men: Innate immunity in pneumococcal pneumonia. Int. J. Antimicrob. Agents 35: 107–113 (2009).

[270] R. Porte, D. Fougeron, N. Muñoz-Wolf, J. Tabareau, A.F. Georgel, F. Wallet, C. Paget, F. Trottein, J.A. Chabalgoity, C. Carnoy, J.C. Sirard. A toll-like receptor 5 agonist improves the efficacy of antibiotics in treatment of primary and influenza virus-associated pneumococcal

mouse infections. Antimicrob. Agents Chemother. 59: 6064–6072 (2015).

[271] W.G. Johanson, S.J. Jay, A.K. Pierce. Bacterial growth in vivo. J. Clin. Invest. 53: 1320–1325 (1974).

[272] D. Chiavolini, G. Pozzi, S. Ricci. Animal models of Streptococcus pneumoniae disease. Clin. Microbiol. Rev. 21: 666–685 (2008).

[273] T. Tängdén, V. Ramos Martín, T.W. Felton, E.I. Nielsen, S. Marchand, R.J. Brüggemann, J.B. Bulitta, M. Bassetti, U. Theuretzbacher, B.T. Tsuji, D.W. Wareham, L.E. Friberg, J.J. De Waele, V.H. Tam, J.A. Roberts. The role of infection models and PK/PD modelling for optimising care of critically ill patients with severe infections. Intensive Care Med. 43: 1021–1032 (2017).

[274] W.A. Craig, D.R. Andes. In vivo pharmacodynamics of ceftobiprole against multiple bacterial pathogens in murine thigh and lung infection models. Antimicrob. Agents Chemother. 52: 3492–3496 (2008).

[275] C.A. Fernandes, R. Vanbever. Preclinical models for pulmonary drug delivery. Expert Opin. Drug Deliv. 6: 1231–1245 (2009).

[276] C.G. Irvin, J.H.T. Bates. Measuring the lung function in the mouse: The challenge of size. Respir. Res. 4: 4 (2003).

[277] F.J. Miller, R.R. Mercer, J.D. Crapo. Lower respiratory tract structure of laboratory animals and humans: Dosimetry implications. Aerosol Sci. Technol. 18: 257–271 (1993).

[278] B.S. Steiniger. Human spleen microanatomy: Why mice do not suffice. Immunology 145: 334–346 (2015).

[279] R.P. Brown, M.D. Delp, S.L. Lindstedt, L.R. Rhomberg, R.P. Beliles. Physiological parameter values for physiologically based pharmacokinetic models. Toxicol. Ind. Health 13: 407–484 (1997).

[280] W.A. Craig. In vitro and animal PK/PD models. In: A. Vinks, H. Derendorf, J. Mouton (eds.). Fundamentals of antimicrobial pharmacokinetics and pharmacodynamics. Springer Science+Business Media, New York, 1st ed.: 23–44 (2014).

[281] B.J. Anderson, N.H.G. Holford. Mechanistic basis of using body size and maturation to predict clearance in humans. Drug Metab. Pharmacokinet. 24: 25–36 (2009).

[282] R.S. Sellers. Translating mouse models. Toxicol. Pathol. 45: 134–145 (2016).

[283] R. Chentouh, C. Fitting, J.M. Cavaillon. Specific features of human monocytes activation by monophosphoryl lipid A. Sci. Rep. 8: 7096 (2018).

[284] M. Matsuura, M. Kiso, A. Hasegawa. Activity of monosaccharide lipid A analogues in human monocytic cells as agonists or antagonists of bacterial lipopolysaccharide. Infect. Immun. 67: 6286–6292 (1999).

[285] K. Buscher, E. Ehinger, P. Gupta, A.B. Pramod, D. Wolf, G. Tweet, C. Pan, C.D. Mills, A.J. Lusis, K. Ley. Natural variation of macrophage activation as disease-relevant phenotype predictive of inflammation and cancer survival. Nat. Commun. 8: 16041 (2017).

[286] J. Zschaler, D. Schlorke, J. Arnhold. Differences in innate immune response between man and mouse. Crit. Rev. Immunol. 34: 433–54 (2014).

[287] H.S. Warren, C. Fitting, E. Hoff, M. Adib-Conquy, L. Beasley-Topliffe, B. Tesini, X. Liang, C. Valentine, J. Hellman, D. Hayden, J. Cavaillon. Resilience to bacterial infection: Difference between species could be due to proteins in serum. J. Infect. Dis. 201: 223–232 (2009).

[288] X. Chu, K. Bleasby, R. Evers. Species differences in drug transporters and implications for translating preclinical findings to humans. Expert Opin. Drug Metab. Toxicol. 9: 237–252 (2013).

[289] A. Sánchez Navarro. New formulations of amoxicillin/clavulanic acid: a pharmacokinetic and pharmacodynamic review. Clin. Pharmacokinet. 44: 1097–115 (2005).

7 Appendix

7.1 Supplementary figures

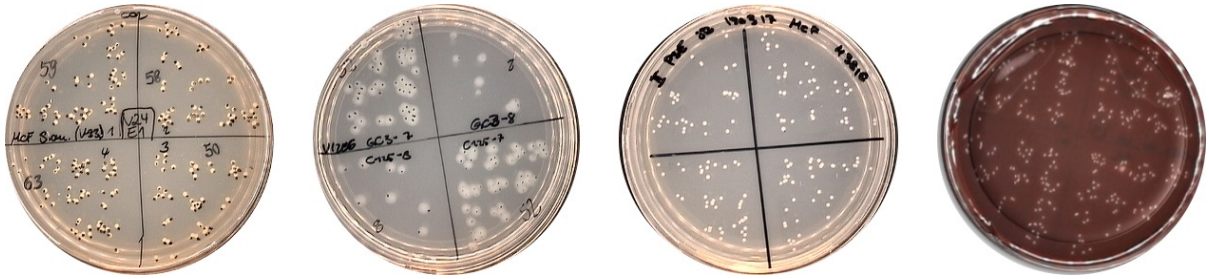

Figure 7.1: Growth of *Staphylococcus aureus* Newman, *Pseudomonas aeruginosa* ATCC 15691, *Klebsiella pneumoniae* ATCC 43816 and *Streptococcus pneumoniae* serotype 1 (from left to right) on their respective growth agar platted by the droplet plate assay. Abbreviations: ATCC: American Type Culture Collection.

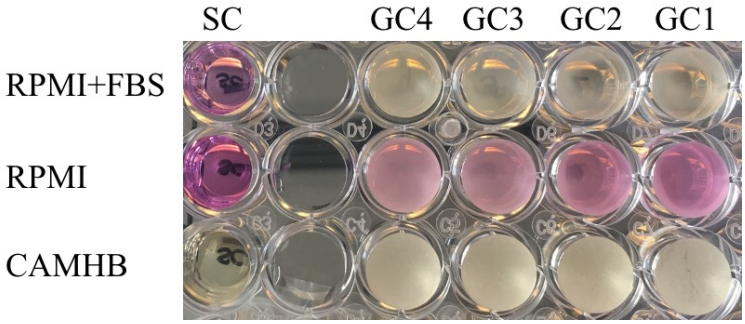

Figure 7.2: Bacterial GC samples of *Staphylococcus aureus* Newman in RPMI1640 with 10% (v/v) FBS ($n_{replicate}$=4), RPMI1640 ($n_{replicate}$=4) and CAMHB ($n_{replicate}$=4), and SC samples ($n_{replicate}$=1 per medium) at 20 h. Abbreviations: CAMHB: Cation-adjusted Mueller-Hinton broth; FBS: Foetal bovine serum; GC: Growth control; RPMI(1640): Roswell Park Memorial Institute 1640 medium; SC: Sterility control.

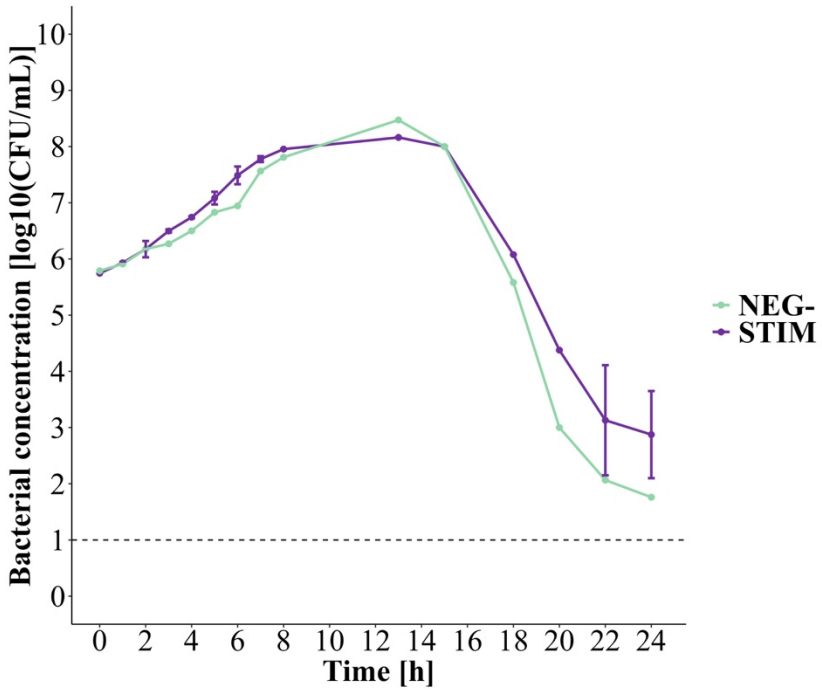

Figure 7.3: (Inhibition of) bacterial growth of *Streptococcus pneumoniae* serotype 1 versus time on a semi-logarithmic scale in NEG- and STIM ($n_{experiment}$=3 with ≥2 replicates each). The median with minimum and maximum bacterial concentrations of the median of single experiments as error bar is depicted for each studied case, LLOQ=1 log10 CFU/mL. Abbreviations: CFU: Colony forming units; LLOQ: Lower limit of quantification; MPLA: Monophosphoryl lipid A; NEG-: Negative control of not-stimulated supernatant; STIM: MPLA-stimulated supernatant.

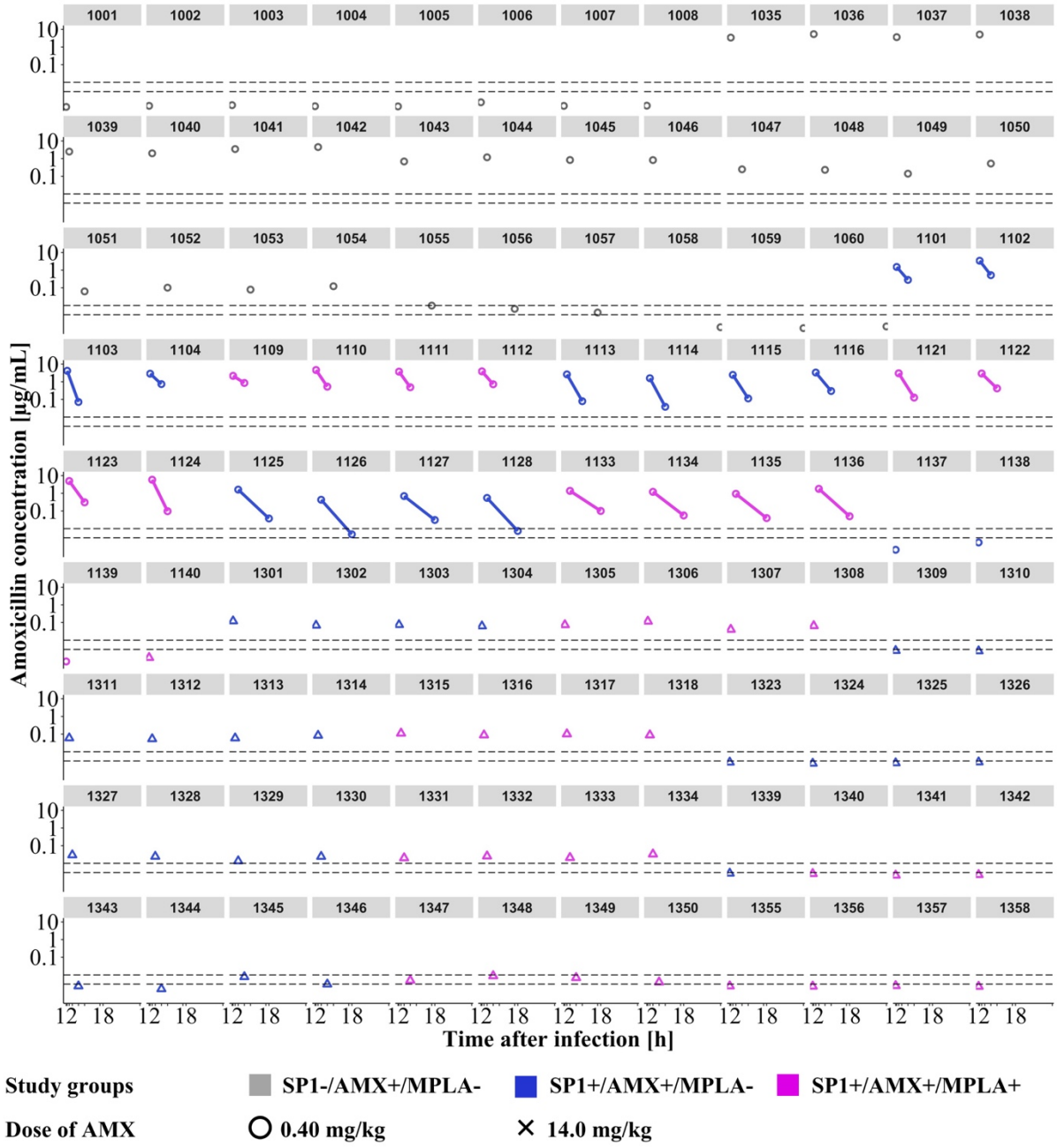

Figure 7.4: Individual serum AMX concentrations of 132 study samples (n_{ID}=108 mice with IDs 1001-1060 in PK1.1, IDs 1101-1136 in PK1.2 and IDs 1301-1358 in PK1.3) in three study groups at a low and a high dose of AMX (0.40 and 14 mg/kg, respectively) on a semi-logarithmic scale versus time. A pharmacokinetic study in mice being non-infected (SP1-) or infected (SP+) with SP1 and treated with either AMX in monotherapy (AMX+/MPLA-) or in combination with MPLA (AMX+/MPLA+) was performed. Dashed lines: LLOQ at 0.01 µg/mL and LOD at 0.003 µg/mL. Symbols: Cross: Mice treated with 14.0 mg/kg AMX; Triangle: Mice treated with 0.40 mg/kg AMX. Abbreviations: AMX: Amoxicillin; ID: Identifier; LLOQ: Lower limit of quantification; LOD: Limit of detection; MPLA: Monophosphoryl lipid A; PK: Pharmacokinetic study; SP1: *Streptococcus pneumoniae* serotype 1. +: Treatment with respective drug; -: No treatment with respective drug.

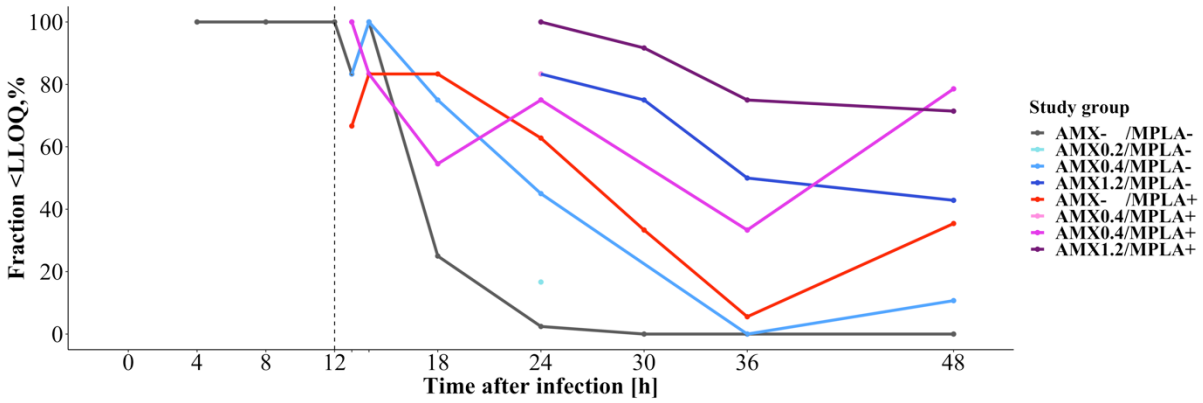

Figure 7.5: Fractions of samples of bacterial numbers being below the LLOQ in spleen of mice being infected with *Streptococcus pneumoniae* serotype 1 at 0 h and drug administration at 12 h (dashed line) for eight study groups: Untreated mice as control (AMX-/MPLA-), mice treated with AMX (AMX0.2/MPLA-, AMX0.4/MPLA-, AMX1.2/MPLA-), MPLA (AMX-/MPLA+) or a combination of AMX and MPLA (AMX0.2/MPLA+, AMX0.4/MPLA+, AMX1.2/MPLA+). The medians of n_{obs}=6-39 observations per study group and timepoint are depicted (lines). Abbreviations: AMX: Amoxicillin (0.20 mg/kg, 0.40 mg/kg or 1.20 mg/kg); LLOQ: Lower limit of quantification (1.22 log10 CFU/lung); MPLA: Monophosphoryl lipid A (2.00 mg/kg); +: Treatment with respective drug; -: No treatment with respective drug.

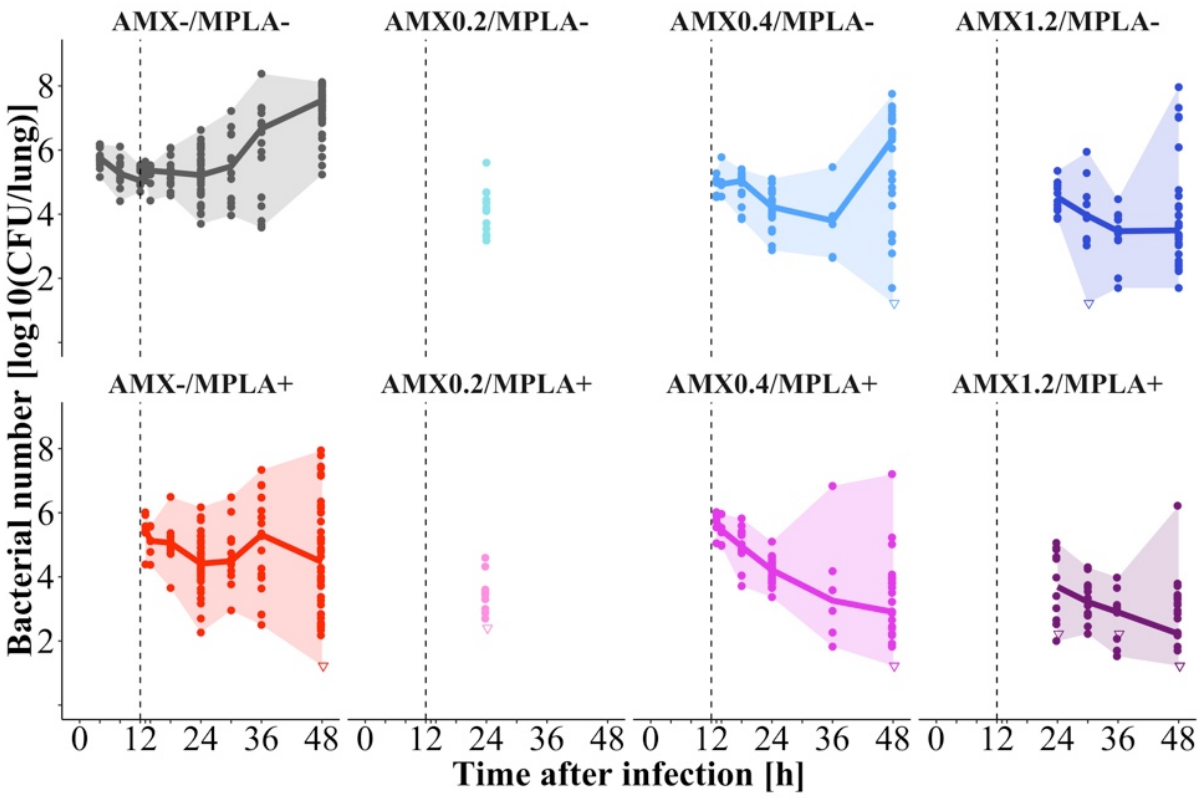

Figure 7.6: Bacterial numbers of *Streptococcus pneumoniae* serotype 1 in lung after intranasal infection at 0 h and drug administration at 12 h (dashed line) stratified by the different study groups: Untreated mice as control (AMX-/MPLA-), mice treated with AMX (AMX0.2/MPLA-, AMX0.4/MPLA-, AMX1.2/MPLA-), MPLA (AMX-/MPLA+) or a combination of AMX and MPLA (AMX0.2/MPLA+, AMX0.4/MPLA+, AMX1.2/MPLA+). The study groups including their individual observations (points; numbers below the LLOQ as triangle) as well as the median of n_{obs}=6-39 observations per study group and timepoint are depicted (lines). Abbreviations: AMX: Amoxicillin (0.20 mg/kg, 0.40 mg/kg or 1.20 mg/kg); CFU: Colony forming units; LLOQ: Lower limit of quantification (1.22-2.40 log10 CFU/lung); MPLA: Monophosphoryl lipid A (2.00 mg/kg); +: Treatment with respective drug; -: No treatment with respective drug.

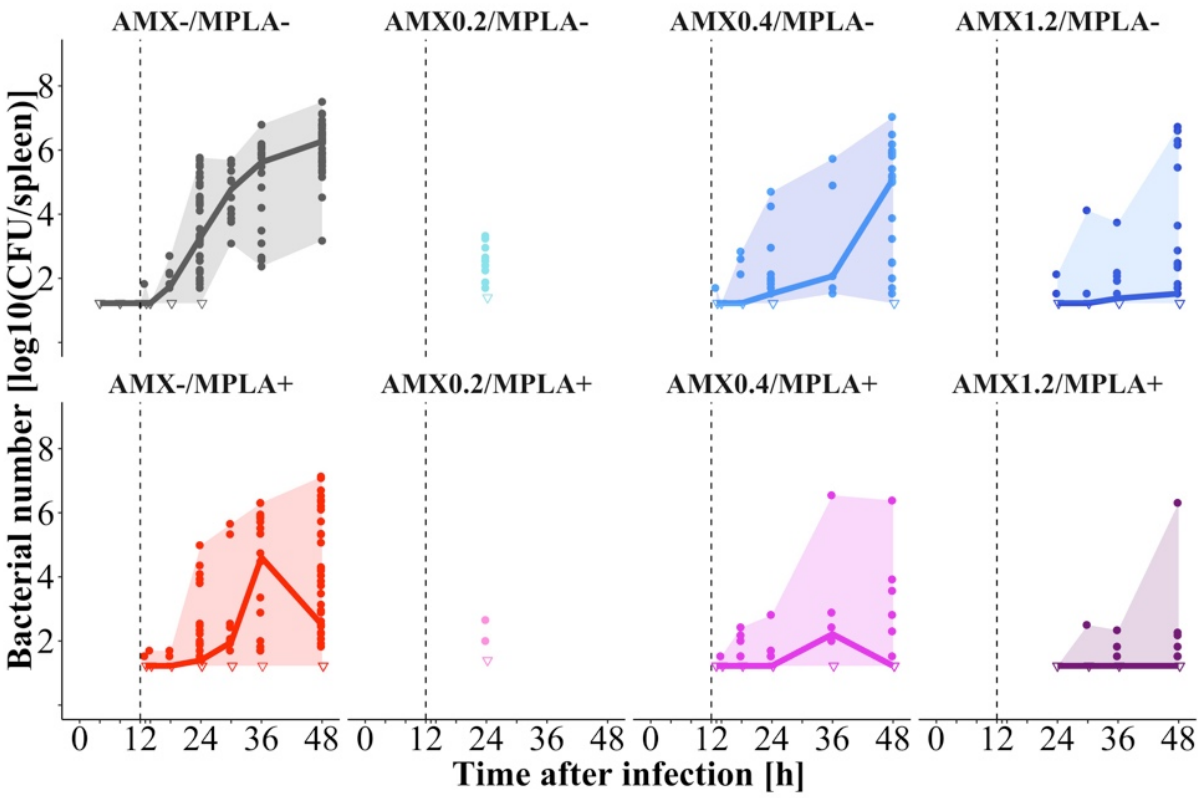

Figure 7.7: Bacterial numbers of *Streptococcus pneumoniae* serotype 1 in spleen after intranasal infection at 0 h and drug administration at 12 h (dashed line) stratified by the different study groups: Untreated mice as control (AMX-/MPLA-), mice treated with AMX (AMX0.2/MPLA-, AMX0.4/MPLA-, AMX1.2/MPLA-), MPLA (AMX-/MPLA+) or a combination of AMX and MPLA (AMX0.2/MPLA+, AMX0.4/MPLA+, AMX1.2/MPLA+). The study groups including their individual measurements (points; numbers below the LLOQ as triangle) as well as the median of n_{obs}=6-39 observations per study group and timepoint are depicted (lines). Abbreviations: AMX: Amoxicillin (0.20 mg/kg, 0.40 mg/kg or 1.20 mg/kg); CFU: Colony forming units; LLOQ: Lower limit of quantification (1.22-2.40 log10 CFU/spleen); MPLA: Monophosphoryl lipid A (2.00 mg/kg); +: Treatment with respective drug; -: No treatment with respective drug.

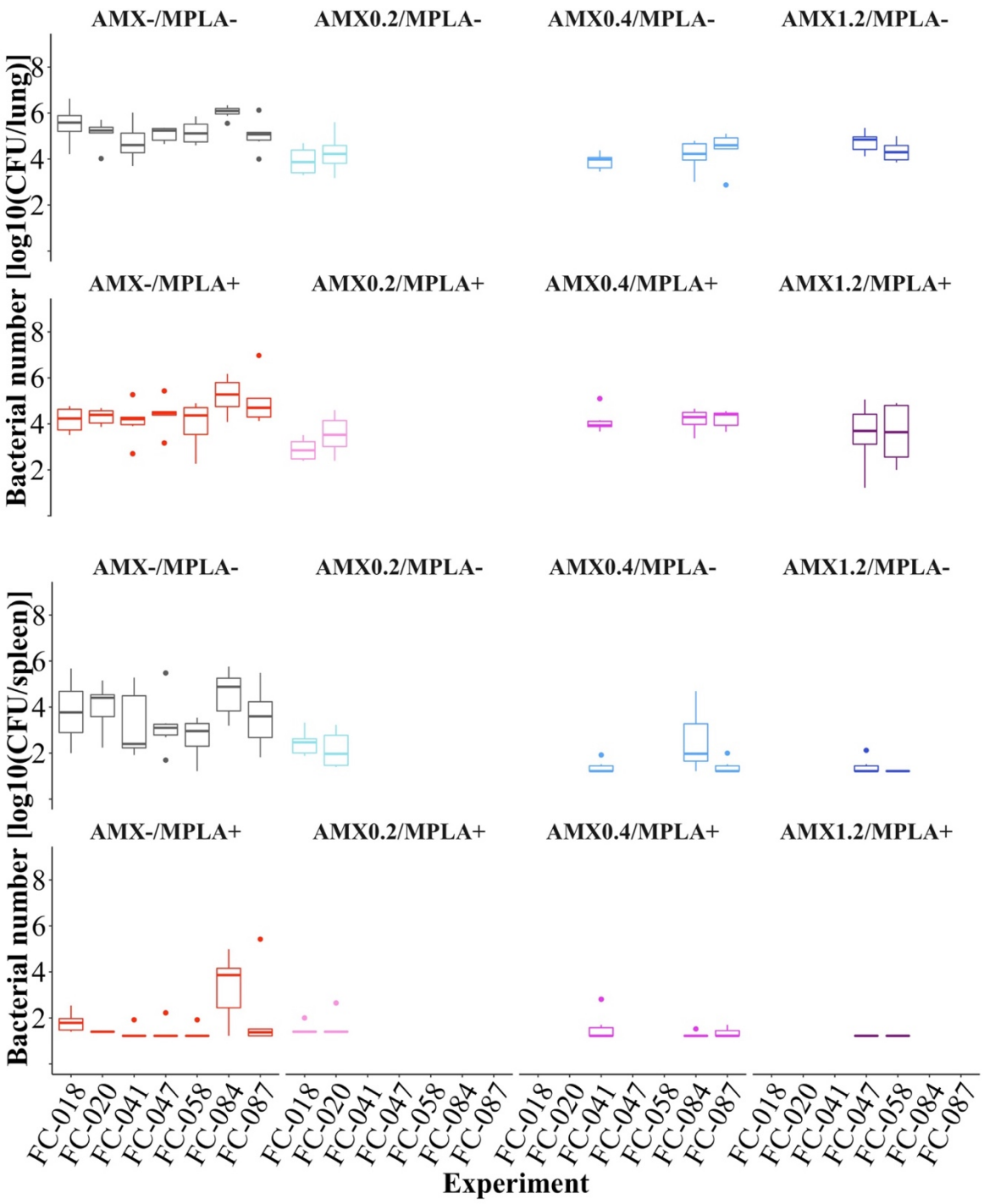

Figure 7.8: Distribution of bacterial numbers of *Streptococcus pneumoniae* serotype 1 per experiment (FC-018 – FC-087) in lung and spleen at 24 h. Different study groups are displayed: Untreated mice as control (AMX-/MPLA-), mice treated with AMX (AMX0.2/MPLA-, AMX0.4/MPLA-, AMX1.2/MPLA-), MPLA (AMX-/MPLA+) or a combination of AMX and MPLA (AMX0.2/MPLA+, AMX0.4/MPLA+, AMX1.2/MPLA+). Bacterial numbers are depicted as median, 25th (Q1) and 75th (Q3) percentile (lower and upper hinge), Q1-1.5×IQR (lower whisker), Q1+1.5×IQR (lower whisker) and outliers (points). Abbreviations: AMX: Amoxicillin (0.20 mg/kg, 0.40 mg/kg or 1.20 mg/kg); CFU: Colony forming units; FC: Code of experiment performed by Fiordiligie Casilag (Institut Pasteur de Lille, France); IQR: Interquartile range; MPLA: Monophosphoryl lipid A (2.00 mg/kg); +: Treatment with respective drug; -: No treatment with respective drug.

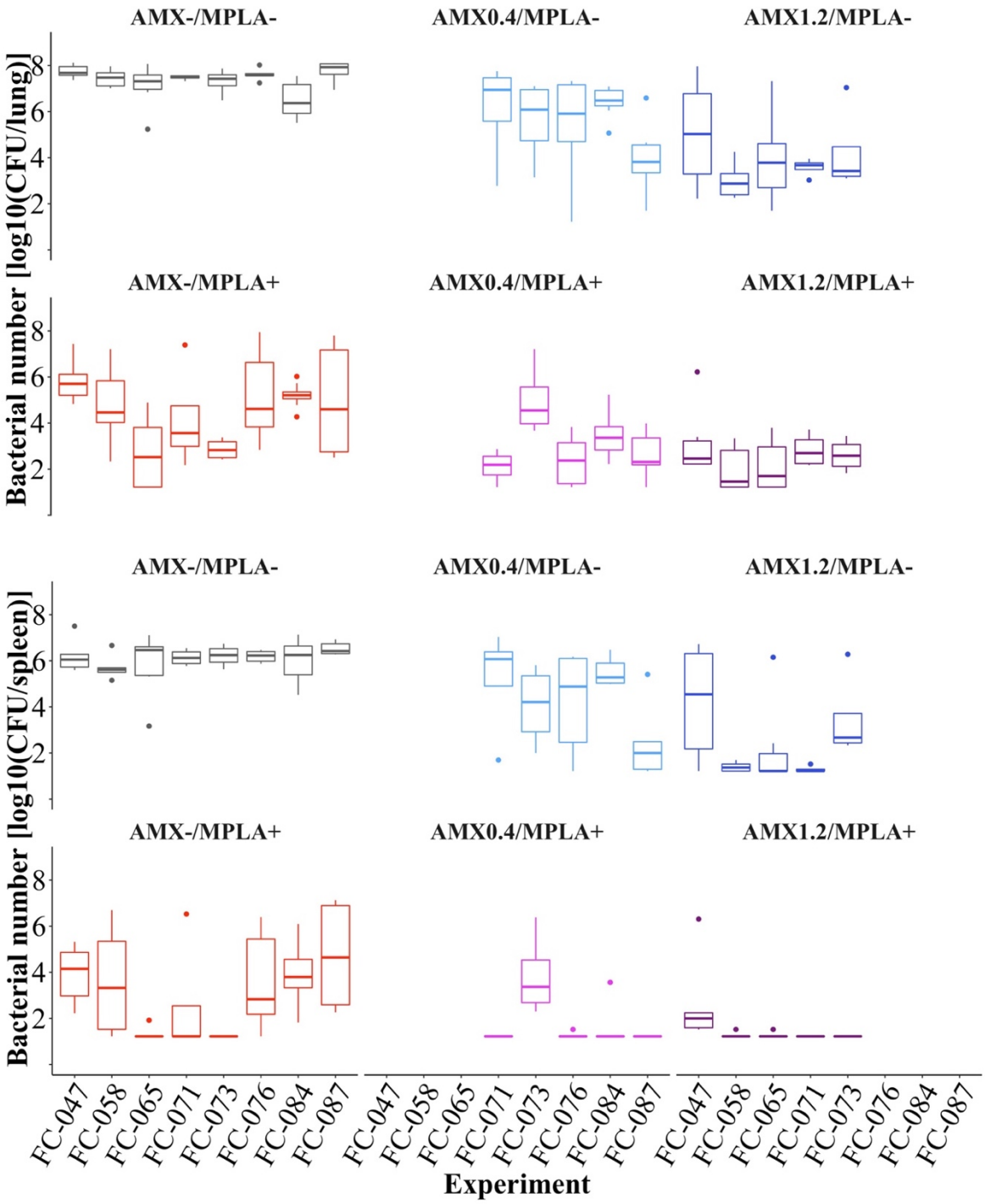

Figure 7.9: Distribution of bacterial numbers of *Streptococcus pneumoniae* serotype 1 per experiment (FC-047 – FC-087) in lung and spleen at 48 h. Different study groups are displayed: Untreated mice as control (AMX-/MPLA-), mice treated with AMX (AMX0.4/MPLA-, AMX1.2/MPLA-), MPLA (AMX-/MPLA+) or a combination of AMX and MPLA (AMX0.4/MPLA+, AMX1.2/MPLA+). Bacterial numbers are depicted as median, 25th (Q1) and 75th (Q3) percentile (lower and upper hinge), Q1-1.5×IQR (lower whisker), Q1+1.5×IQR (lower whisker) and outliers (points). Abbreviations: AMX: Amoxicillin (0.20 mg/kg, 0.40 mg/kg or 1.20 mg/kg); CFU: Colony forming units; FC: Code of experiment performed by Fiordiligie Casilag (Institut Pasteur de Lille, France); IQR: Interquartile range; MPLA: Monophosphoryl lipid A (2.00 mg/kg); +: Treatment with respective drug; -: No treatment with respective drug.

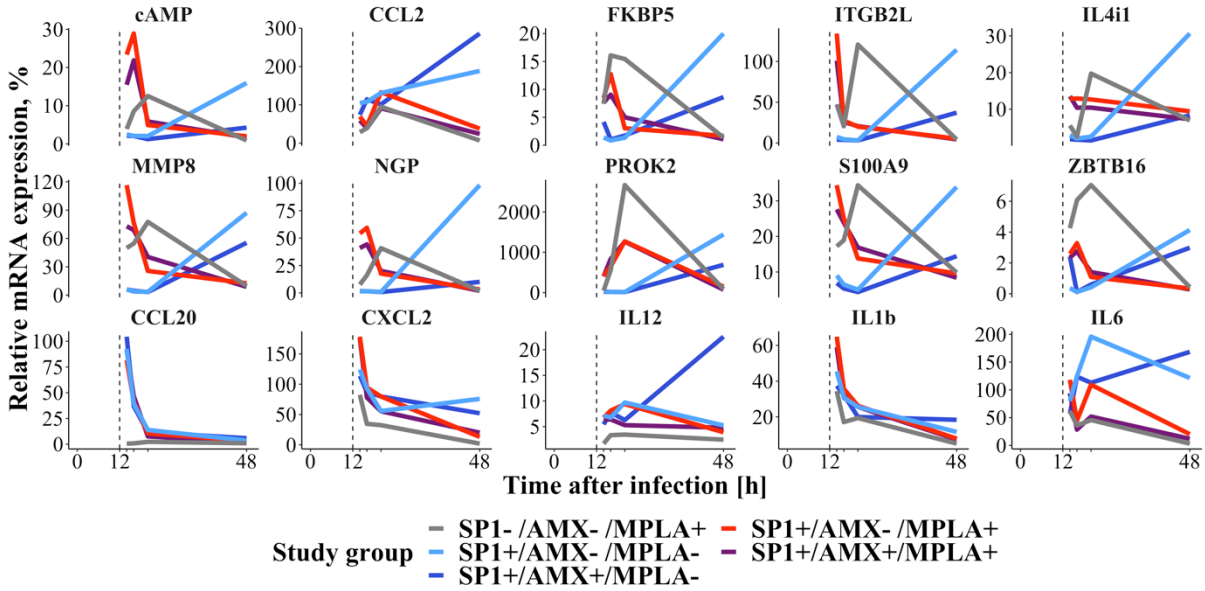

Figure 7.10: Relative mRNA expression of 15 different markers of the immune system in mice after intranasal infection at 0 h and drug administration at 12 h (dashed line) differentiated by five study groups: Non-infected and treated with MPLA (SP1-/AMX-/MPLA+), infected and untreated (SP1+/AMX-/MPLA-), infected and treated with AMX (SP1+/AMX+/MPLA-), MPLA (SP1+/AMX-/MPLA+) or the combination of both (SP1+/AMX+/MPLA+). Relative gene expression normalised to an internal control (β-actin and expression of non-infected, untreated mice) is depicted as median of n_{obs}=3-6 individual observations (lines). Abbreviations: AMX: Amoxicillin; cAMP: Cyclic adenosine monophosphate; CCL2: C-C chemokine ligand 2; CCL20: C-C chemokine ligand 20; CXCL2: C-X-C chemokine ligand 2; FKBP5: FK506 binding protein 5; IL-12 p40: Interleukin-12 subunit p40; IL-1β: Interleukin-1β; IL-4i1: Interleukin-4 induced 1; IL-6: Interleukin-6; ITGB2L: Integrin beta chain 2; MMP8: Matrix metalloproteinase 8; MPLA: Monophosphoryl lipid A; mRNA: Messenger ribonucleic acid; NGP: Neuronal guidance protein; PROK2: Prokineticin 2; S100A9: S100 calcium-binding protein A9; SP1: *Streptococcus pneumoniae* serotype 1; ZTBT16: Zinc finger and BTB region containing-16; +: Treatment with respective drug or bacteria; -: No treatment with respective drug or bacteria.

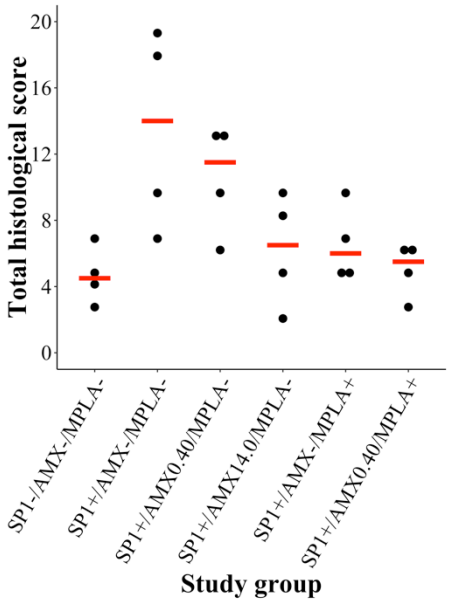

Figure 7.11: Total histological score of 11 different markers of the immune system in mice at 48 h after infection and treatment at 12 h after infection differentiated by different study groups: Non-infected and untreated (SP1-/AMX-/MPLA+), infected and untreated (SP1+/AMX-/MPLA-), infected and treated with two doses of AMX (SP1+/AMX(0.40 or 14.0)/MPLA-), solely treated with MPLA (SP1+/AMX-/MPLA+) or the combination of both (SP1+/AMX0.40/MPLA+). Individual scores (dots) and the median of n_{ID}=4 (line) are depicted. Abbreviations: AMX: Amoxicillin; MPLA: Monophosphoryl lipid A; SP1: *Streptococcus pneumoniae* serotype 1; +: Treatment with respective drug or bacteria; -: No treatment with respective drug or bacteria.

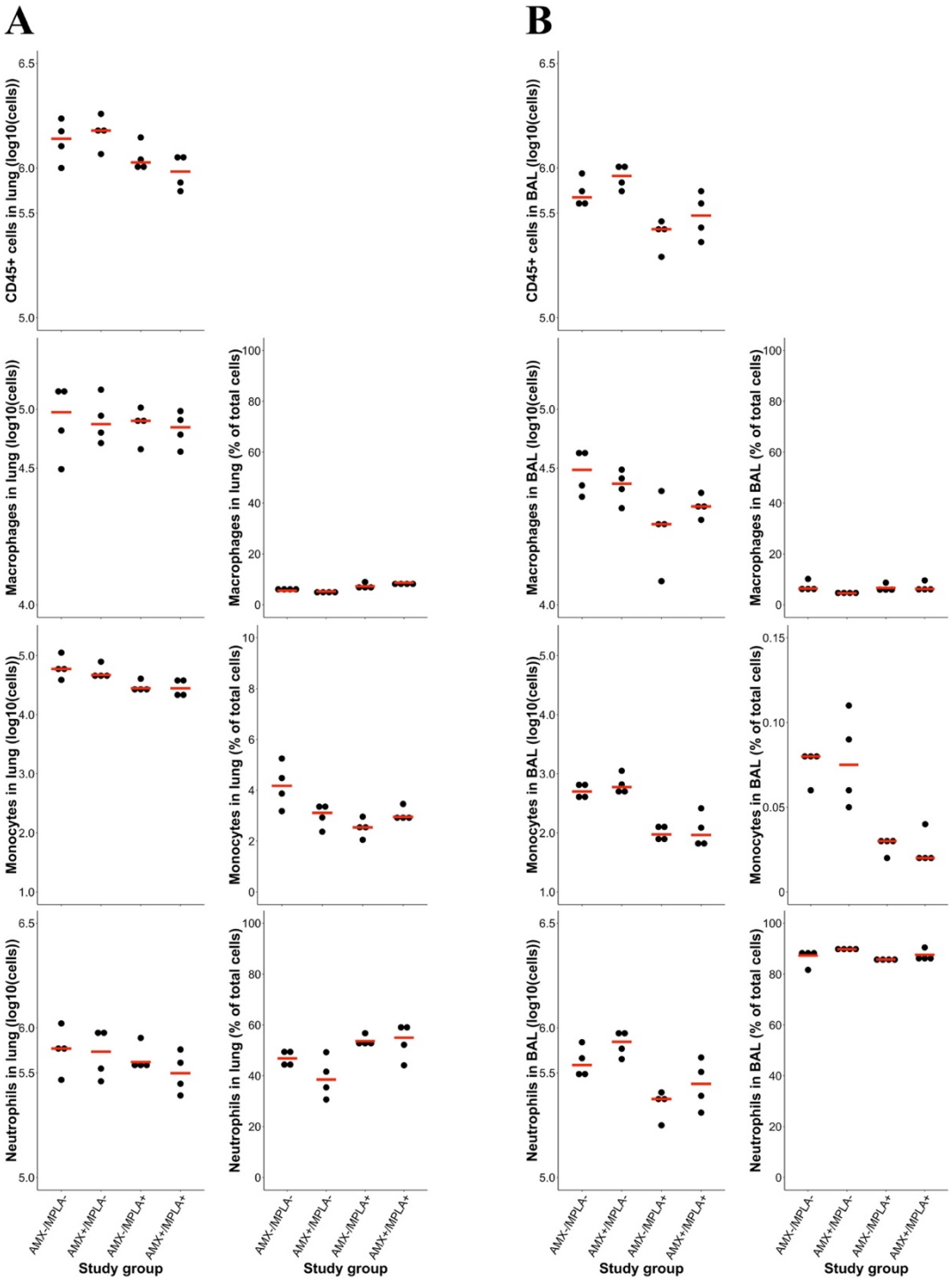

Figure 7.12: Recruitment of different immune system-related cells (CD45+ cells, macrophages, monocytes and neutrophils) of mice being infected with *Streptococcus pneumoniae* serotype 1 and treatment at 12 h after infection as number of cells or % of total cells in lung (A) or BAL (B) differentiated by different study groups: Untreated (AMX-/MPLA-), treated with AMX (AMX+/MPLA-), with MPLA (AMX-/MPLA+) or the combination of both (AMX+/MPLA+). Individual scores (dots) and the median of n_{ID}=4 (line) are depicted. Abbreviations: AMX: Amoxicillin; BAL: Bronchoalveolar lavage; CD45+: Cluster of differentiation 45 positive; MPLA: Monophosphoryl lipid A; SP1: *Streptococcus pneumoniae* serotype 1; +: Treatment with respective drug or bacteria; -: No treatment with respective drug or bacteria.

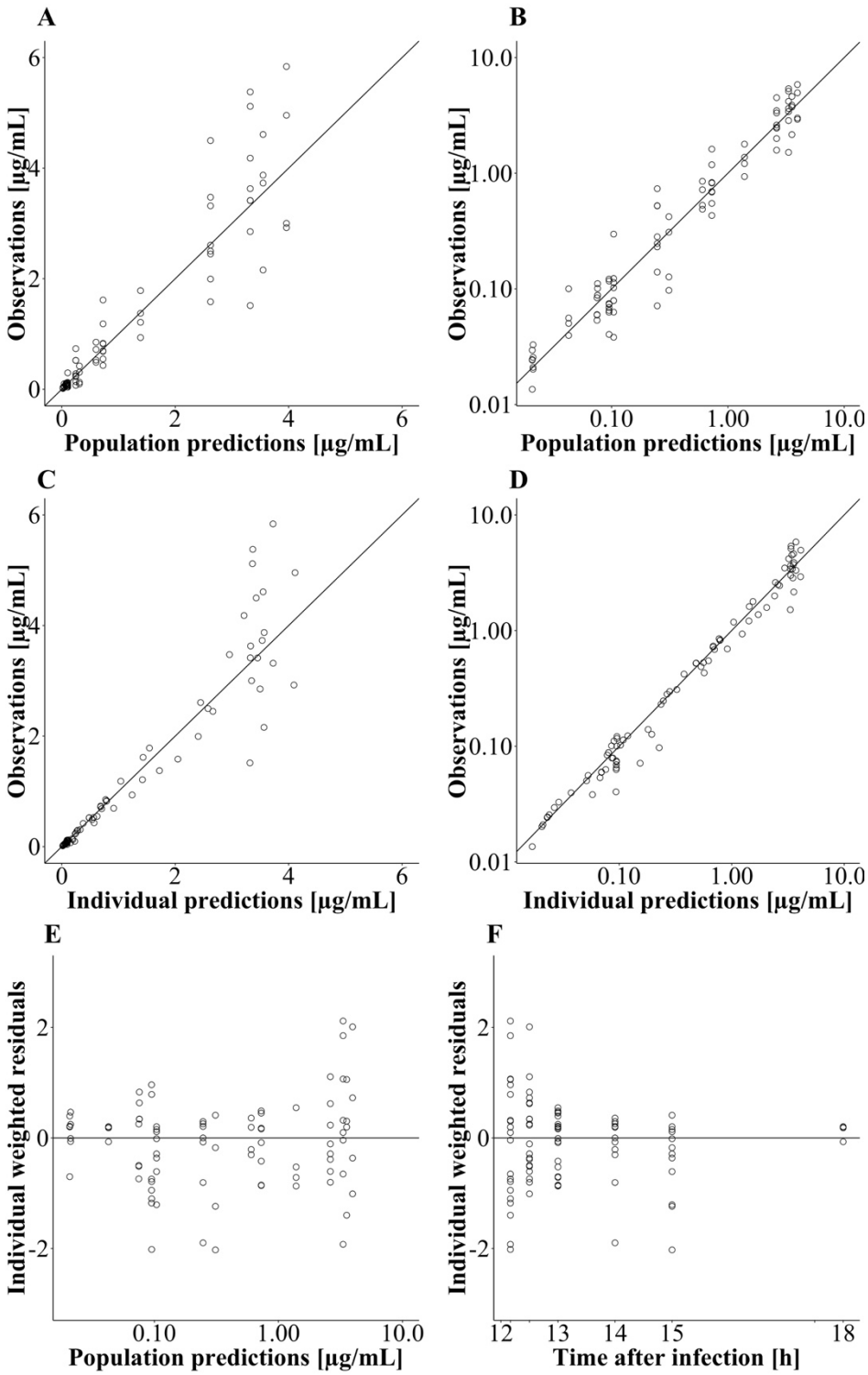

Figure 7.13: Typical GOF plots for the developed pharmacokinetic submodel for AMX serum concentrations in mice with coadministration of MPLA: Observed vs. population-predicted AMX concentrations on a normal (A) and logarithmic scale (B); Observed vs. individual predicted AMX concentrations on a normal (C) and logarithmic scale (D); Individual weighted residuals vs. population-predicted AMX concentrations on a logarithmic scale (E) and vs. time (F); Black line: Line of identity. Abbreviations: AMX: Amoxicillin; GOF: Goodness-of-fit; MPLA: Monophosphoryl lipid A.

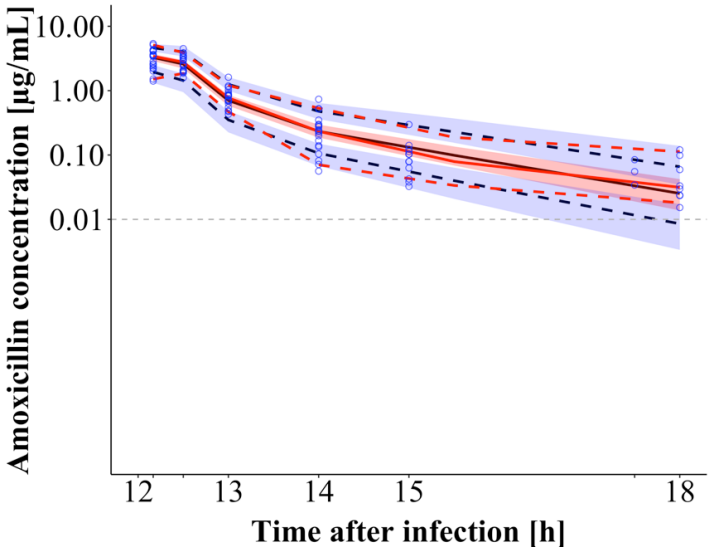

Figure 7.14: Prediction-corrected visual predictive check (n=1000 simulations incl. interindividual variability and residual unexplained variability) of the developed pharmacokinetic submodel for amoxicillin concentrations in mouse serum with MPLA coadministration on a semi-logarithmic scale: Circles: Measurements; Lines: 50th percentile (solid), 5th and 95th percentile (dashed) of measured (red) and simulated (black) amoxicillin concentrations; LLOQ at 0.01 µg/mL (dashed, grey line); Shaded area: 90% confidence interval around simulated percentiles. Abbreviations: LLOQ: Lower limit of quantification; MPLA: Monophosphoryl lipid A.

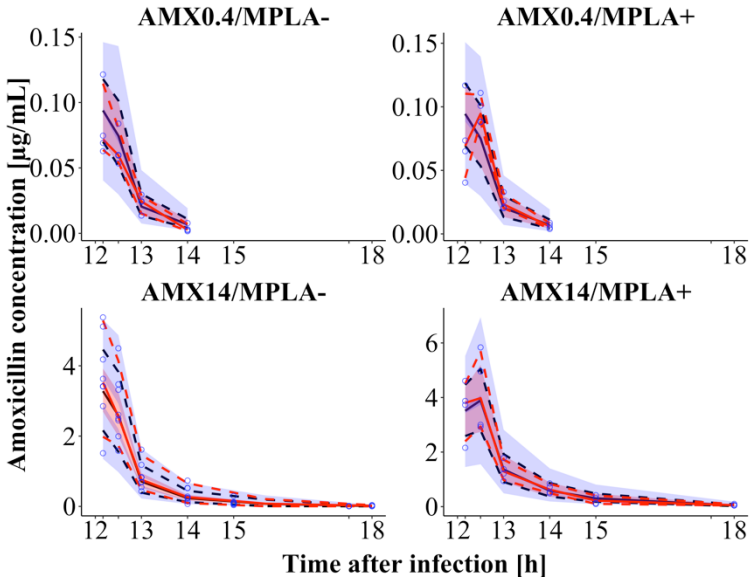

Figure 7.15: Visual predictive check (n=1000 simulations incl. interindividual variability and residual unexplained variability) of the developed pharmacokinetic submodel for AMX concentrations in mouse serum with MPLA coadministration stratified into the different dosing groups: Mice treated with AMX (AMX0.4/MPLA-, AMX14/MPLA-) or a combination of AMX and MPLA (AMX0.4/MPLA+, AMX14/MPLA+). Circles: Measurements; Lines: 50th percentile (solid), 5th and 95th percentile (dashed) of measured (red) and simulated (black) AMX concentrations; Shaded area: 90% confidence interval around simulated percentiles. Abbreviations: AMX: Amoxicillin (0.40 mg/kg or 14.0 mg/kg); MPLA: Monophosphoryl lipid A.

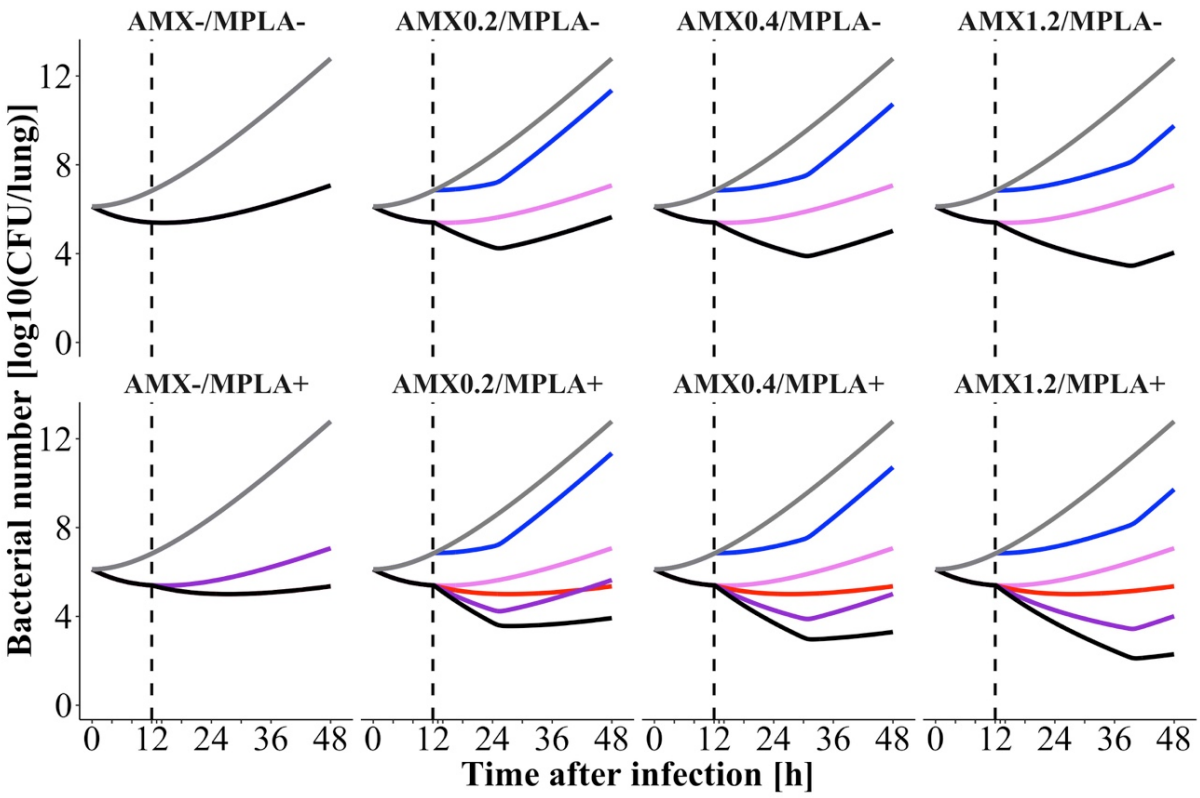

Figure 7.16: Bacterial growth, treatment-unrelated killing and natural death, and drug effects of the semi-mechanistic PK/PD model in lung of mice being infected with *Streptococcus pneumoniae* serotype 1 and treatment at 12 h after infection (dashed line) for eight study groups (Untreated mice as control (AMX-/MPLA-), mice treated with AMX (AMX0.2/MPLA-, AMX0.4/MPLA-, AMX1.2/MPLA-), MPLA (AMX-/MPLA+) or a combination of AMX and MPLA (AMX0.2/MPLA+, AMX0.4/MPLA+, AMX1.2/MPLA+)): (i) Bacterial growth in terms of k_g and k_{lag} without any killing effects (grey); (ii) AMX effects in terms of a sigmoidal E_{max} model depending on AMX concentrations in lung in addition to (i) (blue); (iii) Treatment-unrelated killing and natural death effects in terms of $k_{kill,\ lung}$ in addition to (i) (lightred); (iv) MPLA effect in addition to (iii) (red); (v) AMX effects in terms of a sigmoidal E_{max} model depending on AMX concentrations in lung in addition to (iii) (darkred); (vi) Entire bacterial growth, treatment-unrelated bacterial elimination and drug effects (black). Abbreviations: AMX: Amoxicillin (0.20 mg/kg, 0.40 mg/kg or 1.20 mg/kg); CFU: Colony forming units; k_g: First-order growth rate constant of bacteria in lung; $k_{kill,lung}$: First-order rate constant for treatment-unrelated killing and natural death effects in lung; k_{lag}: First-order rate constant for delay in onset of bacterial growth in lung; MPLA: Monophosphoryl lipid A (2.00 mg/kg); PD: Pharmacodynamics; PK: Pharmacokinetics; +: Treatment with respective drug; -: No treatment with respective drug.

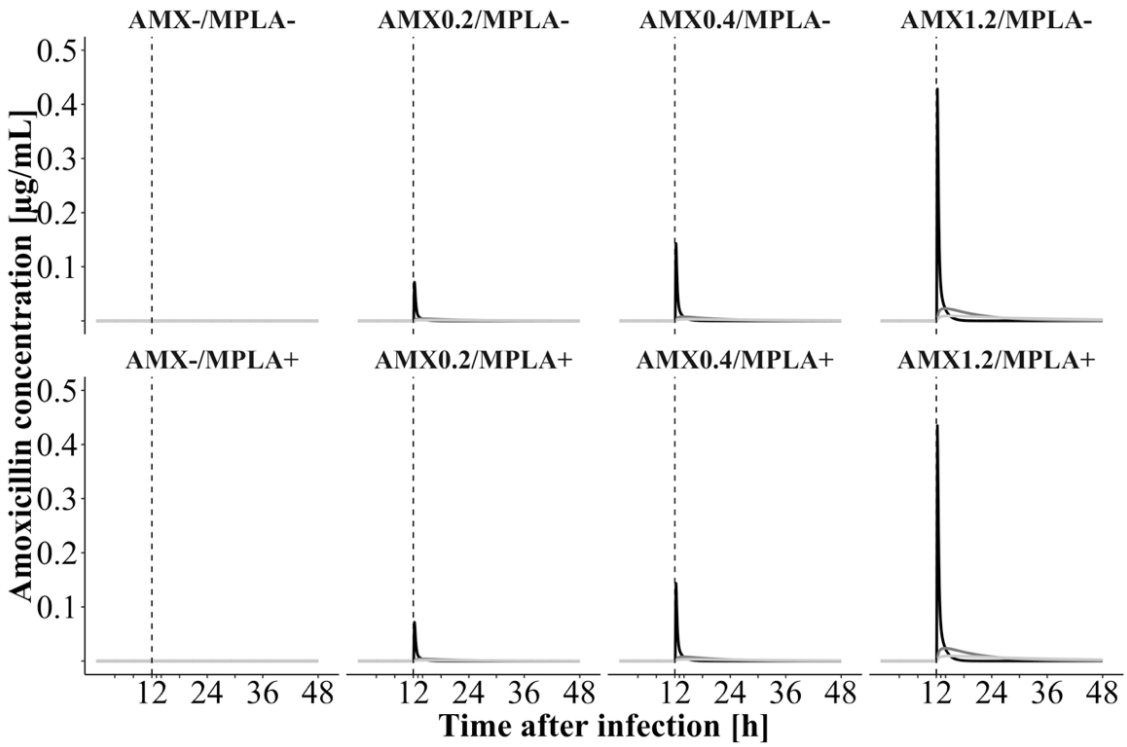

Figure 7.17: Population-predicted AMX concentrations in the central compartment (black), and respective effect compartments in lung (darkgrey) and spleen (lightgrey) over 48 h after infection with *Streptococcus pneumoniae* serotype 1 in mice drug administration at 12 h after infection (dashed line). Different study groups are displayed: Untreated mice as control (AMX-/MPLA-), mice treated with AMX (AMX0.2/MPLA-, AMX0.4/MPLA-, AMX1.2/MPLA-), MPLA (AMX-/MPLA+) or a combination of AMX and MPLA (AMX0.2/MPLA+, AMX0.4/MPLA+, AMX1.2/MPLA+). Abbreviations: AMX: Amoxicillin (0.20 mg/kg, 0.40 mg/kg or 1.20 mg/kg); MPLA: Monophosphoryl lipid A (2.00 mg/kg); +: Treatment with respective drug; -: No treatment with respective drug.

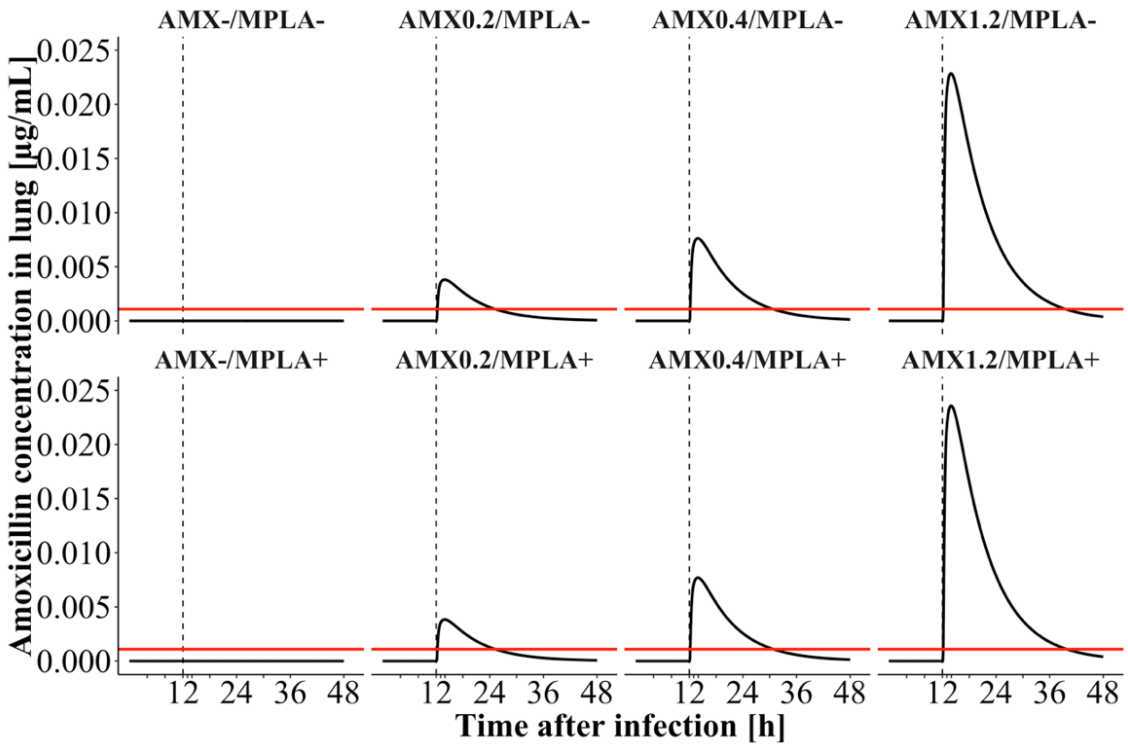

Figure 7.18: Population-predicted AMX concentrations in the lung compartment (black line) over 48 h after infection with *Streptococcus pneumoniae* serotype 1 in mice with drug administration at 12 h after infection (dashed line) and representation of the EC_{50} of 0.00109 µg/mL (red line). Different study groups are displayed: Untreated mice as control (AMX-/MPLA-), mice treated with AMX (AMX0.2/MPLA-, AMX0.4/MPLA-, AMX1.2/MPLA-), MPLA (AMX-/MPLA+) or a combination of AMX and MPLA (AMX0.2/MPLA+, AMX0.4/MPLA+, AMX1.2/MPLA+). Abbreviations: AMX: Amoxicillin (0.20 mg/kg, 0.40 mg/kg or 1.20 mg/kg); EC_{50}: Concentration of AMX to achieve half maximum killing effect; MPLA: Monophosphoryl lipid A (2.00 mg/kg); +: Treatment with respective drug; -: No treatment with respective drug.

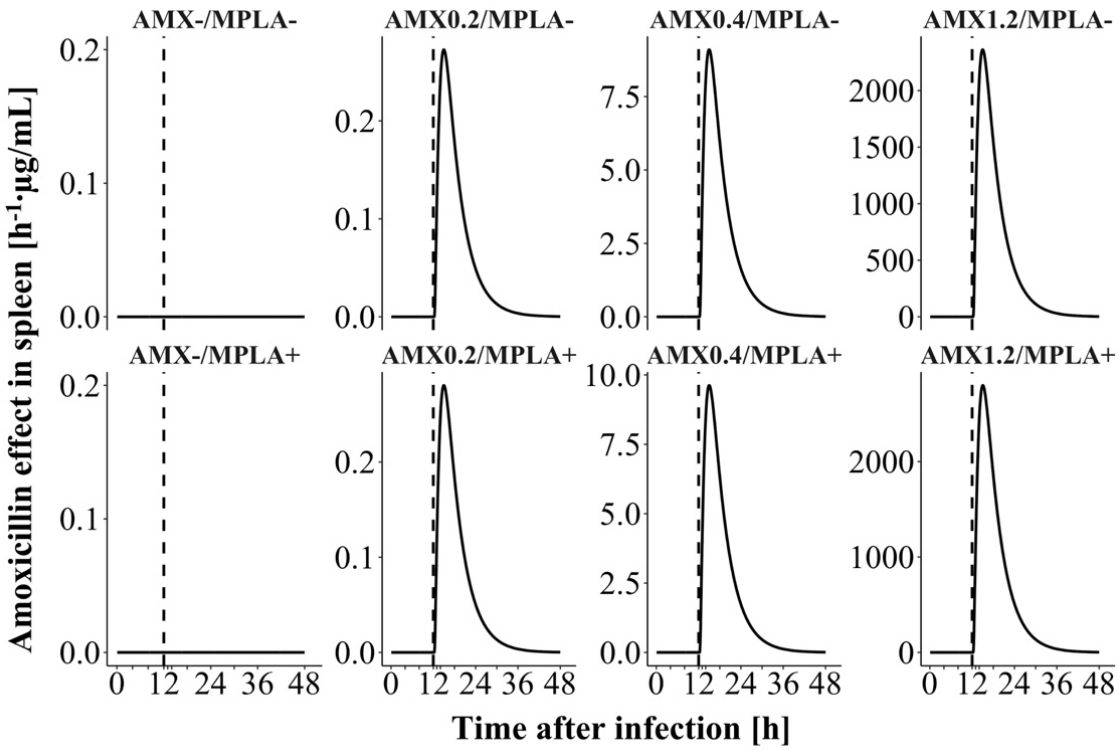

Figure 7.19: PD effect of AMX in spleen depending on a first-order killing rate constant and AMX concentrations in spleen of a PK/PD model defining bacterial growth of *Streptococcus pneumoniae* serotype 1 with drug administration at 12 h (dashed line). Different study groups are displayed: Untreated mice as control (AMX-/MPLA-), mice treated with AMX (AMX0.2/MPLA-, AMX0.4/MPLA-, AMX1.2/MPLA-), MPLA (AMX-/MPLA+) or a combination of AMX and MPLA (AMX0.2/MPLA+, AMX0.4/MPLA+, AMX1.2/MPLA+). Abbreviations: AMX: Amoxicillin (0.20 mg/kg, 0.40 mg/kg or 1.20 mg/kg); MPLA: Monophosphoryl lipid A (2.00 mg/kg); PD: Pharmacodynamic; PK: Pharmacokinetic; +: Treatment with respective drug; -: No treatment with respective drug.

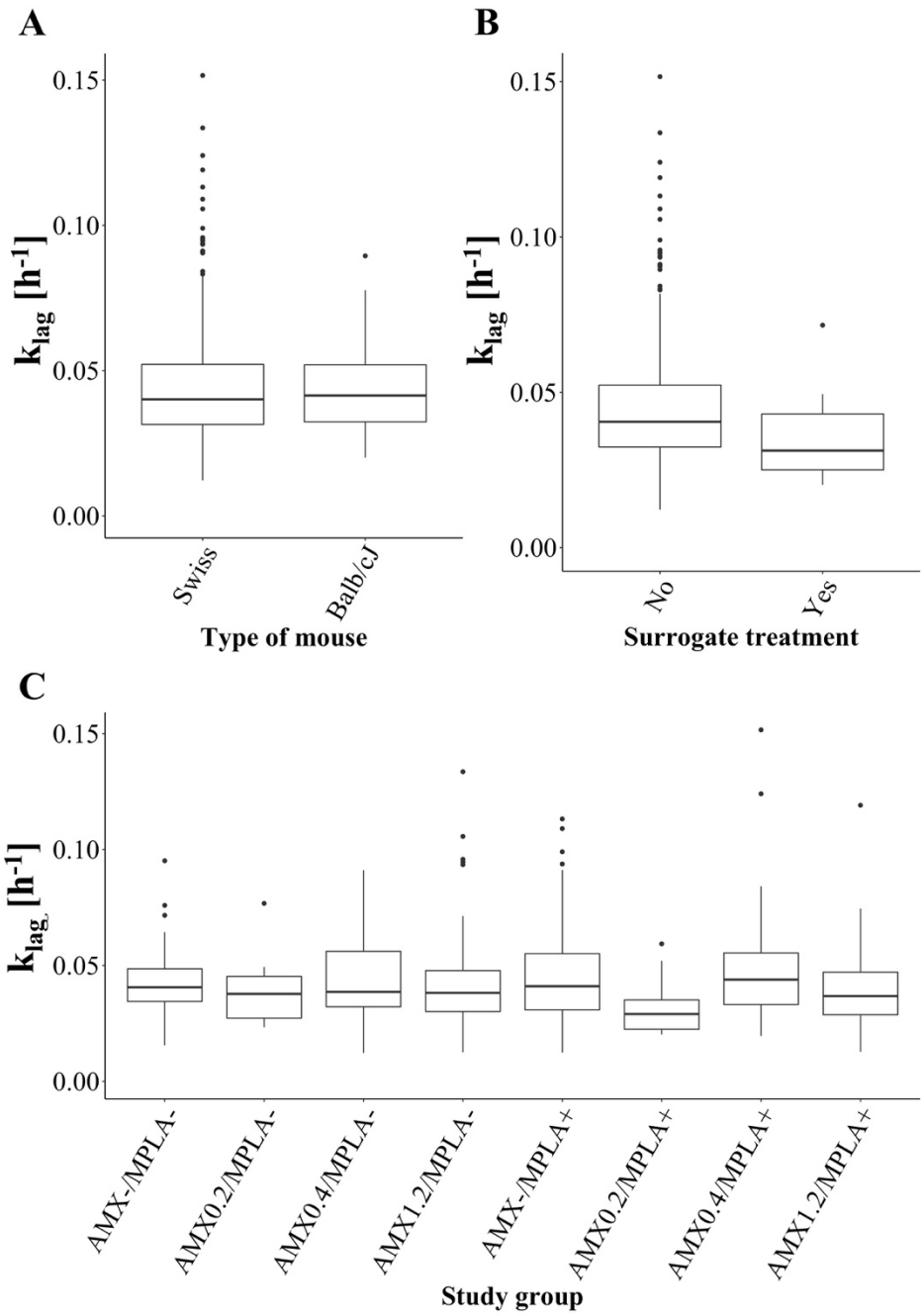

Figure 7.20: Covariate effect of (A) the type of mouse (Swiss, Balb/cJ), (B) dummy administration of the respective other drug (no, yes) and (c) the study groups (untreated mice as control (AMX-/MPLA-), mice treated with AMX (AMX0.2/MPLA-, AMX0.4/MPLA-, AMX1.2/MPLA-), MPLA (AMX-/MPLA+) or a combination of AMX and MPLA (AMX0.2/MPLA+, AMX0.4/MPLA+, AMX1.2/MPLA+)) on the parameter k_{lag} investigating the effect of AMX and MPLA coadministration on *Streptococcus pneumoniae* serotype 1 in mice. k_{lag} is depicted as median, 25th (Q1) and 75th (Q3) percentile (lower and upper hinge), Q1-1.5×IQR (lower whisker), Q1+1.5×IQR (lower whisker) and outliers (points). Abbreviations: AMX: Amoxicillin (0.20 mg/kg, 0.40 mg/kg or 1.20 mg/kg); Balb/cJ: Inbred Balb/cJRj mouse strain; IQR: Interquartile range; k_{lag}: First-order rate constant for delay in onset of bacterial growth in lung; MPLA: Monophosphoryl lipid A (2.00 mg/kg); Swiss: Outbred RjOrl:Swiss (CD-1) mouse strain; +: Treatment with respective drug; -: No treatment with respective drug.

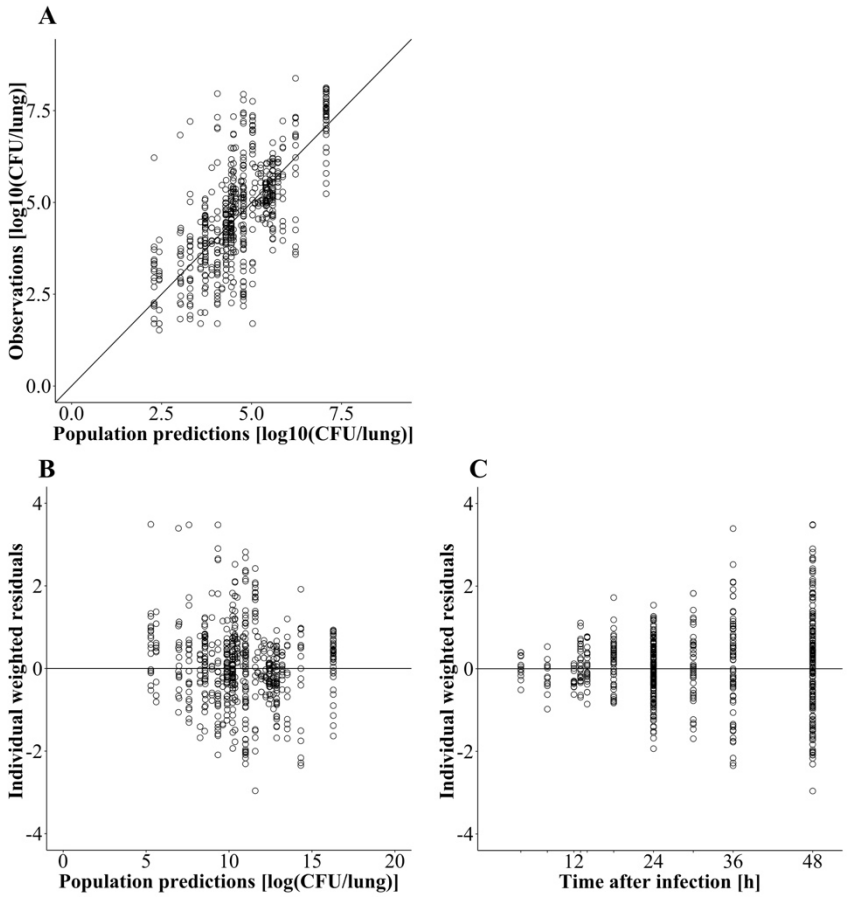

Figure 7.21: Typical GOF plots for the developed semi-mechanistic PK/PD model for bacterial numbers of *Streptococcus pneumoniae* serotype 1 in lungs of mice being untreated or treated with AMX with or without coadministration of MPLA: Observed vs. population-predicted bacterial numbers (A); Individual weighted residuals vs. population-predicted bacterial numbers (B) and vs. time after infection (C); Black line: Line of identity. Abbreviations: AMX: Amoxicillin; CFU: Colony forming units; GOF: Goodness-of-fit; MPLA: Monophosphoryl lipid A; PD: Pharmacodynamic; PK: Pharmacokinetic.

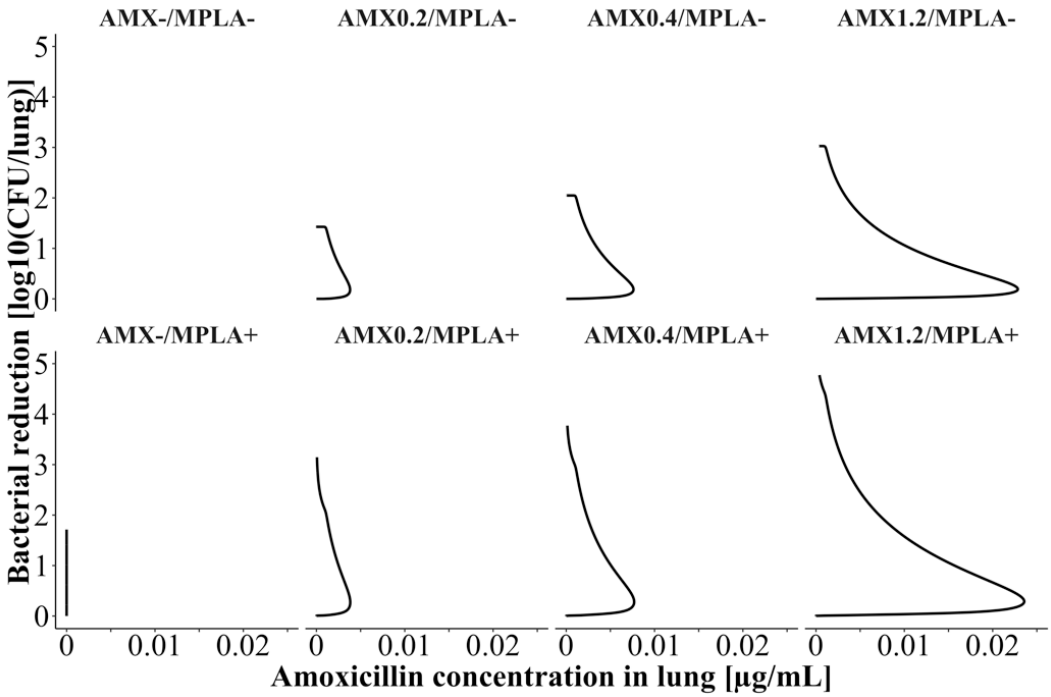

Figure 7.22: Model-predicted PD effect of AMX as bacterial reduction of bacterial numbers of *Streptococcus pneumoniae* serotype 1 in lung of mice compared to bacterial numbers of untreated mice versus model-predicted AMX concentrations in lung. Different study groups are displayed: Untreated mice as control (AMX-/MPLA-), mice treated with AMX (AMX0.2/MPLA-, AMX0.4/MPLA-, AMX1.2/MPLA-), MPLA (AMX-/MPLA+) or a combination of AMX and MPLA (AMX0.2/MPLA+, AMX0.4/MPLA+, AMX1.2/MPLA+). Abbreviations: AMX: Amoxicillin (0.20 mg/kg, 0.40 mg/kg or 1.20 mg/kg); CFU: Colony forming units; MPLA: Monophosphoryl lipid A (2.00 mg/kg); PD: Pharmacodynamics; +: Treatment with respective drug; -: No treatment with respective drug.

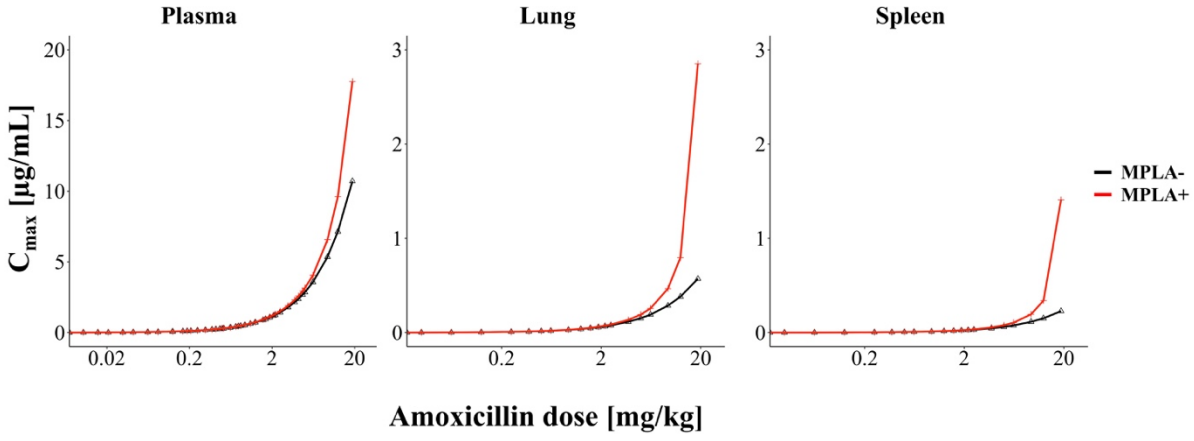

Figure 7.23: Simulated maximum AMX concentrations in serum, lung and spleen of mice infected with *Streptococcus pneumoniae* serotype 1 and being untreated or treated with different total AMX doses without or with MPLA coadministration. Abbreviations: AMX, Amoxicillin; C_{max}: Maximum AMX concentrations in the respective organ; MPLA: Monophosphoryl lipid A; +: Treatment with MPLA; -: No treatment with MPLA.

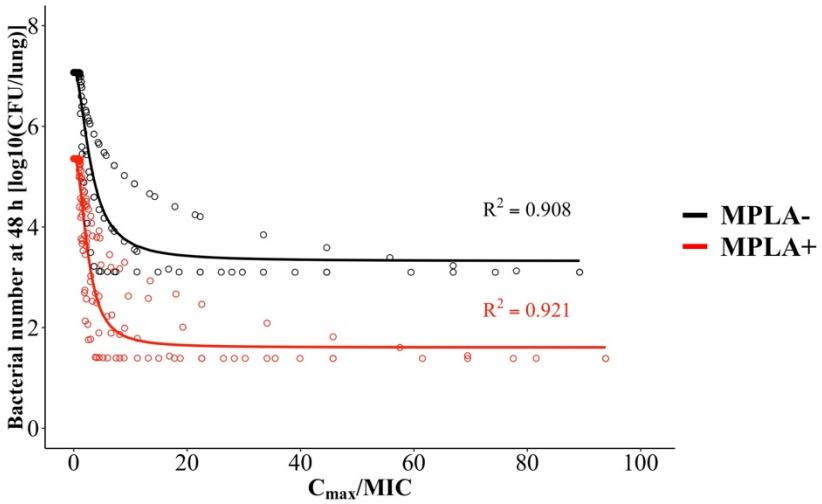

Figure 7.24: Simulated bacterial numbers at 48 h in lung of mice infected with *Streptococcus pneumoniae* with different susceptibility (MIC values ranging from 0.016 to 8 mg/L) versus the C_{max}/MIC. Mice were either untreated, treated with AMX monotherapy (black) or a combined treatment of AMX and MPLA (red) in single to thrice administration. Abbreviations: AMX: Amoxicillin (Total doses ranging from 0.05 to 30.0 mg/kg administered at one dose or split into two or three doses within 36 h); CFU: Colony forming units; C_{max}/MIC: Ratio of maximum AMX concentrations in serum and the minimal inhibitory concentration; MPLA: Monophosphoryl lipid A; +: Treatment with MPLA; -: No treatment with MPLA.

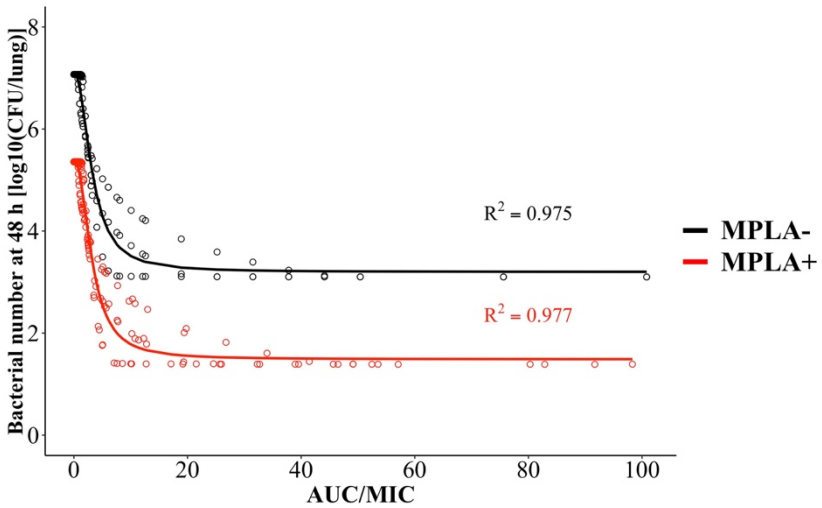

Figure 7.25: Simulated bacterial numbers at 48 h in lung of mice infected with *Streptococcus pneumoniae* with different susceptibility (MIC values ranging from 0.016 to 8 mg/L) versus the AUC/MIC. Mice were either treated with AMX monotherapy (black) or a combined treatment of AMX and MPLA (red) in single to thrice administration. Abbreviations: AMX: Amoxicillin (Total doses ranging from 0.05 to 30.0 mg/kg administered at one dose or split into two or three doses within 36 h); AUC/MIC: Ratio of the area under the concentration-time curve of AMX in serum and the minimal inhibitory concentration; CFU: Colony forming units; MPLA: Monophosphoryl lipid A; +: Treatment with MPLA; -: No treatment with MPLA

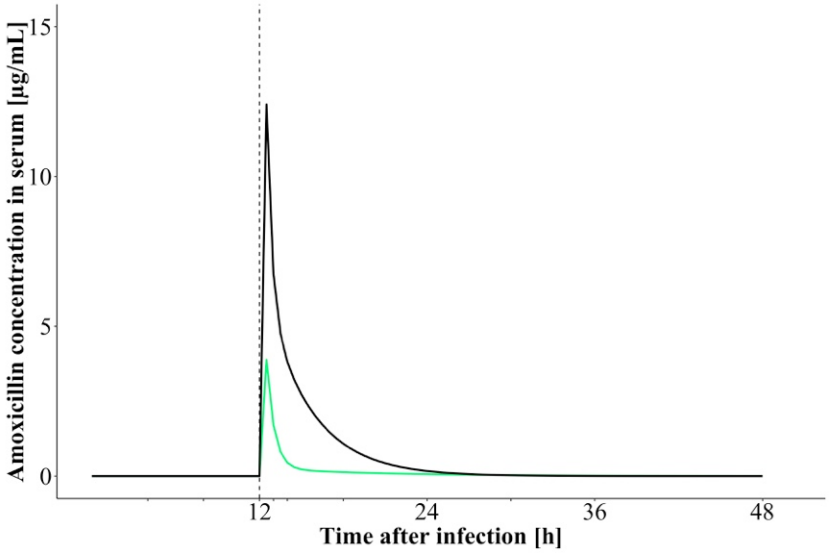

Figure 7.26: Simulated amoxicillin concentrations in serum of humans based on the pharmacokinetic model by Carlier et al. (black, [29]) and on the extrapolated values of parameters of the developed pharmacokinetic submodel (green) versus time after infection. Simulated patients were treated with 3.57 mg/kg, i.e. 250 mg, amoxicillin 12 h after infection (dashed line).

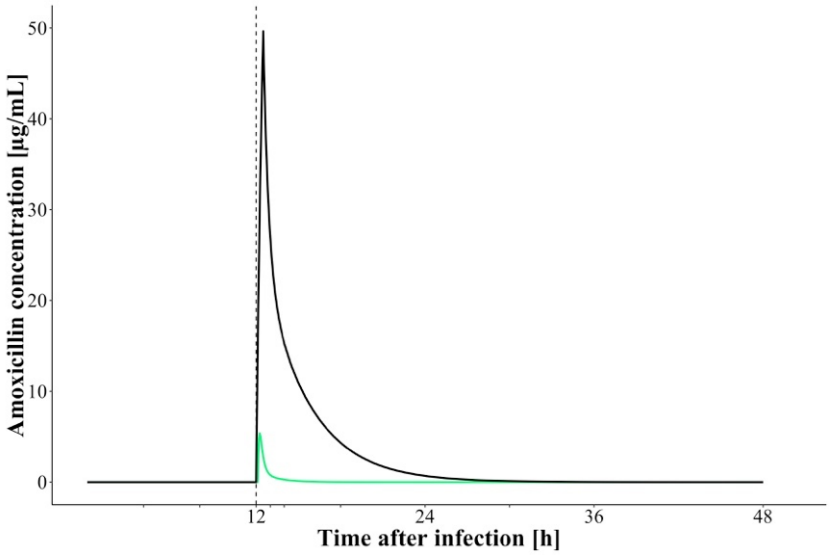

Figure 7.27: Simulated amoxicillin concentrations in serum of humans based on the pharmacokinetic model by Carlier et al. (black, [29]) and of mice based on the developed pharmacokinetic submodel (green) versus time after infection. Simulated humans and mice were treated with 14.3 mg/kg or 15.0 mg/kg amoxicillin, respectively, 12 h after infection (dashed line).

7.2 Supplementary tables

Table 7.1: Mean accuracy and precision of calibrator samples ($n_{replicate}$=3 per concentration per day) of the developed liquid chromatography-tandem mass spectrometry assay for quantification of amoxicillin in mouse serum during the validation process.

	Day 1		Day 2		Day 3	
C_{AMX} [µg/mL]	Accuracy, %	Precision, % CV	Accuracy, %	Precision, % CV	Accuracy, %	Precision, % CV
0.01	100	7.69	101	7.47	99.0	1.97
0.025	99.9	2.04	98.1	3.39	103	3.61
0.1	99.3	3.50	102	8.94	102	8.31
0.5	93.3	4.58	93.5	8.64	93.3	8.50
2.5	98.9	0.54	98.7	4.32	99.6	3.88
5	96.5	9.83	96.0	14.1	95.2	15.0
10	112	5.26	111	2.01	109	0.96

Abbreviations: C_{AMX}: Nominal serum concentration of amoxicillin; CV: Coefficient of variation.

Table 7.2: Within-run (determined on three consecutive days) and between-run accuracy and precision of quality control samples ($n_{replicate}$=5 per concentration level for within-run and between-run, respectively) of the developed liquid chromatography-tandem mass spectrometry assay for quantification of amoxicillin in mouse serum during the validation process.

	Within-run						**Between-run**	
	Day 1		Day 2		Day 3			
C_{AMX} [µg/mL]	Accuracy, %	Precision, %CV	Accuracy, %	Precision, %CV	Accuracy, %	Precision, %CV	Accuracy, %	Precision, %CV
0.01	107	6.96	106	5.57	105	6.00	106	6.44
0.1	114	7.28	108	7.69	107	8.49	110	8.37
1	111	3.46	105	5.75	104	5.98	107	5.88
5	110	9.57	106	10.8	105	12.0	107	11.0

Abbreviations: C_{AMX}: Nominal serum concentration of amoxicillin; CV: Coefficient of variation.

Table 7.3: Back calculated concentrations and accuracy of calibrator samples ($n_{replicate}$=1 per concentration per part of the study sample analysis) of the developed liquid chromatography-tandem mass spectrometry assay for quantification of amoxicillin in mouse serum during application to serum study samples.

	Part 1		Part 2	
C_{AMX} [µg/mL]	Calculated concentration [µg/mL]	Accuracy, %	Calculated concentration [µg/mL]	Accuracy, %
0.01	0.00982	98.2	0.00997	99.7
0.025	0.0261	105	0.0255	102
0.1	0.0992	99.2	0.0955	95.5
0.5	0.485	97.0	0.463	92.7
2.5	2.47	98.8	2.77	111
5	5.10	102	4.57	91.5
10	9.99	99.9	10.8	108

Abbreviations: C_{AMX}: Nominal serum concentration of amoxicillin.

Table 7.4: Mean accuracy and precision of quality control samples ($n_{replicate}$=2 per concentration per part of the study sample analysis) of the developed liquid chromatography-tandem mass spectrometry assay for quantification of amoxicillin in mouse serum during application to serum study samples.

	Part 1		Part 2	
C_{AMX} [µg/mL]	Accuracy, %	Precision, %CV	Accuracy, %	Precision, %CV
0.007	92.4	0.68		
0.01			99.2	30.3
0.07	91.3	1.08		
0.1			87.1	3.31
0.7	92.9	0.57		
1			87.9	8.01
5	94.9	6.62		
7			90.0	1.55

Abbreviations: C_{AMX}: Nominal serum concentration of amoxicillin; CV: Coefficient of variation.

Table 7.5: Determined AMX concentrations of three pharmacokinetic studies in mice being non-infected or infected with *Streptococcus pneumoniae* serotype 1. The bioanalytical assay had a LLOQ of 0.01 µg/mL. Mice were treated with AMX in monotherapy or in combination with monophosphoryl lipid A (AMX dose: 0.40 mg/kg (PK1.3), 14.0 mg/kg (PK1.1, PK1.3)).

Study	Sample ID	Time [h]	Infection	Treatment	Geo. Mean [µg/mL]	Range [µg/mL]	CV, %
PK1.1	1035-1038	0.167	Non-infected	AMX	4.30	3.42-5.38	23.4
PK1.1	1039-1042	0.5	Non-infected	AMX	2.97	1.99-4.50	37.3
PK1.1	1043-1046	1	Non-infected	AMX	0.863	0.686-1.18	24.6
PK1.1	1047-1050	2	Non-infected	AMX	0.254	0.140-0.524	65.3
PK1.1	1051-1054	3	Non-infected	AMX	0.0889	0.0629-0.123	29.6
PK1.1	1055-1057	5.5	Non-infected	AMX	<LLOQ	0.00398-0.00986	
PK1.1	1058-1060	12	Non-infected	AMX	<LLOQ	0.000520-0.000648	
PK1.2	1101-1104	0.167	Infected	AMX	2.80	1.51-4.18	40.1
PK1.2	1109-1112	0.167	Infected	AMX+MPLA	3.46	2.16-4.16	29.8
PK1.2	1113-1117	0.5	Infected	AMX	2.41	1.58-3.32	29.6
PK1.2	1121-1124	0.5	Infected	AMX+MPLA	3.99	2.92-5.84	36.4
PK1.2	1125-1128	1	Infected	AMX	0.717	0.431-1.61	75.2
PK1.2	1133-1136	1	Infected	AMX+MPLA	1.29	0.935-1.78	27.5
PK1.2	1201-1204	2	Infected	AMX	0.296	0.0713-0.735	97.2
PK1.2	1209-1212	2	Infected	AMX+MPLA	0.630	0.488-0.852	26.9
PK1.2	1213-1217	3	Infected	AMX	0.100	0.0382-0.297	114
PK1.2	1221-1224	3	Infected	AMX+MPLA	0.200	0.0971-0.421	76.7
PK1.2	1225-1228	6	Infected	AMX	0.0142	0.00477-0.0376	116
PK1.2	1233-1236	6	Infected	AMX+MPLA	0.0578	0.0396-0.100	46.2
PK1.3	1301-1304	0.167	Infected	AMX	0.0792	0.0628-0.121	33.8
PK1.3	1305-1308	0.167	Infected	AMX+MPLA	0.0689	0.0403-0.117	46.3
PK1.3	1311-1314	0.5	Infected	AMX	0.0632	0.0535-0.0838	21.2
PK1.3	1315-1318	0.5	Infected	AMX+MPLA	0.0965	0.0880-0.111	11.5
PK1.3	1327-1330	1	Infected	AMX	0.0221	0.0135-0.0295	30.5
PK1.3	1331-1334	1	Infected	AMX+MPLA	0.0244	0.0202-0.0329	23.8
PK1.3	1343-1346	2	Infected	AMX	<LLOQ	0.00161-0.00778	
PK1.3	1347-1350	2	Infected	AMX+MPLA	<LLOQ	0.00389-0.00875	

Abbreviations: AMX: Amoxicillin; CV: Coefficient of variation; Geo. Mean: Geometric mean; ID: Identifier; LLOQ: Lower limit of quantification; MPLA: Monophosphoryl lipid A; PK: Pharmacokinetic study.

Table 7.6: Overview of performed experiments including the allocation of each single experiment performed in Balb/cJ and Swiss mice to the respective study groups.

Study group	Experiment										
	Swiss								Balb/cJ		
	FC-041	FC-047	FC-058	FC-065	FC-071	FC-073	FC-076	FC-087	FC-018	FC-020	FC-084
A–M–	x	x	x	x	x	x	x	x	x	x	X
A–M+	x	x	x	x	x	x	x	x	x	x	x
A02M–									x	x	x
A02M+									x	x	x
A04M–	x				x	x	x	x			
A04M+	x				x	x	x	x			
A12M–		x	x	x	x	x					
A12M+		x	x	x	x	x					

Abbreviations: A: Amoxicillin (0.20 mg/kg, 0.40 mg/kg or 1.20 mg/kg); Balb/cJ: Inbred Balb/cJRj mouse strain; FC: Code of experiment performed by Fiordiligie Casilag (Institut Pasteur de Lille, France); M: Monophosphoryl lipid A (2.00 mg/kg); Swiss: Outbred RjOrl:Swiss (CD-1) mouse strain; +: Treatment with respective drug; -: No treatment with respective drug.

7.3 NONMEM® model scripts

7.3.1 Semi-mechanistic pharmacokinetic/pharmacodynamic model

```
$PROBLEM PK/PD

$INPUT
ID            ; Mouse ID
TIME          ; Sampling time [h]
NDV           ; Bacterial number [CFU/organ]
DV            ; Bacterial number [log(CFU/organ)]
AMT           ; Dose AMX [ug]
MDV           ; (0=DV; 1=MissingDV)
EVID          ; (0=DV; 1=Dose; 2=None)
CMT           ; (1=ORAL; 2=SERUM; 3=PERIPHERAL; 5=LUNG; 8=SPLEEN)
BLQ           ; (0=>LLOQ; 1=<LLOQ)
LOQ           ; Respective LLOQ value
TREA          ; Treatment (1=AMX-MPLA-; 2=AMX+MPLA-; 3=AMX-MPLA+; 4=AMX+MPLA+)
PLACE         ; Sampling place (1=GUT; 2=SERUM; 3=LUNG; 4=SPLEEN)
STUDY         ; Data part of lung/spleen (3=Lung; 4=Spleen)
MOUSE         ; Type of mouse (1=SWISS; 2=BALB/CJ)
MOCK          ; Dummy administration (0=NO; 1=YES)
MISSED        ; Missing DV (0=NO; 1=YES)
DOSE          ; AMX Dose [µg]
STRT          ; Stratification into study groups

$DATA 20190506_L+S.csv IGNORE=@ ACCEPT=(MISSED.EQ.0)

$SUBROUTINES ADVAN13 TOL=9

$MODEL NCOMPARTMENTS=8

COMP=(ABS, DEFDOSE)
COMP=(CENTRAL)
COMP=(PERI)

COMP=(CEL)
COMP=(CES)

COMP=(LUNG)
COMP=(TRANSIT)
COMP=(SPLEEN)

;-----------------------------------
$PK
;Pharmacokinetic submodel
KA            =THETA(1)
V1            =THETA(2)
V2            =THETA(3)
V3            =THETA(4)
Q             =THETA(5)*EXP(ETA(1))
TVCL          =THETA(6)
IF(TREA.GE.3)TVCL=THETA(6)+THETA(7)*DOSE
CL            =TVCL*EXP(ETA(2))
ALAG1         =THETA(8)

S1     =V1
S2     =V2
S3     =V3
K23    =Q/V2
K32    =Q/V3
KE     =CL/V2

;Effect compartments
KE0L   =THETA(9) *EXP(ETA(3))
KE0S   =THETA(10)*EXP(ETA(4))
```

```
;Lung compartment
KG     =THETA(11)*EXP(ETA(5))
TVKISL =THETA(12)
IF(TREA.GE.3.AND.TIME.GT.12) TVKISL=THETA(12)*THETA(13)
KISL   =TVKISL   *EXP(ETA(6))
KLAG   =THETA(14)*EXP(ETA(7))
EMAX   =THETA(15)*EXP(ETA(8))
INIT   =THETA(16)*EXP(ETA(9))
EC50   =THETA(17)*EXP(ETA(10))
H      =THETA(18)*EXP(ETA(11))

;Transit compartment
NT     =THETA(19)*EXP(ETA(12))
MTT    =THETA(20)*EXP(ETA(13))
KTR    =(NT+1)/MTT
NFAC   =SQRT(2*3.1415)*NT**(NT+0.5)*EXP(-NT)

;Spleen compartment
TVKISS =THETA(21)
IF(TREA.GE.3.AND.TIME.GT.12) TVKISS=THETA(21)+THETA(22)
KISS   =TVKISS   *EXP(ETA(14))
KKILL  =10**THETA(23)*EXP(ETA(15))
HS     =THETA(24)*EXP(ETA(16))

;Initial conditions
A_0(6)=10**INIT
A_0(7)=0
A_0(8)=0

;Numbers below the LLOQ
IF(BLQ.EQ.1) THEN
  LLOQ=LOQ
ENDIF

;-----------------------------------
$DES
;Pharmacokinetic submodel
DADT(1)=-KA*A(1)
DADT(2)= KA*A(1)+K32*A(3)-K23*A(2)-KE*A(2)
DADT(3)=         -K32*A(3)+K23*A(2)

;Effect compartments
DADT(4)=KE0L*A(2)/V2-KE0L*A(4)
DADT(5)=KE0S*A(2)/V2-KE0S*A(5)

;Lung compartment
DADT(6)=(KG*(1-EXP(-KLAG*T)))*A(6)-KISL*A(6)-((EMAX*A(4)**H)/(EC50**H+A(4)**H))*A(6)

;Transit compartment
DADT(7)=A(6)*KTR*((KTR*T)**NT)*EXP(-KTR*T)/NFAC-A(7)*KTR

;Spleen compartment
DADT(8)=A(7)*KTR-KISS*A(8)-KKILL*A(5)**HS*A(8)

;-----------------------------------
$THETA
(5.04)        FIX    ; 1  KA
(1)           FIX    ; 2  V1
(15.4)        FIX    ; 3  V2
(50.7)        FIX    ; 4  V3
(71.9)        FIX    ; 5  Q
(124)         FIX    ; 6  CL
(-0.145)      FIX    ; 7  CL SL
(0.125)       FIX    ; 8  LAG
(0, 0.136)           ; 9  KE0L
(0, 0.0448)          ; 10 KE0S
(0.48)               ; 11 KG
(0.273)              ; 12 KISL
```

```
(0, 1.41)           ; 13 KISL2
(0.0587)            ; 14 KLAG
(0, 0.255)          ; 15 EMAX
(6.12) FIX          ; 16 INIT
(0, 0.00093)        ; 17 EC50
(0, 20)       FIX   ; 18 H
(0, 23)             ; 19 NT
(0, 40.8)           ; 20 MTT
(0)           FIX   ; 21 KISS
(0, 3.71)           ; 22 KISS2
(0, 13.7)           ; 23 KKILL
(0, 5.06)           ; 24 HS
(0, 2.59)           ; 25 ADD L
(0, 4.17)           ; 26 ADD S

;----------------------------------
$OMEGA
 0 FIX  ; 1  Q
 0 FIX  ; 2  CL
 0 FIX  ; 3  KE0L
 0 FIX  ; 4  KE0S
 0 FIX  ; 5  KG
 0 FIX  ; 6  KIS
 0 FIX  ; 7  KLAG
 0 FIX  ; 8  EMAX
 0 FIX  ; 9  INIT
 0 FIX  ; 10 EC50
 0 FIX  ; 11 H
 0 FIX  ; 12 NT
 0 FIX  ; 13 MTT
 0 FIX  ; 14 KISS
 0 FIX  ; 15 KKILL
 0 FIX  ; 16 HS

;----------------------------------
$SIGMA
 1 FIX  ; RUV1
 1 FIX  ; RUV2

;----------------------------------
$ERROR
IF(PLACE.EQ.3) IPRED=LOG(A(6))
IF(PLACE.EQ.4) IPRED=LOG(A(8))

IF(DV.LT.LLOQ.AND.PLACE.EQ.3) THEN
  F_FLAG=1
  MDVRES=1
  DUM=(LLOQ-IPRED)/(SQRT(THETA(25)**2))
  CUMD=PHI(DUM)
  Y=CUMD
ENDIF

IF(DV.GE.LLOQ.AND.PLACE.EQ.3) THEN
  W1=SQRT(THETA(25)**2)
  RESV=EPS(1)
  IRES=DV-IPRED
  IWRES=IRES/W1
  Y=IPRED+W1*RESV
ENDIF

IF(DV.LT.LLOQ.AND.PLACE.EQ.4) THEN
  F_FLAG=1
  MDVRES=1
  DUM=(LLOQ-IPRED)/(SQRT(THETA(26)**2))
  CUMD=PHI(DUM)
  Y=CUMD
ENDIF
IF(DV.GE.LLOQ.AND.PLACE.EQ.4) THEN
```

```
  W2=SQRT(THETA(26)**2)
  RESV=EPS(2)
  IRES=DV-IPRED
  IWRES=IRES/W2
  Y=IPRED+W2*RESV
ENDIF

CPL = A(2)/V2
CLU = A(4)
CSP = A(5)

;-----------------------------------
$EST METHOD=1 LAPLACIAN MAXEVAL=9999 SIG=3 PRINT=1 NOABORT POSTHOC
$COV
$TABLE ID CMT TIME PRED IPRED RES WRES MDV CPL CLU CSP TREA MOCK PLACE MOUSE DOSE
       IRES IWRES EVID STRT NOPRINT ONEHEADERALL FILE=sdtab698
$TABLE ID KG KLAG KISL EMAX EC50 H KE0S KE0L NT CPL CLU CSP KKILL HCO TREA DOSE MOUSE
       MOCK MDV NOPRINT ONEHEADERALL FILE=patab698
```

7.3.2 Time-to-event model

```
$PROBLEM TTE

$INPUT
ID           ; Mouse ID
TIME         ; Time [h]
DV           ; Survival (0=YES; 2=END OF INTERVAL; 3=START OF INTERVAL)
AMT          ; Dose AMX [ug]
MDV          ; (0=DV; 1=MissingDV)
EVID         ; (0=DV; 2=None)
TREA         ; Treatment (1=AMX-MPLA-; 2=AMX+MPLA-; 3=AMX-MPLA+; 4=AMX+MPLA+)
PLACE        ; Sampling place (1=ORAL; 2=SERUM; 3=LUNG; 4=SPLEEN; 5=TTE)
STUDY        ; Data part of lung/spleen/TTE (3=LUNG; 4=SPLEEN; 5=TTE)
MOUSE        ; Type of mouse (1=SWISS; 2=BALB/CJ)
DOSE         ; Dose AMX [ug]
STRT         ; Stratification into study group
COTR         ; MPLA cotreatment (0=MPLA-; 1=MPLA+)
AUC          ; AUC of AMX [µg/mL*h]
TAM          ; T>MIC of AMX [h]
TAEC         ; T>EC50 of AMX [h]
CMAX         ; CMAX of AMX [µg/mL]
CL24         ; CFU LUNG at 24h [log10(CFU/lung)]
CL48         ; CFU LUNG at 48h [log10(CFU/lung)]
CS24         ; CFU SPLEEN at 24h [log10(CFU/spleen)]
CS48         ; CFU SPLEEN at 48h [log10(CFU/spleen)]
AUCL         ; AUC CFU LUNG [log10(CFU/lung)*h]
AUCS         ; AUC CFU SPLEEN [log10(CFU/spleen)*h]

$DATA 20190716_TTE_PKPD.csv IGNORE=@ IGNORE(DOSE.EQ.20)

$SUBROUTINES ADVAN6 TOL=9

$MODEL NCOMPARTMENTS=1
COMP = (HAZARD)

;-----------------------------------
$PK
SA   =THETA(1)*EXP(ETA(1))
SW   =THETA(2)
GA   =THETA(3)
PE   =THETA(4)
BCOV =THETA(5)
BCOV2=THETA(6)


;-----------------------------------
$DES
```

```
DEL= 1E-6
DADT(1)=(SA/(((T+DEL-PE)**2/SW**2)**GA+1))*EXP(BCOV*TAM+BCOV2*COTR)

;-----------------------------------
$THETA
(0,0.04)      ; SA
(0,30)        ; SW
(0,1)         ; GA
(0,100)       ; PT
(1)           ; BCOV
(1)           ; BCOV2

;-----------------------------------
$OMEGA
0 FIX

;-----------------------------------
;$SIGMA

;-----------------------------------
$ERROR

IF(NEWIND.LE.1) CHLAST=0
IF(TIME.EQ.0)   CUMHAZ=0

CUMHAZ=A(1)
SUR   =EXP(-CUMHAZ)

DELX  =1E-6
HAZNOW=(SA/(((TIME+DELX-PE)**2/SW**2)**GA+1))*EXP(BCOV*TAM+BCOV2*COTR)

IF(DV.EQ.0) THEN          ; Censored event
       Y=SUR
       CHLAST=CUMHAZ
    ELSE
       CHLAST=CHLAST
ENDIF

IF(DV.EQ.1) THEN          ; Exact event
       Y=SUR*HAZNOW
ENDIF

IF(DV.EQ.2) THEN          ; Interval Censored event
       Y=1-EXP(-(CUMHAZ-CHLAST))
ENDIF

;-----------------------------------
$EST METHOD=0 LIKE MAXEVAL=9990 NSIG=3 SIGL=9 PRINT=1
$COV
$TABLE ID TIME PRED CUMHAZ SUR HAZNOW MDV TREA MOUSE DOSE STRT NOPRINT ONEHEADERALL
       FILE=sdtab319
$TABLE ID TREA DOSE MOUSE MDV NOPRINT ONEHEADERALL FILE=patab319
```

8 Publications

Original articles

R. Michelet, M. Ursino, S. Boulet, **S. Franck**, F. Casilag, M. Baldry, J. Rolff, M. van Dyk, S.G. Wicha, J.-C. Sirard, E. Comets, S. Zohar, C. Kloft.
The use of translational modelling and simulation to develop immunomodulatory therapy as an adjunct to antibiotic treatment in the context of pneumonia.
Pharmaceutics: 13: 601 (2021).
doi: 10.3390/pharmaceutics13050601

F. Casilag, L. Matarazzo, **S. Franck**, M. Figeac, R. Michelet, C. Kloft, C. Carnoy, J.C. Sirard.
The biosynthetic monophosphoryl lipid A enhances the therapeutic outcome of antibiotic therapy in pneumococcal pneumonia.
ACS Infect. Dis. (2021).
doi: 10.1021/acsinfecdis.1c00176

S. Franck, R. Michelet, F. Casilag, J.C. Sirard, S.G. Wicha[#], C. Kloft[#].
A model-based pharmacokinetic/pharmacodynamic analysis of the combination of amoxicillin and monophosphoryl lipid A against *S. pneumoniae* in mice.
Pharmaceutics 13:469 (2021).
doi: 10.3390/pharmaceutics13040469
[#]shared senior authorship

S. Franck, T. Fuhrmann-Selter, J.F. Joseph, R. Michelet, F. Casilag, J.C. Sirard, S.G. Wicha, C. Kloft.
A rapid, simple and sensitive liquid chromatography tandem mass spectrometry assay to determine amoxicillin concentrations in biological matrix of little volume.
Talanta 201: 253-258 (2019).
doi: 10.1016/j.talanta.2019.03.098

Conference abstracts (oral/poster)

S. Franck, R. Michelet, F. Casilag, J.C. Sirard, S.G. Wicha, C. Kloft.
Boosting the immune system to enhance amoxicillin activity: Insights provided by semi-mechanistic PK/PD modelling.
29th European Congress of Clinical Microbiology and Infectious Diseases (ECCMID), Amsterdam, The Netherlands, 13-16 April 2019.
https://www.escmid.org/escmid_publications/escmid_elibrary/material/?mid=68652, (2019).
(Oral presentation)

S. Franck, R. Michelet, F. Casilag, J.C. Sirard, S.G. Wicha, C. Kloft.
Boosting the immune system to enhance amoxicillin activity: Insights provided by semi-mechanistic PK/PD modelling.
Annual meeting of the International Society of Anti-Infective Pharmacology (ISAP) 2019, Rotterdam, The Netherlands, 12 April 2019.
https://isap.org/index.php/annual-meeting/annual-meeting-2019, (2019).
(Oral presentation)

S. Franck, F. Casilag, J.C. Sirard, M. Rumbo, S.G. Wicha, C. Kloft.
Towards developing unconventional antibiotic treatments – an in vitro approach to study the direct and indirect effects of immune modulators.
28th European Congress of Clinical Microbiology and Infectious Diseases (ECCMID), Madrid, Spain, 21-24 April 2018.

https://www.escmid.org/escmid_publications/escmid_elibrary/material/?mid=63805, (2018).
(Poster presentation)

F. Casilag, L. Matarazzo, D. Cayet, C. Carnoy, **S. Franck**, S.G. Wicha, C. Kloft, J.C. Sirard.
Targetting innate immunity to improve antibiotic therapy in pneumococcal pneumonia.
28th European Congress of Clinical Microbiology and Infectious Diseases (ECCMID), Madrid, Spain, 21-24 April 2018.
https://www.escmid.org/escmid_publications/escmid_elibrary/material/?mid=62331, (2018).
(Oral presentation)

S. Franck, T. Fuhrmann-Selter, J.F. Joseph, R. Michelet, F. Casilag, J.C. Sirard, S.G. Wicha, C. Kloft.
An in vivo-in silico approach to assess the pharmacokinetics of a novel concept combining amoxicillin with an immunomodulatory drug.
Annual Meeting of the Deutsche Pharmazeutische Gesellschaft (DPhG), Hamburg, Germany, 02-05 October 2018.
https://www.dphg.de/fileadmin/downloads/DPhG2018_ConferenceBook_Final_27-09-2018.pdf, 142, (2018).
(Oral and poster presentation)

S. Franck, M. Si-Tahar, S.G. Wicha, C. Kloft.
Evaluation of pharmacodynamic interactions: Which criterion provides the right answer? A case study with colistin and streptomycin in Pseudomonas aeruginosa.
Annual Meeting of the Deutsche Pharmazeutische Gesellschaft (DPhG), Saarbrücken, Germany, 27-29 September 2017.
https://www.dphg.de/fileadmin/downloads/DPhG2017_ConferenceBook_final.pdf, 114, (2017).
(Poster presentation)

Presentation without abstract

S. Franck, R. Michelet, F. Casilag, J.C. Sirard, M. Rumbo, S.G. Wicha, C. Kloft.
Is the combination of antibiotics and immune modulators a solution for tackling bacterial resistance?
Tag der Pharmazie, Berlin, Germany, 20 June 2018.

9 Curriculum vitae

According to the EU privacy protection prescription (DSGVO)
the curriculum vitae has been removed from the electronic version.